NORTHWESTERN UNIVERSITY

Lipid unsaturation in ovarian cancer

A DISSERTATION

SUBMITTED TO THE GRADUATE SCHOOL

IN PARTIAL FULFILLMENT OF THE REQUIREMENTS

for the degree

DOCTOR OF PHILOSOPHY

Driskill Graduate Program in Life Sciences

By

Guangyuan Zhao

EVANSTON, ILLINOIS

December 2022

ABSTRACT

Fat represents an important source of energy for ovarian cancer (OC) cells and is supplied either through import from the tumor milieu or via de novo lipogenesis. During fast tumor growth, when nutrients are scarce, lipogenesis becomes the primary source of fatty acids. Stearoyl-CoA desaturase (SCD), a rate-limiting enzyme in this pathway converts saturated (SFAs) into unsaturated fatty acids (UFAs) and is highly expressed in OC. The goal of this study was to determine how the balance between SFAs and UFAs tightly controlled by SCD, regulates OC cell survival and tumorigenicity. SCD was knocked down by shRNA or inhibited by using the small molecule CAY10566 and global effects on the lipidome and transcriptome were examined by targeted and untargeted lipidomics, stimulated Raman scattering (SRS), and RNA sequencing. In OC cells in which SCD was blocked or knocked down, the effects of exogenous SFAs and UFAs on cell survival and endoplasmic reticulum (ER) stress pathway were assessed by using annexin V staining, XBP1 splicing assay and Western blotting of PERK/eIF2α/ATF4. Tumorigenicity was assessed by using an intraperitoneal (i.p.) xenograft model in nude mice. RNA-seq analysis of SCD knockdown cells cultured under low serum conditions revealed activation of ER stress response pathways. Targeted lipidomics and SRS microscopy showed downregulation of UFAs vs. SFAs, while untargeted lipidomics discovered decreased fatty acyl chain plasticity among phosphatidylcholines. Activation of IRE1α/XBP1 and PERK/eIF2α/ATF4 axes was observed in cells accumulating SFAs. Stiff and disorganized ER membrane was detected by transmission electron microscopy and Stimulated Raman Scattering microscopy. Annexin V staining demonstrated apoptosis of OC cells under long-term mild ER stress or short-time severe ER stress induced by increased levels of SFAs. ER stress and

apoptosis were rescued by addition of UFAs. In vivo SCD knockdown suppressed tumor growth and treatment with the SCD inhibitor CAY10566 reduced the number of metastases and the volume of ascites in mice fed with SFA enriched diet, but not in mice fed a balanced diet. Our data support that OC cells are highly susceptible to unbalanced intracellular SFAs/UFAs, undergoing ER stress and apoptosis in the presence of excessive intracellular SFAs. SCD inhibition coupled with a diet rich in saturated fats decreased cancer progression *in vivo*. These results support SCD as a key regulator of cancer cell fate during metabolic stress in growing tumors and point to new treatment strategies targeting lipid metabolism.

ACKNOWLEDGEMENT

My PhD journey at the Driskill Graduate Program (DGP) in Biomedical Sciences, Feinberg School of Medicine, Northwestern University began with a mid-night interview on February 9th, 2016 at 1:20am (February 8th, 2016 at 11:20am) with Drs. Mojgan Naghavi, Steve Anderson, and Christopher Payne. I am grateful for my admission interview committee who saw my potential as a graduate student in biomedical sciences and extended an offer to me to pursue my PhD training at Northwestern University Feinberg School of Medicine.

The DGP program designed core courses like biochemistry, molecular biology and in particular cell biology which helped me to establish my initial critical thinking and analytical thinking throughout my six years of PhD research in Dr. Daniela Matei's lab. Elective courses such as biostatistics taught by Dr. Rosemary Braun and advanced data science instructed by Drs. Ramana Davuluri and Manoj Kandpal introduced me to the world of coding and next generation sequencing the skills of which I honed and practiced more during my senior years of research.

I would like to express my foremost gratitude towards my academic/thesis advisor, Dr. Daniela Matei who has been such an amazing mentor and supervisor during my journey towards my Doctor of Philosophy degree. Dr. Matei's semi hands-on and hands-off mentorship style gave me sufficient space to learn and hone the essential bioinformatics skill to help the lab to establish our own bulky RNA-seq, metabolomics, and lipidomics analysis pipeline. At the same time, Dr. Matei oversaw my progress in both thesis project and side project so that I could produce meaningful data to answer our biological questions. As time went by, we transitioned from Dr. Matei frequently sending me most recent articles in my field to me sending her interesting

articles relevant to my projects, exemplifying a virtuous circle. There were times when Dr. Matei was tough on me in terms of my logics and train of thoughts for project progression and experiment design. Later on, I learnt from my friends at World Financial Group that this is called "tough love". It is a special type of mentorship and love that in the long run helped me to establish my scientific and logic thinking. I really appreciate that Dr. Matei showed her care, support and love towards me as a mentee and a future scientist.

I am also really grateful for my other mentor, Dr. Horacio Cardenas who worked side-by-side with me on this project. Dr. Cardenas guided me through the early days of RNA extraction from cultured cancer cells and xenograft tumors. He also assisted me in *in vivo* studies using athymic nude mice. More importantly, Dr. Cardenas' mentorship style is more of asking questions to trigger my thinking over each experiment and the entire project. He enjoys scientific discussion and debates which clearly resonates with Dr. Ali Shilatifard's editorial published in Science Advances in 2022, quoted here "Debate and questioning are integral to the scientific process in proving hunches, theories, and in refining experimental design." We always have heated discussions on the rationale of performing an experiment and the correct interpretation of data we obtained. It was a truly challenging but productive and beneficial experience working under the mentorship of Dr. Cardenas.

My gratitude also goes to Drs. Yinu Wang, Hao Huang, Salvatore Condello and Livia Sima who helped me during my rotation and first couple of months at Matei lab. Dr. Yinu Wang taught me the concept of ovarian cancer stem cell and fluorescence activated cell sorting. Dr. Hao Huang showed me and taught me how to made RNA-seq library and supported me to learn RNA-seq analysis and took over the analysis for Matei lab, which contributed to the establishment of the

RNA-seq analysis pipeline for Matei lab and multiple collaborations within the lab. Dr. Salvatore Condello showed me cell culturing and helped me get started on my thesis project which is part of the R01 project granted to Dr. Daniela Matei. Dr. Livia Sima gave me a lot of guidance and learning material regarding flow cytometry when she knew that I would be using flow cytometry for my thesis project and side project.

I also want to thank our collaborators at Boston University, Drs. Ji-Xin Cheng, Junjie Li and Yuying Chen. Their research focusses on Stimulated Raman Scattering microscopy that enables single-cell level imaging of intracellular metabolites. This collaboration experience made me aware of the exciting interdisciplinary studies and opportunities to tackle challenging questions such as mechanistic studies in cancer and identification of drug targets.

I would like to thank other Matei lab members during my thesis work here, i.e. Dr. Yaqi Zhang and Russell Keathley. We had some very thought-provoking conversations on bioinformatics analysis especially for TCGA data, the Cancer Dependency Map data and the Cancer Cell Line Encyclopedia data. Additionally, I would also like to thank past Matei lab alumni. Drs. Nkechiyere Nwani and Anusha Chaparala, Hyebin Han Roh, Xiaolei Situ, Azza Akasha and Dr. Matthew Cowan. Their company and the peer environment created around me really made me feel at “home” and feel that this is the lab I would love to come every single day.

I also want to express my gratitude for my thesis committee members, Drs. Debabrata Chakravarti (Chair), Ramana Davuluri, Cara Gottardi, and Guillermo Oliver. They provided valuable feedback and comments during every committee meeting so that I received information

from different perspectives for my project. Their scientific rigor and critical thinking serve as the best role model for my current and future career as a junior scientist.

We would like to thank Northwestern University Robert H. Lurie Comprehensive Cancer Center Pathology Core, especially Dr. Jian-Jun Wei for providing the tumor specimens and NUSeq Core, especially Drs. Matthew Schipma and Xinkun Wang for RNA sequencing. Lipidomics analysis was performed by Drs. Christina Ferreira and Amber Jannasch in Metabolite Profiling Facility at Bindley Bioscience Center, Purdue University. Transmission electron microscopy was performed by Lennell Reynolds and Drs. Farida Vadimovna Korobova in the Center for Advanced Microscopy/Nikon Imaging Center (CAM) at Northwestern University. We are also grateful for Drs. Constadina Arvanitis and David Kirchenbuechler for their general support during imaging and image analysis. IncuCyte imaging was performed in the Analytical bioNanoTechnology Core Facility of the Simpson Querrey Institute for BioNanotechnology at Northwestern University. Flow cytometry analysis of ferroptosis was supported by the Northwestern University – Flow Cytometry Core Facility and we would like to thank Paul Mehl and Dr. Suchitra Swaminathan for their support. This thesis work was supported in part through the computational resources and staff contributions provided for the Quest high performance computing facility at Northwestern University which is jointly supported by the Office of the Provost, the Office for Research, and Northwestern University Information Technology.

An indispensable part of my PhD journey is the continuous support from my family, i.e. my parents, grandparents and my uncle's family. Later on, I formed my own family and I was so blessed to have my wife and my wife's parents and their families to be part of my life and my

journey towards my PhD degree. The unconditional love from all these family members made my life simpler outside the lab and I could be laser focus on my thesis project.

I am also fortunate to have a group of peers within the DGP program that I hanged out with and also discussed science with. They are Shuirui Bian, Dr. Triet Bui, Dr. Shang-Yang Chen, Junlong Chi, Zhangying Chen, Dr. Yu Deng, Dr. Yucheng Gao, Dr. Blanca Gutierrez-Diaz, Dr. Yanrong Ji, Hana Kubo, Dr. Shimeng Liu, Dr. Yara Rodriguez, Hyebin Roh, Yishu Qu (The Health Sciences Integrated PhD Program), Dr. Chang Zeng, Dr. Yizhen Zhong, and Dr. Yueming Zhu. Also close friends from the PhD in Chemistry program like Drs. Su Chen, Yuanning Feng, Yiqun Wang, and Wenjie Zhou. Their peer support and mental support are so precious during graduate school study and our mutual journey towards PhD degree.

I would like to end my thesis with this famous sentence by Aristotle, “Amicus Plato, sed magis amica veritas”. We are in the quest for truth in studying science and biomedical sciences are the future for human healthcare. Mentorship and truth are the two cores of my PhD training.

Some of the contents within this thesis were reproduced with permission from Multidisciplinary Digital Publishing Institute (MDPI), Springer Nature and Proceedings of the National Academy of Sciences of the United States of America (PNAS).

LIST OF ABBREVIATIONS

ACC	Acetyl-CoA carboxylase
ACLY	ATP-citrate lyase
ACSL	Acyl-CoA synthetase long-chain family member
ARHI	Aplysia ras homology member I, also known as DIRAS3
AKT	AKT serine/threonine kinase 1
ALDH	Aldehyde dehydrogenase
AML	Acute myeloid leukemia
AMP	Adenosine monophosphate
AMPK	5’ Adenosine monophosphate-activated protein kinase
ANOVA	Analysis of variance
AR	Androgen receptor
ATCC	American Type Culture Collection
ATF3	Activating transcription factor 3
ATF4	Activating transcription factor 4
ATP	Adenosine triphosphate
BRAF	B-Raf proto-oncogene, serine/threonine kinase
BRCA1	BRCA1 DNA repair associated
BRCA2	BRCA2 DNA repair associated
BSA	Bovine serum albumin
CACT	Carnitine-acylcarnitine translocase

cDNA	Complementary DNA
CD133	CD133 antigen, also known as PROM1
CD36	Cluster of differentiation 36, also known as fatty acid translocase
CD4	Cluster of differentiation 4
CD44	CD44 antigen (Indian blood group)
CD8	Cluster of differentiation 8
CEBPB	CCAAT enhancer binding protein beta
CHOP	C/EBP homologous protein, also known as DDIT3
CHTN	Cooperative Human Tissue Network
CLL	Chronic lymphocytic leukemia
CMV	Cytomegalovirus
CNS	Central nervous system
CPT1	Carnitine palmitoyl transferase 1
CPT2	Carnitine palmitoyl transferase 2
CRISPR	Clustered regularly interspaced short palindromic repeats
CSC	Cancer stem cell
CSIOVDB	Ovarian cancer database of Cancer Science Institute Singapore
CXCR1	C-X-C motif chemokine receptor 1
DAB	3,3'-Diaminobenzidine
DDIT3	DNA damage-inducible transcript 3
DEG	Differentially expressed gene
DGAT1	Diacylglycerol O-acyltransferase 1

DMEM	Dulbecco's Modification of Eagle's Medium
DMSO	Dimethyl sulfoxide
DNA	Deoxyribonucleic acid
DNase	Deoxyribonuclease
ECAR	Extracellular acidification rate
EGCG	Epigallocatechin-3-gallate
EGFR	Epidermal growth factor receptor
eIF2α	Eukaryotic translation initiation factor 2A
ELOVL	Fatty acid elongase
ELOVL2	Fatty acid elongase 2
EMT	Epithelial-to-mesenchymal transition
ER	Endoplasmic reticulum
ERBB2	Erb-b2 receptor tyrosine kinase 2
ERK	Extracellular signal-regulated kinase
ERN1	Endoplasmic reticulum to nucleus signaling 1
EZH2	Enhancer of zeste 2 polycomb repressive complex 2 subunit
FA	Fatty acid
FABP	Fatty acid binding protein
FABP3	Fatty acid binding protein 3
FABP4	Fatty acid binding protein 4
FABP5	Fatty acid binding protein 5
FABP7	Fatty acid binding protein 7

$FADH_2$	Flavin adenine dinucleotide, reduced
FADS	Fatty acid desaturase
FADS2	Fatty acid desaturase 2
FAO	Fatty acid oxidation
FASN	Fatty acid synthase
FATP	Fatty acid transport protein
FBS	Fetal bovine serum
FCCP	Carbonyl cyanide-p-trifluoromethoxyphenylhydrazone
FDR	False discovery rate
FITC	Fluorescein isothiocyanate
FTE	Fallopian tube epithelium
FTIR	Fourier transform infrared
GAPDH	Glyceraldehyde-3-phosphate dehydrogenase
GPX4	Glutathione peroxidase 4
GSEA	Gene Set Enrichment Analysis
GTEx	Genotype-Tissue Expression
HER2	Human epidermal growth factor receptor 2, also known as ERBB2
HIF1α	Hypoxia inducible factor 1 subunit alpha
HGSOC	High grade serous ovarian cancer
HRP	Horseradish peroxidase
hSRS	Hyperspectral Stimulated Raman Scattering
IGFBP1	Insulin like growth factor binding protein 1

IHC	Immunohistochemistry
IL-6	Interleukin 6
IL-8	Interleukin 8
IOSE	Immortalized ovarian surface epithelium
IPA	Ingenuity pathway analysis
IRE1α	Endoribonuclease inositol-requiring enzyme 1α, also known as ERN1
JAK2	Janus kinase 2
KEAP1	Kelch like ECH associated protein 1
KO	Knockout
KRAS	Kirsten rat sarcoma virus (proto-oncogene, GTPase)
Ku70	X-ray repair cross complementing 6, also known as XRCC6
LASSO	Least absolute shrinkage and selection operator
LD	Lipid droplet
LDL	Low-density lipoprotein
LDLR	Low-density lipoprotein receptor
LMP	Low malignant potential
LPA	Lysophosphatidic acid
LPAR2	Lysophosphatidic acid receptor 2
LPAR3	Lysophosphatidic acid receptor 3
LOH	Loss of heterozygosity
LRP5	Low-density lipoprotein-receptor-related proteins 5
LRP6	Low-density lipoprotein-receptor-related proteins 6

MDSC	Myeloid derived stromal cell
MET	Mesenchymal-to-epithelial transition
microRNA	Micro-ribonucleic acid
MITF	Microphthalmia-associated transcription factor
MMP9	Matrix metallopeptidase 9
MOI	Multiplicity of infection
MRM	Multiple reaction monitoring
mRNA	Messenger ribonucleic acid
mTOR	Mammalian target of rapamycin
mTORC1	Mammalian target of rapamycin complex 1
MYC	MYC proto-oncogene, bHLH transcription factor
NA	Not applicable
NABP1	Nucleic acid binding protein 1
NADH	Nicotinamide adenine dinucleotide, reduced
NADPH	Nicotinamide adenine dinucleotide phosphate, reduced
NANOG	Nanog Homeobox
NF-κB	Nuclear factor kappa-light-chain-enhancer of activated B cells
NIH	National Institute of Health
NUPR1	Nuclear protein 1, transcriptional regulator
OA	Oleic acid
OC	Ovarian cancer
OCR	Oxygen concentration rate

OCSC	Ovarian cancer stem cell
ORF	Open reading frame
PA	Palmitic acid
PARP	Poly-(ADP-ribose) polymerase
PBS	Phosphate buffered saline
PC	Phosphatidylcholine
PCA	Principal component analysis
PCR	Polymerase chain reaction
PE	Phosphatidylethanolamine
PECR	Peroxisomal trans-2-enoyl-CoA reductase
PEG3	Paternally expressed 3
PERK	Protein kinase R (PKR)-like endoplasmic reticulum kinase, also known as EIF2AK3
PFS	Progression-free survival
PIK3CA	Phosphatidylinositol-4,5-bisphosphate 3-kinase catalytic subunit alpha
PI3K	Phosphatidylinositol-4,5-bisphosphate 3-kinase
PLAGL1	Pleomorphic adenoma gene 1 like zinc finger 1
PML	Promyelocytic leukemia
PPAR	Peroxisome proliferator-activated receptor
PROTAC	Protein-targeting chimeric molecule
PPP1R15A	Protein phosphatase 1 regulatory subunit 15A
PR	Progesterone receptor

PROM1	Prominin 1
PTEN	Phosphatase and tensin homolog
PTPLB	Protein tyrosine phosphatase-like (proline instead of catalytic arginine), member B, also known as 3-hydroxyacyl-CoA dehydratase 2
PVDF	Polyvinylidene difluoride
qRT-PCR	Quantitative reverse transcription polymerase chain reaction
RIPA	Radioimmunoprecipitation assay buffer
RNA	Ribonucleic acid
RNase	Ribonuclease
ROS	Reactive oxygen species
RPMI	Roswell Park Memorial Institute
RSEM	RNA-Seq by Expectation-Maximization
SCD	Stearoyl-CoA desaturase
SCD5	Stearoyl CoA desaturase 5
SD	Standard deviation
SE	Standard error
SFA	Saturated fatty acid
shRNA	Short hairpin ribonucleic acid
SLC22A16	Solute carrier family 22 member 16
SLUG	Snail family transcriptional repressor 2, also known as SNAI2
SM	Sphingomyelin
SNAI1	Snail family transcriptional repressor 1

SP1	Specificity protein 1
SREBF1	Sterol regulatory element binding transcription factor 1
SRC	SRC proto-oncogene, non-receptor tyrosine kinase
SRS	Stimulated Raman Scattering
STAT3	Signal transducer and activator of transcription 3
STK11	Serine/threonine kinase 11
TAG	Triacylglycerol
TCA	tricarboxylic acid
TCGA	The Cancer Genome Atlas
TEM	Transmission Electron Microscopy
TGFα	Transforming growth factor alpha
TIC	Tumor-initiating stem cell-like cell
TMA	Tissue microarray
TOFA	5-(Tetradecyloxy)-2 Furoic Acid
TP53	Tumor protein p53
tRNA	Transfer ribonucleic acid
TXNIP	Thioredoxin interacting protein
UCSC	University of California Santa Cruz
UFA	Unsaturated fatty acid
UMP	Uridine monophosphate
UTP	Uridine triphosphate
VEGF	Vascular endothelial growth factor

WNT	Wingless-type MMTV integration site
WT	Wildtype
XBP1	X-box binding protein 1
YAP1	Yes1 associated transcriptional regulator
ZEB2	Zinc finger E-box binding homeobox 2
3’ UTR	3’ untranslated region
5’ UTR	5’ untranslated region

TABLE OF CONTENTS

LIST OF FIGURES

LIST OF TABLES

Chapter 1 : Introduction

1.1 Ovarian cancer

Epithelial ovarian cancer (OC), an aggressive tumor with origins in the fallopian tube epithelium [1], is characterized by the propensity of metastasizing early and presenting with disseminated implants in the peritoneal cavity and infiltrating the omentum, a fat rich organ. Due to the widely metastatic presentation, OC is rarely curable and most patients die due to the disease. The most common histological subtype is high grade serous ovarian cancer (HGSOC), which is characterized by a tumor protein p53 (*TP53*) mutated signature and deficiency in homologous recombination [2]. Because of the deoxyribonucleic acid (DNA) repair mechanisms commonly deficient in HGSOC, these tumors are initially very chemo-responsive to platinum-based therapy [3, 4]. Most patients reach meaningful near-complete responses and sustained remissions; however, the majority of women with OC eventually relapse, recurring tumors become chemo-resistant and ultimately fatal [4, 5].

Many mechanisms have been implicated in development of acquired platinum resistance, including export pathways, epigenetic modifications, and alterations in DNA damage response. More recently, it has been hypothesized that a key phenomenon implicated in disease recurrence in OC and other solid tumors is the persistence of cancer stem cells (CSCs), which are quiescent and therefore can escape the effects of cytotoxic therapy, survive under the stimulation of certain factors in the peritoneal environment, and eventually become reactivated and give rise to recurrent tumors, which are heterogeneous and highly resistant to treatment [6-8].

1.1.1 Mechanisms involved in ovarian cancer initiation

Ovarian cancer originates from the fallopian tube epithelium [9] with multiple layers of genetic, epigenetic and signaling events [10] that contribute to the initiation of the aggressive disease. From the perspective of tumor suppressors, mutation of *TP53*, the most frequent genetic alteration in ovarian cancer, is detectable in 60-80% of all cases. The mutation and overexpression profile of *TP53* is positively correlated with the stage of cancer [11, 12]. Conversely, genetic mutation of phosphatase and tensin homolog (*PTEN*) is seen in 3-5% of low-grade ovarian cancer cases [10]. Aplysia ras homology member I (*ARHI*) is downregulated in 60% of all cases due to loss of heterozygosity (LOH), hypermethylation at the promoter region or transcriptional regulation [13]. Pleomorphic adenoma gene 1 like zinc finger 1 (*PLAGL1*) is downregulated in 30% of all cases due to LOH and transcriptional regulation [14]. Paternally expressed 3 (*PEG3*) is downregulated in 75% of all cases due to LOH, hypermethylation at promoter region and transcriptional regulation [15]. Homologous recombination-based DNA repair defects are also seen in 10-15% of all cases, of which BRCA1 DNA repair associated (*BRCA1*) mutation accounts for 30-60% of the cases whereas BRCA2 DNA repair associated (*BRCA2*) mutation accounts for 15-30% of the cases [16, 17].

From the perspective of oncogenes, 11 out of 15 genes undergo genetic amplification or copy number variation in ovarian cancer [18]. Of those 11 genes, KRAS proto-oncogene, GTPase (*KRAS*), B-Raf proto-oncogene, serine/threonine kinase (*BRAF*) and phosphatidylinositol-4,5-bisphosphate 3-kinase catalytic subunit alpha (*PIK3CA*) are mostly observed in low histological grade ovarian cancer while *TP53*, *BRCA1* and *BRCA2* are mostly observed in high histological grade ovarian cancer [19].

Multiple known signaling pathways are involved in ovarian tumorigenesis. Epidermal growth factor receptor (*EGFR*) is rarely activated in ovarian cancer [20]. Erb-b2 receptor tyrosine kinase 2 (*ERBB2*, *HER2*) is amplified in 11% of all cases [21]. Phosphatidylinositol-4,5-bisphosphate 3-kinase (*PI3K*) signaling appears active in 70% of all cases, through autocrine and paracrine signaling caused by protein tyrosine kinase growth factor receptors [10]. Interleukin 6 (IL-6) is produced by cancer cells and utilized in an autocrine manner to activate Janus kinase 2 (JAK2) which further phosphorylates signal transducer and activator of transcription 3 (STAT3) to promote proliferation, anti-apoptosis and angiogenesis in 70% of the cases [22]. Lysophosphatidic acid receptor 2/3 (LPAR2/3) are upregulated in tumorigenic transformation and bind to lysophosphatidic acid (LPA) produced by cancer cells to generate unsaturated fatty acids [23]. nuclear factor kappa-light-chain-enhancer of activated B cells (NF-κB) signaling is altered in more than 50% of all cases, mediating anti-apoptosis, anti-oxidation and production of cytokines like IL-6 and angiogenic factors like interleukin 8 (IL-8) [24].

On top of the molecular events summarized above, ovarian CSCs (OCSCs), hub for the malignant transformation activities, have been invoked as key regulators of tumor initiation [25]. CSCs, present in the tumor niche, have the capability of self-renewal, of differentiation into differentiated daughter cells and of plasticity back to CSCs [26], which are critical for tumors to invade local host tissues and survive unfamiliar microenvironment during the process of metastasis. As a proof-of-principle, as few as 10 OCSCs, characterized by high aldehyde dehydrogenase (ALDH) activity and surface expression of CD133 antigen (CD133), were able to initiate tumor in a mouse subcutaneous xenograft model [27].

1.1.2 Mechanisms involved in ovarian cancer metastasis

Metastasis of ovarian cancer cells first of all engages epithelial-to-mesenchymal transition (EMT) [28]. The initial upregulation of zinc finger E-box binding homeobox 2 (*ZEB2)*, snail family transcriptional repressor 1 (*SNAI1*), snail family transcriptional repressor 2 (*SLUG*) repress the expression of E-cadherin [29], membrane marker for epithelial cells. Conversely, N-cadherin and P-cadherin are upregulated in cancer cells [30, 31] to prepare for mesenchymal status when being transported to distant sites in peritoneal fluid or ascites. Clustering of collagen-binding $\alpha_2\beta_1$- and $\alpha_3\beta_1$-integrain induces matrix metallopeptidase 9 (MMP9) to cleave ectodomain of E-cadherin [32] so that cancer cells can detach from the basement membrane. Ovarian cancer cells are then carried by peritoneal fluid in a passive manner inside the peritoneum and towards omentum, the preferential metastatic site [28]. Meanwhile, cancer cells secrete vascular endothelial growth factor (VEGF) to promote the formation of ascites [33] that aids in the process of dissemination of cancer cells throughout the peritoneum. Once at the secondary site, the behavior of ovarian cancer cells follow the traditional "seed and soil" theory [34, 35]. Essentially, ovarian cancer cells, the seed, colonize the mesothelium, the soil, that covers all the organs including omentum and diaphragm in the peritoneal cavity [28]. Disseminated ovarian cancer cells undergo mesenchymal-to-epithelial transition (MET) to reverse to epithelial cell status and establish adhesion to the new sites.

1.1.3 Current treatment for ovarian cancer

Current treatment for ovarian cancer involves two strategies: surgery and chemotherapy [36]. The purpose of surgery is to stage the disease [37] and debulk the tumor [38]. Multiple

procedures are involved in staging including hysterectomy (removal of uterus), bilateral salpingo-oophorectomy (removal of both ovaries and fallopian tubes), omentectomy (removal of omentum), tissue biopsy (sampling of lymph nodes in pelvis and abdomen), and liquid biopsy (sampling of ascites in the peritoneal cavity). Debulking is a process that removes almost all tumors with the size larger than 1cm so that no visible tumors are present in the primary and metastatic sites at the end of the procedure.

Adjuvant therapy for ovarian cancer includes chemotherapy and targeted therapy. Chemotherapy is intended to kill residual tumor cells after debulking, tumor cells at the metastatic sites, and shrink large tumors for easy removal by surgery. Chemotherapy can be administrated intravenous or intraperitoneal. Intraperitoneal administration is done through a catheter into the abdominal cavity to reach a higher drug concentration at the site of disease [39, 40]. Intraperitoneal chemotherapy is usually given to post-debulking stage III ovarian cancer patients. Chemotherapy usually comprises 2 drugs, i.e. platinum and taxanes [41, 42]. Platinum drugs include mainly cisplatin and carboplatin, the latter of which is more prevalent in the current medical practice. Taxane-based drug include mainly paclitaxel and docetaxel. Chemotherapy is usually performed every 3-4 weeks a cycle for 3-6 cycles depending on the stage and type of the ovarian cancer.

Targeted therapy [43] acts on tumor cells without affecting normal cells as compared to chemotherapy. Two major targeted therapies are available for ovarian cancer. The angiogenesis inhibitor bevacizumab which targets VEGF in ovarian cancer cells is administered intravenously. Bevacizumab has been shown to shrink tumor in advanced stage disease and synergize with chemotherapy [44, 45]. The second type of targeted therapy is poly-(ADP-ribose) polymerase

(PARP) inhibitor, mainly olaparib, rucaparib, and niraparib. This family of inhibitors targets the DNA damage repair process in cancer cells. They work better in tumor cells with BRCA1/2 mutation [46, 47]. For patients with BRCA1/2 mutation, PARP inhibitor can be given after chemotherapy or with bevacizumab for maintenance therapy [48]. For patients without BRCA1/2 mutation, PARP inhibitor are given to those tumors bearing high genomic instability score or those patients after initial favorable response to chemotherapy [49].

1.1.4 Metabolism in ovarian cancer

Metabolic alterations have been associated with rapid growth of tumors, early tendency to metastasize, development of resistance to therapy, and survival of CSCs. While abnormal glycolysis and glucose metabolism are well understood in these contexts, new data is emerging associated with the role of lipid metabolism in cancer [50, 51]. Due to the almost symbiotic relationship between OC and fat in the omentum, lipid metabolism adaptations operative in HGSOC are of high interest both to advance the understanding of the mechanisms that fuels peritoneal dissemination, and to achieve the goal of identifying potential new targets for therapeutic interventions.

The concept of metabolic reprogramming and hence metabolic heterogeneity in cancer cells was therefore raised beyond the Warburg effect [52-54] which describes cancer cells' utilization of glucose via less-efficient lactic acid fermentation in spite of presence of ample oxygen resources. Metabolic reprogramming enables cancer cells to shift gears among different metabolic status for fast proliferation at primary site, better survival at distant metastatic sites, and more efficient energy storage and utilization [55]. This applies particularly to critical steps during cancer

development such as metastasis [56, 57] and therapeutic resistance, one key challenge in ovarian cancer treatment. Emerging evidence has associated cancer drug resistance with metabolic reprogramming [58-60]. For example, increased uptake and utilization of lactate present in the uterine cervix enhanced DNA damage repair and development of chemotherapy resistance in cervical cancer [61]. Our group recently unveiled that metabolic reprogramming from glycolysis to fatty acid β-oxidation mediates the acquisition of resistance to chemotherapy [62] in ovarian cancer. This finding corroborates with our previous understanding of the role of adipocyte in cancer drug resistance and underscores the importance of tumor microenvironment in development of resistance [63].

Chemotherapy resistance has been strongly associated with OCSCs in two ways. Platinum treatment can induce cancer cell stemness in ovarian cancer [64, 65] and CSCs contribute to chemotherapy resistance in ovarian cancer [66]. Consequently, identification of metabolic reprogramming in cancer stem cells could also assist in targeting metabolic vulnerability in this unique population [66-68].

1.2 Lipid metabolism

1.2.1 Cellular lipid metabolism

Lipids are hydrophobic biomolecules which include fatty acyls, glycerolipids, glycerophspholipids, sphingolipids, saccharolipids, polyketides, sterol lipids, and prenol lipids [69]. Three major routes participate in how lipids are routed and used inside the cell: uptake, lipogenesis, and utilization (Figure 1-1). The metabolism of lipids is closely aligned with that of glucose and tightly regulated by enzymes which are rate limiting at various steps.

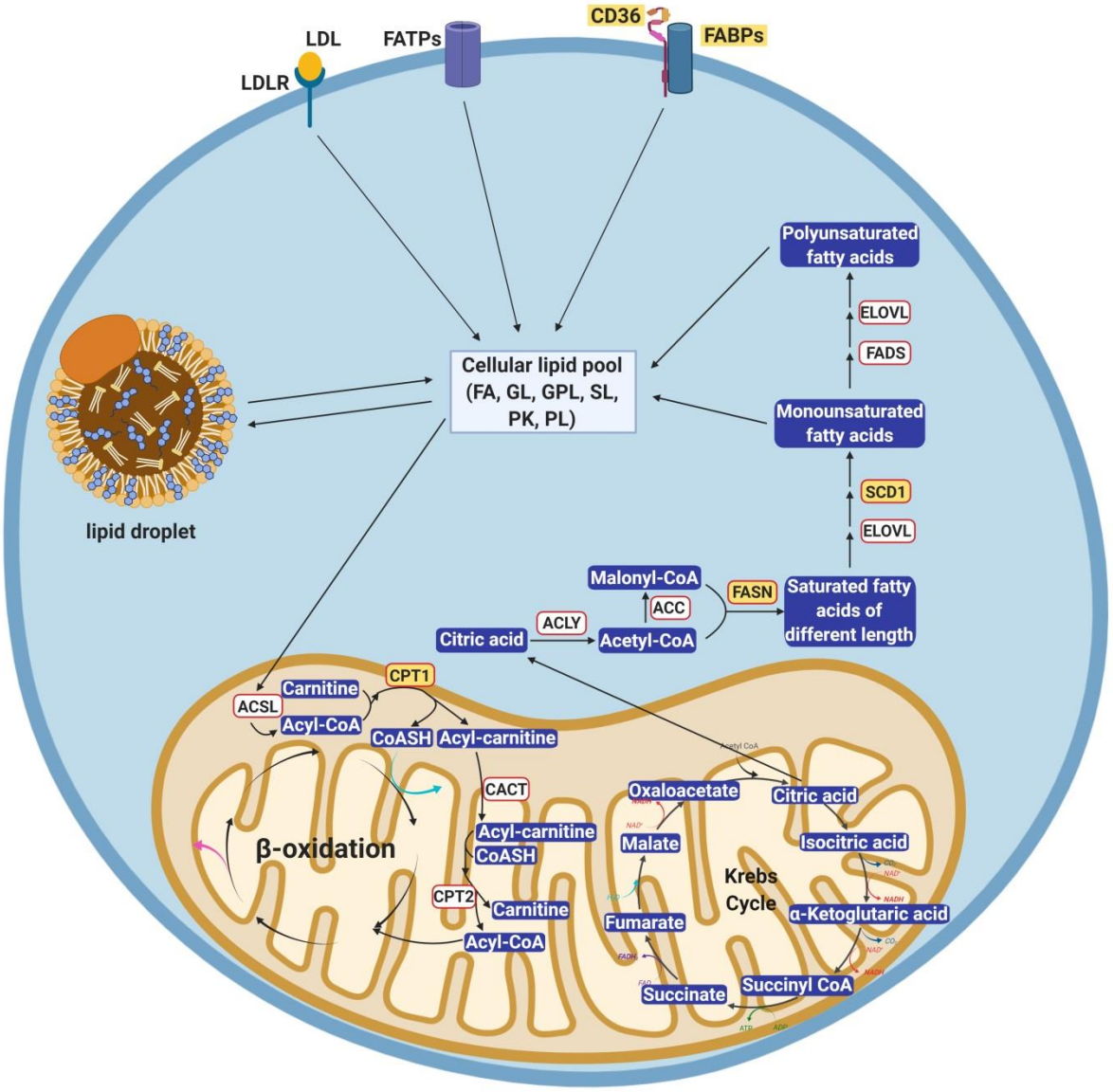

Figure 1-1 Cellular fatty acid uptake, synthesis and oxidation.

Overview of the metabolic pathways involved in fatty acid uptake, *de novo* lipogenesis, and β-oxidation. ACC, acetyl-CoA carboxylase; ACLY, ATP-citrate lyase; ACSL, ATP-dependent acyl-CoA synthetase; CACT, carnitine-acylcarnitine translocase; CD36, fatty acid translocase; CPT1, carnitine palmitoyl transferase 1; CPT2, carnitine palmitoyl transferase 2; ELOVL, fatty acid elongase; FADS, fatty acid desaturase; FASN, fatty acid synthase; FABPs, fatty acid binding proteins; FATPs, fatty acid transport proteins; LDL, low-density lipoprotein; LDLR, low-density lipoprotein receptor; SCD, stearoyl CoA desaturase. Image created using BioRender (https://biorender. com/).

Lipids are imported into cells through a variety of fatty acids transporters present on the plasma membrane [70, 71]. These transporters include low-density lipoprotein receptors, fatty acid transport proteins (FATPs), fatty acid translocase, and fatty acid binding proteins (FABPs). Low-density lipoprotein receptors bind to low-density lipoproteins in blood, transport them inside the cells, where the cholesterol is released after the low-density lipoproteins are broken down [72]. The fatty acid transport protein family includes six members (FATP1-6) with distinct distribution across tissue types [70]. FATPs contain a functional adenosine monophosphate (AMP)-binding motif [73, 74] which actively participates in the fatty acid transport. Fatty acid translocase (CD36) is the predominant fatty acid transporter in many normal cell types, including adipocytes, cardiac myocytes, enterocytes, and skeletal myocytes (reviewed in [75]) and also in cancer cells. Most of the time, CD36 works in concert with FABPs to facilitate the import of fatty acids into the cell. FABPs are fatty acid chaperones also with distinct pattern of expression [71]. So far, nine family members of FABPs have been identified, including adipocyte, brain, epidermal, heart, intestinal, ileal, liver, myelin, and testis FABPs. The plasma membrane-bound fragment of FABPs interacts

with that of CD36 to facilitate the import of free fatty acids sequestered from the extracellular space. Once inside the cell, fatty acids remain bound to cytosolic part of FABPs until their delivery to the destination site for storage in lipid droplets, oxidation in mitochondria, lipid synthesis in the membrane, or transcriptional regulation in the nucleus.

Lipogenesis is the pathway by which lipids are generated in the cell from other metabolites. Cytosolic citrate resulting from glutamine metabolism and citric acid cycle downstream of glucose metabolism is cleaved by adenosine triphosphate (ATP)-citrate lyase into acetyl-CoA [76]. Acetyl-CoA carboxylase (ACC) then turns this metabolite into malonyl-CoA which, together with acetyl-CoA, is condensed into saturated fatty acids of various lengths by the fatty acid synthase (FASN) [77]. These newly synthesized fatty acids undergo further elongation via fatty acid elongases [78]. Until this point, all fatty acids are saturated, bearing carbon-carbon single bonds. Stearoyl CoA desaturases (SCDs), SCD [79-81] and stearoyl CoA desaturase 5 (SCD5) [82] then convert palmitic acid and stearic acid, two of the major free fatty acids generated by FASN and fatty acid elongases into palmitoleic acid and oleic acid, respectively, creating carbon-carbon double bonds at Δ9 position [82, 83]. Palmitoleic acid and oleic acid are further reduced into polyunsaturated fatty acids by other fatty acid desaturases. The majority of those fatty acid species are not present in the cytoplasm in the form of free fatty acids; they are rather esterified with glycerol into triglycerides and stored in lipid droplets [84]. *De novo* synthesized fatty acids participate in different aspects of cellular physiology, such as construction of cell membranes, biogenesis of energy-storing lipids, and formation of signaling molecules through post-translational fatty acylation of proteins [85-87].

Fatty acids represent an important source of fuel in the cell, which is released through a process called oxidation, which is tightly regulated. Free fatty acids in the mitochondrial inter-membrane space are converted into acyl-CoA by ATP-dependent acyl-CoA synthetase. Carnitine palmitoyl transferase 1 tags fatty acyl-CoA with carnitine to form fatty acyl-carnitine which is then transported into mitochondrial inner membrane via carnitine-acylcarnitine translocase. Once inside the mitochondrial matrix, fatty acyl-CoA is reformed by carnitine palmitoyl transferase 2 with free CoA. The subsequent fatty acid β-oxidation strips one acetyl-CoA group off fatty acyl-CoA at a time, generating flavin adenine dinucleotide, reduced ($FADH_2$) and nicotinamide adenine dinucleotide, reduced (NADH) as small and mobile energy storage units that can participate in different biochemical processes including the generation of ATP via electron transport chain [88]. Thus, the cell utilizes the stored energy necessary for its metabolic needs. In cancer, these processes could be augmented to keep up with the increased energetic requirements of growing tumors or tumors stressed by various cancer treatments [89].

1.2.2 Lipid metabolism in cancer

1.2.2.1 Lipid uptake in cancer

Cancer cells utilize various strategies to boost lipid uptake in order to fulfil their high energetic needs for cell growth and altered oncogenic signaling. Alterations in lipid uptake were described in different cancer types, including HGSOC. For example, breast cancer cells were shown to import exogenous oleic acid through upregulated CD36 and this mechanism alleviated the apoptotic effects induced by stearoyl CoA desaturase (SCD) inhibition [90]. The very low-density lipoprotein receptor was found to be overexpressed in clear-cell renal cell carcinoma in a

hypoxia inducible factor 1 subunit alpha (HIF1α)-dependent manner [91], leading to lipid accumulation in tumor cells. Similar observations were reported by Bensaad et al. in a VEGF inhibitor-resistant xenograft mouse model of glioblastoma [92]. Chronic VEGF inhibitor therapy was shown to strongly induce the expression of fatty acid binding protein 3 (FABP3) and fatty acid binding protein 7 (FABP7), resulting in increased lipid uptake and storage of fatty acids in lipid droplets. Another report described upregulation of fatty acid binding protein 5 (FABP5) in malignant prostate cancer versus normal tissue [93] whereas upregulation of FABP5 was found to be associated with poor prognosis in lung cancer [94]. Stable knockdown of FABP5 in prostate cancer cells significantly reduced the tumor burden in a xenograft mouse model, highlighting the significance of lipid uptake to tumor growth *in vivo*. Pascual et al. found that in an oral carcinoma model, among slow cycling tumor initiating cells identified by CD44 antigen (Indian blood group) (CD44) expression, there was a small subpopulation with increased metastatic potential, which was characterized by abnormal lipid metabolic features. In particular, these cells were found to have high expression of CD36 and were sufficient and necessary for metastasis in oral carcinoma [95]. In particular, these cells were found to have high expression of CD36 and were sufficient and necessary for metastasis in oral carcinoma [95]. $CD36^+$ oral carcinoma cells could initiate tumor metastasis more effectively than $CD36^-$ cells, while retaining the same ability to generate tumors at the primary site. Interestingly, tumor metastasis was augmented by a fat rich diet, in a CD36-dependent manner and strategies targeting CD36 with neutralizing antibodies were able to decrease the metastatic potential [95], thus pointing to a potential vulnerability of these highly tumorigenic cells. Similar observation was made by Montero-Calle et al. in colorectal cancer [96]. Kamphorst et al. discovered that hypoxic and Ras-transformed cancer cells scavenge fatty acids from serum lysophospholipids in support of rapid

growth [97]. In addition, Zhou et al. summarized the most recent findings of altered lipogenesis in hepatocellular carcinoma [98]. Collectively, these findings support that cancer cells rely on import of fatty acid during proliferation.

The role of lipid uptake has been also studied in OC. Recognizing that the preferred site of metastasis in OC is the omentum, a fat rich organ, Lengyel's group characterized the symbiotic relationship between adipocytes and OC cells [56]. Direct transfer of lipids between adipocytes and OC cells was shown to be mediated by fatty acid binding protein 4 (FABP4), which was highly upregulated in metastatic versus primary tumor sites. Depletion of FABP4 was sufficient for diminishing the metastatic potential of HGSOC cells. More recently, FABP4 was described by another group as being critical to mediating the metastatic potential of OC both in *in vitro* cell migration and invasion assays and in *in vivo* orthotopic mouse models [99]. Bioinformatics analyses of The Cancer Genome Atlas (TCGA) dataset using chemotherapy-naïve cases of HGSOC demonstrated that the expression level of miR-409-3p, microRNA, was negatively correlated with that of FABP4. Mir-409-3p was further predicted to bind to the 3' untranslated region (3' UTR) of FABP4 and experimentally validated to be a key regulator of FABP4. Metabolomics experiments found higher unsaturation and oxidation of fatty acid species in high FABP4-expression patient tumor specimens, and these metabolic abnormalities were correlated with poor overall and progression-free survival. Lastly, the authors used a known inhibitor of FABP4, tamoxifen, and demonstrated that physiological concentrations could impair the uptake of free fatty acids and inhibit migration and invasion capability of OC cells, perhaps correlating with clinical reports indicating that this anti-estrogen has modest anti-tumor activity in OC [99].

A more recent report focusing on lipid uptake demonstrated the significance of CD36 transporter mediated fatty acid transport into OC cells [57]. The authors found that human primary adipocytes induced CD36 messenger RNA (*mRNA*) level and plasma membrane expression in OC cells in co-culture. Consequently, fatty acid uptake and lipid droplet accumulation was enhanced in OC cells. Interestingly, genes involved in endogenous lipid metabolism and cholesterol biosynthesis were downregulated in tumor cells. These observations indicate that OC cells, in the presence of primary adipocytes, rely more on the uptake of exogenous lipids and cholesterol than on *de novo* lipogenesis. More importantly, knockdown of CD36 suppressed baseline and adipocyte-induced cellular invasion and migration, as well as adhesion to major extracellular matrix components of the peritoneum, i.e. type I collagen and laminin. *In vivo* experiments demonstrated that CD36 knockdown or treatment with a neutralizing antibody significantly reduced tumor burden and metastatic nodules in intraperitoneal OC xenograft models. Together, these data strongly support the significance of increased lipid uptake to tumor metastasis in this cancer type.

1.2.2.2 Lipogenesis in cancer

While the excessive anaerobic metabolism of glucose, i.e. Warburg effect [100, 101], in cancer cells has been well described as means to provide energy for proliferation and survival [102], less is known in terms of lipid metabolism in cancer. Recent cumulative results have pointed to the concept that cancer cells rely on lipogenesis to adapt to cytotoxic stress in the tumor microenvironment. This is particularly important in tumor areas where the exogenous supply of fatty acids is scarce, such as in hypovascular and hypoxic regions [103-109]. Such regions are abundant in large, rapidly growing tumors. Acetyl-CoA carboxylase and FASN-mediated *de*

novo lipogenesis was reported in breast [110, 111], pancreatic cancer [112], clear cell renal cell carcinoma [113] and gastric cancer [114]. It was reported that breast cancer cells upregulate FASN to induce non-homologous end joining DNA repair and to combat genotoxic stress (chemotherapy and radiotherapy) [111]. More comprehensive lipidomics studies found that products of *de novo* lipogenesis were upregulated and incorporated into phospholipids [115] or phosphatidylcholine lipids [116, 117] in tumor tissues, implying multiple enzymes in the pathways contributed to the observation. Integration of lipidomics and transcriptomics analyses demonstrated that tumors from clear cell renal cell carcinoma patients displayed significant enrichment of fatty acid metabolism pathways with particular upregulation of essential fatty acids and glycerolipids while downregulation of glycerophospholipids [118]. New untargeted lipidomics tool like Small Molecule Isotope Resolved Formula Enumerator and ultra-high-resolution Fourier transform mass spectrometry revealed that sterol and sphingolipids are upregulated whereas glycerophospholipids are downregulated in primary non-small cell lung carcinoma [119]. Spatially-resolved metabolic network modeling of tumor microenvironment, on the other hand, identified spatial separation of fatty acid biosynthesis and unsaturation in whole tumor samples of prostate cancer patients, granting additional rationale for SCD inhibition-based therapy [120]. *In vivo* magnetic resonance spectroscopy was able to distinguish the ratios of bis-allyl to vinyl hydrogen proton in the fatty acyl groups of unsaturated fatty acids in liver tissue of transforming growth factor alpha (Tgfα)/c-myc mice and control mice [121]. Upregulation of unsaturated fatty acids were confirmed by high performance liquid chromatography and mass spectrometry and upregulation of Scd1 and Scd2 were confirmed by Western blot and microarray. These findings enabled *in vivo* magnetic resonance spectroscopy as a potential early detection technique [121]. In addition to fatty acids, lipid metabolism-derived cholesterol serves

as a signaling molecule for prostate cancer progression [122]. In liver cancer, alterations in lipid metabolism often take place at the level of a whole class of lipids such as sphingolipids, phospholipids and steroid hormones [123].

Additionally, fatty acid desaturation, a critical step in the process of lipogenesis [124-126], is essential for the maintenance of membrane fluidity, inter- and intra-cellular signaling, and provision of lipid pool for energy generation through oxidation [79, 80, 127-129]. Notably, SCD *vide supra* is the rate-limiting enzyme converting saturated fatty acids to unsaturated fatty acids. SCD was found to be upregulated in various neoplasms [118, 121, 130-144] and its inhibition prevented cancer cell proliferation when exogenous fatty acids were depleted [105, 145-147]. Depletion of SCD *in vivo* led to reduction in hepatic lipogenesis, increased insulin sensitivity and protection from carbohydrate-induced obesity [148, 149]. Expression of SCD was negatively correlated with that of miR-215 which directly targets upstream of SCD mRNA in colorectal cancer [150]. Adipocyte also plays an important role in unsaturated fatty acid pool not only due to its secretion of monounsaturated fatty acids. Adipocyte-induced exosomes under hypoxic condition were reported to carry less miR-433-3p which targets SCD expression to adjacent nasopharyngeal carcinoma cells, resulting in enhanced tumorigenesis [109].

Beyond SCD-mediated desaturation, the Δ6 and Δ5 desaturases in concert with elongases are involved in the synthesis of polyunsaturated fatty acids from exogenously acquired alpha-linolenic and linoleic acid [151] and branched chain fatty acids and normal odd chain fatty acids [152], which are present in the inflammatory environment associated with tumor initiation [153]. To exemplify the role of polyunsaturated fatty acids, Amézaga et al. examined the phospholipid profiles of red blood cell membrane from recently diagnosed breast cancer patients and identified

ω-6 fatty acids upregulated in patients than control [154]. Different upstream acyl-CoA synthetase long-chain family member (ACSL) isoforms, i.e. ACSL1 or ACSL4 or 3' UTR polymorphism in ACSL1, work with SCD to reprogram colon cancer cells demonstrating more glycolytic or lower basal respiratory phenotypes and dictated differential clinical outcomes [155-157]. Recently, our group developed a new imaging approach based on Stimulated Raman Scattering that allowed us to probe the different lipid species in rare cell populations, such as stem cells [158, 159]. By using this technology, the lab demonstrated that unsaturated fatty acids (both monounsaturated fatty acids and polyunsaturated fatty acids) were enriched in OC stem cells [67]. We found that unsaturated fatty acids were essential for the proliferation and survival of OC stem cells and that pharmacological inhibition of SCD activity or short hairpin RNA (shRNA)-mediated knockdown of SCD eliminated OC stem cells and retarded tumor initiation. The role of SCD in ovarian cancer stem cells was also corroborated in colon cancer [160]. Due to the association between SCD and different cellular adaptive signaling [161], the concept of increased lipid unsaturation and the role of fatty acid desaturases in cancer progression are also supported by work from other groups in different cancer models.

Overexpression of acetyl-CoA synthetase and SCD led to increased cellular monounsaturated fatty acids and conferred bioenergetic advantages to EMT and confirmed clinical prognosis in colon cancer, triple negative breast cancer, and aggressive prostate cancer [162]. Interestingly, phosphorylation of tyrosine 55 by EGFR is essential for the stability of SCD [163] whereas proteolytic product of SCD spanning amino acids 130-162 could induce transcriptional activity of androgen receptor (AR) in prostate cancer, promoting proliferation of AR-positive prostate cancer [164]. SCD inhibitors blocked prostate, breast and lung cancer cell proliferation in low

serum conditions (limited exogenous supply of fatty acids) [165-168] and these effects were rescued by addition of exogenous oleic acid. Inhibition of SCD altered the lipid microenvironment around epidermal growth factor receptor and hence undermined downstream signaling via AKT serine/threonine kinase 1 (AKT), extracellular signal-regulated kinase (ERK) and mammalian target of rapamycin (mTOR) in multiple cancer types [169-171]. Similarly, depletion of oleic acid (but not of palmitic acid) inhibited the proliferation of acute myelogenous leukemia and lymphoma cells [172]. Our current understanding of fatty acid desaturation supports that SCD is the sole enzyme responsible for converting saturated fatty acid to monounsaturated fatty acid. However, Vriens et al. discovered that an alternative fatty acid desaturation pathway exists in multiple cancer types, including lung cancer, breast cancer, prostate cancer, and liver cancer [173]. In those cancer cells, palmitic acid can be converted to sapienic acid by fatty acid desaturase 2 (FADS2). Additionally, inhibition of SCD activity accounted for less than 50% of the cancer cell proliferation. Their findings unveiled an unknown property of cancer cells in producing lipids, indicating cancer cell plasticity. Park et al. also found that excessive palmitic acid competes with alpha-linolenic and linoleic acid for FADS2 [174]. Future endeavors could be directed to the population of cancer cells that utilize this alternative lipid metabolism pathway to survive SCD inhibitor therapy. A follow-up research by Triki et al. found that activation of mammalian target of rapamycin complex 1 (mTORC1) signaling was sufficient to induce SREBF1 activity and hence upregulation of FADS2 expression and intracellular sapienic acid level [175].

1.2.2.3 Fatty acid oxidation (FAO) in cancer

Cancer cells utilize FAO mainly for production of ATP as energy storage and nicotinamide adenine dinucleotide phosphate, reduced (NADPH) as energy storage and antioxidant reservoir [176, 177]. Mutations in key FAO enzymes have not been identified yet [178]; nevertheless, overexpression of CD36 [95], carnitine palmitoyl transferase 1 (CPT1)A [179, 180], CPT1B [180, 181], CPT1C [182], carnitine palmitoyl transferase 2 (CPT2) [180], carnitine transporter 2 (SLC22A16, solute carrier family 22 member 16) [183] and ACSL3 [184] were extensively studied in different cancer types. In addition, high FAO activity was observed in KRAS-mutant lung cancer [184], breast cancer [185, 186], acute myeloid leukemia (AML) [183], Hepatitis B-induced liver cancer [187], glioma [188], and low grade astrocytoma [188]. Key FAO enzymes and intermediate metabolites were found to be upregulated by oncoproteins such as c-Myc [189] and JAK/STAT3 [181]. Reciprocally, CPT mediates SRC Proto-Oncogene, Non-Receptor Tyrosine Kinase (SRC) protein activation and SRC-dependence cancer metastasis [190].

The role of FAO in cancer cell growth and survival is mainly through CPT1 functionality. Phenotypically, inhibition of CPT1 suppresses growth in AML [177, 191], ovarian cancer [192], liver cancer [193], prostate cancer [194, 195], glioma [176], myeloma [196] and breast cancer [197]. In ovarian cancer, the metabolic sensor AMP-activated protein kinase (AMPK) senses the availability of ATP the decrease of which, due to CPT1 inhibition, leads to cell cycle arrest at G1/G0 phase [192]. In colon cancer [198], breast cancer [199] and ovarian cancer [56] which metastasize preferentially to the omentum, uptake of free fatty acids facilities FAO in these cancer cells for survival and proliferation [200]. In prostate cancer [201, 202] and glioma [188, 203] where glycolysis is limited for energy production, FAO is the main source of contribution

towards respiration activity. Mechanistically, CPT1 inhibition breaks the homeostasis of redox status, leading to accumulation of oxidative stress and hence apoptosis in myeloid leukemia [191], glioma [188] and liver cancer [187]. It was also reported that FAO regulates expression of proteins in the Bcl-2 family [204, 205]. Furthermore, inhibition of FAO leads to accumulation of long chain fatty acids which exert stress to the ER membrane [206].

FAO is also involved in cancer metastasis [95, 198, 207, 208]. Peroxisome proliferator-activated receptors (PPARs), molecular sensors for fatty acids, bind to fatty acids and serve as transcriptional regulator of FAO enzymes [198, 209] through promyelocytic leukemia (PML) gene [210]. During EMT, when cancer cells detach from the basement membrane, cellular production of glucose uptake, ATP and NADPH drop whereas reactive oxygen species (ROS) increases. FAO provides the energy to counteract the change during EMT to avoid anoikis [208, 210, 211].

Cancer stem cells rely on FAO for maintaining stemness. Inhibition of CPT1 led to reduction of quiescent leukemia progenitor cell population in around 50% human primary AML samples [191]. Leukemia stem cells could be further divided into two distinct populations based on CD36 expression. The CD36-high group of cells had higher FAO activity and thus greater resistance to drug treatment as compared to the CD36-low group [212]. JAK/STAT3 signaling pathway could upregulate CPT1B and hence FAO in breast cancer stem cells to boost stem cell self-renewal [181].

Development of drug resistance, both chemotherapy and targeted therapy, has also been associated with FAO in cancer cells. Pediatric ALL cells upregulated RagB-mTORC1 pathway

to activate FAO upon L-asparaginase administration [213]. Cytarabine treatment induced upregulation of CD36 and hence FAO in AML [214]. Dexamethasone treatment in chronic lymphocytic leukemia (CLL) cells led to upregulation of PPARα which activated FAO [215]. In cases where tumor cells experience hypoxia or nutrient stress, cancer cells turned on CPT1C to boost FAO [182, 216]. CPT1C was also reported to be upregulated in the development of resistance to imatinib/rapamycin in leukemia [217, 218]. Tamoxifen could induce the upregulation of FAO in retinoblastoma deficient breast cancer cells [219]. In most cases, co-treatment of FAO inhibitors re-sensitized cancer cells to either chemotherapy or targeted therapy [213-215, 218, 220, 221].

Abnormalities in lipid metabolism have been linked to several cancer phenotypes, including metastatic potential, cancer stemness and resistance to chemotherapy or targeted therapy. Specific alterations and the cellular mechanisms engaged in these contexts are reviewed below.

1.2.2.4 Specific roles of lipid metabolism in cancer metastasis

Advanced stage OC is typically characterized by omental or peritoneal metastasis. The omentum is mainly comprised of adipocytes which serve as a chemical attractant for OC cells. Nieman et al. identified that IL-6, IL-8, monocyte chemoattractant protein-1, and tissue inhibitor of metalloproteinases-1 are released by omentum to promote the metastasis of OC cells towards omentum [56]. Specifically, they found that IL-8 from the omentum binds to C-X-C motif chemokine receptor 1 (CXCR1) on OC cells to induce p38-mitogen-activated protein kinase and STAT3 phosphorylation, hence initiation of metastasis. The molecular mechanism that distinguished metastatic tumor from primary tumor relied predominantly on FABP4. FABP4 was

highly expressed on the membrane of disseminated OC cells at the adipocyte-cancer cell interface and mediates lipid accumulation in OC cells. Inhibition of FABP4 led to reduced intracellular lipid accumulation and adipocyte-mediated invasion capability of OC cells. It is conceivable that the accumulated lipid droplets could be used through oxidation to generate ample adenosine triphosphate (ATP) for energy consumption during colonization and formation of micrometastases. In addition to *in vitro* experiments, knock out of FABP4 in OC cells caused decreased tumor burden and number of metastatic nodules in intraperitoneal OC mouse models, convincingly establishing the link between lipid metabolism and the metastatic phenotype.

Besides metastatic OC, altered lipid metabolism was also seen regulating tumor metastasis to lymph nodes in melanoma by Lee et al. [222] and to central nervous system in acute lymphoblastic leukemia (ALL) by Savino et al. [223]. Lee et al. utilized subcutaneous xenograft mouse model and compared the cells isolated at primary site, micrometastatic, and macrometastatic tumor-draining lymph nodes. RNA-seq analysis revealed that top up-regulated gene sets in the micro- and macrometastatic tumors were positively correlated with bile acid metabolism, adipogenesis, fatty acid metabolism, cholesterol homeostasis, and oxidative phosphorylation. Pathway analysis demonstrated that lymph node metastatic tumors induced fatty acid oxidation and peroxisome proliferator-activated receptor-α signaling. Further metabolomic experiments showed that lymph node metastatic tumors accumulated more fatty acid species compared to tumors at the primary site. Treatment with etomoxir, an inhibitor of fatty acid oxidation, did not affect the size of primary tumor whereas it significantly suppressed lymph node metastasis. Notably, etomoxir also suppressed lymph node metastasis after removal of the primary tumor.

To identify the underlying mechanism for fatty acid oxidation-dependent metastatic tumor, Lee et al. knocked down each of the oncogenic genes in the metastasis-prone cells and found that knockdown of Yes1 associated transcriptional regulator (YAP1) significantly reduced fatty acid oxidation in the metastasis-prone cells. Conversely, overexpression of YAP1 enhanced fatty acid oxidation in the same cells both in *in vitro* and *in vivo* assays. Immunofluorescent imaging analysis revealed that YAP1 was uniquely localized in the nucleus of cells at the invasive front but cytoplasm of cells at the primary site [222]. Additionally, Kang et al. used breast cancer cell spheroids to study metabolic alterations associated with EMT [224]. They found that ceramides, sphingomyelin, ether-linked phosphatidylcholine and phosphatidylethanolamine were significantly altered during mesenchymal state. In addition, polyunsaturated fatty acids were downregulated in concert with the downregulation of genes like protein tyrosine phosphatase-like (proline instead of catalytic arginine), member B (PTPLB), peroxisomal trans-2-enoyl-CoA reductase (PECR), and fatty acid elongase 2 (ELOVL2). Further investigation of human breast cancer cell lines confirmed their initial findings and drew the conclusion that expression of ELOVL2 is negatively correlated with breast cancer phenotype [224]. Similar observations were made by Angelucci et al. where SCD and its product oleic acid were found to be critical for breast cancer cell migration. Interestingly, SCD5, the other isoform of SCD, was not responsible for cancer cell migration in their study [225]. Controversially, overexpression of Scd5 in mouse breast cancer cells 4T1 dampened the metastatic potential and reversed EMT phenotype [226].

Savino et al., on the other hand, found that central nervous system (CNS)-derived ALL cells demonstrated significant enrichment of genes involved in *de novo* lipogenesis among which SCD was highly upregulated given that cerebrospinal fluid serves as a fatty acid-poor

microenvironment. The consistence of SCD upregulation in CNS metastasis vs primary sites in their and others' studies showed that unsaturated fatty acids are critical for adaptation and survival of ALL cells in the CNS microenvironment. Savino et al. further examined that SCD overexpressed ALL cells possessed enhanced CNS infiltration whereas suppression of SCD activity using pharmacological inhibitor SW203668 could alleviate tumor growth [223]. It would be more interesting to investigate the mechanism underlying the development of fatty acid metabolism-dominant molecular signature.

Early studies using Fourier transform infrared (FTIR) microspectroscopy revealed the translocation of palmitic acid from adipocytes to metastatic prostate cancer cells in coculturing system, depicting the role of fatty acid in tumor metastasis [227]. A more recent study from Benitah lab found that dietary palmitic acid possesses prometastatic features in oral carcinoma and melanoma [228]. Specifically, *in vitro* palmitic acid treatment could prime tumor cells for subsequent *in vivo* metastasis after withdrawal of palmitic acid in advance. In another orthotopic mouse xenograft model, mice were fed with palmitic acid-rich diet after tumor cell implantation and showed more metastatic tumor burden as compared to those fed with control diet. Vivas-García et al. unveiled a metabolic switch that controls phenotypic plasticity in melanoma [229]. Interestingly, the microphthalmia-associated transcription factor (MITF)/SCD axis that upregulated SCD suppressed the metastatic/invasive phenotype while induced the proliferative phenotype.

The role of lipid metabolism in tumor metastasis was previously reviewed by Mounier et al. [230]. Additional studies of the role of SCD in metastasis were performed in breast cancer cells

[231-233], colon cancer cells [234, 235], lung cancer cells [236-238] esophageal cancer cells [239], and liver cancer cells [240, 241].

1.2.2.5 Specific roles of lipid metabolism in cancer stem cells

A small population residing within heterogeneous tumors is referred to as cancer stem cells and was reported to mediate OC initiation *in vivo* [27, 242, 243]. These cancer stem cells which represent about 1% of the tumor mass have also implicated in tumor progression [242], resistance to chemotherapy or radiotherapy [242, 244, 245], and metastasis to distant tissues [246]. The underlying signaling pathways that maintain cancer cell stemness have been extensively studied, and include the Wnt-β-catenin pathway [247], NF-κB pathway [248], and Notch signaling [249]. Nevertheless, less is known about the metabolic regulation of cancer stem cells due to difficulties studying these rare cells by using traditional mass spectrometry-based methods, which typically require large numbers of cells for analysis. Some early studies approached this question from a different angle by examining the molecular signatures of monolayer vs spheroid cells formed by OC cells [250-252].

A recent report from our group utilized stimulated Raman Scattering Microscopy to study OC stem cells and found that these cells harbor higher level of unsaturated fatty acids and increased levels of SCD *mRNA* as compared to non-stem cancer cells [67]. Cancer stem cells possess the metabolic signature of lipid metabolism [253]. Suppression of fatty acid desaturation by small molecule inhibitors against SCD downregulated stemness markers in cancer stem cells isolated from both cancer cell lines and primary patient samples. SCD inhibitor-treated cancer stem cells, when injected subcutaneously into athymic mice, displayed impaired *in vivo* tumor initiation

capacity, delayed time-to-tumor formation, and reduced tumor burden. Additionally, our group found that OC stem cells relied on *de novo* biosynthesis of unsaturated fatty acids instead of uptake of exogenous fatty acids from the immediate environment [67].

In order to identify the molecular mechanisms linking unsaturated fatty acids and OC cell stemness, OC stem cells treated with vehicle and an SCD inhibitor were probed by using a pathway-specific quantitative reverse transcription polymerase chain reaction (qRT-PCR) array. Transcriptional activity of NF-κB was found to be compromised in OC stem cells upon suppression of SCD enzymatic activity. Furthermore, the NF-κB signaling pathway was shown to directly regulate the transcription of SCD, through a positive feedback loop.

These observations were corroborated in other cancer types, such as colon cancer [254-257], breast cancer [258-260], liver cancer [261, 262], bladder cancer [263], gallbladder cancer [264], chronic myeloid leukemia [265], glioblastoma [266, 267], gastric cancer [268], lung cancer [269, 270] and melanoma [271]. For example, the stemness associated-transcription factor NANOG Homeobox (NANOG) was shown to suppress mitochondrial oxidative phosphorylation and tilt the metabolic balance in tumor initiating cells towards fatty acid oxidation to support stem cell self-renewal [221]. Inhibition of lipogenesis mediated by acetyl-CoA carboxylase was shown to inhibit mammosphere generation and the $ALDH^+$ stem cell population in a breast cancer model [272]. ELOVL2, an enzyme involved in the biogenesis of poly-unsaturated fatty acids, was found to be epigenetically upregulated in glioma cancer stem cells. Its inhibition caused disruption of phospholipids in the plasma membrane leading to altered EGFR signaling and suppression of tumorigenicity and self-renewal in this cell population, further consolidating the concept that unsaturated fatty acids play a role in the maintenance of cancer stem cells [273].

Targeting SCD in breast cancer stem cells, miR-600 down-regulates post-translational modification of wingless-type MMTV integration site (WNT), hence reduced self-renewal and increased differentiation of breast cancer stem cells [274]. Blockage of production of monounsaturated fatty acid in mouse liver tumor-initiating stem cell-like cells (TICs) prevented the stabilization of low-density lipoprotein-receptor-related proteins 5 (LRP5) and 6 (LRP6) mRNA and therefore Wnt/β-catenin signaling pathways critical for self-renewal of the TICs [275].

Furthermore, while lipid unsaturation is critical to cancer stem cells, it has also been linked to normal stem cell physiology. FASN was found to be upregulated in neural progenitors and suppression of its activity affected normal neurogenesis [276]. SCD5 was highly expressed in brain and increased abundance of phosphatidylcholine and cholesterol esters and decreased those of phosphatidylethanolamine and triacylglycerol [277]. SCD5 induced cellular proliferation and meanwhile suppressed neuronal differentiation [277]. Embryonic stem cells, characterized by the presence of highly unsaturated lipidome, became differentiated in response to *in vivo* oxidative processes such as inflammation [278]. These findings were also corroborated by the observations of lipid droplets in mouse oocytes and early embryos till blastocyst stage by using live Raman scattering microscopy [279]. Taken together, results from cancer biology and developmental biology support the concept that lipid unsaturation is associated with stemness.

1.2.2.6 Specific roles of lipid metabolism in drug resistance

Based on the significance of lipid metabolism to cancer stem cells, it was reasonable to hypothesize that similar deregulation is associated with development of resistance to

chemotherapy. A report using used OC cell lines Hey, Igrov-1, and SKOV-3 as model for different levels of cisplatin-resistance, i.e. sensitive, intermediate-resistant and resistant, described the potential role of lipogenesis to this process [280]. Pre-treatment of cisplatin-resistant Hey-cis generated *in vitro* with FASN inhibitor cerulenin reversed platinum resistance whereas no changes were observed in the parental cells. Exogenous addition of palmitic acid, one of the major products of FASN, rescued the re-sensitization to cisplatin caused by combined treatment with cerulenin and cisplatin, supporting the involvement of fatty acid synthesis in this phenomenon. In a more recent study, Papaevangelou et al. used xenograft models generated from cisplatin-resistant A2780-cis cells [281]. Intraperitoneal administration of the FASN inhibitor orlistat together with cisplatin significantly reduced tumor growth and tumor burden in these tumors. Interestingly, monotherapy with orlistat or with the combination decreased the abundance of hydrophilic metabolites involved in glutamine metabolism in addition to decreasing FASN activity and fatty acid production.

The role of fatty acid metabolism was also studied in other cancer types. For example, Wu et al. found that FASN mediated cellular responses to cisplatin treatment in breast cancer cells [111]. The underlying mechanism involved upregulated specificity protein 1 (SP1) which was upregulated by FASN and, in turn, induced the expression of poly(ADP-ribose) polymerase 1. The later promoted recruitment of repair proteins X-ray repair cross complementing 6 (Ku70) and DNA-dependent protein kinase at sites of double-strand breaks, initiating non-homologous end joining DNA repair machinery. Peng et al. found that colorectal cancer patients proficient DNA damage repair bear higher SCD expression and level of most phospholipids than patients deficient in DNA damage repair [282], implying the importance of SCD and lipid metabolism in

chemotherapy resistance in colorectal cancer. Similar observations were made by Schlaepfer et al. in progesterone receptor (PR)-positive breast cancer cells [283]. Essentially, progesterone analogs induced SCD upregulation and subsequence accumulation of oleic acid in phospholipids and cellular lipid droplets in PR-positive breast cancer cells. The presence of unsaturated fatty acids and lipid droplets confer PR-positive breast cancer cells to chemotherapy agent docetaxel. Similar observation was seen in breast cancer patients [284]. Chemotherapy-induced SCD upregulation was also detected in liver cancer where researchers found that c-Jun N-terminal kinases 1/2 and phosphatidylinositol 3 kinase mediated the transcriptional upregulation [285]. ALL cells, when co-cultured with adipocytes, take up secreted monounsaturated fatty acids and store them as triglycerides and phospholipids. The monounsaturated fatty acids partially protect the cancer cells from chemotherapy-induced death [286]. Interestingly, adipocytes could alter leukemia cells' dependence on glucose metabolism to fatty acid metabolism for energy generation.

The development of resistance to targeted therapy also engages fatty acid metabolism, especially unsaturated fatty acid biogenesis. Sorafenib, multikinase inhibitor, was used to treat advanced liver cancer by disrupting SCD expression and AMPK/mTORC1/sterol regulatory element binding transcription factor 1 (SREBF1) signaling pathway [287]. Shueng et al. used radioactive labelling technique revealed that sorafenib-resistant hepatocellular carcinoma cells depend on *de novo* synthesis of fatty acids and treatment of FASN inhibitor orlistat could sensitize the cancer cells to sorafenib treatment [288]. While Ma et al. found that SCD was upregulated in sorafenib-resistant hepatocellular carcinoma cells and patient-derived xenograft model [289]. Treatment of SCD inhibitor A939572 could resensitize liver cancer cells to sorafenib. Similarly, Lounis et al.

found that *de novo* lipogenesis was enriched in enzalutamide-sensitive prostate cancer and co-treatment with SCD inhibitor and enzalutamide reduced tumor growth [290]. Zhang et al. found that SCD inhibition could sensitize cancer cells that are less sensitive to enhancer of zeste 2 polycomb repressive complex 2 subunit (EZH2) inhibitor GSK126 [291]. Hu et al. found that SCD inhibitor and amodiaquine had synergistic effect in preventing *in vitro* and *in vivo* tumor growth of lung cancer cells [292]. Huang et al. revealed that SCD was upregulated in gefitinib-resistant non-small cell lung cancer cells than their gefitinib-sensitive counterparts [293]. Co-administration of 20(S)-protopanaxatriol could re-sensitize lung cancer cells to gefitinib treatment. Dai et al. identified SCD as key fatty acid metabolism enzyme involved in temozolomide-resistance in glioblastoma. Combined treatment of SCD inhibitor A939572 and temozolomide showed enhanced inhibition of growth of glioma cells than individual drugs [294]. Similar observation was also made by Parik et al. where the authors found synergy between accumulated palmitic acid due to SCD inhibition and temozolomide [295]. New technologies using single cell mass spectrometry revealed that SCD and unsaturated fatty acids were upregulated in irinotecan-resistant colorectal cancer and its inhibition led to sensitization to irinotecan treatment [296]. However, the authors did not further their investigations on the mechanism behind that.

Furthermore, recent reports have suggested that drug-tolerant cells adopt a mesenchymal state and are dependent on lipid peroxidation mediated by the lipid hydroperoxidase glutathione peroxidase 4 (GPX4) [297]. Targeting GPX4 induced ferroptosis which selectively eliminated the “persister” cells responsible for treatment resistance *in vitro* and *in vivo* models. Interestingly, inhibition of the enzyme SCD in OC cells induced both ferroptosis and apoptosis and combined

inhibition of SCD with inducers of ferroptosis induced potent tumor inhibition in OC models [298, 299]. These findings were also supported by *in silico* computation work from Konstorum et al. [300]. In addition to OC, aggressive lung cancer with serine/threonine kinase 11 (STK11) and Kelch like ECH associated protein 1 (KEAP1) co-mutation is more susceptible to inhibition of SCD in the context of ferroptosis [301]. Likewise, breast cancer cells utilize upregulated tumor SCD as well as FABP4 derived from tumor endothelial cells for deposition of unsaturated fatty acids into lipid droplets. These lipid droplets serve as the antioxidant and anti-ferroptotic pool during tyrosine kinase inhibitor, i.e. sunitinib or sorafenib administration [302]. On the contrary, breast cancer cells that are tolerant to the anti-tumor effect of statins activated fatty acid unsaturation genes and cholesterol biosynthesis pathway to store neutral lipids for survival and proliferation [303]. These examples strongly support the involvement of lipogenesis in response to chemotherapy and suggest that inhibitors for these pathways may be added to the armamentarium of cancer therapy.

1.3 Targeting lipid metabolism in ovarian cancer

Given the importance of lipid metabolism in tumor progression and metastasis, much effort has been laid in the past years on the development of small molecular inhibitors targeting different enzymes involved in this metabolism network (Table 1). Inhibitors of fatty acid biosynthesis include inhibitors for SREBF1, ATP-citrate lyase (ACLY), ACC, FASN, SCD, and CPT1.

Multiple inhibitors are under development for SREBF1; however, none has yet entered the clinical arena. One interesting finding was that lipid extract from *N. commune*, a blue-green alga, showed significant reduction of maturation of SREBF1 and hence expression of FASN and SCD

[304]; yet the chemical composition of the extract remains to be elucidated. Inhibitors for ATP citrate lyase are being developed as cholesterol lowering drugs, with the most advanced being ETC-1002, a first in class compound, which completed phase III studies, demonstrating efficacy in blocking cholesterol synthesis [305]. Evaluation of this agent in cancer contexts has not yet been initiated. Acetyl-CoA carboxylase is indirectly targeted by metformin and directly blocked by specific inhibitors ND-646 and ND-654. The latter are being studied in preclinical models of lung cancer and hepatoma, while metformin has been studies extensively in combination with chemotherapy in clinical trials in breast, ovarian, and endometrial cancer or as a preventive cancer agent.

Multiple FASN inhibitors are currently in clinical development, including GSK 2194069, IPI-9119, and TVB-2640. The latter is being studied for the treatment of non-alcoholic steatohepatitis and was assessed in a phase I clinical trial in patients with solid tumors, either alone or in combination with paclitaxel. TVB-2640 was reasonably well tolerated and most common adverse event were alopecia, palmar-plantar rash, and decreased appetite. Responses were observed in patients with ovarian cancer (5 of 12 patients), breast cancer (3 of 14 patients), and KRAS mutated lung cancer [306]. Based on these promising results, further development of this agent includes combinations with bevacizumab in glioblastoma and with paclitaxel and trastuzumab in breast cancer.

SCD is the most extensively studied for drug development among all the enzymes in lipid metabolism. A whole spectrum of different classes of inhibitors have been developed and tested at different stages as summarized in Table 1. One special group of inhibitors not listed here is

isomers of linoleic acid, they were previously shown to have inhibitory effects on protein expression or enzymatic activity in human breast cancer cells [307].

CPT1 is the rate limiting enzyme controlling fatty acid oxidation, which is a major source of energy for several tumor types. The best studied CPT1 inhibitor is etomoxir which has been evaluated in preclinical models of prostate, breast, and bladder cancer and leukemia [194]. Etomoxir was found to synergize with glutaminase inhibitors in triple negative breast cancer cells [308]. The agent also inhibited proliferation of prostate cancer cells, especially under hypoxia [194], and blocked the proliferation of chronic lymphocytic leukemia cells resistant to ibrutinib [309]. Further exploration of inhibitors blocking fatty acid oxidation in various cancer contexts is warranted.

Interestingly, inhibition of lipid metabolism can also affect normal cells, particularly the immune system, including T cells, tumor-associated macrophages, regulatory T cells and myeloid derived stromal cells (MDSCs). An example is the fatty acid transport proteins which are upregulated in MDSCs, cells with immunosuppressive roles in tumors [310]. By reducing this cell population, inhibitors of FATP2, currently under preclinical development, could augment the effects of immunotherapy by selectively eliminating MDSCs. While at high doses, etomoxir was also shown to inhibit the survival of T regulatory and T memory cells as well as the polarization of macrophages, more recent work demonstrated that these effects were independent of CPT1 [311, 312], refuting the previously proposed role of fatty acid oxidation in these processes. Future development of combinations of immunotherapy strategies with agents targeting lipid metabolism is a new direction beginning to be explored in cancer treatment.

Our current understanding of lipid metabolism, specifically fatty acid desaturation, dictates that SCD is the sole enzyme responsible for converting saturated fatty acid to monounsaturated fatty acid. However, Vriens et al. discovered that an alternative fatty acid desaturation pathway exists in multiple cancer types, including lung cancer, breast cancer, prostate cancer, and liver cancer [173]. In those cancer cells, palmitic acid can be converted to sapienic acid by fatty acid desaturase 2. Additionally, inhibition of SCD activity accounted for less than 50% of the cancer cell proliferation. Their findings unveiled an unknown property of cancer cells in producing lipids, indicating cancer cell plasticity. Future endeavours could be directed to the population of cancer cells that utilize this alternative lipid metabolism pathway to survive SCD inhibitor therapy.

A summary of various lipid metabolism inhibitors that have been tested in preclinical cancer models is included bellow. While anti-tumorigenic effects have been documented, concerns regarding systemic toxicity and activation of parallel metabolic pathways have thwarted clinical development thus far.

Table 1. Inhibitors targeting different enzymes in the lipid metabolism network with their known IC_{50} and preclinical models and clinical studies

Target	Compound name	IC_{50}	Preclinical models or clinical trials	Refs
Sterol regulatory element-binding protein 1	Fatostatin	11.2 μM	Prostate cancer cells, subcutaneous xenograft mouse model	[313-315]
	Betulin	10s' μM range	Different types of cancer cells Different types of primary tumor cells Different types of xenograft mouse models	[316]
	PF429242	24.5 μM	Pancreatic cancer cells	[317]
ATP citrate lyase	Cucurbitacin B	0.3 μM	Prostate cancer cells	[318]
	Emodin anthraquinones	3-30 μM	Lung cancer cells	[319]
	ETC-1002	2-13 μM	Primary rat hepatocytes, obese female Zucker rat Hypercholesterolemia, phase III Hypercholesterolemia and type 2 diabetes mellitus	[320-324]

	Furan carboxylate derivatives	4.1 μM	Breast cancer stem cells	[325]
	(-)-Hydroxycitrate	NA	Liver cancer cells Mouse bladder cancer, melanoma and lung cancer	[326-328]
	MEDICA 16	70 μM	*In vitro* biochemical assay	[329]
	NDI-091143	7 nM	Precursors tested in liver cancer cells, high-fat diet fed mice *In vitro* biochemical assay	[330, 331]
	SB-204990	24-53 μM	Lung cancer cells	[332]
Acetyl-CoA carboxylase	Benzofuranyl α-pyrone (TEI-B00422)	17-36 μM	*In vitro* biochemical assay Rat liver cells Liver cancer cells	[333]
	Metformin	NA	Advanced pancreatic cancer, phase IB Prostate cancer, phase II Non-small-cell lung cancer, phase II Papillary renal cell carcinoma, phase I/II	[334-341]

			Colorectal cancer, phase II High-grade serous ovarian, or peritoneal cancer, phase II Advanced melanoma, phase I Head and Neck Squamous Cell Carcinoma, phase I/II Advanced stage ovarian cancer, phase II	
	ND-646	3.5 nM	Non-small-cell lung cancer cells	[342]
	ND-654	3 nM	Liver cancer cells	[305]
	MEDICA 16	NA	Rat	[343]
	Spiropentacylamide compounds	0.008-5 μM	*In vitro* biochemical assay Lung cancer cells Colon cancer cells	[344]
	Spiro-pyrazole compounds	6.9-650 nM	*In vitro* biochemical assay Glioblastoma cells	[345, 346]

	5-(Tetradecyloxy)-2 Furoic Acid (TOFA)	NA	Liver cancer cells	[347, 348]
Fatty acid synthase [349, 350]	3-Aryl-4-hydroxyquinolin-2(1H)-one compounds	19-15,000 nM	*In vitro* biochemical assay	[351]
	C75	NA	Breast cancer cells, HER2/neu transgenic mice Ovarian cancer mouse xenograft	[352-356]
	C93 (FAS93)	30 μg/mL	Non-small cell lung cancer cells, subcutaneous xenograft mouse model, chemically induced lung carcinogenesis murine model Ovarian cancer cells, intraperitoneal xenograft mouse model or subcutaneous xenograft mouse model	[357-359]
	Cerulenin	NA	*In vitro* biochemical assay Breast cancer cells	[360-363]

	Polyphenol compounds (e. g. , epigallocatechin-3-gallate (EGCG), luteolin)	2.33-250 μM	*In vitro* biochemical assay Prostate cancer cells Breast cancer cells, subcutaneous xenograft mouse model	[364-368]
	Fasnall	1.57-7.13 μM	Breast cancer cells Liver cancer cells Mammary tumor mice	[369]
	G28UCM	NA	Breast cancer cells, subcutaneous xenograft mouse model	[370]
	GSK2194069	15 nM	Non-small-cell lung cancer cells	[371]
	GAK837149A	15.8 nM	*In vitro* biochemical assay	[372]
	Imidazopyridine compounds	0.012-50 μM	*In vitro* biochemical assay Cervical cancer cells Rat breast cancer cells Rats	[373]

	IPI-9119	0.3 nM	Metastatic castration-resistant prostate cancer cells and xenograft mice	[374]
	JNJ-54302833	28 nM	Ovarian and prostate cancer cells, subcutaneous xenograft mouse model	[375]
	Orlistat	100 nM	Prostate cancer cells, subcutaneous xenograft mouse model Mouse melanoma cells Breast cancer cells Gastric cancer cells, C57BL/6J APC-Min (multiple intestinal neoplasia) mice	[376-379]
	Platensimycin	0.18-0.30 μM	*In vitro* biochemical assay Rat liver cells Type II diabetes mice	[380]
	(5R)-Thiolactomycin	2.1-80 μg/mL	Breast cancer cells	[381, 382]
	TVB-2640	NA	Colon cancer, phase I	[383-

			HER2-positive advanced breast cancer, phase II Refractory high grade astrocytoma, phase II Non-small cell lung cancer, phase I	386]
	TVB-3166	0.042-0.1 μM	*In vitro* biochemical assay Breast, colorectal, lung, ovarian, pancreatic, prostate, and hematopoietic cancer cells Ovarian and pancreatic cancer cell subcutaneous xenograft mouse model Patient-derived non-small cell lung cancer mouse xenograft	[387]
Stearoyl-CoA desaturase [143, 388-390]	A939572	6-65 nM	Clear cell renal cell carcinoma cells Subcutaneous athymic nude mice	[391, 392]
	Agrimonolide	NA	Ovarian cancer cells Subcutaneous mouse xenograft	[393]
	2-Aminothiazole compounds	0.1-8,200 nM	Immortalized human embryonic kidney cells C57BL/6J mice	[394, 395]

	Aniline compounds (lead compound: CVT-11563 & CVT-12012)	49-30,000 nM	Liver microsomal assay Liver cancer cells Sprague–Dawley rats	[396, 397]
	2-Aryl benzimidazole compounds	27-4,400 nM	*In vitro* biochemical assay Liver cells and liver cancer cells C57BL/6 mice	[398]
	Azetidinyl pyridazine compounds	2.3-8,100 nM	*In vitro* biochemical assay Liver cancer cells C57BL/6 mice	[399]
	Benzimidazolecarboxamide compounds (lead compound: SAR224)	0.078-100 μM	Liver microsomal assay Liver cancer cells Obese Zucker diabetic fatty rats	[400]
	Benzothiazole compounds (lead compound: SW001286)	0.3-6,000 nM	Lung cancer cells	[5, 401]

	Benzoylpiperidine compounds	2-1,048 nM	Liver microsomal assay Obese Zucker diabetic fatty rats	[402]
	Benzo-fused spirocyclic oxazepine compounds	0.003-10 μM	AKR/J mice Rats	[403]
	Bicyclic heteroaryl compounds	2-10,600 nM	*In vitro* biochemical assay Liver cancer cells	[404]
	BZ36	100 nM	Prostate cancer cells Subcutaneous athymic nude mice	[167]
	CVT-11127	NA	Lung cancer cells	[168, 405]
	4,4-Disubstituted piperidine compounds(lead compound: T-3764518)	1.2-220 nM	Liver microsomal assay Colon cancer cells, subcutaneous athymic nude mice	[406, 407]
	GSK993	0.18 μM	*In vitro* biochemical assay Liver cancer cells Obese Zucker diabetic fatty rats	[408]

			Insulin-resistant Sprague Dawley rats	
	Icaritin derivative 2 (ICT2)	NA	Breast cancer cells	[409]
	MF-438	3-220 nM	Non-small cell lung cancer cells Melanoma cells	[271, 410, 411]
	MK-8245	1.066 μM	Liver cancer cells Type 2 diabetes, phase I	[412, 413]
	N-benzylimidazolecarboximde compounds	11-2,700 nM	Liver microsomal assay Sprague–Dawley rats	[414]
	Nicotinic acid compounds	8-20,000 nM	Liver cells Liver cancer cells C57BL/6 mice Sprague–Dawley rats	[415]
	Oxalamide compounds (lead compound:	0.3-6,000 nM	Lung cancer cells	[401]

	SW027951)			
	1-(4-Phenoxypiperidin-1-yl)-2-arylaminoethanone compounds	0.03-10 μM	NA	[416]
	Phenoxy acyclic link compounds	2-100,000 nM	Liver microsomal assay Liver cells Liver cancer cells Mice	[417]
	Phenoxy bispyrrolidine isoxazole compounds	3-100,000 nM	Liver microsomal assay Liver cells Liver cancer cells Mice	[418]
	Piperidine arylurea compounds	0.004-10 μM	Liver microsomal assay	[419]
	Pteridinone compounds	0.5-30,000 nM	Liver microsomal assay Liver cancer cells	[420]

	Pyridazine heteroaryl compounds	3-7,300 nM	*In vitro* biochemical assay Liver cancer cells	[421]
	Pyridin-2-ylpiperazine compounds (lead compound: XEN103)	10s' μM range	Liver cancer cells	[421, 422]
	SAR707	39 nM	Liver cancer cells Obese Zucker diabetic fatty rats	[423]
	Spiropiperidine compounds	0.03 nM-10 μM	Liver microsomal assay C57BL/6J mice	[424-426]
	Thiadiazole compounds	1-6,500 nM	Rat liver microsomal assay Liver cancer cells	[427]
	Thiazole compounds (lead compound: MF-152)	0.3-100+ μM	Rat liver microsomal assay Liver cancer cells	[428]
	Thiazole-4-acetic acid compounds	3.0-3,600 nM	Liver microsomal assay C57BL/6J mice Sprague Dawley rats	[429]

	Thiazolylpyridinone compounds	14-3,400 nM	Mouse liver microsomal assay Liver cancer cells Lewis rats	[430]
	Triazolone compounds	7-10,000 nM	Liver cancer cells Liver microsomal assay Lewis rats	[431]
Peroxisome proliferator-activated receptor α	TPST-1120	NA	Different types of advanced cancer, phase I	[432]

1.4 Summary and research objectives

To summarize, cancer cells thwart physiological metabolic pathways to meet their augmented energetic needs for limitless proliferation and metastatic spread. When glucose and oxygen are in short supply, fat becomes convenient fuel. Whether taken up from the tumor microenvironment or newly synthesized, lipids function as alternative energy source for rapidly growing tumors. A unique property of ovarian cancer is its tropism to the omentum, a fat-laden organ, which has been thought to function as feeding soil for rapidly expanding tumors. While lipid uptake by cancer cells has been studied to some extent, the roles of *de novo* lipogenesis and of the ensuing balance between unsaturated and saturated lipids remain not fully understood. Within the *de novo* lipogenesis pathway, lipid desaturation is a key step required for the generation of unsaturated lipids to maintain the membrane fluidity, the integrity of cellular signaling, and the lipid pool for β-oxidation. SCD converts saturated to unsaturated fatty acids, i.e. palmitic and stearic acids to palmitoleic and oleic acids, respectively. SCD is upregulated in different cancers, and its inhibition was shown to suppress cancer cell proliferation, in conditions depleted of exogenous lipids. However, the mechanisms by which SCD regulates cancer cells' survival under stress conditions are not elucidated. The main focus of this thesis work is to study how lipid metabolism and in particular lipid unsaturation contributes to the aberrant functions of ovarian cancer cells. We are asking whether and how the disturbance of the dynamic between saturated and unsaturated fatty acids regulated by SCD impacts the survival and tumorigenicity of ovarian cancer cells.

Chapter 2 : Materials and Methods

2.1 Cell culture

OVCAR-5 cells were provided by Dr. Marcus Peter, Northwestern University. COV362 and OVCAR-8 cells were provided by Dr. Kenneth Nephew, Indiana University. PEO1 and PEO4 cells were purchased from MilliporeSigma (cat#: 10032308 and 10032309). OVCAR-3 (cat#: HTB-161) and SKOV-3 (cat#: HTB-77) cells were purchased from the American Type Culture Collection (ATCC). FT-190 cells (immortalized human fallopian tube luminal epithelial cells) were provided by Dr. Ronny Drapkin, University of Pennsylvania [433]. OVCAR-5 cells were cultured in Roswell Park Memorial Institute (RPMI)-1640 with L-glutamine (Corning cat#: 10-040-CV) supplemented with 10% fetal bovine serum (FBS) (Corning cat#: 35011CV), 1% GlutaMAX (Gibco cat#: 35050-061), and 100 μg/mL penicillin/streptomycin (Cytiva cat#: SV30010). OVCAR-8 cells were cultured in DMEM (Dulbecco's Modification of Eagle's Medium, Corning cat#: 10-017-CV) supplemented with 10% FBS and 100 μg/mL penicillin/streptomycin. COV362 cells were cultured in DMEM supplemented with 10% FBS, 1% GlutaMAX and 100 μg/mL penicillin/streptomycin. PEO1 and PEO4 cells were cultured in RPMI-1640 with L-glutamine supplemented with 10% FBS, 1% GlutaMAX, 2mM Sodium Pyruvate (Gibco cat#: 11360-070), and 100 μg/mL penicillin/streptomycin. OVCAR-3 cells were cultured in RPMI-1640 (ATCC cat#: 30-2001) supplemented with 20% FBS, 0.01 mg/mL insulin human recombinant zinc (Gibco cat#: 12585-014) and 100 μg/mL penicillin/streptomycin. SKOV-3 and FT190 cells were cultured in medium composed of 1:1 combination of MCDB 105 (MilliporeSigma cat#: M6395) and Medium 199 (Corning cat#: 10-060-CV) supplemented with 10% FBS and 100μg/mL penicillin/streptomycin. All cells were maintained at 37℃ in an incubator with 5% CO_2 and 100% humidity. Palmitic acid (MilliporeSigma cat#: P0500) was

dissolved in dimethyl sulfoxide (DMSO) and treatment of 50 μM palmitic acid under low serum condition (1% FBS) was intended to recapitulate the concentration of palmitic acid in 10% FBS media [434]. 10% lipid depleted FBS (Biowest cat#: S162L) was used in some experiments to validate the findings from low serum condition (1% FBS). Oleic acid (MilliporeSigma cat#: O3008) was added at different doses with the lowest dose of 13 μM equivalent to that in media containing 10% FBS [434]. All cell lines were authenticated by IDEXX BioAnalytics and were determined to be free of mycoplasma contamination by IDEXX BioAnalytics or Charles River Laboratories. In addition, cells were regularly tested for mycoplasma in our laboratory using a Universal Mycoplasma Detection Kit (ATCC cat#: 30-1012K).

2.2 Reagents

Palmitic acid (cat#: P0500), oleic acid (cat#: O3008), dimethyl sulphoxide (DMSO) (cat#: D2650), Tween® 80 (cat#: P4780), cisplatin (cat#: 1134357) and carboplatin (cat#: C2538) were purchased from MilliporeSigma. CAY10566 (cat#: HY-15823) and PEG300 (cat#: HY-Y0873) were purchased from MedChemExpress. Saline (cat#: Z1376) was purchased from Intermountain Life Sciences. Etomoxir (cat#: 11969) was purchased from Cayman Chemical.

2.3 *In vitro* development of cisplatin-resistant cell lines

SKOV-3, OVCAR-5, COV362, and OVCAR-3 cells were treated with three or four repeated or increasing doses of cisplatin or carboplatin for 24 hours. Surviving cells were allowed to recover for 3 to 4 weeks before receiving the next treatment. Changes in resistance to platinum were estimated by calculating half maximal inhibitory concentration (IC_{50}) values determined by the CCK-8 assay (Dojindo cat#: CK04) (Table 2). Specifically, 5,000 OC cells/well were seeded in

96-well plates and 24 hours after plating, treated with different concentrations of cisplatin (0, 0.5, 1, 2.5, 5, 10, 25, 50, 75, 100, 250, 500 μM) or carboplatin (0, 0.5, 1, 2.5, 5, 10, 25, 50, 75, 100, 250, 500 μg/ml) for 24 hours. Cisplatin was then removed (washed off), cells were cultured for 72 hours and cell viability was measured with CCK8 assay (). IC_{50} values were determined by logarithm-normalized sigmoidal dose curve fitting using Graphpad Prism 8 (GraphPad Software).

Table 2. Generation of platinum resistant ovarian cancer cells *in vitro*. IC_{50} of SKOV-3, OVCAR-3, OVCAR-5 and COV362 parental and cisplatin/carboplatin resistant cells are shown

Cell line	IC_{50} range	Cell line	IC_{50} range
SKOV-3	Cisplatin: 6.5 μM (5.22 μM – 8.18 μM)	SKOV-3 cisplatinR	Cisplatin: 11.08 μM (9.73 μM – 12.62 μM)
	Carboplatin: 4.16 μg/mL (3.10 μg/mL – 5.59 μg/mL)		Carboplatin: 15.01 μg/mL (10.36μg/mL – 21.74 μg/mL)
OVCAR-3	Cisplatin: 0.0083 μM (0.00044 μM – 0.15 μM)	OVCAR-3 cisplatinR	Cisplatin: 0.35 μM (0.23 μM – 0.52 μM)
	Carboplatin: 2.86 μg/mL (1.58 μg/mL – 5.17 μg/mL)		Carboplatin: 15.2 μg/mL (12.64 μg/mL – 18.29 μg/mL)
OVCAR-5	Cisplatin: 2.59 μM (2.31 μM – 2.82 μM)	OVCAR-5 cisplatinR	Cisplatin: 8.38 μM (7.47 μM – 9.42 μM)
COV362	Cisplatin: 3.32 μM (3.05 μM – 3.63 μM)	COV362 cisplatinR	Cisplatin: 8.45 μM (6.58 μM – 10.84 μM)

2.4 Human specimens

Primary tumors or ascites from high grade serous OC patients were collected at Northwestern Memorial Hospital from consenting donors (IRB#: STU00202468). Tumor tissues were minced into small pieces and digested with in DMEM/F-12 medium (Gibco cat#: 11320-033) supplemented with 300U/mL collagenase (MilliporeSigma cat#: C7657) and 300U/mL hyaluronidase (MilliporeSigma cat#: H3506) at room temperature overnight. The next day, tissues were digested with trypsin (Corning cat#: 25054CI) at 37℃ for 10min, followed by treatment with 1× red blood cell lysis buffer (Biolegend cat#: 420301) on ice for 10min, and then with DNase I (MilliporeSigma cat#: DN25) at 37℃ for 10min to produce a single-cell suspension. Cells were resuspended in RPMI-1640 with L-glutamine supplemented with 10% FBS, 1% GlutaMAX, and 1% Pen/Strep. For ascites, cells were spun down and resuspended in RPMI-1640 as described above.

2.5 Cell transfection

For generation of gene knockdown or overexpression cells, ovarian cancer cells were seeded at a density of 40,000 cells per well in a 24-well plate on day 0. On day 1, lentiviral particles containing shRNAs targeting human SCD (MilliporeSigma cat#: SHCLNV) or scrambled (control) shRNAs (MilliporeSigma cat#: SHC001V) or containing human SCD cDNA were diluted in complete medium containing 8 μg/mL polybrene to obtain a multiplicity of infection (MOI) of 5. Cells were incubated with lentiviruses for 24 hours followed by removal of lentiviruses and cultured in complete medium for another 24 hours. On day 3, complete medium

containing 2.0 μg/mL puromycin (Gibco cat#: A1113803) or neomycin (Fisher Scientific cat#: 10-131-027) was added to cells to start selection of stably transfected cells.

2.6 Construction of SCD expression vector

The SCD coding sequence was amplified by PCR from SCD Human Tagged open reading frame (ORF) Clone plasmid (OriGene cat#: RC209148) using primers (forward: 5'-GCTCTAGA GGATCCACCGGTCGCCACCATGCCGGCCCACTTG-3' and reverse: 5'-GACGTCGACGCGGCCGCTTCAGCCACTCTTGTAGTTTCCATC-3'), and inserted into pLenti-CMV-Neo vector (Addgene plasmid#: 17447). Lentiviral particles containing the cloned plasmid were packaged in HEK-293T cells via co-transfection using branched polyethylenimine (MilliporeSigma cat#: 408719) with pMD2.G (Addgene plasmid#: 12259) and psPAX2 (Addgene plasmid#: 12260). Viral particles were harvested 48hrs and 72hrs post transfection and pooled for concentration using Lenti-X Concentrator (TaKaRa cat#: 631231). Pellets of lentiviral particles were resuspended in phosphate buffered saline (PBS) (Cytiva cat#: SH30256.LS), aliquoted and stored at -80℃.

2.7 Ribonucleic acid (RNA) extraction and real-time qPCR

Total cellular RNA was extracted using TRI reagent according to the manufacturer's instruction (MilliporeSigma cat#:T9424). 1 μg of total RNA was used to synthesize complementary DNA (cDNA) with a High Capacity cDNA Reverse Transcription Kit (Applied Biosystems cat#: 4368814). Genes of interest were amplified by PCR using PowerUp SYBR Green Master Mix (Applied Biosystems cat#: A25742) on a QuantStudio 5 Real-Time PCR System (Thermo Fisher Scientific cat#: A28140) and quantified applying the $2^{-\Delta\Delta CT}$ method [435] using glyceraldehyde-

3-phosphate dehydrogenase (GAPDH) for normalization. Primers used for real-time qPCR are described [436-439] in Table 3.

Table 3. Primers used for real-time RT-PCR

Target gene	Forward (5'- 3')	Reverse (5'- 3')
SCD	ACGATATCTCTAGCTCCTATACC	GGCATCGTCTCCAACTTATC
GAPDH	GTATGACAACAGCCTCAAGAT	GTCCTTCCACGATACCAAAG
XBP1 (splicing assay)	CCTGGTTGCTGAAGAGGAGG	CTCCAGAACTCCCCATGG

2.8 X-box binding protein 1 (XBP1) splicing assay

Synthesized cDNA as described above was used to measure levels of unspliced and spliced XBP1 mRNA were measured by regular PCR performed with GoTaq Green Master Mix (Promega cat#: M7123) on a T100 Thermo Cycler (Bio-Rad cat#: 186-1096). The primers targeting the spliced XBP1 region (116bp) (Table 3) were designed according to a previous study [440]. PCR products were resolved by 3.5% agarose (Invitrogen cat#: 16550100) gel electrophoresis and visualized using GelGreen stain (Biotium cat#: 41005) on an ImageQuant LAS 4000 machine (GE Healthcare). Densitometric analysis of product bands was performed using the Gel Analyzer function in Fiji from National Institute of Health (NIH) [441]. For rare XBP1 splicing event, unspliced and spliced XBP1 mRNA were PCR amplified for total 36 cycles and resolved by 6% agarose gel electrophoresis.

2.9 Western blot

Cell lysates were prepared using Radio-immunoprecipitation assay (RIPA) buffer. Protein concentrations were measured with the Bradford reagent (Bio-Rad Protein Assay, cat#: 5000006) using bovine serum albumin (BSA) as standard. Protein lysates were denatured and 20 μg of protein per sample were resolved by polyacrylamide-gel electrophoresis and then transferred to a polyvinylidene difluoride (PVDF) membrane. The membrane was incubated with 5% milk and then with primary antibody overnight at 4℃, followed by incubation with horseradish peroxidase (HRP)-conjugated secondary antibody for 1hr at room temperature. Signal was developed using SuperSignal West Pico PLUS Chemiluminescent Substrate (Thermo Fisher Scientific cat#: 34580) and captured with an ImageQuant LAS 4000 machine. To detect additional proteins, membranes were treated with Restore Western Blot Stripping Buffer (Thermo Fisher Scientific cat#: 21059), blocked, and then incubated with primary antibody. Antibodies against SCD (ab19862, 1:1000) and ATF4 (ab184909, 1:1000) were purchased from Abcam. Antibodies against PERK (3192, 1:1000), p-eIF2α (3597, 1:1000), eIF2α (9722, 1:1000), CHOP (2895, 1:1000), caspase-3 (14220, 1:1000), and cleaved caspase-3 (9664, 1:1000) were from Cell Signaling Technology. Antibody against GAPDH (H86504M, 1:20,000) was from Meridian Life Science, Inc. Antibody against β-actin (A1978, 1:20,000) was from MilliporeSigma. GAPDH and β-actin were used as loading control.

2.10 Immunohistochemistry (IHC)

SCD protein was detected by IHC staining on ovarian cancer and fallopian tube paraffin-embedded sections of a tissue array from the Cooperative Human Tissue Network (CHTN) and

one built by the Lurie Cancer Center Pathology Core. The OVCA2 Tissue microarray (TMA) contains 12 cases of serous papillary carcinoma, 12 cases of clear cell carcinoma, 12 cases of endometrioid adenocarcinoma and 12 cases of mucinous adenocarcinoma, 6 cases of serous borderline tumor and 6 cases of mucinous borderline tumor. Non-malignant tissue types were also included, namely 6 cases of proliferative endometrium, 6 cases of fallopian tube fimbriae, 6 cases of ovarian serous cystadenoma and 6 cases of ovarian mucinous cystadenoma. Each specimen is represented by 4 replicate cores on the array. The Lurie Cancer Center Pathology Core TMA contains 50 cases of high grade serous carcinoma, 3 cases of low grade serous carcinoma, 2 cases of endometrium, 6 cases of endometrioid carcinoma, 13 cases of borderline tumor, 1 case of benign tumor and 10 cases of fallopian tube epithelium. The array slide was heated at 56°C for 30 minutes to melt the paraffin. Removal of paraffin was completed using xylene and then sections were rehydrated by immersing the array in decreasing concentrations of ethanol solutions. Heat-induced antigen retrieval was performed with 10mM sodium citrate buffer (pH = 6.0) at 95℃ for 30 min, followed by cool down at room temperature for 1 hour. Sections were treated with 3% hydrogen peroxide for 15 minutes, washed with PBS, blocked with 3% normal goat serum to decrease non-specific binding, and then incubated with anti-SCD antibody (5µg/mL; ab19862, Abcam), overnight at 4°C. Mouse IgG was used as negative control (sc-2025, Santa Cruz Biotechnology) on an ovarian cancer xenograft run in parallel. Sections were incubated with biotinylated secondary antibody for 15 minutes and then with streptavidin-HRP of a Dako (K0675, Agilent Technologies) and continued with incubation with Dako DAB+ Substrate Chromogen System (K3467, Agilent Technologies) to generate colored signal. Sections were counterstained with hematoxylin and imaged with a digital camera attached to a

compound microscope. SCD staining was scored by a board-certified pathologist (JJW) recording the level of staining intensity (0, 1+, 2+, or 3+) for each tumor section. Each tumor or normal specimen was represented by 4 cores, the average of staining intensity for the 4 cores was calculated for the analysis.

2.11 Metabolomics

OVCAR-5, SKOV-3 wildtype (WT) and cisplatin-resistant and PEO1 and PEO4 cells were seeded at a density of 500,000 cells on a 10 cm dish, cultured in regular media for 72hrs. Cells were quickly washed twice with 7mL ice cold normal saline solution with residual solution completely aspirated. Plates were placed on dry ice and 1mL 80% (v/v) methanol pre-cooled to -80℃ was added to each plate to harvest the cell lysate with a cell lifter. Cell lysate was transferred to 1.5mL conical tube and subject to three freeze-thaw cycles between liquid nitrogen and 37℃ with 30 seconds vortex after each thaw. Cells were spun down at 20,000 ×g for 15 minutes at 4℃. Metabolite-containing supernatant was transferred to a new 1.5mL conical tube and stored on dry ice until used for analysis at the Northwestern University Metabolomics Core Facility.

2.12 Lipidomics

OVCAR-5 cells transduced with shRNA targeting SCD vs. control shRNA cells were seeded at a density of 400,000 cells on a 10 cm dish, cultured in regular media for 48h, and then in low serum medium (1% FBS) for an additional 48 hours. Cells were washed twice with ice cold PBS, harvested in 800 μL ice cold PBS and spun down at 1000 rpm at 4℃ for 5min. Supernatants were discarded and cell pellets were stored on dry ice until used for analysis at the Bindley

Bioscience Center, Purdue University. Lipidomic analysis was performed using multiple reaction monitoring (MRM) profiling which has been designed to provide rapid and comprehensive analysis of several classes of lipids in biological samples [442]. The MRM Profiling method workflow includes direct injection of diluted lipid extracts and the selection of signature fragments of lipid classes in a triple quadrupole mass spectrometer. Briefly, lipids were extracted using the Bligh & Dyer (1959) method [443]. Dried lipid extracts were diluted in the injection solvent (acetonitrile/methanol/ammonium acetate 300mM 3:6.65:0.35 [v/v/v]) to obtain a stock solution. The stock solution was further diluted into injection solvent spiked with 0.1 ng/μL of EquiSPLASH LIPIDOMIX (Avanti Polar Lipids cat#: 330731) for sample injection. The MRM-profiling methods and instrumentation used have been recently described in previous reports [444-449]. Data acquisition was performed using flow-injection (no chromatographic separation) from 8 μL of the diluted lipid extract stock solution delivered using a micro-autosampler (G1377A) to the electrospray ionization (ESI) source of an Agilent 6410 triple quadrupole mass spectrometer (Agilent Technologies, Santa Clara, CA, USA). A capillary pump was connected to the autosampler and operated at a flow rate of 7 μL/min and pressure of 100bar. Capillary voltage on the instrument was 5kV and the gas flow 5.1L/min at 300°C. The MS data obtained from these methods was processed using an in-house script to obtain a list of MRM transitions with their respective sum of absolute ion intensities over the acquisition time. For the reporting of relative amounts using normalization by the internal standards, the amount of each fatty acid was expressed as pg/1000 cells. For lipidomics profiling using the relative amounts, cells were lysed in ultrapure water for lipid extraction. MetaboAnalystR 3.0 [450] was used to process mass spectrometry peak intensity data for each lipid species. Data on the relative amounts from different lipid classes were autoscaled to obtain a normal distribution, and evaluated by

univariate analysis, principal component analysis (PCA), and cluster analysis/heatmap. Informative lipids were analyzed according to class, fatty acyl residue chain unsaturation level [451].

2.13 SRS imaging

Stimulated Raman scattering (SRS) imaging was performed to measure isotope labelled cellular saturated/unsaturated fatty acids on a previously described lab-built system with a femtosecond laser source operating at 80MHz (InSight DeepSee, Spectra-Physics, Santa Clara, CA, USA) [67, 452]. Briefly, the laser source provides two synchronized output beams, a tunable pump beam ranging from 680 nm to 1300 nm and a fixed 1040 nm Stokes beam, modulated at 2.3MHz by an acousto-optic modulator (1205-C, Isomet). SRS spectrum is obtained by controlling the temporal delay of two chirped femtosecond pulse. A 12.7 cm long SF57 glass rod was used to chirp Stoke path to compensate for its longer wavelength. After combination, the path of both beams was further chirped by five 12.7 cm long SF57 glass rods before sent to a laser-scanning microscope. A 60x water immersion objective (NA = 1.2, UPlanApo/IR, Olympus) was used to focus the light on the sample, followed by signal collection via an oil condenser (NA = 1.4, U-AAC, Olympus). For hyperspectral SRS (hSRS) imaging, a stack of 120 images was recorded at various pump-Stokes temporal delay, implemented by tuning the optical path difference between pump and Stokes beam through a translation delay stage. Pump beam was tuned to 798 nm for imaging at the C-H vibration region (2800 ~ 3050 cm^{-1}), and to 850 nm for imaging at C-D vibration region (2100 ~ 2300 cm^{-1}). The power of pump and Stokes beam before microscope was 30mW and 200mW respectively. Raman shift was calibrated by standard samples, including DMSO, DMSO-d6, palmitic acid-d31 (PA-d31) and oleic acid-d34 (OA-d34). Hyperspectral

SRS images were analyzed using ImageJ and previously described pixel-wise least absolute shrinkage and selection operator (LASSO) regression algorithm [453]. In brief, LASSO can effectively decompose hSRS imaging into maps of different biomolecules by introducing a sparsity constraint to suppress the crosstalk between different chemical maps. PA-d31 and OA-d34 was used to provide reference spectrum of SFA and UFA respectively for LASSO unmixing analysis.

To study cellular uptake of fatty acids by SRS microscopy, cells were seeded on 35 mm glass-bottom dishes (Cellvis, D35-20-1.5-N) overnight, and then cultured in low serum medium for 24 hours, followed by treatment with 12.5 μM PA-d31 (Cambridge Isotope Lab) for 24 hours. Rescue experiments were conducted by adding 52 μM oleic acid to the low serum medium containing 12.5 μM PA-d31 or changing to full serum medium with 12.5 μM PA-d31. For quantitative SRS imaging, cells were fixed with 10% neutral buffered formalin for 30 min followed by 3 times of PBS wash.

2.14 Flow cytometry for lipid peroxidation

After treatment with CAY10566 at the indicated concentrations, cells were stained with 5 μM BODIPY 581/591 C11 (Thermo Fisher Scientific cat#: D3861) for 2 hours at 37℃. Cells were then trypsinized and fixed at room temperature for 30 minutes. Flow cytometry analysis was performed on a Fortessa analyzer with fluorescein isothiocyanate (FITC) channel for oxidized BODIPY-C11 and PE-YG for reduced BODIPY-C11.

2.15 Cell viability assay

OVCAR-5 WT cells were seeded at a density of 6,000 cells in a 96-well plate, cultured in regular media for 48h, and then washed once with 1×PBS and switched to medium containing low serum (1% FBS) and 21.6 nM CAY10566, 25 μM Ferrostatin-1 and/or 25 μM Z-VAD-FMK for an additional 72 hours. CCK-8 was used to determine cell viability after 72 hours.

2.16 FAO assay

FAO was measured using Fatty Acid Oxidation Assay kit (Abcam cat#: ab217602) following the provided protocol. Briefly, cells were seeded in 96-well plate with 150k cells/well. After incubation overnight, medium was replaced. 10 μL Extracellular O_2 consumption reagent and 2 drops of high sensitivity mineral oil (pre-heated at 37℃) were added to each well. Fluorescence was measured in plate reader at 2min intervals for 180min at excitation/emission = 380/650 nm. Etomoxir was added at final concentration of 40 μM to block FAO. Oxygen consumption rate (OCR) is presented as $\Delta_{\text{Fluorescence intensity}}$/min/cell and FAO rate is calculated as $OCR_{FAO} = OCR_{total} - OCR_{Etomoxir}$. At least three replicates were included for each measurement.

2.17 Measurement of OCR and extracellular acidification rate (ECAR) by Seahorse

Cell lines were seeded in a Seahorse XF96 Cell Culture Microplate (Agilent cat#: 101085-004) at density of 60,000 (OVCAR-5 WT/cisR pair) or 40,000 (PEO1/4 pair) cells per well. After incubation at 37℃ overnight for cell attachment, OCR and ECAR were measured via Seahorse XFe96 Analyzer (Agilent). Measurement time was 30 seconds following 3 minutes mixture and 30 seconds waiting time. First three cycles were used for basal respiration measurement. Effects

of 4 μM oligomycin, 4 μM carbonyl cyanide-4-(trifluoromethoxy)phenylhydrazone (FCCP), 25 μM rotenone, 50 μM antimycin A, 26.4 μM cisplatin, or 40 μM etomoxir on OC cells OCR and ECAR were measured. Basal respiration, ATP production and maximal respiration reduction were calculated following the manufacturer's instructions.

2.18 Xenograft experiments

Athymic nude mice (strain: *Foxn1*^{nu}), 6-8 weeks old, were obtained from Envigo (Indianapolis, IN, USA). OVCAR-5 cells, untransformed, or cells stably transduced with shRNAs targeting SCD or control shRNA were injected intraperitoneally (i.p., 5 million cells) into the mice to induce tumors. Mice were euthanized 28 days after injection of cells to evaluate tumor growth and abdominal ascites. To determine the effects of a palmitic acid-enriched diet and SCD inhibitor combination, athymic nude mice were randomized to be fed with a palmitic acid-enriched or a control diet beginning one week before i.p. injection of OVCAR-5 cells, and continued for the duration of the experiment (28 days). Mice were treated i.p. with the SCD inhibitor CAY10566 (8 mg/kg body weight) or diluent (10% DMSO, 40% PEG300, 5% Tween-80, 45% saline), every other day during weekdays. The contents of palmitic acid in the palmitic acid-enriched diet and control were 30% and 11.7% of the total fatty acids, respectively. The levels of total fat (58g/kg) were the same, and levels of saturated fat, monounsaturated fat, polyunsaturated fat, stearic acid, and oleic acid were similar (< 2% difference) between the palmitic acid-enriched and control diets. The diets were custom-made by Teklad (Envigo).

A subcutaneous tumor xenograft mouse model was also used to determine the effect of SCD KD on tumor development. For this, mice were injected with 2×10^6 OVCAR-3 cells stably

transduced with shRNAs targeting SCD or control shRNA resuspended in 1/1 mix of RPMI 1640 basal medium and Matrigel (Corning cat#: 356234). Tumor length (L), width (W) and height (H) were measured every three days with digital calipers. Tumor volume was calculated using the formula $V = L \times H \times W/2$.

2.19 RNA sequencing (RNA-seq)

RNA-sequencing was performed as described previously [436, 437]. RNA was extracted using TRI reagent. Genomic DNA was removed from 1 μg total RNA with an RNeasy MinElute Cleanup Kit (QIAGEN cat#: 74204). Thereafter, mRNA was isolated from total RNA using a NEBNext Poly(A) mRNA Magnetic Isolation Module (New England Biolabs cat#: E7490S). This was followed by first strand cDNA synthesis, second strand cDNA synthesis, adaptor ligation, PCR enrichment, and purification for RNA-seq library preparation (New England Biolabs cat#: E7770S). RNA-seq library quality was determined with a BioAnalyzer. RNA-seq libraries were sequenced on an Illumina NextSeq 500 machine producing single-end reads with 75bp read length. Illumina software called bcl2fastq (v2.17.1.14) was used to convert base call files (*.bcl) to FASTQ format (*.fastq) with the following parameters: -r 4 -d 3 -p 8 -w 4. Raw RNA-seq reads were aligned to the human reference genome GRCh38 ENSEMBL release 91 [454] using STAR (v2.5.2) [455] and SAMtools (v1.6) [456]. Mapped reads were then counted using HTSeq (Anaconda v3.6) [457]. Differentially expressed genes (DEGs) between experimental groups were determined and false discovery rate (FDR) corrected for multiple hypothesis testing with the edgeR package [458] in R. Pathway analysis based on the DEGs was performed using Ingenuity Pathway Analysis (IPA) software (QIAGEN). Normalized counts for

all genes and all biological replicates were exported from R and subject to Gene Set Enrichment Analysis [459] and Gene Ontology analysis using clusterProfiler [460].

2.20 The Genotype-Tissue Expression (GTEx) and The Cancer Genome Atlas (TCGA) ovarian cancer RNA-seq data analysis

Recomputed RNA-Seq by Expectation-Maximization (RSEM) expected counts of fallopian tube samples (GTEx) and primary tumor samples from TCGA ovarian cancer patients were downloaded from University of California Santa Cruz (UCSC) Xena Browser. Expression of SCD (Ensembl ID: ENSG00000099194) was extracted from matrix of all genes and Student's t test was performed on log2 transformed RSEM expected counts between fallopian tube samples and primary tumor samples.

2.21 Cancer Dependency Map data analysis

Dependency score data from clustered regularly interspaced short palindromic repeats (CRISPR) screening in cancer cell lines was downloaded from Depmap Portal [461]. Ovarian cancer cell lines were selected and Pearson correlation score was calculated between SCD and transcriptional regulators identified from IPA (Qiagen).

2.22 Microarray gene expression analysis

SCD expression levels among different ovarian cancer subtypes (clear cell, endometrioid, mucinous, serous, serous-low malignant potential) and assessed by microarray hybridization and deposited on the Ovarian cancer database of Cancer Science Institute Singapore (CSIOVDB) website [462] was analyzed by using the Mann-Whitney U test.

2.23 Patient Survival Analysis

Progression-free survival (PFS) for women with high grade serous, stages III-IV ovarian cancer in the TCGA database was analyzed using Kaplan-Meier Plotter online tool. In total data from 1001 patients were analyzed and dichotomized into two groups: high and low expression.

2.24 Apoptosis assay by IncuCyte imaging

OVCAR-5 cells were seeded on 96-well plates at 500 per well and cultured in an IncuCyte S3 live-cell analysis system. Serum was reduced in the medium to 1% FBS, and Annexin V Green Dye (Sartorius cat#: 4642) was added for detection of apoptotic cells under different experimental conditions. Bright field and green fluorescence were captured for four wells and five images per well at three-hour intervals during a 72hr evaluation period. Cell confluence were calculated on the images and expressed as apoptotic cells (green cells vs total cells under bright field).

2.25 Transmission Electron Microscopy

Cells were seeded at a density of 32,000 on glass bottom dishes (Cellvis cat#: D35-14-1.5-N) and cultured in regular medium for 48 hours. Culture conditions were changed to low serum medium (1% FBS) for an additional 48 hours. Cells were rinsed twice with PBS and fixed with 0.1M sodium cacodylate buffer, pH 7.3, containing 2% paraformaldehyde and 2.5% glutaraldehyde. Cells were post-fixed with 2% osmium tetroxide in unbuffered aqueous solution followed by rinsing with distilled water. Subsequently, cells were *en-bloc* stained with 3% uranyl acetate and rinsed with distilled water. Finally, cells were dehydrated in ascending grades of

ethanol, transitioned with 1:1 mixture of ethanol and resin, and embedded in resin mixture of EMbed 812 Kit (Electron Microscopy Sciences cat#: 14120), cured in a 60℃ oven. Samples were sectioned on a Leica Ultracut UC6 ultramicrotome. Sections (70 nm) were collected on 200mesh copper grids and post stained with 3% uranyl acetate and Reynolds lead citrate. Electron microscopic images were captured on a FEI Tecnai Spirit G2 transmission electron microscope.

2.26 Statistical Analyses

Data were analyzed by two-tailed Student t test or non-parametric U test when necessary. Two-way ANOVA was used for the analyses of the *in vivo* experiment with CAY10566 and palmitic acid-enriched diet. IHC staining analysis employed the Fisher exact test to compare the groups. Tumor weights and volumes from the subcutaneous mouse xenograft experiment were log transformed as paired samples before statistical analysis. $P < 0.05$ was considered statistically significant. All statistical analyses except for RNA-seq and lipidomics were performed using GraphPad Prism v8.0.

2.27 Rigor and Reproducibility

All experiments were performed for at least 3 biological replicates except for western blot measurements of SCD protein levels in immortalized fallopian tube luminal epithelial cells (FT-190), immortalized ovarian surface epithelial (IOSE) and eleven ovarian cancer cell lines and XBP1 splicing and western blot of proteins of the PERK/eIF2α/ATF4 axis in shCtrl and shSCD OVCAR-5 cells cultured under low serum conditions and treated with 50 μM PA for different time points. Appropriate statistical analysis was applied to determine the significance of the

results. Conclusions were drawn from adequate repetition of experiments and from different observations. Materials and methods have been written in sufficient detail in order for my lab members and researchers in the scientific community to repeat my experiments. Work that was done or helped by others have been attributed in the Acknowledgement section as well as in the figure legends. Permissions for reproducing contents of my own published articles were stated in the Acknowledgement section. Cell lines, mouse models, primary patient tumors and reagents were authenticated by external entities and notated.

Chapter 3 : Results

This section is largely adapted from Ovarian cancer cell fate regulation by the dynamics between saturated and unsaturated fatty acids published in Proceedings of the National Academy of Sciences of the United States of America.

3.1 SCD is highly expressed in OC cell lines and tumors

SCD expression was assessed by using representative cancer cell lines, human OC specimens included in two tissue microarrays (TMAs), and RNA sequencing data from human specimens profiled by TCGA [463] and the GTEx Project. *SCD* expression was significantly higher in HGSOC profiled by the TCGA (n = 427) compared to normal fallopian tube epithelium (FTE, n = 5, Fig. 3-1 A, left panel) and normal ovarian tissue (n = 93, Figure 3-1 A, right panel). Further, *SCD* was highly expressed in OC cell lines as compared to immortalized fallopian tube epithelial (FT-190) cells and immortalized ovarian surface epithelial (IOSE) cells at both *mRNA* and protein levels (Figure 3-1 B and C). IHC analysis demonstrated significant upregulation of SCD in HGSOC tumors (n = 62) vs. fallopian tube epithelium (FTE) (n = 15), with 46 of 62 tumors displaying intense staining vs. FTE (Figure 3-1 D, $p = 0.0016$). Other histological subtypes of OC also displayed increased SCD expression compared to FTE ($p = 0.0027$), while non-malignant ovarian tumors (borderline tumors and cystadenoma) did not overexpress SCD (Table 4). Additionally, analysis of mRNA expression data from a publicly available dataset (CSIOVDB [462]) showed a significant difference in SCD expression levels between all and each histological subtype of OC vs. low malignant ovarian tumors, (Figure 3-1 E and Table 5), further supporting the significance of SCD in OC.

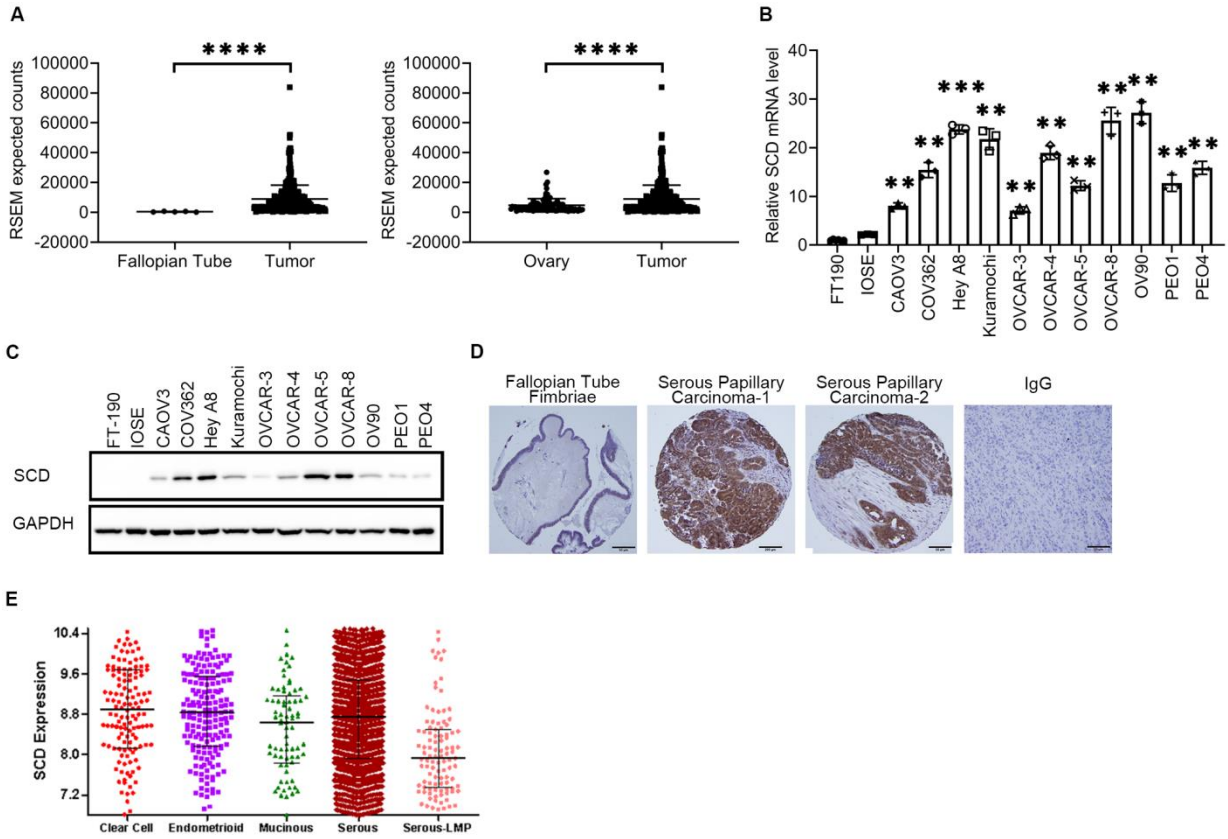

Figure 3-1 SCD is highly expressed in ovarian cancer.

(A) *SCD* expression from RNA-seq data in fallopian tube (left) and normal ovary tissue (right) compared to ovarian cancer tumors in patients from the UCSC Xena Browser. Expression is shown as RSEM expected counts. Russell Keathley helped with data retrieval. (B, C) qRT-PCR analysis of SCD expression (mean ± SD, n = 3) (B), and western blot measurements of SCD protein levels (C) in immortalized fallopian tube luminal epithelial cells (FT-190), immortalized ovarian surface epithelial (IOSE) and eleven ovarian cancer cell lines. (D) Representative images of IHC staining for SCD under 20X magnification in fallopian tube fimbriae (left panel), HGSOC specimens (middle panels). Negative control (IgG) is shown in right panel (tumor tissue). Scale bar corresponds to 50 μm. Dr. Jian-Jun Wei helped with image acquisition and

scoring. (E) SCD expression levels among clear cell (n = 146), endometrioid (n = 185), mucinous (n = 78) and high grade serous (n = 2433) ovarian cancer as compared to low malignant potential serous ovarian tumors (n = 106). Y axis presents relative SCD mRNA expression levels. Dr. Sandra Orsulic helped with data retrieval. ** $p < 0.01$, *** $p < 0.001$, **** $p < 0.0001$.

Table 4. Summary of SCD immunohistochemistry staining in gynecologic tissue (graded from 0 to 3+)

Tissue type	Total number of samples	Number of samples with score <= 1	Number of samples with score >1	P value[#]
Fallopian tube fimbriae	15	11	4	NA
Serous papillary carcinoma	62	16	46	0.0016
All ovarian cancers (serous, endometrioid, mucinous, clear cell)	101	31	70	0.0027
All non-malignant ovarian tumors (serous cystadenoma and borderline tumors)	33	21	12	0.7422

[#]Statistical significance was calculated by using the Fisher's exact test comparing each group with the control (fallopian tube fimbriae)

Table 5. Expression of SCD in different histologic subtypes of ovarian cancer compared to low malignant potential serous ovarian tumors

Mann-Whitney U Test	Clear Cell	Endometrioid	Mucinous	Serous	Serous-LMP	Rest
Clear Cell		6.96e-01	1.67e-02	1.54e-01	4.25e-09	8.63e-02
Endometrioid			1.99e-02	2.38e-01	2.04e-10	1.29e-01
Mucinous				6.86e-02	8.72e-04	8.56e-02
Serous					7.76e-11	5.17e-02
Serous-LMP						3.35e-11

Data were obtained from the CSIOVDB: a microarray gene expression database of ovarian cancer subtype [462].

3.2 SCD knockdown in OC cells

For functional studies, two shRNA sequences targeting *SCD* (shSCD-1 and shSCD-2) or control shRNA (shCtrl) were stably transduced in OVCAR-5, OVCAR-8, OVCAR-3 and PEO1 cells. *SCD* knockdown (KD) was verified by quantitative PCR and western blotting (Figure 3-2).

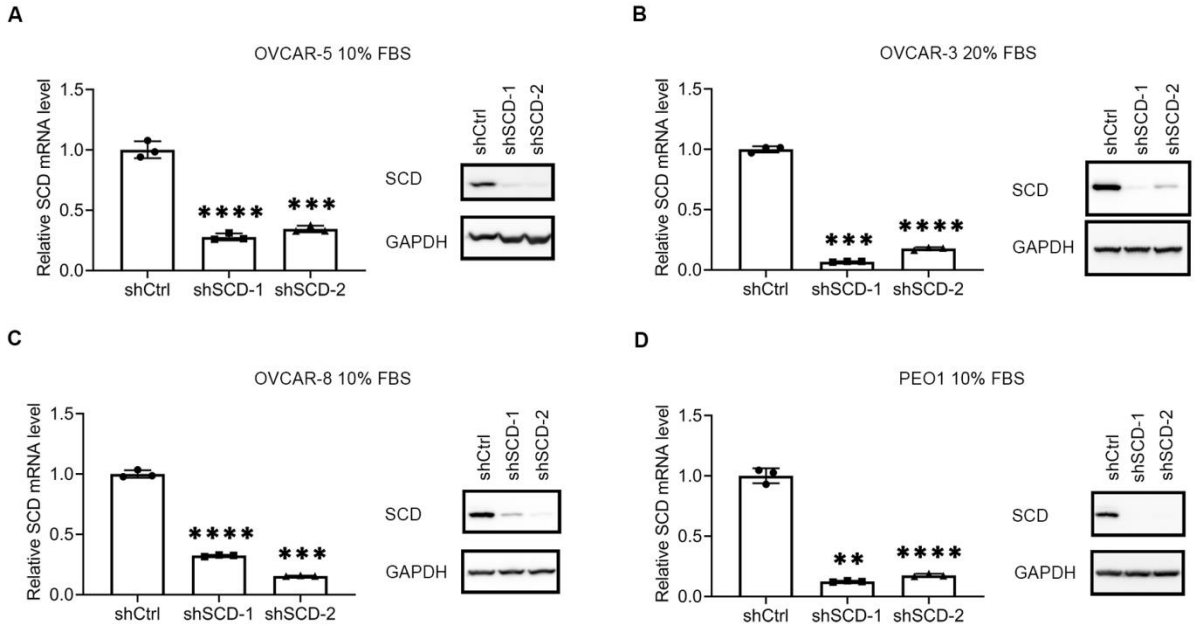

Figure 3-2 SCD is knocked down in ovarian cancer cell lines.

(A-D) *SCD* expression measured by qRT-PCR (mean ± SD, n = 3) and western blot in OVCAR-5 (A), OVCAR-3 (B), OVAR-8 (C) and PEO1 (D) cells transduced with shRNAs (1 or 2) targeting *SCD* (shSCD), or control shRNA (shCtrl). ** $p < 0.01$, *** $p < 0.001$, **** $p < 0.0001$.

3.3 SCD regulates the balance between SFAs and UFAs in OC cells

Lipidomics and isotopic hSRS assessed the abundance of SFAs and UFAs in OC cells transduced with shRNA targeting SCD vs. control shRNA and cultured under low serum conditions to limit the impact of exogenous lipid uptake. A significant reduction in UFAs (palmitoleic and oleic acids), but no difference in abundance of SFAs (palmitic and stearic acids, Figure 3-3 A) were recorded in cells transduced with shRNA targeting SCD vs. control shRNA.

Further, isotopic hSRS imaging compared the levels of UFAs converted from newly imported SFAs in shSCD vs shCtrl transduced cells (Figure 3-3 B and C). After being maintained in low serum medium for 24 hours, cells were cultured with deuterated SFA (PA-d31) for 24 hours. The C-D bond signal, corresponding to UFAs was measured by hSRS imaging (Figure 3-3 C), and intracellular deuterated SFA and UFA levels were distinguished through a LASSO unmixing analysis using the distinctive Raman spectra of PA-d31 and OA-d34, as reference for SFA and UFA respectively (Figure 3-3 B). Images and quantitative analyses of UFA levels and UFA/SFA ratio (Figure 3-3 D) show that cells in which SCD was knocked down contain significantly less deuterated UFA synthesized from newly imported PA-d31, indicating diminished efficiency of converting SFA to UFA in cells depleted of SCD compared to controls.

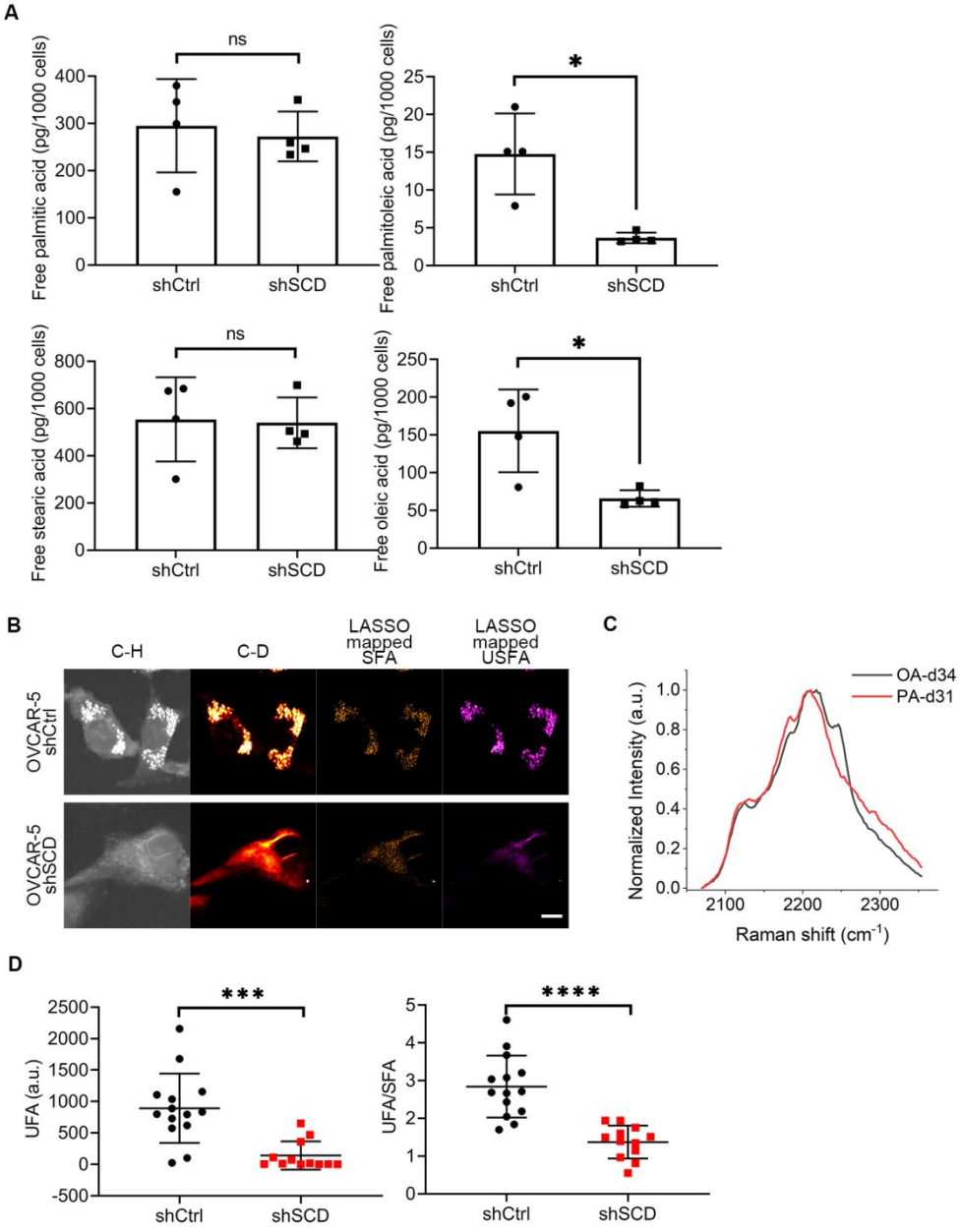

Figure 3-3 SCD is associated with increased levels of free unsaturated fatty acids.

(A) Lipidomics analysis of PA (16:0), palmitoleic acid (16:1), stearic acid (18:0), and OA (18:1) in shCtrl and shSCD OVCAR-5 cells cultured in medium containing low serum (1% FBS) for 48 hours (means ± SD, n = 4). (B) Representative SRS images in C-H and C-D regions, and LASSO

mappings of saturated fatty acid (SFA) and unsaturated fatty acids (UFA) in shSCD vs shCtrl OVCAR-5 cells treated with 12.5 μM PA-d31 and cultured in low serum conditions. Scale bar: 10 μm. (C) Normalized SRS spectra of OA-d34 and PA-d31 (PA-d31) as reference spectrum of UFA and SFA respectively for LASSO analysis. (D) Quantitative analysis of LASSO mapped UFA and ratio between UFA and SFA in shSCD vs shCtrl OVCAR-5 cells. Each data point represents quantitative result from a single cell (n = 12-14). Yuying Tan helped with image acquisition and data analysis. * $p < 0.05$, *** $p < 0.001$, **** $p < 0.0001$.

To understand which lipid species were most affected by the decrease of UFAs caused by SCD depletion, lipidomics by MRM profiling [442] measured the abundance of phosphatidylcholines (PC), phosphatidylethanolamine (PE), sphingomyelin (SM), and triglycerides (TAGs) in OVCAR-5 cells stably transduced with control or shRNA targeting SCD and cultured under low serum conditions for 48 hours. After data normalization, PCA confirmed the separation of the two groups (i.e. shCtrl and shSCD) and heatmaps for each lipid species generated by using unsupervised hierarchical clustering demonstrated separation and clustering of the two groups (Figure 3-4, Figure 3-5, Figure 3-6, and Figure 3-7). The most affected (fold-change) lipid species by SCD depletion were PC and SM, followed by triacylglycerol (TAG) and PE (Figure 3-8 A). A deeper examination of each lipid class revealed that both PC and SM phospholipids with 1° plasticity (one or two carbon-carbon double bonds within the fatty acid tail) [464] were significantly less abundant in shSCD compared with shCtrl transduced cells ($p < 0.0001$, Figure 3-8 B). Further, a significant reduction of 16:1 or 18:1 fatty acyl chains integrated TAGs was observed in OC cells stably transduced with shRNA targeting SCD compared to cells transduced

with control shRNA (p = 0.0382, Figure 3-8 C). Combined, the lipidomics analyses coupled with hSRS imaging demonstrate that cells depleted of this key desaturase, contain less abundant UFAs, and less plastic lipid species, particularly PC and SM.

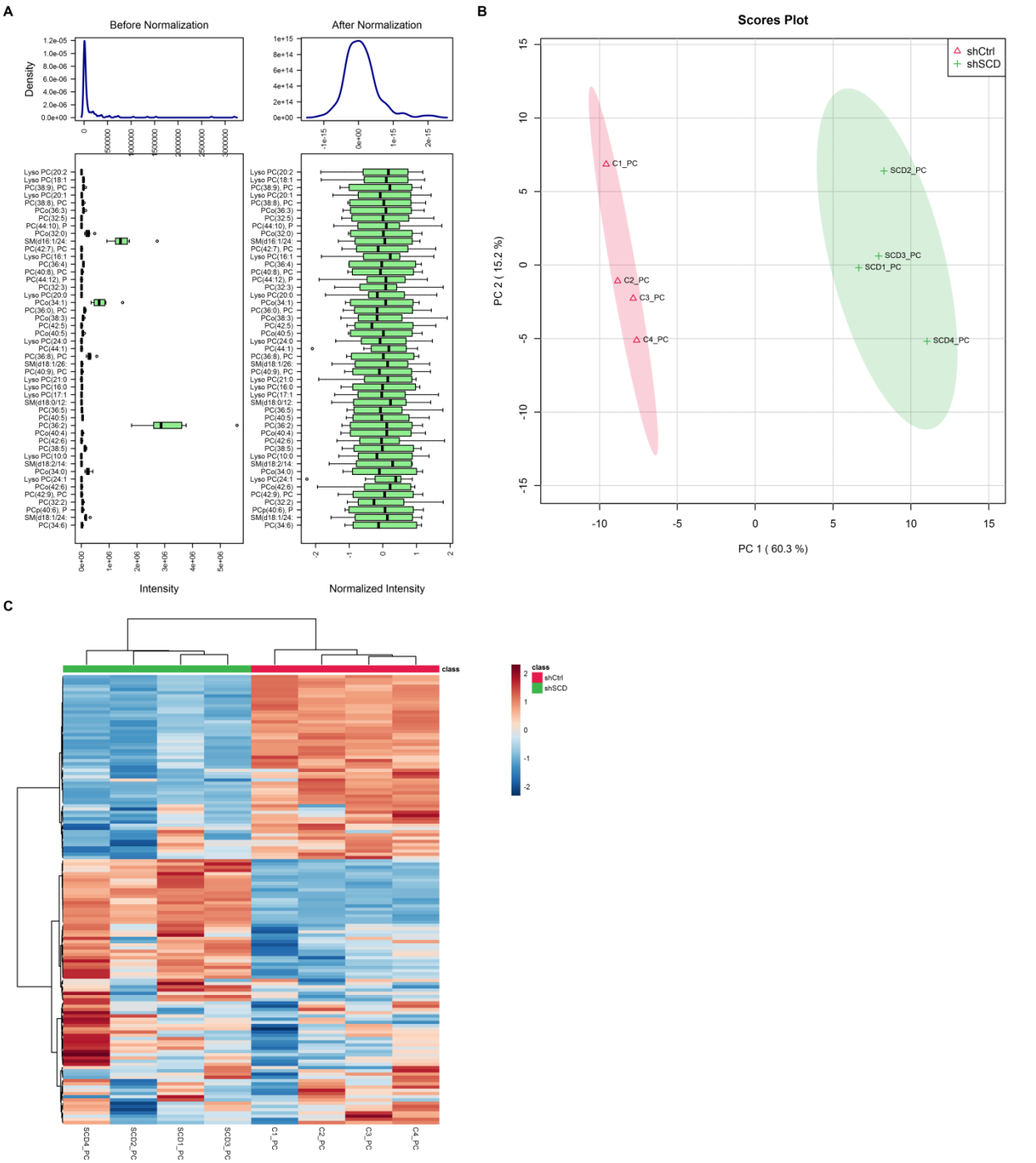

Figure 3-4 Quality control of lipidomics analysis of phosphatidylcholine & sphingomyelin lipids.

(A-C) Normalization plot, principal component analysis and hierarchical clustering of phosphatidylcholine & sphingomyelin lipids from lipidomics profiling of shCtrl and shSCD OVCAR-5 cells cultured under low serum condition for 48 hours.

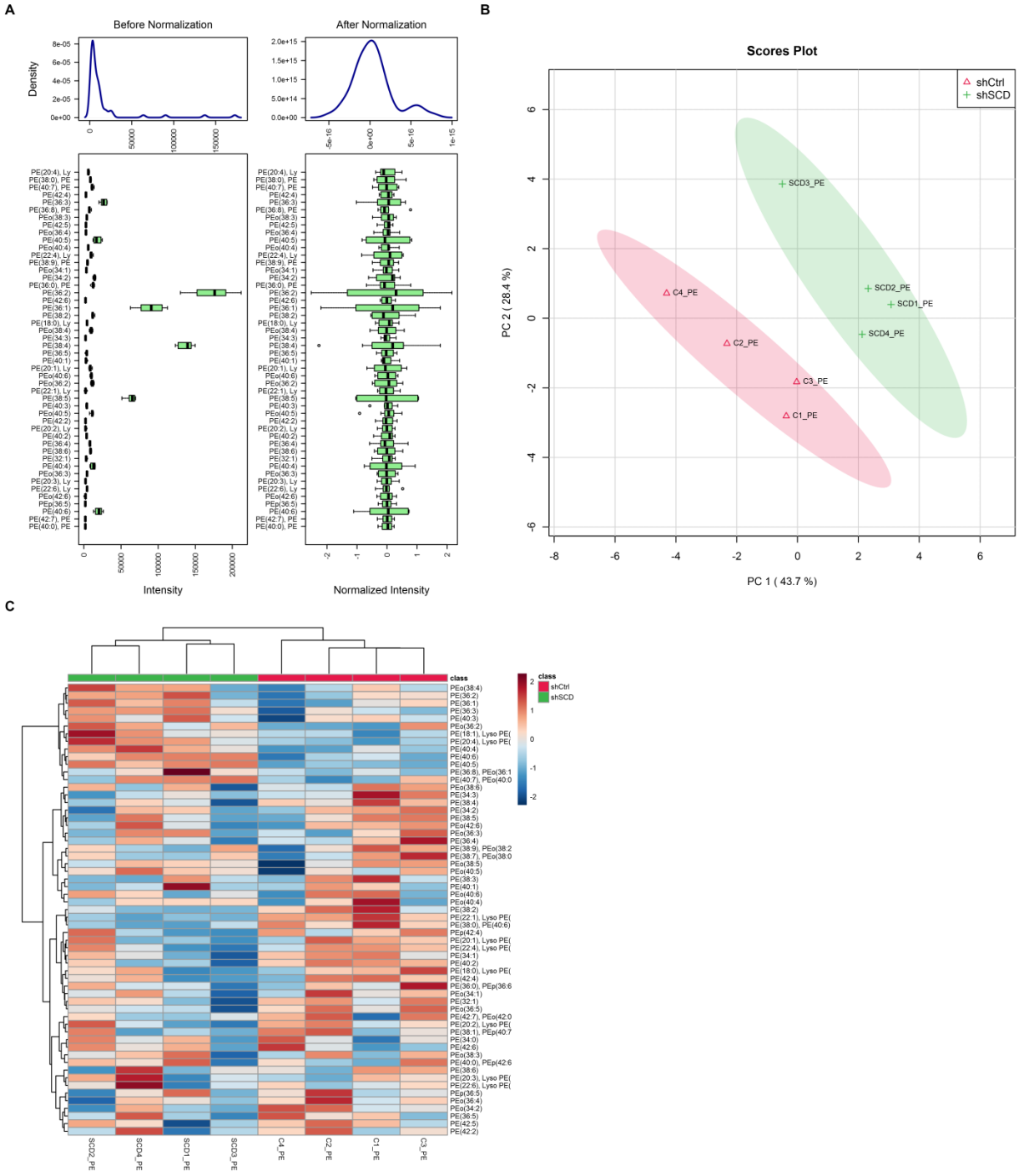

Figure 3-5 Quality control of lipidomics analysis of phosphatidylethanolamine lipids.

(A-C) Normalization plot, principal component analysis and hierarchical clustering of phosphatidylethanolamine lipids from lipidomics profiling of shCtrl and shSCD OVCAR-5 cells cultured under low serum condition for 48 hours.

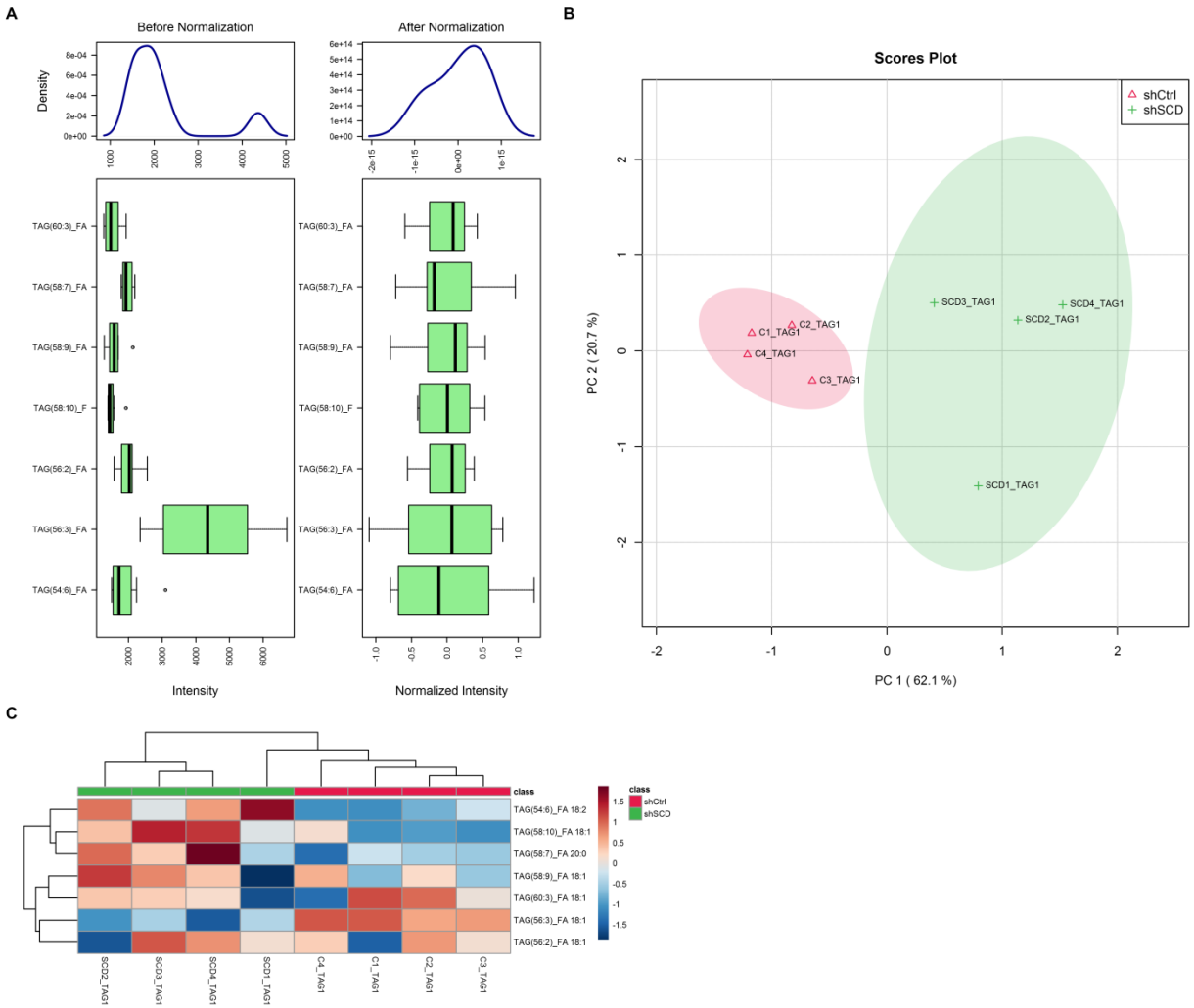

Figure 3-6 Quality control of lipidomics analysis of triacylglycerols 1.

(A-C) Normalization plot, principal component analysis and hierarchical clustering of triacylglycerols 1 from lipidomics profiling of shCtrl and shSCD OVCAR-5 cells cultured under low serum condition for 48 hours.

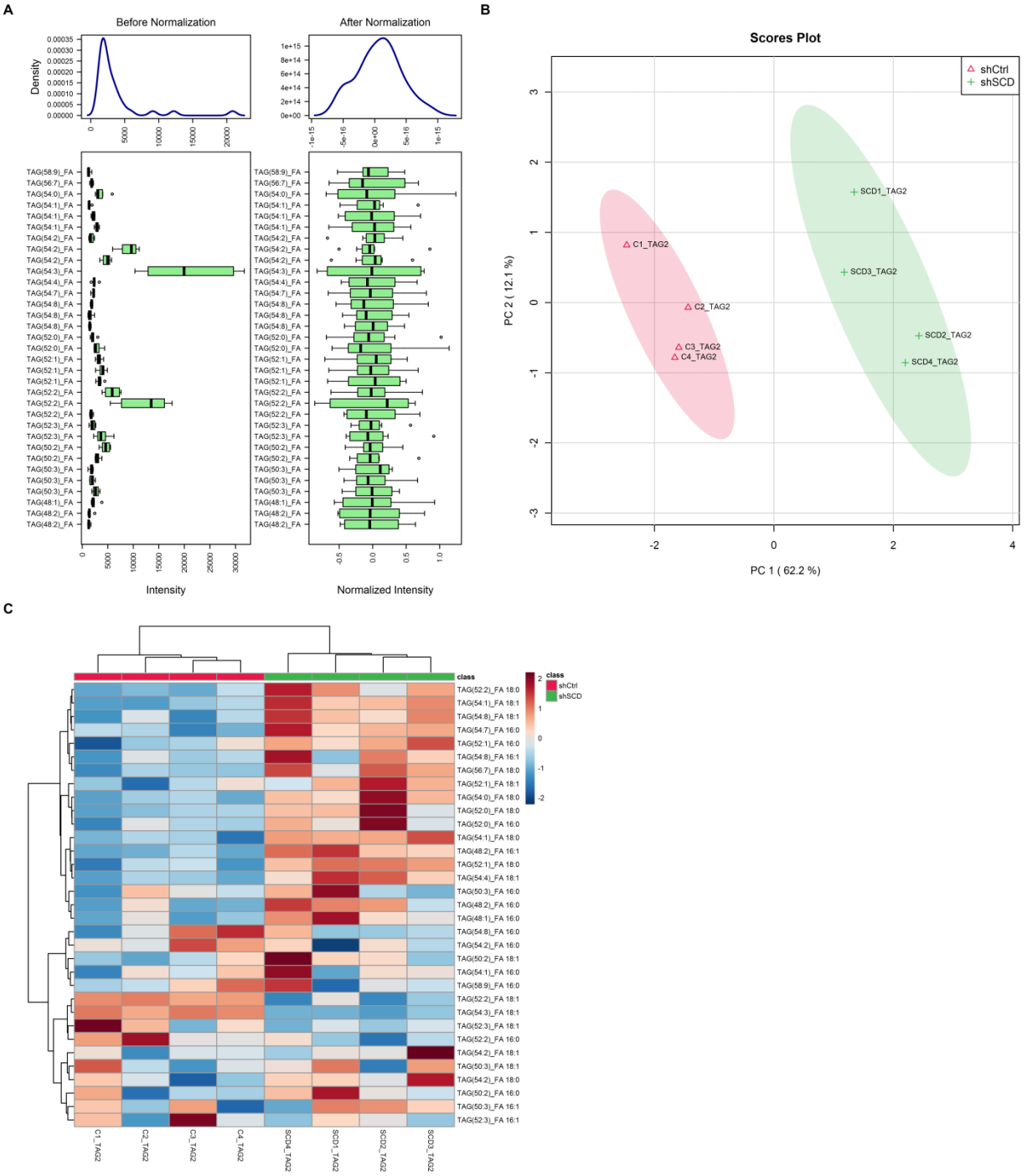

Figure 3-7 Quality control of lipidomics analysis of triacylglycerols 2.

(A-C) Normalization plot, principal component analysis and hierarchical clustering of triacylglycerols 2 from lipidomics profiling of shCtrl and shSCD OVCAR-5 cells cultured under low serum condition for 48 hours.

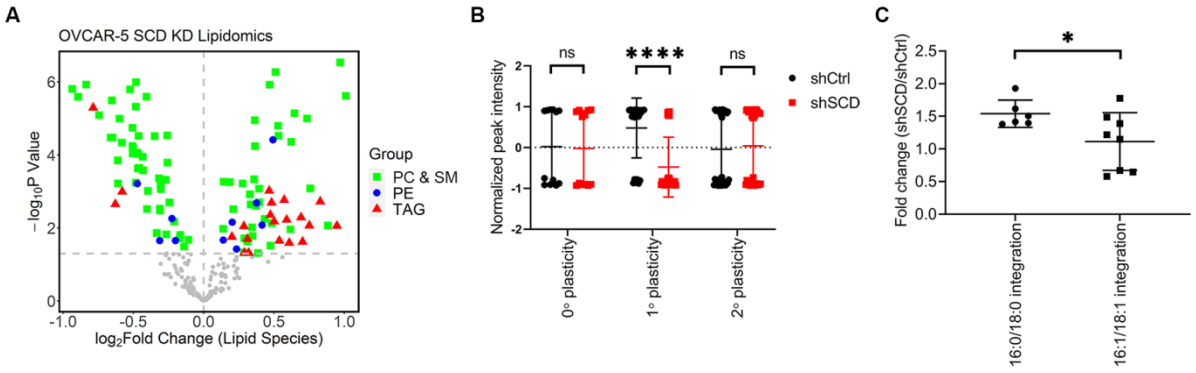

Figure 3-8 Global and lipid species-specific changes in ovarian cancer cells when restricting monounsaturated fatty acids.

(A) Volcano plot of changes in phosphatidylcholine and sphingomyelin (PC & SM, green), phosphatidylethanolamine (PE, blue) and triacylglycerol (TAG, red) relative peak intensities measured by lipidomics profiling analysis in shSCD vs shCtrl OVCAR-5 cells cultured in low serum conditions for 48 hours. (B) Normalized peak intensities of phosphatidylcholine (PC) lipids with differing fatty chain plasticity (0°, no carbon-carbon double bond; 1°, 1 or 2 carbon-carbon double bonds; 2°, more than 2 carbon-carbon double bonds) in shSCD vs shCtrl OVCAR-5 cells. ShSCD cells have significantly fewer 1° PC lipids than shCtrl cells whereas no difference was observed for 0° or 2° PC lipids. (C) Fold change of triacylglycerol (TAG) lipids containing 16:0 or 18:0 fatty acyl chains integration and 16:1 or 18:1 fatty acyl chains integration

determined by lipidomics profiling analysis in shSCD vs shCtrl OVCAR-5 cells. * $p < 0.05$, **** $p < 0.0001$.

3.4 SCD knock down triggers ER stress response

To further understand the global effects of UFA restriction in OC cells, RNA-seq compared the transcriptomic profiles of cells transduced with shRNA targeting SCD or control shRNA. Quality control of RNA-sequencing is included in Figure 3-9. Cells were cultured under low serum conditions for 48 hours. There were 1513 DEGs (FDR < 0.05), of which 707 were upregulated and 806 downregulated between OVCAR-5 cells stably transduced with control or shRNA targeting SCD (Figure 3-10 A). Gene Ontology analysis of significantly upregulated genes revealed that the ER stress response was the top affected pathway by SCD KD (Figure 3-10 B). Gene Set Enrichment Analysis (GSEA) of all genes also indicated that ER stress response gene sets (Hallmark Unfolded Protein Response; Reactome_IRE1α Activities Chaperones, Reactome PERK Regulates Gene Expression, Reactome ATF4 Activities Genes in Response to Endoplasmic Reticulum Stress) were upregulated in cancer cells in which SCD was knocked down (Figure 3-10 C). Several genes (DNA damage-inducible transcript 3 (*DDIT3*), activating transcription factor 3 (*ATF3*), protein phosphatase 1 regulatory subunit 15A (*PPP1R15A*), CCAAT enhancer binding protein beta (*CEBPB*)) involved in ER stress response are highlighted in the volcano plot depicting DEGs between SCD KD and control cells (Figure 3-10 A). Furthermore, upstream regulator analysis performed with IPA software identified several transcription factors (activating transcription factor 4 (*ATF4*), *DDIT3*, Nuclear protein 1,

transcriptional regulator (*NUPR1*)) involved in the ER stress response pathway among the top ones predicted to be activated in OC cells transduced with shRNA targeting *SCD* vs control cells (Figure 3-10 D). A heatmap including significant genes in the ER stress response pathway (n = 64 genes) illustrates clear differences in expression levels for these transcripts between cells in which SCD was knocked down vs. control cells (Figure 3-10 E).

General Statistics

Copy table | Configure Columns | Plot | Showing 6/16 rows and 3/9 columns.

Sample Name	M Aligned	% GC	M Seqs
OVCAR5-shCtrl-1_S8_R1_001	49%	32.6	
OVCAR5-shCtrl-2_S13_R1_001	50%	20.1	
OVCAR5-shCtrl-3_S15_R1_001	50%	29.3	
OVCAR5-shSCD-1_S5_R1_001	49%	28.2	
OVCAR5-shSCD-2_S19_R1_001	51%	18.3	
OVCAR5-shSCD-3_S1_R1_001	51%	29.3	

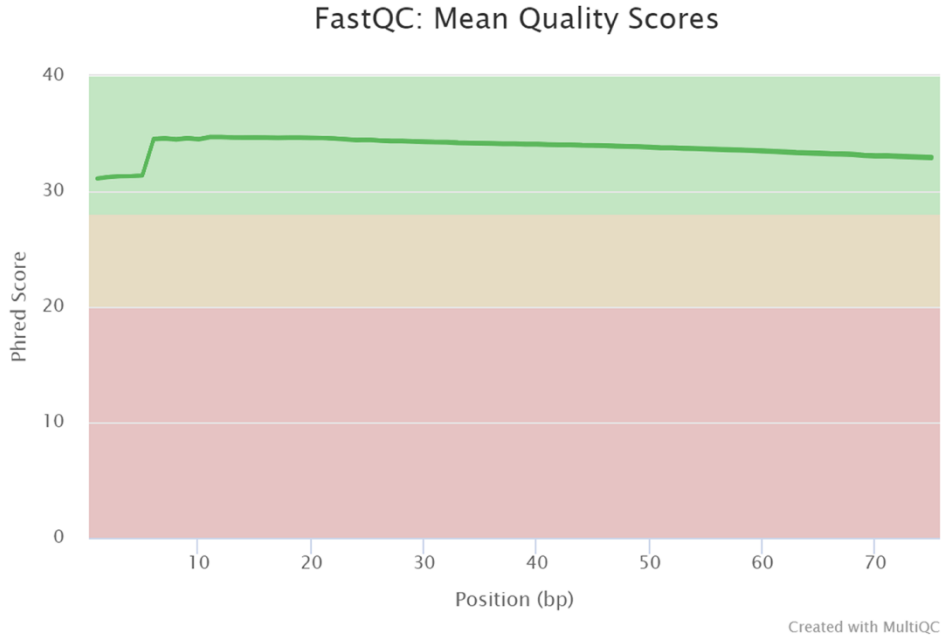

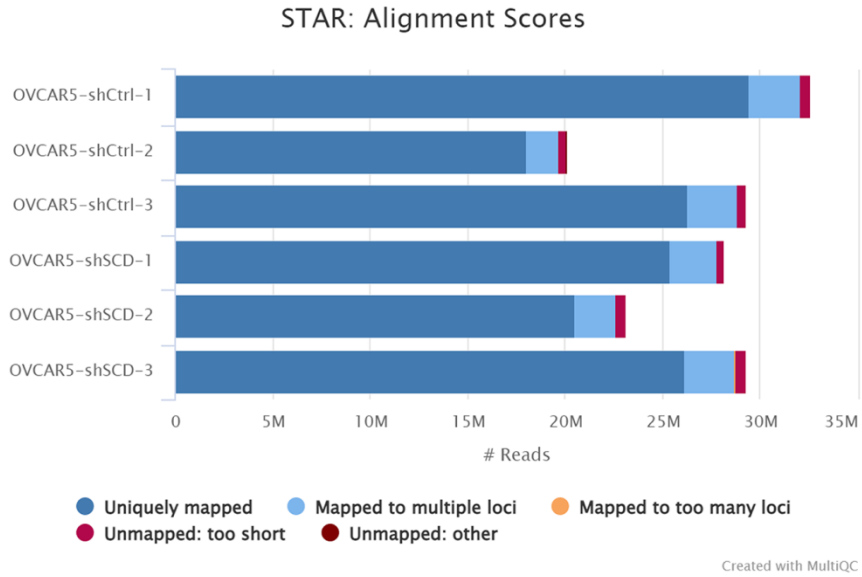

Figure 3-9 Quality control of RNA-seq analysis.

Quality control of RNA-seq analysis of shCtrl and shSCD OVCAR-5 cells cultured under low serum condition for 48 hours.

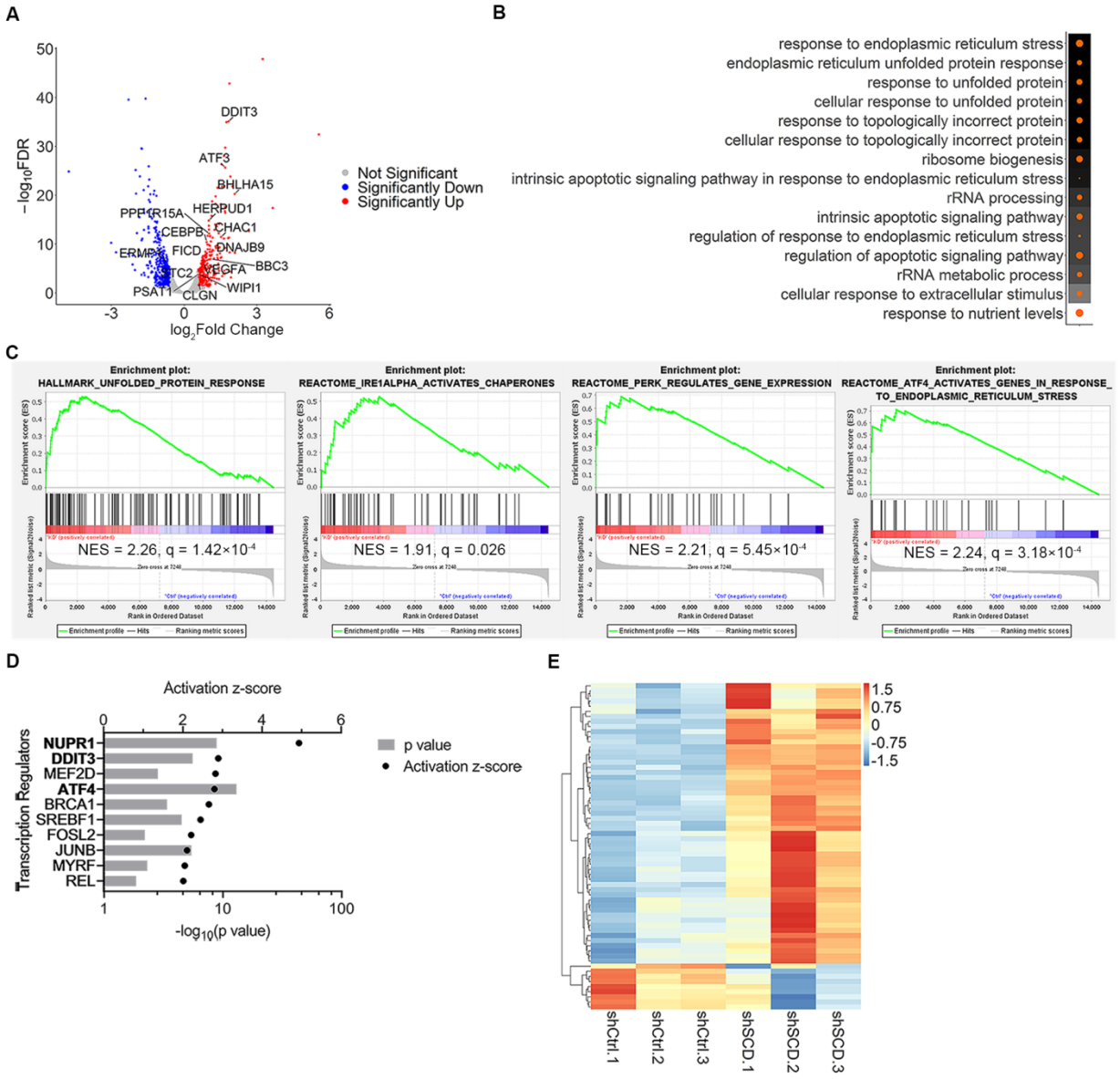

Figure 3-10 Restricting monounsaturated fatty acids activates the endoplasmic reticulum stress response pathway.

(A) Volcano plot of changes in gene expression measured by RNA-seq in shSCD vs shCtrl OVCAR-5 cells. Red dots represent upregulated genes and blue dots, downregulated genes. Genes of the ER stress response pathway are indicated by lines. (B) Dot plot of the top 15 enriched Gene Ontology terms identified by analysis of upregulated genes (RNA-seq) in shSCD vs shCtrl OVCAR-5 cells. Dot size corresponds to ratio of genes on the pathway vs total number of upregulated genes. Background color corresponds to FDR q value. (C) Enrichment plots generated by Gene Set Enrichment Analysis of gene expression (RNA-seq normalized counts) in OVCAR-5 shSCD vs shCtrl using Hallmark and C2 gene sets from Molecular Signatures Database. (D) Top ten significant upstream regulators identified by Ingenuity Pathway Analysis using DEGs from RNA-seq analysis of OVCAR-5 shSCD vs shCtrl cells. Transcription factors involved in the ER stress response pathway are in bold characters. (E) Heatmap of expression (RNA-seq normalized counts) and supervised hierarchical clustering of significant genes of the ER stress response pathway in shCtrl and shSCD OVCAR-5 cells (n = 3).

Further, exploration of the transcriptomic dataset associated with the Cancer Dependence Map [461] and Cancer Cell Line Encyclopedia [465] shows that dependency score of key transcription regulators in the ER stress response pathway such as *ATF4* and *DDIT3* were positively correlated with that of SCD (r = 0.3117 and 0.3878 respectively, Figure 3-11 A and B), indicating that OC cells that are highly dependent on SCD also have higher dependency on

ATF4/DDIT3. Additionally, expression levels of several important ER stress response genes (insulin like growth factor binding protein 1 (*IGFBP1*), endoplasmic reticulum to nucleus signaling 1 (*ERN1*), thioredoxin interacting protein (*TXNIP*), nucleic acid binding protein 1 (*NABP*1)) were negatively correlated with SCD (Figure 3-11 C-F), corroborating the association between SCD and ER stress response found through transcriptomic analysis.

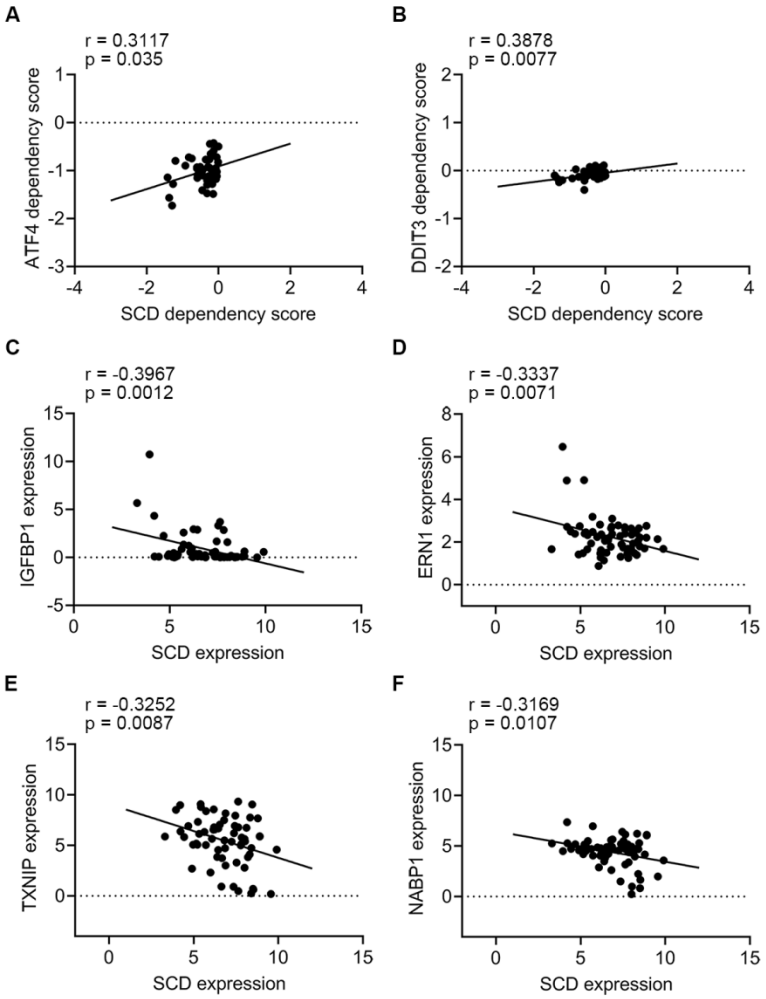

Figure 3-11 Co-dependency of SCD with ER stress response transcription regulators and co-expression of SCD with ER stress response genes.

(A, B) Pearson correlation analysis of dependency scores of SCD, ATF4 (A), and DDIT3 (B) in ovarian cancer cell lines (n = 46 cell lines). (C-F) Pearson correlation analysis between mRNA expression of SCD with IGFBP1 (C), ERN1 (D), TXNIP (E), and NABP1 (F) in ovarian cancer cell lines (n = 64 cell lines).

3.5 Excess SFAs caused by depletion or pharmacological inhibition of SCD induces ER stress

To further investigate how the imbalance between SFAs and UFAs caused by SCD depletion or inhibition in cancer cells activates the ER stress responses, we next evaluated the two key sensing mechanisms of this pathway: activation of endoribonuclease inositol-requiring enzyme 1α (IRE1α) and protein kinase R (PKR)-like endoplasmic reticulum kinase (PERK). ER-spanning transmembrane domain of IRE1α and PERK are critical sensors of the levels of lipid saturation in the cell and activate the ER stress response [466]. IRE1α causes splicing of the X-box-binding protein 1 (XBP1) mRNA which leads to a spliced form (XBP1s) with potent transcriptional activity [467]. PERK autophosphorylates itself upon ER stress and then phosphorylates the eukaryotic translation initiation factor 2α (eIF2α) to halt translation of proteins [468]. Translation of ATF4 mRNA, due to its unique 5’ untranslated region (5’ UTR) sequence, is upregulated upon phosphorylation of eIF2α [469].

XBP1 splicing was assessed in OVCAR-5 cells stably transduced with shRNA targeting SCD or control shRNA or in cells treated with the SCD inhibitor, CAY10566. Increased baseline XBP1s levels were noted in OVCAR-5 and OVCAR-8 cells transduced with shRNA targeting SCD vs

control and cultured in low serum medium or in 10% lipid depleted serum for 48 hours (Figure 3-12 A-C). XBP1 splicing was also increased in OVCAR-5 and OVCAR-8 cells transduced with shRNA targeting SCD vs control even under full serum conditions, but to a lesser degree (Figure 3-12 D and E). Additionally, activation of PERK/ C/EBP homologous protein (CHOP) was detected in shSCD vs shCtrl stably transduced OVCAR-8 cells (Figure 3-12 F) under low serum conditions.

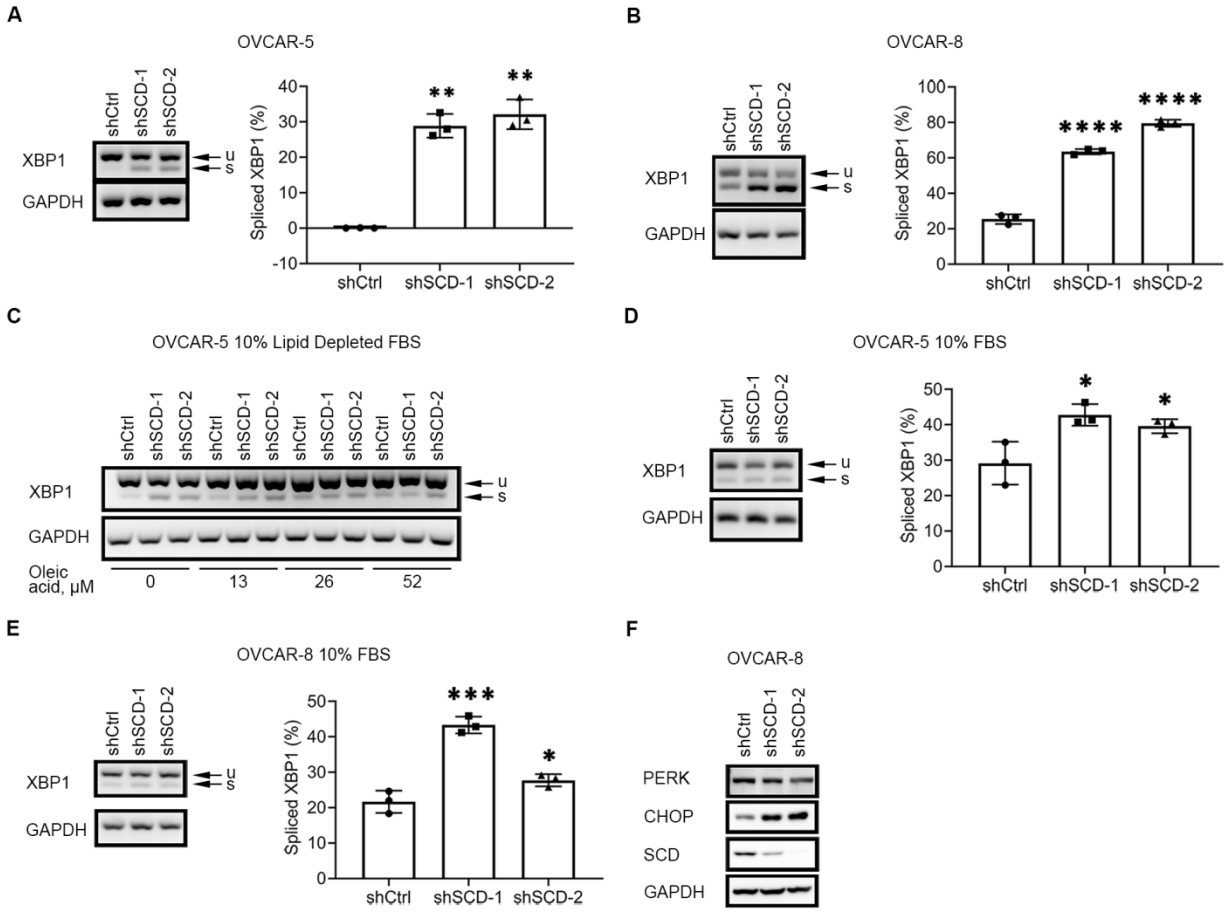

Figure 3-12 The IRE1α/XBP1 axis of the ER stress response pathway are activated in ovarian cancer cells under restricted availability of unsaturated fatty acid.

(A, B) XBP1 splicing (u, unspliced transcript; s, spliced transcript) measured by RT-PCR and agarose-gel electrophoresis in OVCAR-5 (A) and OVCAR-8 (B) cells transduced with control shRNA (shCtrl) or shRNAs (1 or 2) targeting SCD (shSCD) and cultured in low serum conditions (1% FBS) for 48 hours. Densitometric analysis of XBP1 splicing products shown in left panel. Bars represent percent of spliced XBP1 relative to total XBP1 (mean ± SD, n = 3). (C) XBP1 splicing (u, unspliced transcript; s, spliced transcript) measured by RT-PCR and agarose gel electrophoresis in OVCAR-5 cells transduced with control shRNA (shCtrl) or shRNAs (1 or 2) targeting SCD (shSCD), cultured in medium containing 10% lipid depleted FBS, and treated with indicated doses of OA for 48 hours. (D, E) XBP1 splicing (u, unspliced transcript; s, spliced transcript) measured by RT-PCR and agarose-gel electrophoresis in OVCAR-5 (D) and OVCAR-8 (E) cells transduced with control shRNA (shCtrl) or shRNAs (1 or 2) targeting SCD (shSCD) and cultured in full serum conditions for 48 hours. Densitometric analysis of XBP1 splicing products is shown on the right. Bars represent percent of spliced XBP1 (mean ± SD, n = 3). (F) Western blot of SCD and proteins of the PERK/eIF2α/ATF4 axis in OVCAR-8 shCtrl and shSCD cells cultured in low serum medium for 48 hours. * $p < 0.05$, *** $p < 0.001$, **** $p < 0.0001$.

Likewise, a dose-dependent increase in XBP1s levels was observed in OVCAR-5 cells treated with CAY10566 under low serum conditions (Figure 3-13 A and B), in 10% lipid depleted serum (Figure 3-13 C) and in full serum (Figure 3-13 D). Having hypothesized that the major trigger of ER stress induced by SCD depletion is the excess of SFAs, XBP1 splicing and activation of PERK/eIF2α/ATF4 were measured in OC cells in which SCD was either knocked down or

pharmacologically inhibited in the presence of exogenously added SFA (palmitic acid, PA). We chose a concentration of PA (50 μM) equivalent to that found in media supplemented by 10% FBS [434]. Further, as the consequences of ER stress depend on both the length of exposure to cellular stress and the severity of the stress [470], time-dependency was assessed along both the IRE1α/XBP1 and the PERK/eIF2α/ATF4 axes in OC cells supplemented with PA. The XBP1 splicing signal was increased in OC cells in which SCD was knocked down compared with control cells after supplementation with 50 μM of PA, peaking at approximately 8-12 hours and diminishing at 24 hours (Figure 3-13 E). Likewise, western blotting analysis of the PERK/eIF2α/ATF4 axis showed increased phosphorylation levels of eIF2α in OC cells in which SCD was knocked down, starting 2 hours after addition of PA and peaking at 8-12 hours (Figure 3-13 F). The downstream transcription factors ATF4 and CHOP were upregulated starting 4 hours after addition of PA and remaining persistently high up to 24 hours.

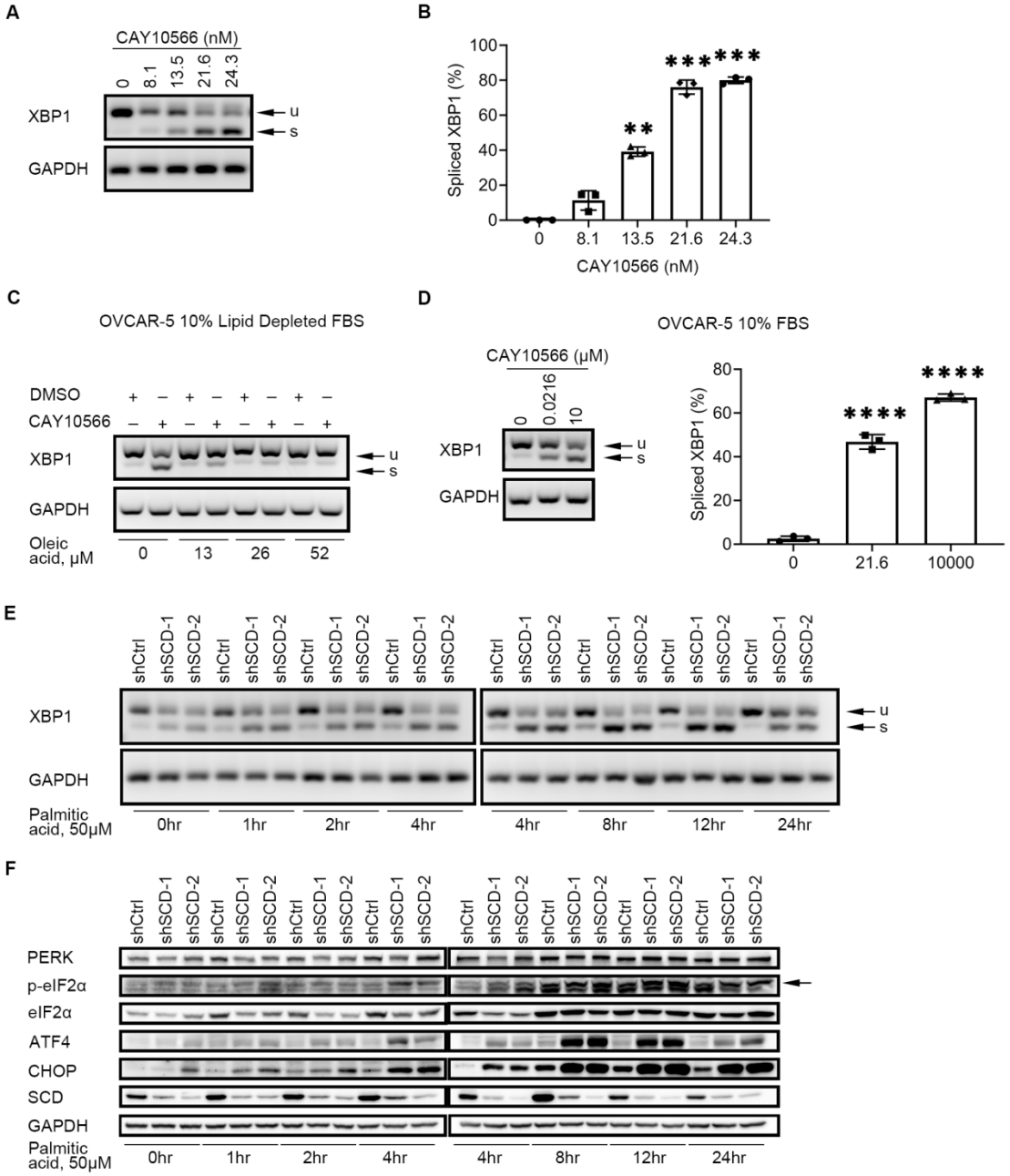

Figure 3-13 The IRE1α/XBP1 and PERK/eIF2α/ATF4 axes of the ER stress response pathway are activated in ovarian cancer cells under restricted availability of unsaturated fatty acid.

(A) XBP1 splicing (u, unspliced transcript; s, spliced transcript) in OVCAR-5 cells cultured in low serum conditions and treated with SCD inhibitor CAY10566 for 48 hours. (B) Percent of spliced XBP1 isoform measured by densitometric analysis of PCR products shown in C (mean ± SD, n = 3). (C) XBP1 splicing (u, unspliced transcript; s, spliced transcript) in OVCAR-5 cells cultured in medium containing 10% lipid depleted FBS and treated with 21.6 nM CAY10566 and indicated doses of OA for 48 hours. (D) XBP1 splicing (u, unspliced transcript; s, spliced transcript) in OVCAR-5 cells cultured in full serum conditions and treated with SCD inhibitor CAY10566 for 48 hours. (E, F) XBP1 splicing (u, unspliced transcript; s, spliced transcript) (E), and western blot of proteins of the PERK/eIF2α/ATF4 axis (F) in shCtrl and shSCD OVCAR-5 cells cultured under low serum conditions and treated with 50 μM PA for the time periods indicated. ** $p < 0.01$, *** $p < 0.001$, **** $p < 0.0001$.

To confirm these observations in human specimens, we used primary tumor cells dissociated from freshly obtained HGSOC tumors (Table 6). Treatment with CAY10566 induced XBP1 splicing in primary HGSOC cells and the XBP1s levels were further augmented by addition of PA (Figure 3-14).

Table 6. Information for the ovarian cancer tumors used in this study

Patient ID	Final pathology report	Tumor origin
81	high grade serous carcinoma (stage IIIC)	omentum
83	high grade serous carcinoma (stage IIIC)	ovary

85	high grade serous carcinoma (stage IIIC)	omentum

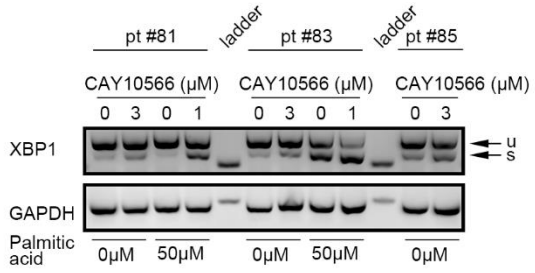

Figure 3-14 The IRE1α/XBP1 axis of the ER stress response pathway is activated in primary tumor cells isolated from ovarian cancer patients under restricted availability of unsaturated fatty acid.

XBP1 splicing (u, unspliced transcript; s, spliced transcript) in primary cells from tumors of three ovarian cancer patients cultured in low serum conditions and treated with 3 μM CAY10566 (SCD inhibitor) for 48 hours, or with 1 μM CAY10566 and 50 μM palmitic acid for 12 hours.

Next, to visualize the status of the ER under these conditions, hSRS imaging was performed after treating OVCAR-5 cells stably transduced with control or shRNA targeting SCD with PA-d31 under low serum condition (Figure 3-15 A). Most of OVCAR-5 shCtrl cells displayed C-D signal derived from PA-d31 in lipid droplet (LD) (depicted as a dot, gray arrow), while a considerable portion of OVCAR-5 shSCD cells displayed the C-D signal on rigid ER (shown as a linear structure, yellow arrow), consistent with an ER stress related morphology [471]. Both cell lines contained a small portion of cells harboring detectable C-D signal all over the

cytoplasm (Figure 3-15 A, blue arrow). After PA-d31 treatment alone under low serum conditions, the cell population with rigid ER structures represented the major population of OVCAR-5 shSCD cells, while the cell population with detectable C-D signal in LD was the majority in OVCAR-5 shCtrl cells (Figure 3-15 A and B). Rescue treatment with UFA (OA or full serum medium) led to the disappearance of rigid ER and increased PA-d31 accumulation in lipid droplets for both shSCD and shCtrl OC cells (Figure 3-15 A and B), suggesting that supplementation with UFAs can rescue SFA-induced ER stress and facilitate SFA storage in LD. These data support that the balance of intracellular SFA and UFA is essential to prevent ER stress.

Further, examination of OVCAR-5 cells stably transduced with control or shRNA targeting SCD cultured in low serum medium for 48 hours by using transmission electron microscopy (TEM) demonstrated smooth ER membrane disorganization and irregular and compromised smooth ER structure in OVCAR-5 shSCD cells compared to shCtrl cells (Figure 3-15 C), confirming the biochemical and hSRS imaging results.

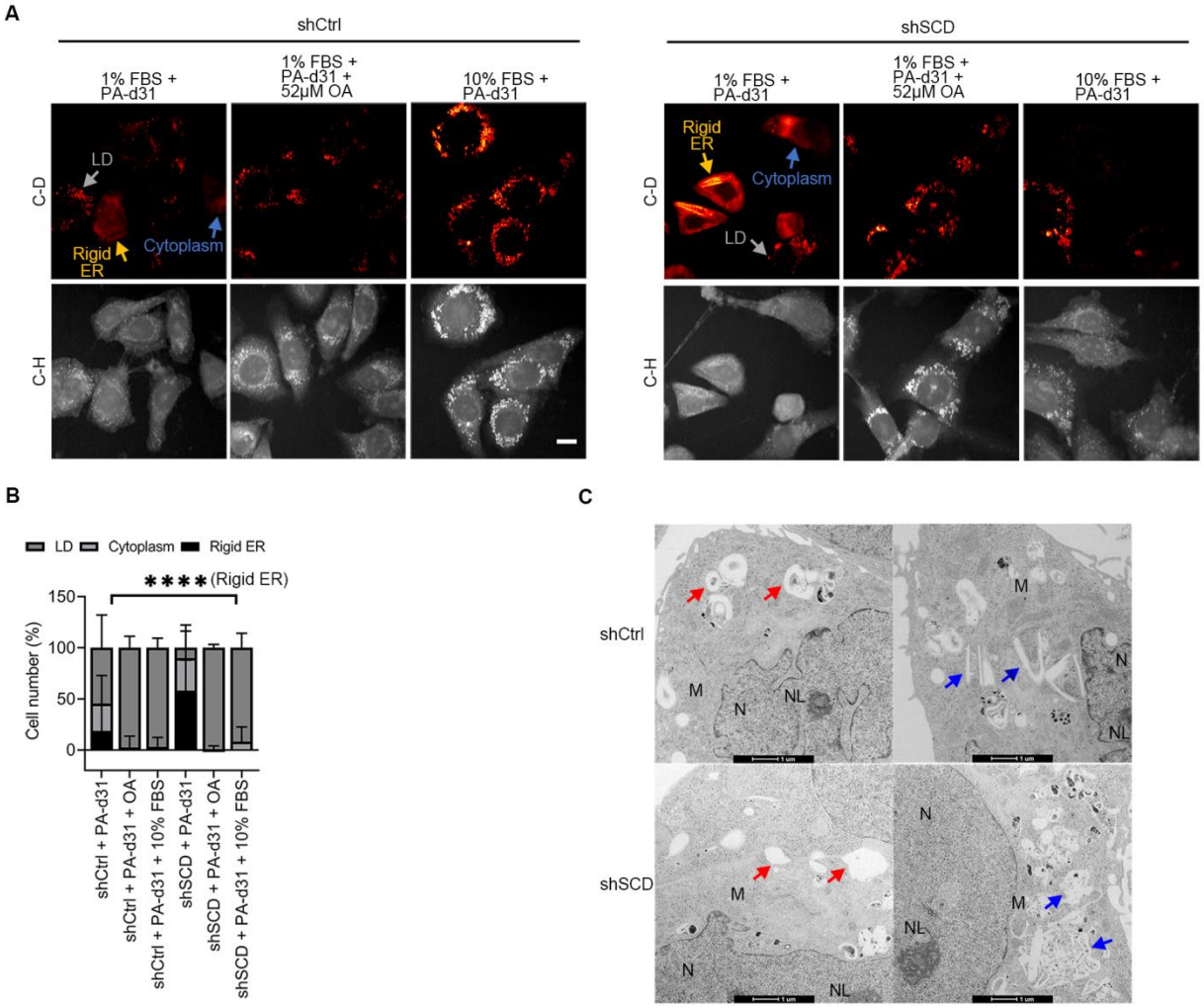

Figure 3-15 Visualization of the ER stress response pathway in ovarian cancer cells at cellular and subcellular level under restricted availability of unsaturated fatty acid.

(A) Representative SRS images in the C-H and C-D regions of OVCAR-5 shCtrl and shSCD cells cultured in low serum conditions (1% FBS) and treated with 12.5 μM PA-d31, with or without 52 μM OA, or cultured in medium with full serum (10% FBS) and treated with PA-d31 for 24 hr. Yellow arrows indicate rigid ER, gray arrows indicate lipid droplet (LD), and blue arrows indicate cytoplasm. Scale bar: 20 μm. (B) Percentages of shCtrl and shSCD OVCAR-5

cells treated as described in (A) showing C-D SRS signal mainly in rigid ER, lipid droplet (LD), and cytoplasm (n = 139-191). Yuying Tan helped with image acquisition and data analysis. (C) TEM imaging of smooth ER (donut shaped, red arrows; ski board shaped, blue arrows) in OVCAR-5 shCtrl vs shSCD cells cultured in low serum conditions for 48 hours. Other organelles are highlighted (M, mitochondria; N, nucleus; NL, nucleolus). **** $p < 0.0001$.

3.6 UFAs prevent ER stress in OC cells

To exclude the contribution of potential desaturase-independent functions of SCD to the induction of ER stress in OC cells, we examined whether the effects of SCD depletion or inhibition could be rescued by OA, its main enzymatic product. Supplementation with OA reversed XBP1 splicing in OVCAR-5 cells in which SCD was knocked down (Figure 3-12 C and Figure 3-16 A), as well as in OVCAR-5 cells depleted of SCD and treated with PA (Figure 3-16 B). Likewise, supplementation with OA reduced the up-regulation of ATF4 and CHOP along the PERK/eIF2α/ATF4 axis observed in OVCAR-5 cells stably transduced with shRNA targeting SCD and maintained under low serum conditions (Figure 3-16 C and D). Similar rescue effects of OA on XBP1 splicing were observed in OVCAR-8 and PEO1 cells stably transduced with shRNA targeting SCD (Figure 3-16 E and F).

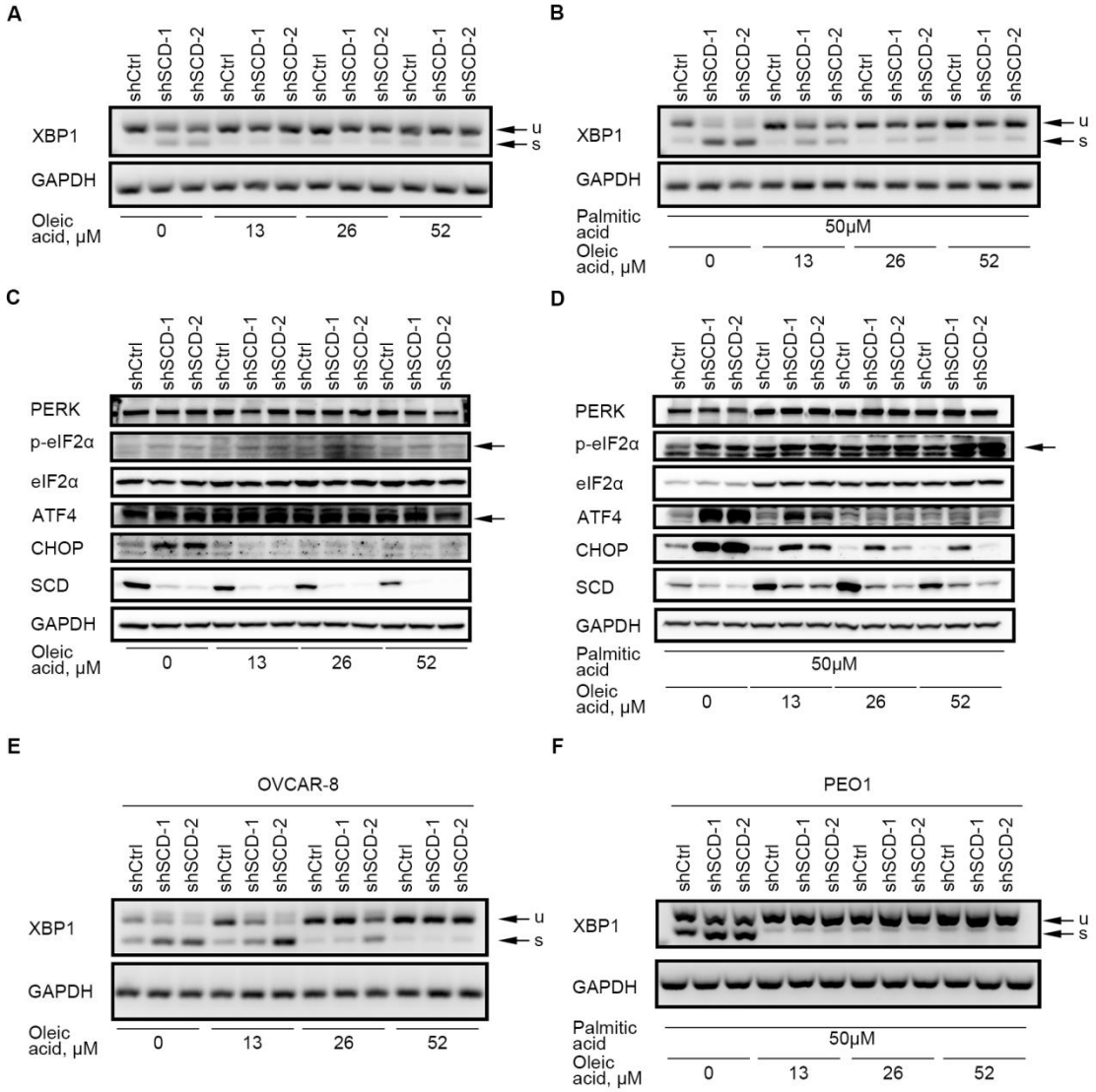

Figure 3-16 SCD knockdown and saturated fatty acid-induced ER stress response is reversed by exogenous oleic acid.

(A, B) XBP1 splicing (u, unspliced transcript; s, spliced transcript) measured by RT-PCR and agarose gel electrophoresis in OVCAR-5 cells transduced with control shRNA (shCtrl) or shRNAs (1 or 2) targeting SCD (shSCD), cultured in medium containing low serum, and treated with indicated doses of OA for 48 hours (A), or with 50 μM PA and indicated doses of OA for

12 hours (B). (C, D) Western blot of SCD and proteins of the PERK/eIF2α/ATF4 axis in shCtrl and shSCD cells cultured in low serum medium, and treated with different doses of OA for 48 hours (C), or with 50 μM PA and indicated doses of OA for 12 hours (D). (E) XBP1 splicing (u, unspliced transcript; s, spliced transcript) measured by RT-PCR and agarose gel electrophoresis in OVCAR-8 cells transduced with control shRNA (shCtrl) or shRNAs (1 or 2) targeting SCD (shSCD), cultured in medium containing low serum, and treated with indicated doses of oleic acid for 48 hours. (F) XBP1 splicing (u, unspliced transcript; s, spliced transcript) measured by RT-PCR and agarose gel electrophoresis in PEO1 cells transduced with control shRNA (shCtrl) or shRNAs (1 or 2) targeting SCD (shSCD), cultured in medium containing low serum, and treated with 50 μM palmitic acid and indicated doses of oleic acid for 12 hours.

Likewise, supplementation with OA reduced XBP1s levels in OVCAR-5 cells treated with CAY10566 (Figure 3-13 C and Figure 3-17 A), as well as XBP1s levels in cells treated with CAY10566 and PA (Figure 3-17 B). OA also reduced the upregulation of ATF4 and CHOP induced by the SCD inhibitor in OVCAR-5 cells maintained under low serum conditions (Figure 3-17 C) or in cells treated with 50 μM PA (Figure 3-17 D).

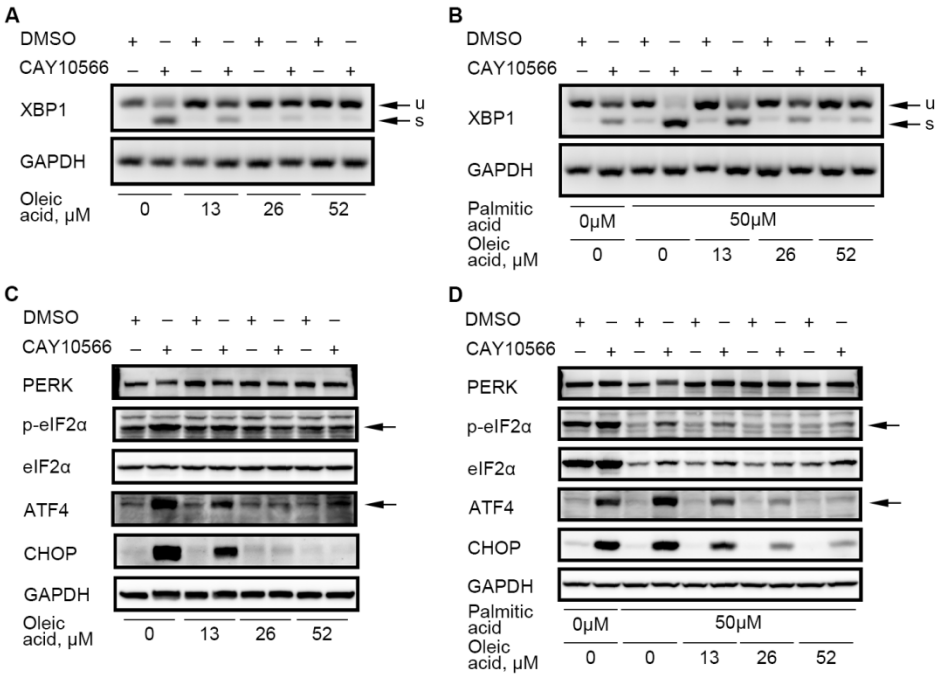

Figure 3-17 SCD inhibition and saturated fatty acid-induced ER stress response is reversed by exogenous oleic acid.

(A, B) XBP1 splicing (u, unspliced transcript; s, spliced transcript) in OVCAR-5 cells cultured in medium containing low serum and treated with 21.6 nM CAY10566 and indicated doses of OA for 48 hours (A), or with 8.1 nM CAY10566, 50 μM PA and indicated doses of OA for 12 hours (B). (C) Proteins of the PERK/eIF2α/ATF4 pathway measured by western blot in OVCAR-5 cells treated as described in (A). (D) Western blot of proteins of the PERK/eIF2α/ATF4 pathway in OVCAR-5 cells treated as described in (B). Arrows indicate the band of interest.

Lastly, to test the sufficiency of SCD in regulating ER stress triggered by an imbalance of SFA and UFA in OC cells, the enzyme was overexpressed in OVCAR-5 cells. Increased SCD *mRNA*

and protein levels were observed in cells stably transfected with pLenti-SCD compared to pLenti-Ctrl (Figure 3-18 A and B). XBP1 splicing induced by addition of PA in control cells was significantly reduced by SCD overexpression (Figure 3-18 C and D, p = 0.0277). Collectively, our data support the significance of the balance between SFAs and UFAs regulated by SCD in fine tuning the functions of the ER, likely mediated through direct effects on the ER membrane.

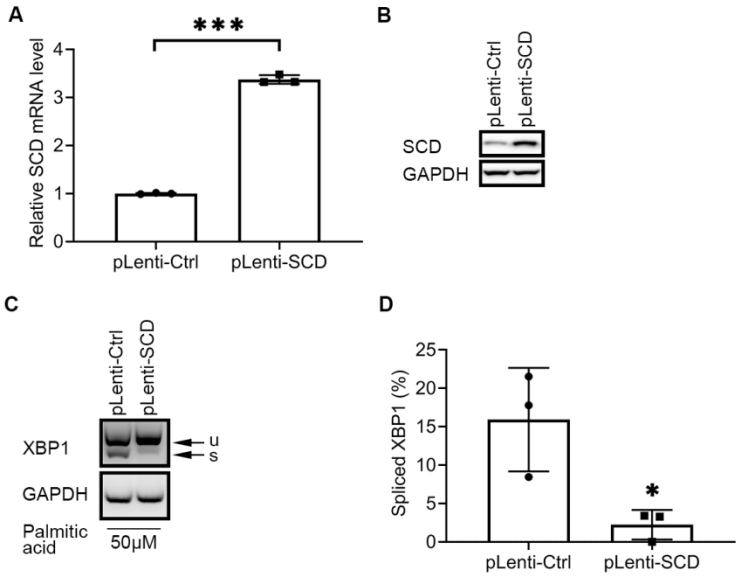

Figure 3-18 Saturated fatty acid-induced ER stress response is reversed by SCD overexpression.

(A, B) Verification of SCD overexpression by qRT-PCR (A) and western blotting (B) in OVCAR-5 cells transduced with a SCD expression vector (pLenti-SCD). Cells transduced with empty vector (pLenti-Ctrl) served as control. Bars represent means ± SD, n = 3. (K) XBP1 splicing (u, unspliced transcript; s, spliced transcript) in pLenti-SCD vs pLenti-Ctrl cells cultured in low serum conditions and treated with 50 μM PA for 12 hours. (L) Percent of spliced isoform

(mean ± SD, n = 3) calculated by densitometric analysis of PCR products shown in (K). *** $p < 0.001$.

3.7 SCD depletion or inhibition induces apoptosis of OC cells

It is accepted that long-term exposure to mild ER stress or short-term exposure to severe ER stress leads to CHOP-mediated apoptosis [470]. We therefore hypothesized that OC cells depleted of SCD and cultured under low serum conditions over long period of time would undergo apoptosis. IncuCyte imaging examining Annexin V staining showed increased percentage of apoptotic cells among OVCAR-5 SCD KD cells cultured in low serum medium compared with control cells. Supplementation with OA rescued the phenotype (Figure 3-19 A). Further, addition of PA (50 μM) induced early onset of apoptosis in shSCD cells as compared to shCtrl cells, and supplementation with OA reversed the phenotype (Figure 3-19 B). Likewise, CAY10566 induced apoptosis in OVCAR-5 cells; while OA supplementation blocked this effect (Figure 3-19 C). Addition of PA to CAY10566 caused earlier onset of apoptosis (less than 24 hours) and augmented cell death (Figure 3-19 D), while OA rescued the phenotype (Figure 3-19 D).

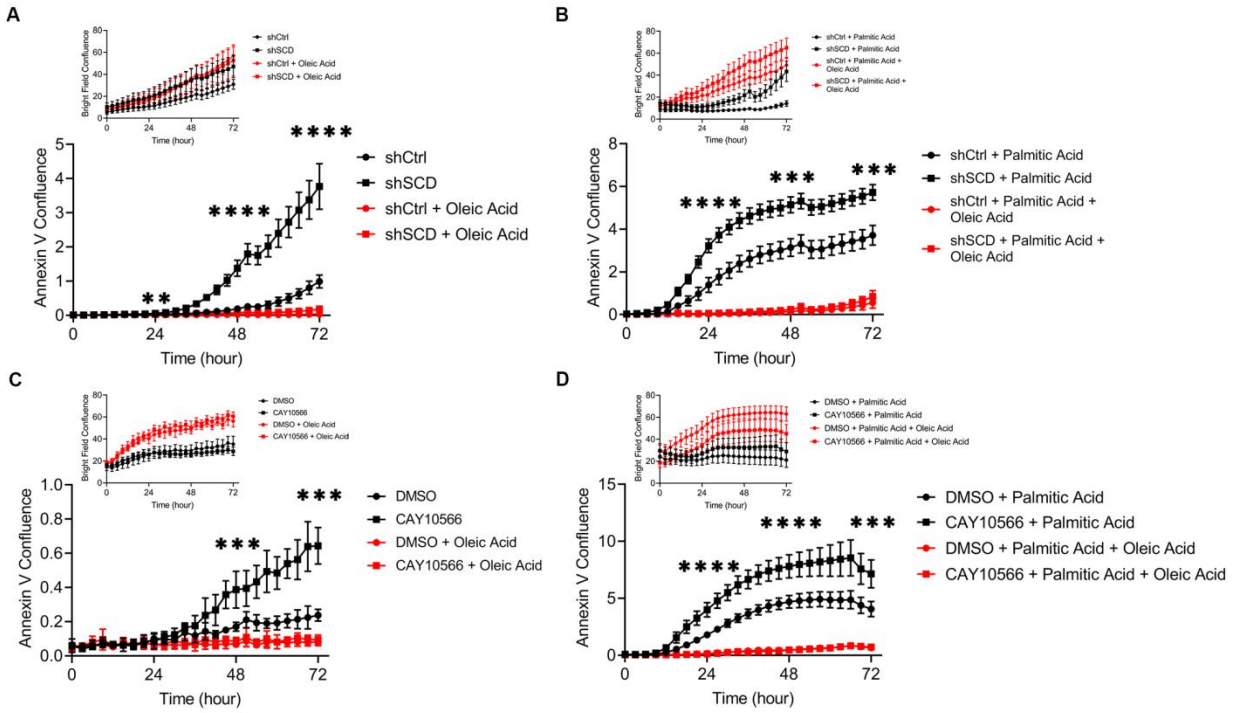

Figure 3-19 Apoptosis induced by SCD inhibition, or treatment with PA, is attenuated by exogenous oleic acid.

(A-B) Time-lapse imaging of Annexin V staining (bright field signal as inset) to measure apoptosis in OVCAR-5 cells transduced with control shRNA (shCtrl) or shRNA targeting SCD (shSCD), cultured in low serum conditions, and treated with 52 μM OA (A), or with 50 μM PA alone or in combination with 52 μM OA (B). (C-D) Time-lapse of Annexin V imaging (bright field signal as inset) to measure apoptosis in OVCAR-5 cells cultured in low serum conditions and treated with 21.6 nM CAY10566, 52 μM OA or combination (C), or with 8.1 nM CAY10566, 50 μM PA, 52 μM OA, or combinations (D). Values in panels A-D are means ± SD, n = 6. ** $p < 0.01$, *** $p < 0.001$, **** $p < 0.0001$.

To confirm the apoptosis phenotype, we examined cleaved caspase-3 levels. Increased caspase-3 cleavage was observed in OVCAR-5 shSCD compared to shCtrl cells (Figure 3-20 A) and this was reversed by OA (Figure 3-20 A). Caspase-3 cleavage was also induced by CAY10566, augmented by addition of PA and rescued by repletion of OA (Figure 3-20 B).

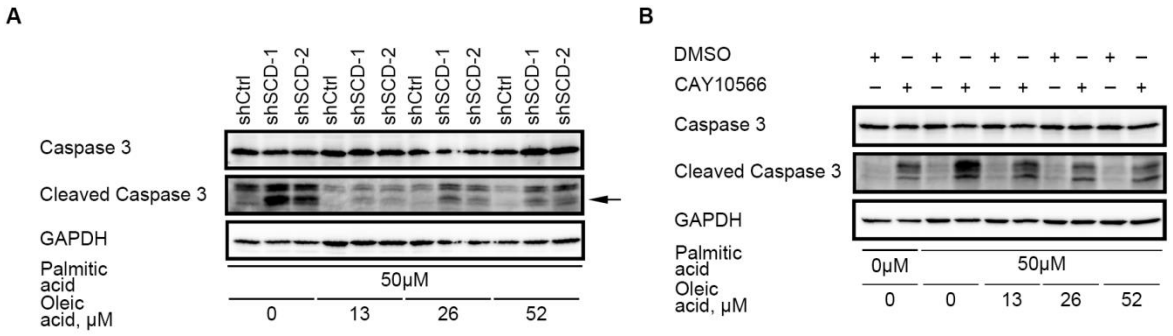

Figure 3-20 Cleavage of Caspase 3 induced by SCD inhibition, or treatment with PA, is attenuated by exogenous oleic acid.

(A) Western blot of full-length and cleaved caspase-3 in shSCD vs shCtrl cells cultured under low serum medium and treated with 50 μM PA and indicated doses of OA for 12 hours. (B) Western blot of full-length and cleaved caspase-3 in OVCAR-5 cells cultured in low serum medium and treated with 8.1 nM CAY10566, 50 μM PA and indicated doses of OA for 12 hours.

As the numbers of apoptotic cells appeared insufficient to explain the decreased numbers of surviving cells (insets Figure 3-19 A and C) and SCD inhibition had been shown to induce non-apoptotic cell death through ferroptosis [298], we examined whether SCD depletion or blockade could promote cell death through a combination of apoptosis and ferroptosis. C11 BODIPY

staining measured lipid peroxidation in cells in which SCD was knocked down or inhibited by CAY10566. A clear peak shift in the oxidized lipid channel was observed after SCD knockdown or inhibition (Figure 3-21 A), supporting induction of ferroptosis. Cell viability inhibited by CAY10566 was not rescued by either a caspase 3 inhibitor (Z-VAD-FMK) or by ferrostatin-1 (ferroptosis inhibitor) alone, but was blocked by the combination of Z-VAD-FMK) and ferrostatin-1 (Figure 3-21 B). Together these data support that decreased UFAs induced by SCD blockade or depletion blocks cell survival through both apoptosis and non-apoptotic cell death.

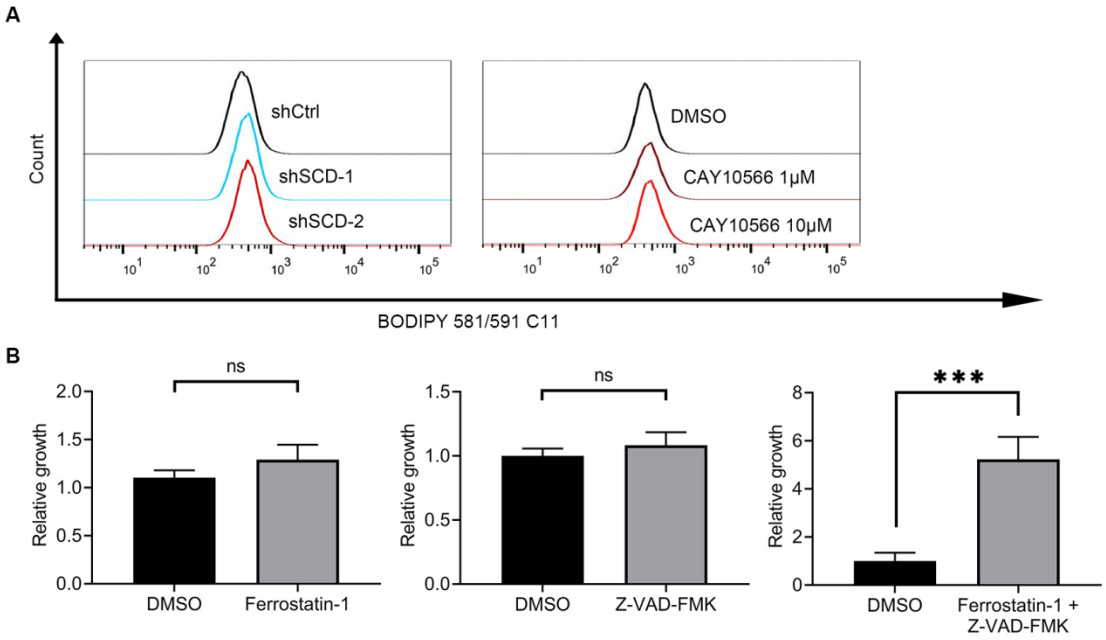

Figure 3-21 Concurrent onsets of apoptosis and ferroptosis in ovarian cancer cells upon SCD inhibition.

(A) Histogram of oxidized BODIPY 581/591 C11 dye in OVCAR-5 cells transduced with control shRNA (shCtrl) or shRNAs (1 or 2) targeting SCD (shSCD), cultured in medium containing low serum for 48 hours or in OVCAR-5 cells cultured in low serum conditions and

treated with different concentrations of CAY10566 (SCD inhibitor) for 48 hours. Dr. Yinu Wang helped with flow cytometry analyzer setup and data visualization. (B) Cell viability measured by CCK-8 in OVCAR-5 cells cultured in low serum conditions (1% FBS) and treated with 21.6 nM CAY10566, 25 μM Ferrostatin-1 and/or 25 μM Z-VAD-FMK for an additional 72 hours. *** $p < 0.001$.

Lastly, to test the sufficiency of SCD to this phenotype, OVCAR-5 cells in which SCD was overexpressed (pLenti-SCD) vs control cells (pLenti-Ctrl) were maintained under low serum and treated with PA. The percentage of apoptotic cells was significantly reduced in cells in which SCD was overexpressed compared to controls (Figure 3-22), supporting that OC cells with higher SCD expression could survive the stress induced by SFAs. Together, the data demonstrate that the UFAs, the direct product of SCD, act as a buffer against SFAs, promoting the survival of OC cells.

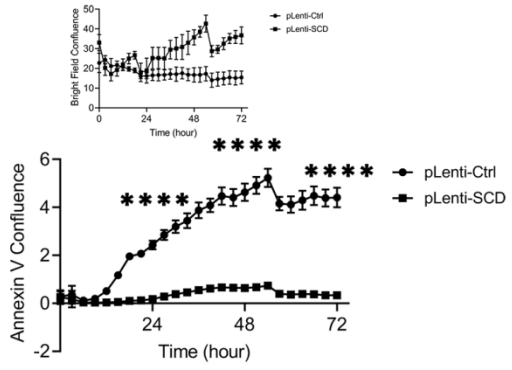

Figure 3-22 Apoptosis induced by SCD inhibition, or treatment with PA, is attenuated by SCD overexpression.

Time-lapse of Annexin V imaging (bright field signal as inset) to determine apoptosis in OVCAR-5 cells overexpressing SCD (pLenti-SCD) and control cells (pLenti-Ctrl), cultured in medium containing low serum and treated with 50 μM PA. Values in are means ± SD, n = 6. **** $p < 0.0001$.

3.8 SCD depletion or inhibition suppresses tumor growth in vivo

Whether the observed effects of SCD on cancer cell survival impact tumor progression *in vivo* remains unknown. Tumorigenicity of OC cells depleted of SCD was tested by using an intraperitoneal (i.p.) xenograft model in athymic nude mice. SCD knockdown compared to control OVCAR-5 cells led to significantly reduced tumor weight (234.3 mg vs. 360.1 mg, $p = 0.0343$) and tumor volume (209.2 mm^3 vs. 404.8 mm^3, $p = 0.0212$; Figure 3-23 A and B), although the numbers of peritoneal metastases (Figure 3-23 C, 208.8 vs. 217.3, $p = 0.7602$) and ascites volume (Figure 3-23 D) were similar between groups.

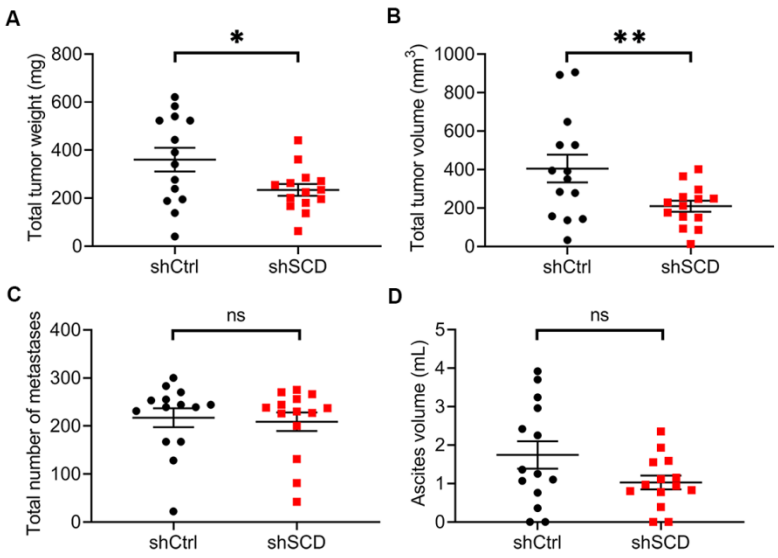

Figure 3-23 SCD knockdown inhibited growth of ovarian cancer intraperitoneal xenografts in mice.

(A-D) Total tumor weight (A), total tumor volume (B), total number of metastases (C) and ascites volume (D) in athymic nude mice intraperitoneally injected with OVCAR-5 cells transduced with control shRNA (shCtrl) or shRNA targeting SCD (shSCD), and evaluated after 28 days (values are means ± SE, n = 14 per group). Dr. Horacio Cardenas helped with cancer cell injection and mouse dissection. * $p < 0.05$, ** $p < 0.01$.

SCD knock down was maintained *in vivo*, as demonstrated by qRT-PCR (Figure 3-24 A, $p = 0.0015$) and increased XBP1s levels were detected in xenografts derived from OVCAR-5-shSCD compared to controls (Figure 3-24 B and C, $p = 0.0018$), supporting that an increased susceptibility to ER stress is maintained *in vivo* in tumors depleted of the enzyme. Similar

inhibitory effects on tumor growth were observed in a subcutaneous mouse xenograft model derived from OVCAR-3 cells stably transduced with shRNA targeting SCD vs. shRNA control (Figure 3-24 D and E).

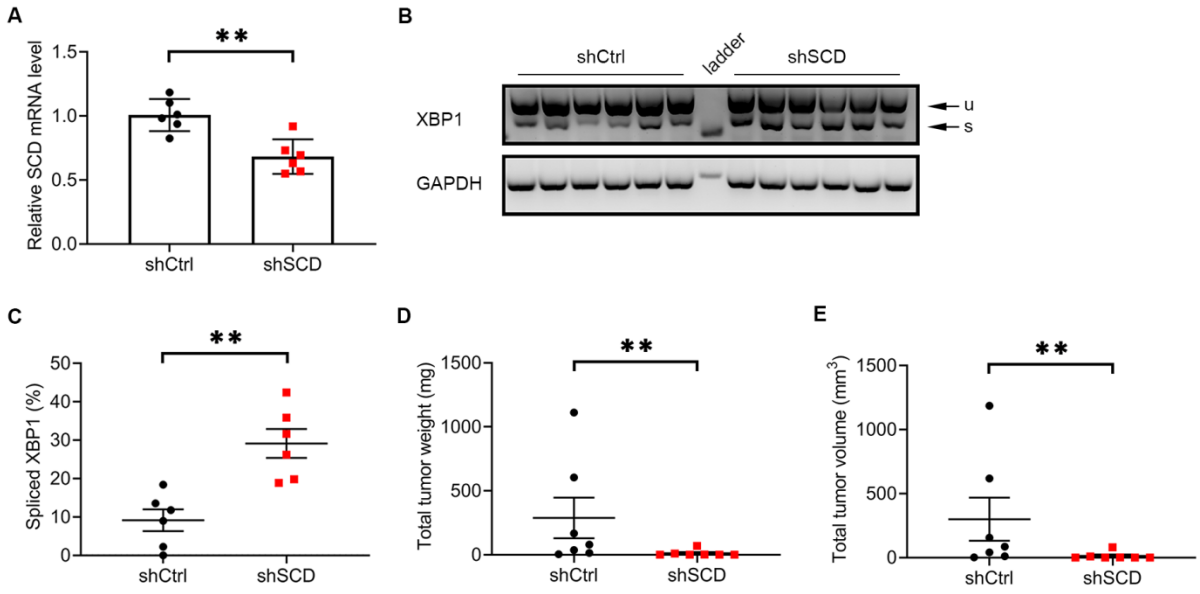

Figure 3-24 SCD knockdown induced XBP1 splicing in xenograft tumors and inhibited growth of ovarian cancer subcutaneous xenografts in mice.

(A) qRT-PCR measurements of SCD expression (mean ± SD, n = 6) in a random sample of tumor xenografts described in (Fig. 3-23 A). (B, C) Agarose gel electrophoresis of XBP1 splicing products (u, unspliced transcript; s, spliced transcript) (B), and percent spliced XBP1 isoform estimated by image analysis of transcript bands (mean ± SD, n = 6) (C) in a random sample of tumor xenografts described in (Fig. 3-23 A). (D, E) Total tumor weight (D) and total tumor volume (E) in athymic nude mice injected subcutaneously with OVCAR-3 cells transduced with control shRNA (shCtrl) or shRNA targeting SCD (shSCD) (means ± SE, n = 7

per group). Dr. Horacio Cardenas helped with cancer cell injection and mouse dissection. ** $p < 0.01$.

Interestingly, HGSOC patients with high (n = 590) vs. low (n = 411) SCD expressing tumors in the TCGA database [472] had shorter progression free survival (PFS; Figure 3-25, p = 0.015), supporting the potential functional relevance of SCD to OC progression.

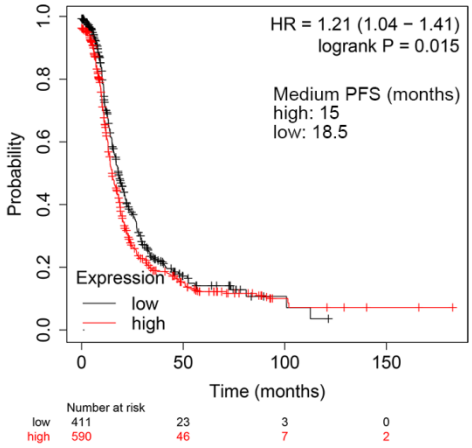

Figure 3-25 Survival of HGSOC patients with dichotomous SCD expression.

PFS Kaplan-Meier plot in HGSOC patients with high SCD (n = 590) vs low SCD (n = 411) expression.

Our observations that ER stress and apoptosis are augmented *in vitro* by inhibition of the desaturase coupled with an excess of SFAs led us to hypothesize that the effects of a

pharmacological inhibitor targeting this pathway would be enhanced through dietary modifications tilting the fatty acid (FA) balance towards increased saturation levels. To test this hypothesis, we used an i.p. model fed a PA rich or control diet, and treatment with CAY10566 or diluent. While CAY10566 did not significantly alter the numbers of peritoneal metastases and the ascites volume in mice fed a control diet (Figure 3-26 A and B), the inhibitor significantly decreased both the ascites volume ($p < 0.0001$) as well as the numbers of metastases ($p = 0.0003$) in mice fed PA rich diet (Figure 3-26 A and B). Interestingly, an unanticipated, but significant increase in ascites volume was observed in the group receiving the SFA rich diet compared with the control diet (Figure 3-26 A, $p = 0.0252$). No significant differences were observed in total tumor weights and total tumor volumes (Figure 3-26 C and D). XBP1s levels were not significantly different in tumors derived from mice fed the control diet and treated with vehicle vs CAY10566 (Figure 3-26 E and F, $p = 0.6370$), but were significantly increased in tumors derived from mice fed PA rich diet and treated with CAY10566 vs. control (Figure 3-26 G and H, $p = 0.0369$). The data support that SCD inhibition or depletion exerts anti-tumorigenic effects through an ER stress-dependent mechanism caused by decreased levels of lipid desaturation.

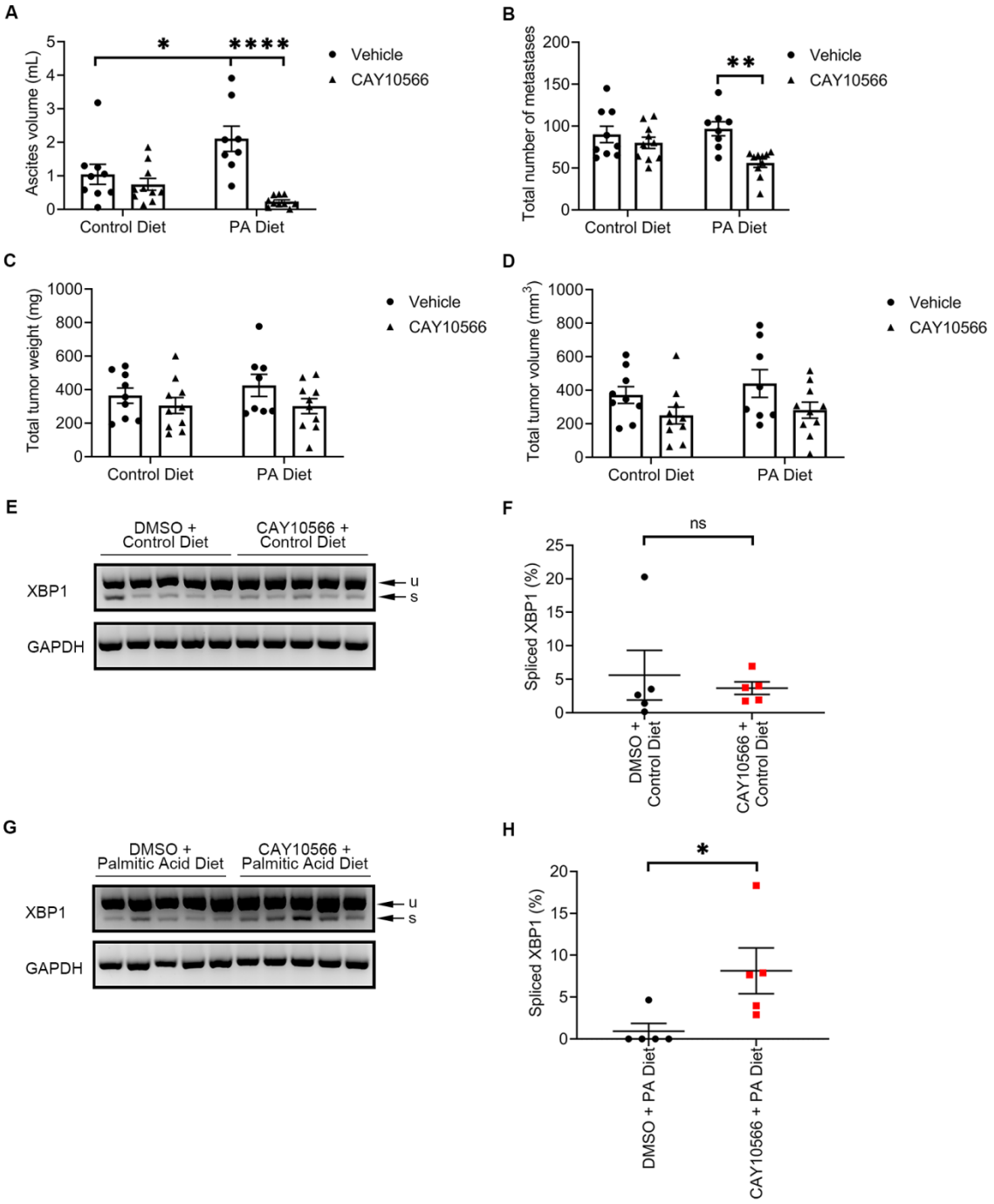

Figure 3-26 SCD knockdown and palmitic acid rich diet inhibited growth of ovarian cancer intraperitoneal xenografts in mice and induced XBP1 splicing in xenograft tumors.

(A-D) Ascites volume (A), total number of metastases (B), total tumor weight (C) and total tumor volume (D) in athymic nude mice intraperitoneally injected with OVCAR-5 cells, fed with a PA-rich diet or control diet, and treated with SCD inhibitor CAY10566 or vehicle for 28 days. Values are means ± SE, n = 10. Dr. Horacio Cardenas helped with cancer cell injection and mouse dissection. (E-H) XBP1 splicing products (u, unspliced transcript; s, spliced transcript) (E, G), and percent intensity of the spliced transcript estimated by image analysis (F, H) in a random sample (n = 5) of tumor xenografts described in (F). Values are means ± SD. * $p < 0.05$, ** $p < 0.01$, **** $p < 0.0001$.

3.9 Increased FAO rate contributes to cisplatin resistance

Given the importance of metabolic reprogramming in ovarian cancer beyond Warburg effect summarized in Section 1.1.4 and the role of fatty acid metabolism in drug resistance reviewed in Section 1.2.2.6, and given that ovarian cancer stem cells are enriched in unsaturated fatty acids [67], we hypothesized that fatty acid metabolism is involved in cisplatin resistance in ovarian cancer. More recently, our lab has demonstrated that fatty acid uptake and storage were significantly upregulated whereas glycolysis and *de novo* lipogenesis were significantly downregulated in cisplatin-resistant than sensitive ovarian cancer cells [62]. We sought to investigate if FAO serves as a major source of energy production during the development of cisplatin resistance. We have developed multiple pairs of cisplatin-sensitive and -resistant ovarian cancer cells (Section 2.3) *in vitro* by repeated cycles of cisplatin treatment and recovery in wildtype (WT)/parental ovarian cancer cells.

To characterize FAO in parental and resistant ovarian cancer cells, we measured cellular OCR. OVCAR-5 cisplatinR cells bore significantly faster oxygen consumption than OVCAR-5 WT cells (Figure 3-27 A and D, p = 0.00044). To verify that the observed oxygen consumption arises from FAO, we used etomoxir, an inhibitor of CPT1A that transports FA into mitochondria for FAO. Etomoxir treatment did not alter oxygen consumption in OVCAR-5 WT cells (Figure 3-27 B); however, it significantly reduced oxygen consumption in OVCAR-5 cisplatinR cells (Figure 3-27 C and D, p = 0.041).

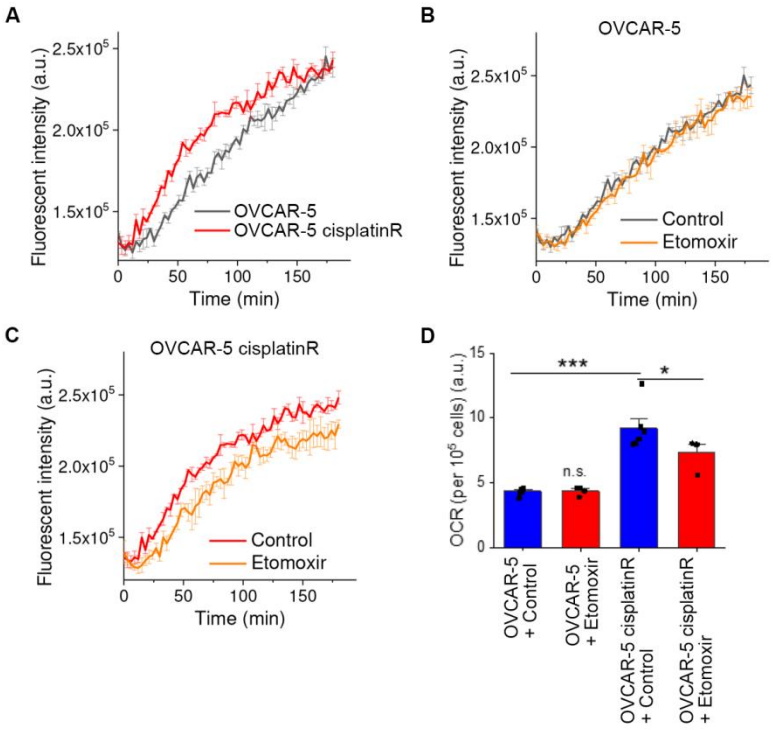

Figure 3-27 Fatty acid contributes to cisplatin resistance via increasing FAO.

(A) Oxygen consumption curves of OVCAR-5 and OVCAR-5 cisplatinR over 3 hours. (B, C) Oxygen consumption curves of OVCAR-5 (B) and OVCAR-5 cisplatinR (C) with 40 μM

etomoxir treatment over 3 hours. Values are means ± SD, n = 4. (D) Quantification of OCR for OVCAR-5 and OVCAR-5 cisplatinR cells treated with (n = 4) or without (n = 6) etomoxir (40 μM) measured by the Fatty Acid Oxidation Assay kit (Abcam). Yuying Tan helped with experimental setup and data acquisition. * $p < 0.05$, *** $p < 0.001$.

Additionally, FAO was characterized by Seahorse FAO assay to assess the changes in mitochondrial respiration upon etomoxir treatment. OVCAR-5 cisplatinR cells demonstrated an overall higher OCR than the parental cells and a clear reduction of OCR after treatment with etomoxir (Figure 3-28 A). In contrast, OCR of OVCAR-5 WT cells was less sensitive to etomoxir treatment. Basal respiration, ATP production and maximal respiration were significantly increased upon etomoxir treatment in OVCAR-5 cisplatinR cells than those in OVCAR-5 WT cells, indicating a significantly upregulated FAO in resistant cells (Figure 3-28 B, $p = 0.0021$, 0.018 and 0.0046). Further, Seahorse measurement of OCR in PEO1 and PEO4 cells corroborates a significant increase of FAO rate in PEO4 cells compared to PEO1 cells (Figure 3-28 C, $p = 8.9\times10^{-5}$). Together, these data support significant increase of FAO in cisplatin-resistant cells.

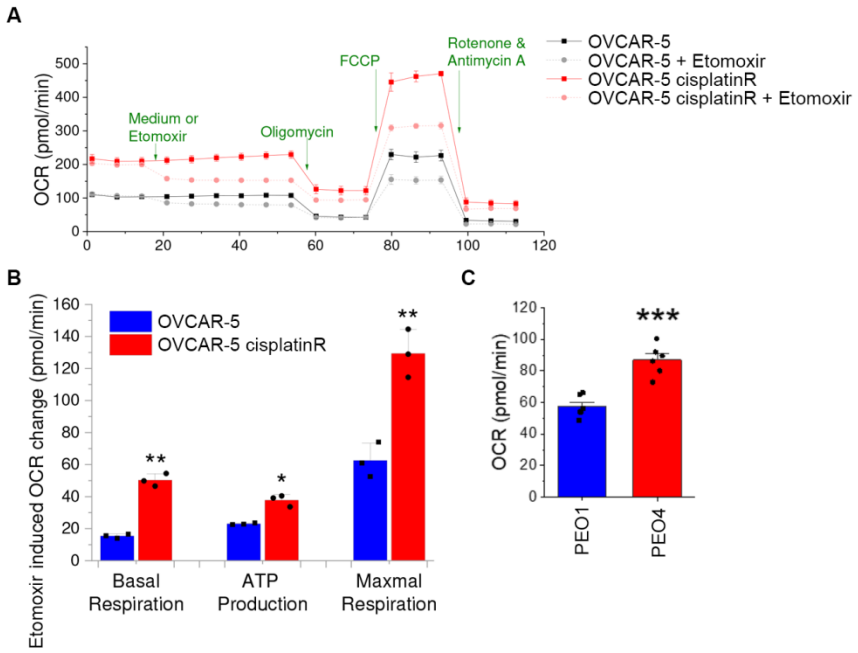

Figure 3-28 Fatty acid contributes to cisplatin resistance by increasing mitochondrial respiration.

(A) Seahorse XF Analyzer measured OCR profile of OVCAR-5 and OVCAR-5 cisplatinR cells with or without etomoxir treatment, followed by injections of mitochondrial respiration inhibitors oligomycin, FCCP, rotenone and antimycin A indicated by arrows. n = 3 technical replicates. (B) Quantified etomoxir-induced basal respiration, ATP production and maximal respiration reduction in OVCAR-5 and OVCAR-5 cisplatinR cells. Data are presented as means + SD, n = 3 technical replicates. (C) Quantification of OCR for PEO1 and PEO4 cells measured by Seahorse XF Analyzer. Data are presented as means + SD, n = 6 technical replicates. Yuying Tan helped with experimental setup and data acquisition. *** $p < 0.001$.

To further explore the possibility of increased FAO contributing to cisplatin resistance, we studied cell viability in response to different doses of etomoxir in cisplatin-resistant and -sensitive cells. We observed a higher sensitivity to etomoxir treatment in cisplatin-resistant cells as compared to the sensitive cells, in PEO1 and PEO4 cells (Figure 3-29 A), OVCAR-5 and OVCAR-5 cisplatinR cells (Figure 3-29 B), and COV362 and COV362 cisplatinR cells (Figure 3-29 C). This result implies a higher dependence on FAO in cisplatin-resistant cells. Subsequently, we investigated if etomoxir treatment could re-sensitize the resistant cells to cisplatin treatment. Indeed, we observed a significant shift in the dose-response curve to cisplatin upon etomoxir treatment in PEO4 (Figure 3-29 D), OVCAR-5 cisplatinR (Figure 3-29 E), and COV362 cisplatinR cells (Figure 3-29 F), indicating a potential synergy between etomoxir and platinum drug in treating chemo-resistant OC tumors.

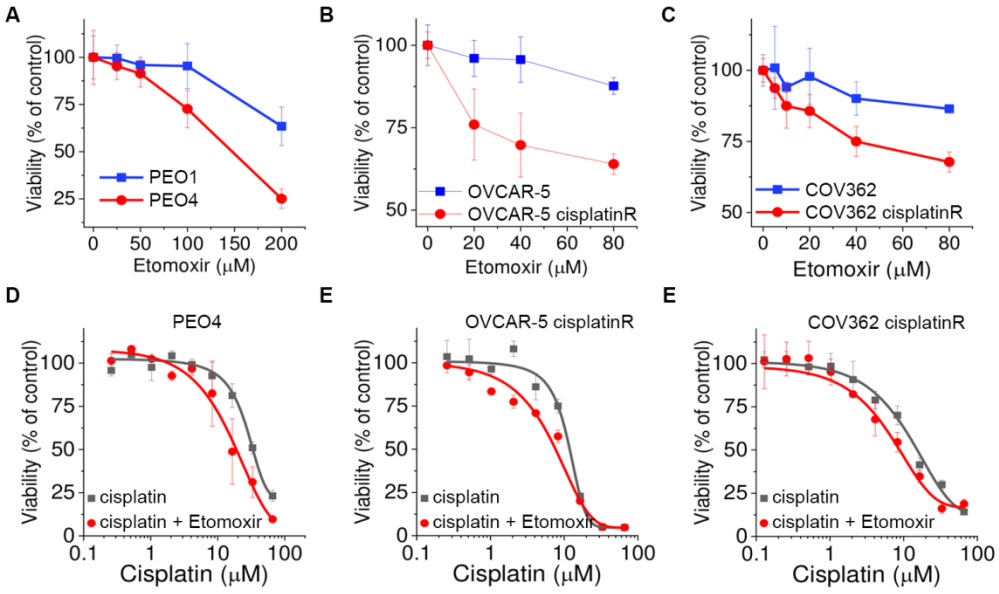

Figure 3-29 Cisplatin-resistant cells are sensitive to FAO inhibition.

(A-C) Dose-response to etomoxir for cisplatin resistant cell lines and their parental cell lines including PEO1 and PEO4 (A), OVCAR-5 and OVCAR-5 cisplatinR (B) and COV362 and COV362 cisplatinR (C). (D-F) Dose-response to cisplatin with or without supplemental etomoxir treatment at 40 μM for PEO4 (D), OVCAR-5 cisplatinR (E) and COV362 cisplatinR (F) cells. Yuying Tan helped with experimental setup and data acquisition.

3.10 Altered pyrimidine metabolism contributes to cisplatin resistance

A recent paper from Sarah-Maria Fendt and Peter Carmeliet laboratories found that in endothelial cells carbon atoms from fatty acid contributed to *de novo* DNA synthesis [473]. The authors revealed that carbon atoms from fatty acids participated in tricarboxylic acid (TCA) cycle and TCA cycle-derived metabolites including citrate, α-ketoglutarate, fumarate, malate and amino acids including aspartate, proline, glutamate and asparagine through FAO. Nevertheless, CPT1A KD did not alter intracellular levels of all amino acids or *de novo* protein synthesis or RNA synthesis. Interestingly, isotope-labelled carbon of palmitic acid was incorporated into uridine monophosphate (UMP) and uridine triphosphate (UTP), a precursor for *de novo* DNA synthesis. Furthermore, exogenous treatment of acetate could completely restore the levels of pyrimidine. Given the relationship between FAO and pyrimidine synthesis and the roles of DNA synthesis in cisplatin-induced DNA repair and potential involvement in the development of resistance to cisplatin in cancer cells [474, 475], we hypothesized that pyrimidine synthesis was significantly altered in cisplatin-resistant ovarian cancer cells as compared to sensitive cancer cells.

We performed metabolomic profiling (hydrophilic panel) of paired cisplatin-sensitive and -resistant ovarian cancer cells. There were 23 differential metabolites (FDR < 0.05), of which 21 were upregulated and 2 downregulated between OVCAR-5 and OVCAR-5 cisplatinR cells. For SKOV-3 and SKOV-3 cisplatinR cells, there were 32 differential metabolites (FDR < 0.05), of which 22 were upregulated and 10 downregulated. For PEO1 and PEO4 cells, there were 90 differential metabolites (FDR < 0.05), of which 62 were upregulated and 28 downregulated. Pathway analysis of significant metabolites revealed that pyrimidine metabolism is universally significantly altered in OVCAR-5 vs. OVCAR-5 cisplatinR, SKOV-3 vs. SKOV-3 cisplatinR and PEO1 vs. PEO4 cells (Table 7).

Table 7. Pathway analysis for metabolomic profiling of OVCAR-5 vs. OVCAR-5 cisplatinR, SKOV-3 vs. SKOV-3 cisplatinR and PEO1 vs. PEO4 cells

OVCAR-5 vs. OVCAR-5 cisplatinR					
Name of pathway	Total metabolites	Expected	Hits	P value	FDR
Pyrimidine metabolism	60	0.37391	6	7.84e-07	6.27e-05
D-Arginine and D-ornithine metabolism	8	0.049855	1	0.04885	1
Arginine and proline metabolism	77	0.47985	2	0.081065	1
Tryptophan metabolism	79	0.49231	2	0.084753	1
Purine metabolism	92	0.57333	2	0.10995	1
SKOV-3 vs. SKOV-3 cisplatinR					

Name of pathway	Total metabolites	Expected	Hits	P value	FDR
Pyrimidine metabolism	60	0.64811	8	1.02e-07	8.15e-06
Alanine, aspartate and glutamate metabolism	24	0.25924	3	0.001949	0.067852
Purine metabolism	92	0.99377	5	0.002544	0.067852
Arginine and proline metabolism	77	0.83174	4	0.008476	0.16952
Pentose phosphate pathway	32	0.34566	2	0.04564	0.73024
PEO1 vs. PEO4					
Name of pathway	Total metabolites	Expected	Hits	P value	FDR
Alanine, aspartate and glutamate metabolism	24	0.70794	9	9.29e-09	7.43e-07
Pyrimidine metabolism	60	1.7698	12	7.68e-08	3.07e-06
Aminoacyl-tRNA biosynthesis	75	2.2123	12	1.01e-06	2.11e-05
Nitrogen metabolism	39	1.1504	9	1.06e-06	2.11e-05
Purine metabolism	92	2.7138	13	1.49e-06	2.39e-05

Our observations demonstrate that platinum-resistant cells undergo complex metabolic reprogramming. These processes entail changes in choice of nutrients, alternative paths towards energy production, and source of molecules for biosynthesis of the DNA. Some of the features

we discovered during acquisition of platinum-resistance provide directions for future investigation.

Chapter 4 : Conclusion, Discussion and Future Directions

Our data based on transcriptomic and lipidomic analyses, SRS and TEM imaging demonstrate that the imbalance between SFAs and UFAs caused by depletion or inhibition of the enzyme SCD has a key function in determining cancer cell survival or death and impacts tumor progression *in vivo*. These findings hone on a largely understudied metabolic process in cancer cells and suggest the possibility of using an intervention combining an SCD enzymatic inhibitor together with a dietary intervention to increase levels of lipid saturation in cancer cells and trigger a potent anti-tumor effect.

Additionally, we unveiled that platinum-resistant ovarian cancer cells undergo metabolic reprogramming and become more dependent on FAO for energy production and its end product for participation into *de novo* DNA synthesis in the acquisition of platinum resistance.

Our findings have several important consequences.

4.1 Lipid unsaturation in cancer

The role of SCD and lipid unsaturation in cancer patient survival and prognosis has been extensively documented in epidemiological studies of various cancer types [476-490]. Our results point to the significance of the process of lipid unsaturation in cancer. Lipid synthesis includes the synthesis of FA from acetyl-coA mediated by FASN and ACSL, followed by addition of double carbon bonds catalyzed by FA desaturases. Among the three desaturases, Δ9 (stearoyl-CoA desaturase-1, SCD) catalyzes the synthesis of monounsaturated fatty acids by adding one double bond to saturated fatty acids (mostly stearic acid), while the Δ6 and Δ5 desaturases are involved predominantly in the synthesis of polyunsaturated fatty acids [491]. The current study builds on our previous observations that highly tumorigenic ovarian CSCs are

enriched in UFAs, caused by SCD upregulation, which in turn, induce pro-survival NF-κB signaling allowing CSCs to proliferate as spheres and effectively initiate tumors in immunodeficient mice [67]. Here we show that beyond the previously observed effects on CSCs, SCD knockdown, and to a lesser extent its inhibition, induces anti-tumor effects in i.p. xenografts. The intracellular free fatty acids levels of palmitoleic acid and oleic acid were 4.0 fold and 2.4 fold less when cells were depleted of SCD and cultured in low serum condition. The culturing condition adapted here [434] closely mimics the last step of the metastatic progression of solid tumors: colonization at secondary tumor sites where nutritional conditions are different and supply is not optimal. It is possible that the observed repression of tumor growth is due to reduced intracellular lipid unsaturation in cancer cells when they arrive and establish new colonies at the secondary tumor sites.

A limitation of the study is that using low serum (1% FBS) culturing medium as performed in many experiments might introduce some potential confounding factors. It is known that serum contains a multitude of proteins, organic compounds, metal ions, hormones and fatty acids. Lowering the serum percentage by 10 fold not only reduced fatty acids in the medium but also all other components, including growth factors. For example, insulin and insulin-like growth factors were identified as a risk factor in ovarian cancer [492]. Admittedly, certain patients or ovarian cancer cell lines might be more sensitive and hence responsive to insulin level in the serum as compared to others, leading to inconclusive or discrepant findings. In this sense, using serum that is specifically depleted of free fatty acids would be a better approach to this question. To mitigate this limitation, we performed several control experiments using lipid depleted serum and replicated key findings under these conditions.

Overexpression of ACSL and SCD leading to increased UFA levels was described in association with epithelial to mesenchymal transition and aggressive clinical prognosis in colon cancer, and SCD upregulation was observed in basal type breast cancer and aggressive prostate cancer [165, 167]. In renal cell carcinoma, triacylglycerols stored in lipid droplets could release OA and counter the stress induced by SFAs [107]. Depletion of OA (but not of PA) inhibited the proliferation of AML and lymphoma cells [172]. Moreover, inhibition of SREBF1 uncoupled fatty acid synthesis from fatty acid desaturation primarily due to the transcriptional repression of SCD through SREBF1 [493]. The consequent imbalance between saturated fatty acids and unsaturated fatty acids could be reversed by addition of oleic acid. However, it remains not clear how the balance between UFAs and SFAs alter cancer predisposition or cancer progression, a concept we addressed here. Due to the clinical and anatomical behavior of ovarian cancer, we used the intraperitoneal mouse xenograft model [494]. Our results indicate that SCD KD significantly decreased tumor burden in intraperitoneal mouse xenograft. More recently, a study found that polyunsaturated ether phospholipids were critical in the induction of ferroptosis, non-apoptotic cell death [495]. This finding implies that certain polyunsaturated fatty acid species are not pro-survival and further studies of lipid unsaturation in cancer are needed. Taken together, our findings suggest that imbalance of saturated/unsaturated fatty acids is important for tumor survival and proliferation.

4.2 Lipid unsaturation-dependent ER stress in tumorigenesis, stemness and metastasis

Our findings demonstrate that the imbalance between SFAs and UFAs impedes cancer cell survival and *in vivo* tumor growth through induction of ER stress. We observed that two branches of the ER stress response, regulated by the PERK and IRE1α were activated in

response to SCD depletion or inhibition, and that this activation was augmented in the presence of SFA supplementation and could be rescued by addition of UFAs. Our observations are consistent with previous reports [145, 161, 391, 496-498]. More recent studies found that lipid unsaturation is critical for cancer stem cell maintenance and tumor growth in hepatocellular carcinoma with high N-MYC expression [499] and in glioblastoma stem cell and corresponding mouse model [267] via regulation of ER stress. Interestingly, Xie et al. found that SCD inhibition even phenocopied the suppression of IRE1α ribonuclease (RNase) activity [500]. Potze et al. found that inhibition of SCD by betulinic acid specifically increased the saturation of cardiolipin, major component of the mitochondrial inner membrane lipid, leading to damage of mitochondrial membrane structure. Subsequently, cytochrome c was released to induce apoptosis in cancer cells [501]. Similarly, Chen et al. revealed that SCD inhibition triggered biosynthesis of ceramide in cancer cells, resulting in dysfunction of mitochondria and hence onset of apoptosis [502]. Zheng et al. had similar observation on SCD inhibition-induced *de novo* synthesis of ceramide and identified NF-κB as the underlying mechanism mediating subsequent apoptosis [503]. On the other hand, one study found that inhibition of SCD in ovarian cancer partially induced ferroptosis instead of apoptosis [298]. Mechanistically, upregulation of SCD through hyperactivation of PI3K/AKT/mTOR signaling pathway produced more monounsaturated fatty acids that protected multiple cancers from ferroptosis [504]. While a definitive mechanistic explanation is still lacking, our hSRS and TEM imaging suggest that increased levels of lipid unsaturation in cancer cells alter the morphology of the ER, causing increased membrane rigidity and potentially direct activation of the sensor proteins.

We speculate that SCD as the critical desaturase in ovarian cancer cells converts saturated fatty acids into their monounsaturated counterparts that are universally pro-survival. Further down the *de novo* synthesis pathway, polyunsaturated fatty acids are structurally more specialized and could have distinctive functions depending on their engagement in different cellular processes. In addition to their involvement in the context of cancer, lipid unsaturation and ER stress participate in stem cell growth and survival. For instance, neural stem/progenitor cells are susceptible to lipid accumulation and consequent ER stress [505]. PA treatment will induce ER stress and apoptosis in human bone marrow-derived mesenchymal stem cells [506]. Interestingly, intestinal stem cells with diacylglycerol O-acyltransferase 1 (DGAT1) deficiency undergo ER stress induced by OA [507]. It is possible that cancer stem cells have unique molecular signatures that make them favor unsaturated fatty acids whereas normal embryonic stem cells are generally sensitive to lipid accumulation disregard of the unsaturation level.

The role of ER stress in tumor metastasis was recently discovered. Specifically, in orthotopic xenografts of cervical cancer, hypoxia-triggered metastasis to lymph node was blocked by PERK inhibition [508]. Another study however found that PERK/eIF2α/ATF4 axis of the ER stress response is critical for epithelial-to-mesenchymal transition of breast cancer cells [509]. Importantly, PERK/eIF2α/ATF4 axis was implicated as a protective means that cells activate during EMT. Given our observations on combination treatment with SCD inhibitor and palmitic acid-enriched diet, we were able to conclude that prolonged severe ER stress inhibited metastasis of ovarian cancer cells. Our study, together with previous reports, unravel the biphasic role of PERK/eIF2α/ATF4 axis of the ER stress response.

4.3 Stimulated Raman Spectroscopic imaging and image analysis

A powerful tool that allowed us to quantify UFAs and SFAs at the single cell level in this study was SRS microscopy, an innovative label-free chemical imaging technique which we have previously employed to characterize metabolic reprograming from glycolysis to fatty acid uptake and β-oxidation in platinum-resistant cancer cells [452], increased lipid desaturation in OCSCs [67], and cholesteryl ester accumulation as a metabolic marker for multiple aggressive cancers [510, 511]. Combined with post-processing methods such as least-square fitting, multivariate curve resolution and phasor segmentation, hSRS can distinguish different intracellular biomolecules such as protein and fatty acid [158, 512]. Here, SRS imaging visualized SFA-induced ER stress in OC cells depleted of SCD and the rescue observed by manipulating the ratio between SFAs and UFAs. We recognize that highly spatially overlapping biomolecules with similar spectrum profile such as SFAs and UFAs are difficult to decompose by using conventional analysis methods. We propose that pixel-wise LASSO unmixing can resolve such shortcomings, enabling the simultaneous evaluation of multiple metabolites, facilitating better assessment of cancer cell metabolism and metabolic changes in response to gene modification and drug treatment. The innovative hSRS-LASSO imaging method utilized here provides a new way to explore cancer lipid metabolism in deeper detail.

4.4 Customized diet in cancer treatment

The role of diet in cancer treatment has been studied for long time [513] with particular focus on the Mediterranean diet [514] and the ketogenic diet [515]. The Mediterranean diet provides ample antioxidants and anti-inflammatory nutrients from food. Conversely, the ketogenic diet

manipulates the ratio among fat, carbohydrate and protein in the food so that fat serves as the main source of energy during metabolism. The underlying concept of such diets is to alter metabolite levels in the tumor microenvironment and create metabolic challenges for tumor cells to survive. Till now, diet therapy remains speculative as adjuvant cancer therapy. A recent study however found that caloric restriction diet downregulates SCD expression in pancreatic and lung tumor in subcutaneous mouse xenograft model. As a result, the balance between saturated fatty acids and unsaturated fatty acids was broken, leading to inhibited tumor growth [516]. The authors also raised an important point that SCD inhibition induces cell death only when saturated fatty acids accumulate. Their observations and speculations were corroborated by our *in vitro* and *in vivo* experiments where prolonged exposure to SCD inhibition or short-term exposure to SCD inhibition in the presence of extra palmitic acid induced apoptosis.

SCD expression and hence dynamics between saturated and unsaturated fatty acids is highly regulated by diet and hormone levels [128, 517]. Early attempts to examine the relationship between SCD and dietary fatty acid composition found that diet rich in saturated fatty acids induces SCD expression [518], which is agrees with our observation that palmitic acid-rich diet resulted in significantly higher ascites volume and number of metastases (Fig. 3-26 A-B). Park et al. found that mice fed with diet containing Panicum miliaceum L. , basically whole grains, demonstrated reduced lipid anabolism and ratio of unsaturated fatty acids to saturated fatty acids but increased lipid catabolism [519]. Other recent studies combining intestinal-specific Scd1 knockout (KO) and customized diet showed upregulation of inflammation and fibrosis in liver of Scd1 KO mice. More importantly, intestinal-specific Scd1 KO mice developed chemical-induced

liver cancer [520] or colon cancer upon mutation of one allele of adenomatous polyposis coli [521].

A more recent study from Benitah lab found that dietary palmitic acid possesses prometastatic features in oral carcinoma and melanoma [228]. Specifically, *in vitro* palmitic acid treatment could prime tumor cells for subsequent *in vivo* metastasis after withdrawal of palmitic acid in advance. In another orthotopic mouse xenograft model, mice were fed with palmitic acid-rich diet after tumor cell implantation and showed more metastatic tumor burden as compared to those fed with control diet.

A starting point towards the investigation on how lipid unsaturation gauges ER stress, ER stress response and metastasis is our attempt to combine SCD inhibition with a dietary intervention. We demonstrate that this intervention resulting in accumulation of toxic SFAs has potent anti-tumor effects (numbers of metastases and ascites) and induces ER stress responses detectable in tumor tissue. Whether the effects of the combined intervention target peritoneal dissemination more than tumor growth, as observed in experiments using SCD knockdown, remains to be elucidated.

The intraperitoneal mouse xenograft model used in this study is appropriate for examining *in vivo* tumor growth and progression. However, it is not the optimal mouse xenograft model to investigate tumor metastasis, as we reported for which we observed reduced ascites volume and number of metastases in our combination of SCD inhibitor and customized diet. The intraperitoneal mouse xenograft model is representative of advanced stage ovarian cancer. In this model injection of cancer cells in fact bypassed the intravasation, transport and extravasation

steps during metastatic progression of solid tumors. To better define the effects of the combination treatment on metastasis, we could utilize the intrabursal orthotopic mouse xenograft model [522]. Essentially, cancer cells are injected into the ovary bursa which serves as a containment for the cancer cells. Cancer cells later travel from the ovary to the peritoneal space to establish their metastatic sites. The proposed combination treatment, as an alternative to chemotherapy, could potentially restrict the cancer cells at the primary site for surgical debulking. Yet, intrabursal injection possesses technical challenges as compared to intraperitoneal injection such as potential leakage of cancer cells from ovary bursa during injection [523]. Additionally, anatomically mouse ovary is separated from the peritoneal cavity by ovary bursa whereas human ovary is located in peritoneal cavity without an ovary bursa, adding extra complexity to this xenograft model and potential failure to observe metastasis due to the confinement by ovary bursa [522]. The orthotopic model could be studied in the future for investigating the effects of SCD inhibition on metastasis.

The putative role of diet in cancer treatment has remained a “holy grail” and is based on the concept that altered metabolite levels in the tumor microenvironment could create metabolic challenges impeding tumor cells’ survival. The role of saturated lipids in cancer remains controversial, with the overwhelming belief that saturated fat is pro-tumorigenic. Indeed, a recent study showed that dietary PA promoted metastasis in oral carcinoma and melanoma models [228]. Consistent with these observations, we found that the PA-rich diet induced increased accumulation of malignant ascites, the main vehicle of OC metastasis. However, the combination of a PA-rich diet and CAY10566 caused a significant reduction in ascites and peritoneal implants. Given the plasticity and redundancy of metabolic pathways, which have by and large thwarted

prior attempts to use metabolic interventions to target cancer, our results highlight the importance of combination strategies.

Taken together our findings support SCD's key role in regulating cancer cell fate and tumorigenicity and point to new modalities to block OC progression.

4.5 Future directions

In 2015 Bowtell et al. wrote a comprehensive review on ovarian cancer pointing out some key challenges faced by researchers and clinicians [1]. The first and foremost barrier remains chemotherapy resistance which emerges after initial favorable response to treatment. Our discovery of the metabolic reprogramming in platinum-resistant ovarian cancer cells, especially fatty acid oxidation-mediated resistance to platinum opened up new areas for identification of new drug targets in fatty acid oxidation pathways in addition to CPT1A combined with platinum-based drugs for treatment. Furthermore, the metabolic index concept introduced in our recent publication [2] provides an extra tool for predicting patient's response to chemotherapy, potentially serving as a new precision medicine tool in the near future. As a promising idea, future endeavors could focus on the acceleration of the mapping of metabolic index for each tumor biopsy from the patients.

Another critical factor is tumor microenvironment. Due to the symbiotic relationship between ovarian cancer cells and adipocytes at metastatic sites, future therapeutic strategy could be focused on how to halt the communications between cancer cells and adipocytes to disable fast and adaptive colonization in the peritoneal space. Our mouse intraperitoneal xenograft experiment with SCD inhibitor administration and customized palmitic acid-rich diet

demonstrated the possibility of altering cancer cell fate by manipulating the dynamics between SFAs and UFAs in the tumor microenvironment. Future applications of combination treatment with targeted therapy and customized diet are one of the areas to explore in addition to dual drug treatment to enhance cancer cell sensitivity to platinum drugs after tumor relapse.

The combination treatment of SCD inhibitor and customized diet could be too toxic systemically while using SCD inhibitor alone would trigger ER stress response in the cancer cells. To overcome the potential development of resistance to SCD inhibition from ER stress response, key pro-survival molecules the in ER stress response such as IRE1α or splice XBP1 are good drug targets in this scenario. An alternative combination treatment to be tested could be SCD inhibitor and an inhibitor of the ER stress response. Most inhibitors targeting the IRE1α/XBP1 axis in the ER stress response are actually designed against IRE1α endoribonuclease activity which might have off-target effect beyond shutting down ER stress response. There are ongoing efforts to develop inhibitors of spliced XBP1 by utilizing the ubiquitin-proteasome system, i.e. protein-targeting chimeric molecule (PROTACs) [3, 4]. Due to the nature of transcriptional factors, design of small molecular inhibitors might be difficult and PROTAC-based repression of spliced XBP1 can be used.

In addition to its role in the tumor, lipid metabolism is also essential to the immune system. For example, de novo lipogenesis mediates differentiation of T effector cells [5]. Fatty acid biosynthesis and β-oxidation regulates cluster of differentiation 8 $(CD8)^+$ T cell development and normal function. Cell development decision between regulatory T cell vs. T helper cells from cluster of differentiation 4 $(CD4)^+$ T effectors also depend on fatty acid biosynthesis and β-oxidation. How the proposed combination treatment of SCD inhibitor and customized diet

interferes with the immune system is worth future investigation. Leveraging immune competent mice for studying the combination treatment after tumor implantation is necessary for evaluating the treatment regimen further.

Apart from ovarian cancer, future approaches towards eradicating other cancers can be envisioned from Hanahan and Weinberg's summary of the newly emerging hallmarks of cancer. Specifically, deregulating cellular energy is now being recognized as an emerging hallmark of cancer [6]. Our combination treatment, when reflected on the hallmarks of cancer, is targeting both deregulating cellular energy (SCD inhibitor) and resisting cell death (palmitic acid). A most recent study from Zender and Dauch laboratories on liver cancer also demonstrated the synergy between lipotoxiticy and SCD inhibition [524]. For developing future combination treatments, a potential strategy is to find a synergy between blockers of two hallmarks of cancer. For different cancers, the strategy and target hallmarks might be different and a scoring system could be developed to assess the dependency on each hallmark.

We have taken a systematic and multidisciplinary approach towards understanding the role of lipid unsaturation in ovarian cancer and metabolism in platinum resistance in ovarian cancer. Lipid metabolism is an essential and key component of ovarian cancer tumor progression and metastasis. Our findings contribute to future efforts towards developing targeted therapy against lipid metabolism pathways. Mechanistic studies at the molecular and cellular level will unveil the interaction between ovarian cancer cells, ovarian cancer stem cells and adipocytes during metastasis and acquisition of platinum resistance to far greater detail and clarity, expanding our knowledge of ovarian cancer.

REFERENCES

[1] R.J. Kurman, M. Shih Ie, The origin and pathogenesis of epithelial ovarian cancer: a proposed unifying theory, The American journal of surgical pathology, 34 (2010) 433-443.
[2] K. Tomczak, P. Czerwinska, M. Wiznerowicz, The Cancer Genome Atlas (TCGA): an immeasurable source of knowledge, Contemporary oncology, 19 (2015) A68-77.
[3] J.S. Berek, K. Bertelsen, A. du Bois, M.F. Brady, J. Carmichael, E.A. Eisenhauer, M. Gore, S. Grenman, T.C. Hamilton, S.W. Hansen, P.G. Harper, G. Horvath, S.B. Kaye, H.J. Luck, B. Lund, W.P. McGuire, J.P. Neijt, R.F. Ozols, M.K. Parmar, M.J. Piccart-Gebhart, R. van Rijswijk, P. Rosenberg, G.J. Rustin, C. Sessa, P.H. Willemse, et al., Advanced epithelial ovarian cancer: 1998 consensus statements, Annals of oncology : official journal of the European Society for Medical Oncology, 10 Suppl 1 (1999) 87-92.
[4] S. Vaughan, J.I. Coward, R.C. Bast, Jr., A. Berchuck, J.S. Berek, J.D. Brenton, G. Coukos, C.C. Crum, R. Drapkin, D. Etemadmoghadam, M. Friedlander, H. Gabra, S.B. Kaye, C.J. Lord, E. Lengyel, D.A. Levine, I.A. McNeish, U. Menon, G.B. Mills, K.P. Nephew, A.M. Oza, A.K. Sood, E.A. Stronach, H. Walczak, D.D. Bowtell, F.R. Balkwill, Rethinking ovarian cancer: recommendations for improving outcomes, Nature reviews. Cancer, 11 (2011) 719-725.
[5] D.D. Bowtell, S. Bohm, A.A. Ahmed, P.J. Aspuria, R.C. Bast, Jr., V. Beral, J.S. Berek, M.J. Birrer, S. Blagden, M.A. Bookman, J.D. Brenton, K.B. Chiappinelli, F.C. Martins, G. Coukos, R. Drapkin, R. Edmondson, C. Fotopoulou, H. Gabra, J. Galon, C. Gourley, V. Heong, D.G. Huntsman, M. Iwanicki, B.Y. Karlan, A. Kaye, E. Lengyel, D.A. Levine, K.H. Lu, I.A. McNeish, U. Menon, S.A. Narod, B.H. Nelson, K.P. Nephew, P. Pharoah, D.J. Powell, Jr., P. Ramos, I.L. Romero, C.L. Scott, A.K. Sood, E.A. Stronach, F.R. Balkwill, Rethinking ovarian cancer II: reducing mortality from high-grade serous ovarian cancer, Nature reviews. Cancer, 15 (2015) 668-679.
[6] Y. Wang, H. Cardenas, F. Fang, S. Condello, P. Taverna, M. Segar, Y. Liu, K.P. Nephew, D. Matei, Epigenetic targeting of ovarian cancer stem cells, Cancer research, 74 (2014) 4922-4936.
[7] T. Shibue, R.A. Weinberg, EMT, CSCs, and drug resistance: the mechanistic link and clinical implications, Nature reviews. Clinical oncology, 14 (2017) 611-629.
[8] B.B. Liau, C. Sievers, L.K. Donohue, S.M. Gillespie, W.A. Flavahan, T.E. Miller, A.S. Venteicher, C.H. Hebert, C.D. Carey, S.J. Rodig, S.J. Shareef, F.J. Najm, P. van Galen, H. Wakimoto, D.P. Cahill, J.N. Rich, J.C. Aster, M.L. Suva, A.P. Patel, B.E. Bernstein, Adaptive Chromatin Remodeling Drives Glioblastoma Stem Cell Plasticity and Drug Tolerance, Cell Stem Cell, 20 (2017) 233-246 e237.
[9] L. Dubeau, The cell of origin of ovarian epithelial tumours, The Lancet. Oncology, 9 (2008) 1191-1197.
[10] R.C. Bast, Jr., B. Hennessy, G.B. Mills, The biology of ovarian cancer: new opportunities for translation, Nature reviews. Cancer, 9 (2009) 415-428.
[11] A. Berchuck, M.F. Kohler, J.R. Marks, R. Wiseman, J. Boyd, R.C. Bast, Jr., The p53 tumor suppressor gene frequently is altered in gynecologic cancers, American journal of obstetrics and gynecology, 170 (1994) 246-252.
[12] L. Havrilesky, M. Darcy k, H. Hamdan, R.L. Priore, J. Leon, J. Bell, A. Berchuck, S. Gynecologic Oncology Group, Prognostic significance of p53 mutation and p53 overexpression in advanced epithelial ovarian cancer: a Gynecologic Oncology Group Study, Journal of clinical oncology : official journal of the American Society of Clinical Oncology, 21 (2003) 3814-3825.
[13] Y. Yu, R. Luo, Z. Lu, W. Wei Feng, D. Badgwell, J.P. Issa, D.G. Rosen, J. Liu, R.C. Bast, Jr., Biochemistry and biology of ARHI (DIRAS3), an imprinted tumor suppressor gene whose expression is lost in ovarian and breast cancers, Methods in enzymology, 407 (2006) 455-468.

[14] D. Cvetkovic, D. Pisarcik, C. Lee, T.C. Hamilton, A. Abdollahi, Altered expression and loss of heterozygosity of the LOT1 gene in ovarian cancer, Gynecologic oncology, 95 (2004) 449-455.
[15] W. Feng, R.T. Marquez, Z. Lu, J. Liu, K.H. Lu, J.P. Issa, D.M. Fishman, Y. Yu, R.C. Bast, Jr., Imprinted tumor suppressor genes ARHI and PEG3 are the most frequently down-regulated in human ovarian cancers by loss of heterozygosity and promoter methylation, Cancer, 112 (2008) 1489-1502.
[16] S.C. Rubin, M.A. Blackwood, C. Bandera, K. Behbakht, I. Benjamin, T.R. Rebbeck, J. Boyd, BRCA1, BRCA2, and hereditary nonpolyposis colorectal cancer gene mutations in an unselected ovarian cancer population: relationship to family history and implications for genetic testing, American journal of obstetrics and gynecology, 178 (1998) 670-677.
[17] J.M. Lancaster, R. Wooster, J. Mangion, C.M. Phelan, C. Cochran, C. Gumbs, S. Seal, R. Barfoot, N. Collins, G. Bignell, S. Patel, R. Hamoudi, C. Larsson, R.W. Wiseman, A. Berchuck, J.D. Iglehart, J.R. Marks, A. Ashworth, M.R. Stratton, P.A. Futreal, BRCA2 mutations in primary breast and ovarian cancers, Nature genetics, 13 (1996) 238-240.
[18] J. Mendelsohn, The molecular basis of cancer, 3rd ed., Saunders/Elsevier, Philadelphia, PA, 2008.
[19] R.J. Kurman, M. Shih Ie, Pathogenesis of ovarian cancer: lessons from morphology and molecular biology and their clinical implications, International journal of gynecological pathology : official journal of the International Society of Gynecological Pathologists, 27 (2008) 151-160.
[20] R.J. Schilder, M.W. Sill, X. Chen, K.M. Darcy, S.L. Decesare, G. Lewandowski, R.B. Lee, C.A. Arciero, H. Wu, A.K. Godwin, Phase II study of gefitinib in patients with relapsed or persistent ovarian or primary peritoneal carcinoma and evaluation of epidermal growth factor receptor mutations and immunohistochemical expression: a Gynecologic Oncology Group Study, Clinical cancer research : an official journal of the American Association for Cancer Research, 11 (2005) 5539-5548.
[21] M.A. Bookman, K.M. Darcy, D. Clarke-Pearson, R.A. Boothby, I.R. Horowitz, Evaluation of monoclonal humanized anti-HER2 antibody, trastuzumab, in patients with recurrent or refractory ovarian or primary peritoneal carcinoma with overexpression of HER2: a phase II trial of the Gynecologic Oncology Group, Journal of clinical oncology : official journal of the American Society of Clinical Oncology, 21 (2003) 283-290.
[22] D.G. Rosen, I. Mercado-Uribe, G. Yang, R.C. Bast, Jr., H.M. Amin, R. Lai, J. Liu, The role of constitutively active signal transducer and activator of transcription 3 in ovarian tumorigenesis and prognosis, Cancer, 107 (2006) 2730-2740.
[23] M. Murph, T. Tanaka, S. Liu, G.B. Mills, Of spiders and crabs: the emergence of lysophospholipids and their metabolic pathways as targets for therapy in cancer, Clinical cancer research : an official journal of the American Association for Cancer Research, 12 (2006) 6598-6602.
[24] M. Karin, Nuclear factor-kappaB in cancer development and progression, Nature, 441 (2006) 431-436.
[25] T. Reya, S.J. Morrison, M.F. Clarke, I.L. Weissman, Stem cells, cancer, and cancer stem cells, Nature, 414 (2001) 105-111.
[26] S. Valle, L. Martin-Hijano, S. Alcala, M. Alonso-Nocelo, B. Sainz, Jr., The Ever-Evolving Concept of the Cancer Stem Cell in Pancreatic Cancer, Cancers, 10 (2018).
[27] I.A. Silva, S. Bai, K. McLean, K. Yang, K. Griffith, D. Thomas, C. Ginestier, C. Johnston, A. Kueck, R.K. Reynolds, M.S. Wicha, R.J. Buckanovich, Aldehyde dehydrogenase in combination with CD133 defines angiogenic ovarian cancer stem cells that portend poor patient survival, Cancer research, 71 (2011) 3991-4001.
[28] E. Lengyel, Ovarian cancer development and metastasis, The American journal of pathology, 177 (2010) 1053-1064.

[29] S. Elloul, M.B. Elstrand, J.M. Nesland, C.G. Trope, G. Kvalheim, I. Goldberg, R. Reich, B. Davidson, Snail, Slug, and Smad-interacting protein 1 as novel parameters of disease aggressiveness in metastatic ovarian and breast carcinoma, Cancer, 103 (2005) 1631-1643.
[30] I.S. Patel, P. Madan, S. Getsios, M.A. Bertrand, C.D. MacCalman, Cadherin switching in ovarian cancer progression, International journal of cancer, 106 (2003) 172-177.
[31] L.G. Hudson, R. Zeineldin, M.S. Stack, Phenotypic plasticity of neoplastic ovarian epithelium: unique cadherin profiles in tumor progression, Clinical & experimental metastasis, 25 (2008) 643-655.
[32] J. Symowicz, B.P. Adley, K.J. Gleason, J.J. Johnson, S. Ghosh, D.A. Fishman, L.G. Hudson, M.S. Stack, Engagement of collagen-binding integrins promotes matrix metalloproteinase-9-dependent E-cadherin ectodomain shedding in ovarian carcinoma cells, Cancer research, 67 (2007) 2030-2039.
[33] A.T. Byrne, L. Ross, J. Holash, M. Nakanishi, L. Hu, J.I. Hofmann, G.D. Yancopoulos, R.B. Jaffe, Vascular endothelial growth factor-trap decreases tumor burden, inhibits ascites, and causes dramatic vascular remodeling in an ovarian cancer model, Clinical cancer research : an official journal of the American Association for Cancer Research, 9 (2003) 5721-5728.
[34] S. Paget, The distribution of secondary growths in cancer of the breast. 1889, Cancer metastasis reviews, 8 (1989) 98-101.
[35] I.J. Fidler, The pathogenesis of cancer metastasis: the 'seed and soil' hypothesis revisited, Nature reviews. Cancer, 3 (2003) 453-458.
[36] B. Orr, R.P. Edwards, Diagnosis and Treatment of Ovarian Cancer, Hematology/oncology clinics of North America, 32 (2018) 943-964.
[37] M. Morgan, J. Boyd, R. Drapkin, M.V. Seiden, Cancers Arising in the Ovary, (2014) 1592-1613.e1596.
[38] J.O. Schorge, C. McCann, M.G. Del Carmen, Surgical debulking of ovarian cancer: what difference does it make?, Reviews in obstetrics & gynecology, 3 (2010) 111-117.
[39] D.K. Armstrong, B. Bundy, L. Wenzel, H.Q. Huang, R. Baergen, S. Lele, L.J. Copeland, J.L. Walker, R.A. Burger, G. Gynecologic Oncology, Intraperitoneal cisplatin and paclitaxel in ovarian cancer, The New England journal of medicine, 354 (2006) 34-43.
[40] C. Gourley, J.L. Walker, H.J. Mackay, Update on Intraperitoneal Chemotherapy for the Treatment of Epithelial Ovarian Cancer, American Society of Clinical Oncology educational book. American Society of Clinical Oncology. Annual Meeting, 35 (2016) 143-151.
[41] M. Markman, P.Y. Liu, J. Moon, B.J. Monk, L. Copeland, S. Wilczynski, D. Alberts, Impact on survival of 12 versus 3 monthly cycles of paclitaxel (175 mg/m2) administered to patients with advanced ovarian cancer who attained a complete response to primary platinum-paclitaxel: follow-up of a Southwest Oncology Group and Gynecologic Oncology Group phase 3 trial, Gynecologic oncology, 114 (2009) 195-198.
[42] S. Pecorelli, G. Favalli, A. Gadducci, D. Katsaros, P.B. Panici, A. Carpi, G. Scambia, M. Ballardini, O. Nanni, P. Conte, G. After 6 Italian Cooperative, Phase III trial of observation versus six courses of paclitaxel in patients with advanced epithelial ovarian cancer in complete response after six courses of paclitaxel/platinum-based chemotherapy: final results of the After-6 protocol 1, Journal of clinical oncology : official journal of the American Society of Clinical Oncology, 27 (2009) 4642-4648.
[43] R.L. Coleman, J. Liu, K. Matsuo, P.H. Thaker, S.N. Westin, A.K. Sood, Carcinoma of the Ovaries and Fallopian Tubes, (2020) 1525-1543.e1527.
[44] C. Aghajanian, S.V. Blank, B.A. Goff, P.L. Judson, M.G. Teneriello, A. Husain, M.A. Sovak, J. Yi, L.R. Nycum, OCEANS: a randomized, double-blind, placebo-controlled phase III trial of chemotherapy with or without bevacizumab in patients with platinum-sensitive recurrent epithelial ovarian, primary peritoneal, or fallopian tube cancer, Journal of clinical oncology : official journal of the American Society of Clinical Oncology, 30 (2012) 2039-2045.

[45] E. Pujade-Lauraine, F. Hilpert, B. Weber, A. Reuss, A. Poveda, G. Kristensen, R. Sorio, I. Vergote, P. Witteveen, A. Bamias, D. Pereira, P. Wimberger, A. Oaknin, M.R. Mirza, P. Follana, D. Bollag, I. Ray-Coquard, Bevacizumab combined with chemotherapy for platinum-resistant recurrent ovarian cancer: The AURELIA open-label randomized phase III trial, Journal of clinical oncology : official journal of the American Society of Clinical Oncology, 32 (2014) 1302-1308.
[46] K.A. Gelmon, M. Tischkowitz, H. Mackay, K. Swenerton, A. Robidoux, K. Tonkin, H. Hirte, D. Huntsman, M. Clemons, B. Gilks, R. Yerushalmi, E. Macpherson, J. Carmichael, A. Oza, Olaparib in patients with recurrent high-grade serous or poorly differentiated ovarian carcinoma or triple-negative breast cancer: a phase 2, multicentre, open-label, non-randomised study, The Lancet. Oncology, 12 (2011) 852-861.
[47] R. Kristeleit, G.I. Shapiro, H.A. Burris, A.M. Oza, P. LoRusso, M.R. Patel, S.M. Domchek, J. Balmana, Y. Drew, L.M. Chen, T. Safra, A. Montes, H. Giordano, L. Maloney, S. Goble, J. Isaacson, J. Xiao, J. Borrow, L. Rolfe, R. Shapira-Frommer, A Phase I-II Study of the Oral PARP Inhibitor Rucaparib in Patients with Germline BRCA1/2-Mutated Ovarian Carcinoma or Other Solid Tumors, Clinical cancer research : an official journal of the American Association for Cancer Research, 23 (2017) 4095-4106.
[48] I. Ray-Coquard, P. Pautier, S. Pignata, D. Perol, A. Gonzalez-Martin, R. Berger, K. Fujiwara, I. Vergote, N. Colombo, J. Maenpaa, F. Selle, J. Sehouli, D. Lorusso, E.M. Guerra Alia, A. Reinthaller, S. Nagao, C. Lefeuvre-Plesse, U. Canzler, G. Scambia, A. Lortholary, F. Marme, P. Combe, N. de Gregorio, M. Rodrigues, P. Buderath, C. Dubot, A. Burges, B. You, E. Pujade-Lauraine, P. Harter, P.-. Investigators, Olaparib plus Bevacizumab as First-Line Maintenance in Ovarian Cancer, The New England journal of medicine, 381 (2019) 2416-2428.
[49] J.A. Watkins, S. Irshad, A. Grigoriadis, A.N. Tutt, Genomic scars as biomarkers of homologous recombination deficiency and drug response in breast and ovarian cancers, Breast cancer research : BCR, 16 (2014) 211.
[50] Z. Ji, Y. Shen, X. Feng, Y. Kong, Y. Shao, J. Meng, X. Zhang, G. Yang, Deregulation of Lipid Metabolism: The Critical Factors in Ovarian Cancer, Frontiers in oncology, 10 (2020) 593017.
[51] S.A. Mir, S.B.J. Wong, K. Narasimhan, C.W.L. Esther, S. Ji, B. Burla, M.R. Wenk, D.S.P. Tan, A.K. Bendt, Lipidomic Analysis of Archival Pathology Specimens Identifies Altered Lipid Signatures in Ovarian Clear Cell Carcinoma, Metabolites, 11 (2021).
[52] W.H. Koppenol, P.L. Bounds, C.V. Dang, Otto Warburg's contributions to current concepts of cancer metabolism, Nature reviews. Cancer, 11 (2011) 325-337.
[53] P.S. Ward, C.B. Thompson, Metabolic reprogramming: a cancer hallmark even warburg did not anticipate, Cancer cell, 21 (2012) 297-308.
[54] J. Kim, R.J. DeBerardinis, Mechanisms and Implications of Metabolic Heterogeneity in Cancer, Cell metabolism, 30 (2019) 434-446.
[55] B. Faubert, A. Solmonson, R.J. DeBerardinis, Metabolic reprogramming and cancer progression, Science, 368 (2020).
[56] K.M. Nieman, H.A. Kenny, C.V. Penicka, A. Ladanyi, R. Buell-Gutbrod, M.R. Zillhardt, I.L. Romero, M.S. Carey, G.B. Mills, G.S. Hotamisligil, S.D. Yamada, M.E. Peter, K. Gwin, E. Lengyel, Adipocytes promote ovarian cancer metastasis and provide energy for rapid tumor growth, Nature medicine, 17 (2011) 1498-1503.
[57] A. Ladanyi, A. Mukherjee, H.A. Kenny, A. Johnson, A.K. Mitra, S. Sundaresan, K.M. Nieman, G. Pascual, S.A. Benitah, A. Montag, S.D. Yamada, N.A. Abumrad, E. Lengyel, Adipocyte-induced CD36 expression drives ovarian cancer progression and metastasis, Oncogene, 37 (2018) 2285-2301.
[58] C. Holohan, S. Van Schaeybroeck, D.B. Longley, P.G. Johnston, Cancer drug resistance: an evolving paradigm, Nature reviews. Cancer, 13 (2013) 714-726.

[59] Y. Zhao, E.B. Butler, M. Tan, Targeting cellular metabolism to improve cancer therapeutics, Cell death & disease, 4 (2013) e532.
[60] J. Lin, L. Xia, J. Liang, Y. Han, H. Wang, L. Oyang, S. Tan, Y. Tian, S. Rao, X. Chen, Y. Tang, M. Su, X. Luo, Y. Wang, H. Wang, Y. Zhou, Q. Liao, The roles of glucose metabolic reprogramming in chemo- and radio-resistance, Journal of experimental & clinical cancer research : CR, 38 (2019) 218.
[61] W. Wagner, W.M. Ciszewski, K.D. Kania, L- and D-lactate enhance DNA repair and modulate the resistance of cervical carcinoma cells to anticancer drugs via histone deacetylase inhibition and hydroxycarboxylic acid receptor 1 activation, Cell communication and signaling : CCS, 13 (2015) 36.
[62] Y. Tan, J. Li, G. Zhao, K.C. Huang, H. Cardenas, Y. Wang, D. Matei, J.X. Cheng, Metabolic reprogramming from glycolysis to fatty acid uptake and beta-oxidation in platinum-resistant cancer cells, Nature communications, 13 (2022) 4554.
[63] Y. Cao, Adipocyte and lipid metabolism in cancer drug resistance, The Journal of clinical investigation, 129 (2019) 3006-3017.
[64] N. Zhou, X. Wu, B. Yang, X. Yang, D. Zhang, G. Qing, Stem cell characteristics of dormant cells and cisplatininduced effects on the stemness of epithelial ovarian cancer cells, Molecular medicine reports, 10 (2014) 2495-2504.
[65] A. Wiechert, C. Saygin, P.S. Thiagarajan, V.S. Rao, J.S. Hale, N. Gupta, M. Hitomi, A.B. Nagaraj, A. DiFeo, J.D. Lathia, O. Reizes, Cisplatin induces stemness in ovarian cancer, Oncotarget, 7 (2016) 30511-30522.
[66] S. Ramadoss, S. Sen, I. Ramachandran, S. Roy, G. Chaudhuri, R. Farias-Eisner, Lysine-specific demethylase KDM3A regulates ovarian cancer stemness and chemoresistance, Oncogene, 36 (2017) 6508.
[67] J. Li, S. Condello, J. Thomes-Pepin, X. Ma, Y. Xia, T.D. Hurley, D. Matei, J.X. Cheng, Lipid Desaturation Is a Metabolic Marker and Therapeutic Target of Ovarian Cancer Stem Cells, Cell Stem Cell, 20 (2017) 303-314 e305.
[68] Y.C. Chae, J.H. Kim, Cancer stem cell metabolism: target for cancer therapy, BMB reports, 51 (2018) 319-326.
[69] E. Fahy, D. Cotter, M. Sud, S. Subramaniam, Lipid classification, structures and tools, Biochimica et biophysica acta, 1811 (2011) 637-647.
[70] R.E. Gimeno, Fatty acid transport proteins, Current opinion in lipidology, 18 (2007) 271-276.
[71] M. Furuhashi, G.S. Hotamisligil, Fatty acid-binding proteins: role in metabolic diseases and potential as drug targets, Nature reviews. Drug discovery, 7 (2008) 489-503.
[72] H. Jeon, S.C. Blacklow, Structure and physiologic function of the low-density lipoprotein receptor, Annual review of biochemistry, 74 (2005) 535-562.
[73] J. Pohl, A. Ring, T. Hermann, W. Stremmel, Role of FATP in parenchymal cell fatty acid uptake, Biochimica et biophysica acta, 1686 (2004) 1-6.
[74] H. Doege, A. Stahl, Protein-mediated fatty acid uptake: novel insights from in vivo models, Physiology, 21 (2006) 259-268.
[75] J.F. Glatz, J.J. Luiken, From fat to FAT (CD36/SR-B2): Understanding the regulation of cellular fatty acid uptake, Biochimie, 136 (2017) 21-26.
[76] N. Zaidi, J.V. Swinnen, K. Smans, ATP-citrate lyase: a key player in cancer metabolism, Cancer research, 72 (2012) 3709-3714.
[77] T. Maier, M. Leibundgut, N. Ban, The crystal structure of a mammalian fatty acid synthase, Science, 321 (2008) 1315-1322.
[78] A. Jakobsson, R. Westerberg, A. Jacobsson, Fatty acid elongases in mammals: their regulation and roles in metabolism, Progress in lipid research, 45 (2006) 237-249.

[79] M. Miyazaki, J.M. Ntambi, Role of stearoyl-coenzyme A desaturase in lipid metabolism, Prostaglandins, leukotrienes, and essential fatty acids, 68 (2003) 113-121.
[80] J.M. Ntambi, M. Miyazaki, Regulation of stearoyl-CoA desaturases and role in metabolism, Progress in lipid research, 43 (2004) 91-104.
[81] H. Wang, M.G. Klein, H. Zou, W. Lane, G. Snell, I. Levin, K. Li, B.C. Sang, Crystal structure of human stearoyl-coenzyme A desaturase in complex with substrate, Nature structural & molecular biology, 22 (2015) 581-585.
[82] R.A. Igal, D.I. Sinner, Stearoyl-CoA desaturase 5 (SCD5), a Delta-9 fatty acyl desaturase in search of a function, Biochimica et biophysica acta. Molecular and cell biology of lipids, 1866 (2021) 158840.
[83] J. Wang, L. Yu, R.E. Schmidt, C. Su, X. Huang, K. Gould, G. Cao, Characterization of HSCD5, a novel human stearoyl-CoA desaturase unique to primates, Biochemical and biophysical research communications, 332 (2005) 735-742.
[84] Y. Guo, K.R. Cordes, R.V. Farese, Jr., T.C. Walther, Lipid droplets at a glance, J Cell Sci, 122 (2009) 749-752.
[85] J. Rios-Esteves, M.D. Resh, Stearoyl CoA desaturase is required to produce active, lipid-modified Wnt proteins, Cell reports, 4 (2013) 1072-1081.
[86] A.H. Nile, R.N. Hannoush, Fatty acylation of Wnt proteins, Nature chemical biology, 12 (2016) 60-69.
[87] V.I. Torres, J.A. Godoy, N.C. Inestrosa, Modulating Wnt signaling at the root: Porcupine and Wnt acylation, Pharmacology & therapeutics, 198 (2019) 34-45.
[88] P. Rinaldo, D. Matern, M.J. Bennett, Fatty acid oxidation disorders, Annual review of physiology, 64 (2002) 477-502.
[89] H. Lee, W.J. Park, Unsaturated fatty acids, desaturases, and human health, Journal of medicinal food, 17 (2014) 189-197.
[90] J. Zhao, Z. Zhi, C. Wang, H. Xing, G. Song, X. Yu, Y. Zhu, X. Wang, X. Zhang, Y. Di, Exogenous lipids promote the growth of breast cancer cells via CD36, Oncology reports, 38 (2017) 2105-2115.
[91] J.P. Sundelin, M. Stahlman, A. Lundqvist, M. Levin, P. Parini, M.E. Johansson, J. Boren, Increased expression of the very low-density lipoprotein receptor mediates lipid accumulation in clear-cell renal cell carcinoma, PloS one, 7 (2012) e48694.
[92] K. Bensaad, E. Favaro, C.A. Lewis, B. Peck, S. Lord, J.M. Collins, K.E. Pinnick, S. Wigfield, F.M. Buffa, J.L. Li, Q. Zhang, M.J.O. Wakelam, F. Karpe, A. Schulze, A.L. Harris, Fatty acid uptake and lipid storage induced by HIF-1alpha contribute to cell growth and survival after hypoxia-reoxygenation, Cell reports, 9 (2014) 349-365.
[93] J. Adamson, E.A. Morgan, C. Beesley, Y. Mei, C.S. Foster, H. Fujii, P.S. Rudland, P.H. Smith, Y. Ke, High-level expression of cutaneous fatty acid-binding protein in prostatic carcinomas and its effect on tumorigenicity, Oncogene, 22 (2003) 2739-2749.
[94] K.A. Garcia, M.L. Costa, E. Lacunza, M.E. Martinez, B. Corsico, N. Scaglia, Fatty acid binding protein 5 regulates lipogenesis and tumor growth in lung adenocarcinoma, Life sciences, 301 (2022) 120621.
[95] G. Pascual, A. Avgustinova, S. Mejetta, M. Martin, A. Castellanos, C.S. Attolini, A. Berenguer, N. Prats, A. Toll, J.A. Hueto, C. Bescos, L. Di Croce, S.A. Benitah, Targeting metastasis-initiating cells through the fatty acid receptor CD36, Nature, 541 (2017) 41-45.
[96] A. Montero-Calle, M. Gomez de Cedron, A. Quijada-Freire, G. Solis-Fernandez, V. Lopez-Alonso, I. Espinosa-Salinas, A. Pelaez-Garcia, M.J. Fernandez-Acenero, A. Ramirez de Molina, R. Barderas, Metabolic Reprogramming Helps to Define Different Metastatic Tropisms in Colorectal Cancer, Frontiers in oncology, 12 (2022) 903033.
[97] J.J. Kamphorst, J.R. Cross, J. Fan, E. de Stanchina, R. Mathew, E.P. White, C.B. Thompson, J.D. Rabinowitz, Hypoxic and Ras-transformed cells support growth by scavenging unsaturated fatty acids

from lysophospholipids, Proceedings of the National Academy of Sciences of the United States of America, 110 (2013) 8882-8887.
[98] Y. Zhou, J. Tao, D.F. Calvisi, X. Chen, Role of Lipogenesis Rewiring in Hepatocellular Carcinoma, Seminars in liver disease, 42 (2022) 77-86.
[99] K.M. Gharpure, S. Pradeep, M. Sans, R. Rupaimoole, C. Ivan, S.Y. Wu, E. Bayraktar, A.S. Nagaraja, L.S. Mangala, X. Zhang, M. Haemmerle, W. Hu, C. Rodriguez-Aguayo, M. McGuire, C.S.L. Mak, X. Chen, M.A. Tran, A. Villar-Prados, G.A. Pena, R. Kondetimmanahalli, R. Nini, P. Koppula, P. Ram, J. Liu, G. Lopez-Berestein, K. Baggerly, S.E. L, A.K. Sood, FABP4 as a key determinant of metastatic potential of ovarian cancer, Nature communications, 9 (2018) 2923.
[100] O. Warburg, On the metabolism of cancer cells, Naturwissenschaften, 12 (1924) 1131-1137.
[101] O. Warburg, On the origin of cancer cells, Science, 123 (1956) 309-314.
[102] M.G. Vander Heiden, L.C. Cantley, C.B. Thompson, Understanding the Warburg effect: the metabolic requirements of cell proliferation, Science, 324 (2009) 1029-1033.
[103] Y. Zhang, H. Wang, J. Zhang, J. Lv, Y. Huang, Positive feedback loop and synergistic effects between hypoxia-inducible factor-2alpha and stearoyl-CoA desaturase-1 promote tumorigenesis in clear cell renal cell carcinoma, Cancer science, 104 (2013) 416-422.
[104] D. Ackerman, M.C. Simon, Hypoxia, lipids, and cancer: surviving the harsh tumor microenvironment, Trends in cell biology, 24 (2014) 472-478.
[105] B. Peck, Z.T. Schug, Q. Zhang, B. Dankworth, D.T. Jones, E. Smethurst, R. Patel, S. Mason, M. Jiang, R. Saunders, M. Howell, R. Mitter, B. Spencer-Dene, G. Stamp, L. McGarry, D. James, E. Shanks, E.O. Aboagye, S.E. Critchlow, H.Y. Leung, A.L. Harris, M.J.O. Wakelam, E. Gottlieb, A. Schulze, Inhibition of fatty acid desaturation is detrimental to cancer cell survival in metabolically compromised environments, Cancer & metabolism, 4 (2016) 6.
[106] T.R. Stoyanoff, J.P. Rodriguez, J.S. Todaro, J.D. Espada, J.P. Colavita, N.C. Brandan, A.M. Torres, M.V. Aguirre, Tumor biology of non-metastatic stages of clear cell renal cell carcinoma; overexpression of stearoyl desaturase-1, EPO/EPO-R system and hypoxia-related proteins, Tumour biology : the journal of the International Society for Oncodevelopmental Biology and Medicine, 37 (2016) 13581-13593.
[107] D. Ackerman, S. Tumanov, B. Qiu, E. Michalopoulou, M. Spata, A. Azzam, H. Xie, M.C. Simon, J.J. Kamphorst, Triglycerides Promote Lipid Homeostasis during Hypoxic Stress by Balancing Fatty Acid Saturation, Cell reports, 24 (2018) 2596-2605 e2595.
[108] J.P. Melana, F. Mignolli, T. Stoyanoff, M.V. Aguirre, M.A. Balboa, J. Balsinde, J.P. Rodriguez, The Hypoxic Microenvironment Induces Stearoyl-CoA Desaturase-1 Overexpression and Lipidomic Profile Changes in Clear Cell Renal Cell Carcinoma, Cancers, 13 (2021).
[109] H. Yin, X. Qiu, Y. Shan, B. You, L. Xie, P. Zhang, J. Zhao, Y. You, HIF-1alpha downregulation of miR-433-3p in adipocyte-derived exosomes contributes to NPC progression via targeting SCD1, Cancer science, 112 (2021) 1457-1470.
[110] V. Chajes, M. Cambot, K. Moreau, G.M. Lenoir, V. Joulin, Acetyl-CoA carboxylase alpha is essential to breast cancer cell survival, Cancer research, 66 (2006) 5287-5294.
[111] X. Wu, Z. Dong, C.J. Wang, L.J. Barlow, V. Fako, M.A. Serrano, Y. Zou, J.Y. Liu, J.T. Zhang, FASN regulates cellular response to genotoxic treatments by increasing PARP-1 expression and DNA repair activity via NF-kappaB and SP1, Proceedings of the National Academy of Sciences of the United States of America, 113 (2016) E6965-E6973.
[112] Y. Zhao, H. Li, Y. Zhang, L. Li, R. Fang, Y. Li, Q. Liu, W. Zhang, L. Qiu, F. Liu, X. Zhang, L. Ye, Oncoprotein HBXIP Modulates Abnormal Lipid Metabolism and Growth of Breast Cancer Cells by Activating the LXRs/SREBP-1c/FAS Signaling Cascade, Cancer research, 76 (2016) 4696-4707.

[113] Z. Zhao, Y. Liu, Q. Liu, F. Wu, X. Liu, H. Qu, Y. Yuan, J. Ge, Y. Xu, H. Wang, The mRNA Expression Signature and Prognostic Analysis of Multiple Fatty Acid Metabolic Enzymes in Clear Cell Renal Cell Carcinoma, Journal of Cancer, 10 (2019) 6599-6607.
[114] C. Li, L. Zhang, Z. Qiu, W. Deng, W. Wang, Key Molecules of Fatty Acid Metabolism in Gastric Cancer, Biomolecules, 12 (2022).
[115] M. Hilvo, C. Denkert, L. Lehtinen, B. Muller, S. Brockmoller, T. Seppanen-Laakso, J. Budczies, E. Bucher, L. Yetukuri, S. Castillo, E. Berg, H. Nygren, M. Sysi-Aho, J.L. Griffin, O. Fiehn, S. Loibl, C. Richter-Ehrenstein, C. Radke, T. Hyotylainen, O. Kallioniemi, K. Iljin, M. Oresic, Novel theranostic opportunities offered by characterization of altered membrane lipid metabolism in breast cancer progression, Cancer research, 71 (2011) 3236-3245.
[116] Y. Ide, M. Waki, T. Hayasaka, T. Nishio, Y. Morita, H. Tanaka, T. Sasaki, K. Koizumi, R. Matsunuma, Y. Hosokawa, H. Ogura, N. Shiiya, M. Setou, Human breast cancer tissues contain abundant phosphatidylcholine(36ratio1) with high stearoyl-CoA desaturase-1 expression, PloS one, 8 (2013) e61204.
[117] S. Guo, L. Qiu, Y. Wang, X. Qin, H. Liu, M. He, Y. Zhang, Z. Li, X. Chen, Tissue imaging and serum lipidomic profiling for screening potential biomarkers of thyroid tumors by matrix-assisted laser desorption/ionization-Fourier transform ion cyclotron resonance mass spectrometry, Analytical and bioanalytical chemistry, 406 (2014) 4357-4370.
[118] G. Lucarelli, M. Ferro, D. Loizzo, C. Bianchi, D. Terracciano, F. Cantiello, L.N. Bell, S. Battaglia, C. Porta, A. Gernone, R.A. Perego, E. Maiorano, O. Cobelli, G. Castellano, L. Vincenti, P. Ditonno, M. Battaglia, Integration of Lipidomics and Transcriptomics Reveals Reprogramming of the Lipid Metabolism and Composition in Clear Cell Renal Cell Carcinoma, Metabolites, 10 (2020).
[119] J.M. Mitchell, R.M. Flight, H.N.B. Moseley, Untargeted Lipidomics of Non-Small Cell Lung Carcinoma Demonstrates Differentially Abundant Lipid Classes in Cancer vs. Non-Cancer Tissue, Metabolites, 11 (2021).
[120] Y. Wang, S. Ma, W.L. Ruzzo, Spatial modeling of prostate cancer metabolic gene expression reveals extensive heterogeneity and selective vulnerabilities, Scientific reports, 10 (2020) 3490.
[121] J. Griffitts, Y. Tesiram, G.E. Reid, D. Saunders, R.A. Floyd, R.A. Towner, In vivo MRS assessment of altered fatty acyl unsaturation in liver tumor formation of a TGF alpha/c-myc transgenic mouse model, Journal of lipid research, 50 (2009) 611-622.
[122] J. Dlubek, J. Rysz, Z. Jablonowski, A. Gluba-Brzozka, B. Franczyk, The Correlation between Lipid Metabolism Disorders and Prostate Cancer, Current medicinal chemistry, 28 (2021) 2048-2061.
[123] B. Paul, M. Lewinska, J.B. Andersen, Lipid alterations in chronic liver disease and liver cancer, JHEP reports : innovation in hepatology, 4 (2022) 100479.
[124] R.A. Igal, Stearoyl-CoA desaturase-1: a novel key player in the mechanisms of cell proliferation, programmed cell death and transformation to cancer, Carcinogenesis, 31 (2010) 1509-1515.
[125] R.A. Igal, Roles of StearoylCoA Desaturase-1 in the Regulation of Cancer Cell Growth, Survival and Tumorigenesis, Cancers, 3 (2011) 2462-2477.
[126] R.A. Igal, Stearoyl CoA desaturase-1: New insights into a central regulator of cancer metabolism, Biochimica et biophysica acta, 1861 (2016) 1865-1880.
[127] B. Peck, A. Schulze, Lipid desaturation - the next step in targeting lipogenesis in cancer?, The FEBS journal, 283 (2016) 2767-2778.
[128] J.M. Ntambi, M. Miyazaki, A. Dobrzyn, Regulation of stearoyl-CoA desaturase expression, Lipids, 39 (2004) 1061-1065.

[129] H. Zhang, Q. Liu, C. Zhao, Y. Zhang, S. Wang, R. Liu, Y. Pu, L. Yin, The dysregulation of unsaturated fatty acid-based metabolomics in the MNNG-induced malignant transformation of Het-1A cells, Environmental science and pollution research international, (2022).
[130] F.S. Falvella, R.M. Pascale, M. Gariboldi, G. Manenti, M.R. De Miglio, M.M. Simile, T.A. Dragani, F. Feo, Stearoyl-CoA desaturase 1 (Scd1) gene overexpression is associated with genetic predisposition to hepatocarcinogenesis in mice and rats, Carcinogenesis, 23 (2002) 1933-1936.
[131] N. Scaglia, J.M. Caviglia, R.A. Igal, High stearoyl-CoA desaturase protein and activity levels in simian virus 40 transformed-human lung fibroblasts, Biochimica et biophysica acta, 1687 (2005) 141-151.
[132] X. Du, Q.R. Wang, E. Chan, M. Merchant, J. Liu, D. French, A. Ashkenazi, J. Qing, FGFR3 stimulates stearoyl CoA desaturase 1 activity to promote bladder tumor growth, Cancer research, 72 (2012) 5843-5855.
[133] C.A. von Roemeling, L.A. Marlow, A.B. Pinkerton, A. Crist, J. Miller, H.W. Tun, R.C. Smallridge, J.A. Copland, Aberrant lipid metabolism in anaplastic thyroid carcinoma reveals stearoyl CoA desaturase 1 as a novel therapeutic target, The Journal of clinical endocrinology and metabolism, 100 (2015) E697-709.
[134] G. Pampalakis, A.L. Politi, A. Papanastasiou, G. Sotiropoulou, Distinct cholesterogenic and lipidogenic gene expression patterns in ovarian cancer - a new pool of biomarkers, Genes & cancer, 6 (2015) 472-479.
[135] T. Vargas, J. Moreno-Rubio, J. Herranz, P. Cejas, S. Molina, M. Gonzalez-Vallinas, M. Mendiola, E. Burgos, C. Aguayo, A.B. Custodio, I. Machado, D. Ramos, M. Gironella, I. Espinosa-Salinas, R. Ramos, R. Martin-Hernandez, A. Risueno, J. De Las Rivas, G. Reglero, R. Yaya, C. Fernandez-Martos, J. Aparicio, J. Maurel, J. Feliu, A. Ramirez de Molina, ColoLipidGene: signature of lipid metabolism-related genes to predict prognosis in stage-II colon cancer patients, Oncotarget, 6 (2015) 7348-7363.
[136] J. Huang, X.X. Fan, J. He, H. Pan, R.Z. Li, L. Huang, Z. Jiang, X.J. Yao, L. Liu, E.L. Leung, J.X. He, SCD1 is associated with tumor promotion, late stage and poor survival in lung adenocarcinoma, Oncotarget, 7 (2016) 39970-39979.
[137] C.A. von Roemeling, J.A. Copland, Targeting lipid metabolism for the treatment of anaplastic thyroid carcinoma, Expert opinion on therapeutic targets, 20 (2016) 159-166.
[138] F. Rosignolo, M. Sponziello, C. Durante, C. Puppin, C. Mio, F. Baldan, C. Di Loreto, D. Russo, S. Filetti, G. Damante, Expression of PAX8 Target Genes in Papillary Thyroid Carcinoma, PloS one, 11 (2016) e0156658.
[139] M. Gaggini, M. Cabiati, S. Del Turco, T. Navarra, P. De Simone, F. Filipponi, S. Del Ry, A. Gastaldelli, G. Basta, Increased FNDC5/Irisin expression in human hepatocellular carcinoma, Peptides, 88 (2017) 62-66.
[140] M. Presler, A. Wojtczyk-Miaskowska, B. Schlichtholz, A. Kaluzny, M. Matuszewski, A. Mika, T. Sledzinski, J. Swierczynski, Increased expression of the gene encoding stearoyl-CoA desaturase 1 in human bladder cancer, Molecular and cellular biochemistry, 447 (2018) 217-224.
[141] W. Li, H. Bai, S. Liu, D. Cao, H. Wu, K. Shen, Y. Tai, J. Yang, Targeting stearoyl-CoA desaturase 1 to repress endometrial cancer progression, Oncotarget, 9 (2018) 12064-12078.
[142] C. Wang, M. Shi, J. Ji, Q. Cai, Q. Zhao, J. Jiang, J. Liu, H. Zhang, Z. Zhu, J. Zhang, Stearoyl-CoA desaturase 1 (SCD1) facilitates the growth and anti-ferroptosis of gastric cancer cells and predicts poor prognosis of gastric cancer, Aging, 12 (2020) 15374-15391.
[143] C.S. Kubota, P.J. Espenshade, Targeting stearoyl-CoA desaturase in solid tumors, Cancer research, (2022).
[144] L. Wang, G. Ye, Y. Wang, C. Wang, Stearoyl-CoA desaturase 1 regulates malignant progression of cervical cancer cells, Bioengineered, 13 (2022) 12941-12954.

[145] U.V. Roongta, J.G. Pabalan, X. Wang, R.P. Ryseck, J. Fargnoli, B.J. Henley, W.P. Yang, J. Zhu, M.T. Madireddi, R.M. Lawrence, T.W. Wong, B.A. Rupnow, Cancer cell dependence on unsaturated fatty acids implicates stearoyl-CoA desaturase as a target for cancer therapy, Molecular cancer research : MCR, 9 (2011) 1551-1561.
[146] P. Mason, B. Liang, L. Li, T. Fremgen, E. Murphy, A. Quinn, S.L. Madden, H.P. Biemann, B. Wang, A. Cohen, S. Komarnitsky, K. Jancsics, B. Hirth, C.G. Cooper, E. Lee, S. Wilson, R. Krumbholz, S. Schmid, Y. Xiang, M. Booker, J. Lillie, K. Carter, SCD1 inhibition causes cancer cell death by depleting mono-unsaturated fatty acids, PloS one, 7 (2012) e33823.
[147] C.A. von Roemeling, T.R. Caulfield, L. Marlow, I. Bok, J. Wen, J.L. Miller, R. Hughes, L. Hazlehurst, A.B. Pinkerton, D.C. Radisky, H.W. Tun, Y.S.B. Kim, A.L. Lane, J.A. Copland, Accelerated bottom-up drug design platform enables the discovery of novel stearoyl-CoA desaturase 1 inhibitors for cancer therapy, Oncotarget, 9 (2018) 3-20.
[148] J.M. Ntambi, M. Miyazaki, J.P. Stoehr, H. Lan, C.M. Kendziorski, B.S. Yandell, Y. Song, P. Cohen, J.M. Friedman, A.D. Attie, Loss of stearoyl-CoA desaturase-1 function protects mice against adiposity, Proceedings of the National Academy of Sciences of the United States of America, 99 (2002) 11482-11486.
[149] H. Sampath, J.M. Ntambi, The role of stearoyl-CoA desaturase in obesity, insulin resistance, and inflammation, Annals of the New York Academy of Sciences, 1243 (2011) 47-53.
[150] X. Xu, Y. Ding, J. Yao, Z. Wei, H. Jin, C. Chen, J. Feng, R. Ying, miR-215 Inhibits Colorectal Cancer Cell Migration and Invasion via Targeting Stearoyl-CoA Desaturase, Computational and mathematical methods in medicine, 2020 (2020) 5807836.
[151] M.T. Nakamura, T.Y. Nara, Structure, function, and dietary regulation of delta6, delta5, and delta9 desaturases, Annual review of nutrition, 24 (2004) 345-376.
[152] Z. Wang, H.G. Park, D.H. Wang, R. Kitano, K.S.D. Kothapalli, J.T. Brenna, Fatty acid desaturase 2 (FADS2) but not FADS1 desaturates branched chain and odd chain saturated fatty acids, Biochimica et biophysica acta. Molecular and cell biology of lipids, 1865 (2020) 158572.
[153] K. Muir, A. Hazim, Y. He, M. Peyressatre, D.Y. Kim, X. Song, L. Beretta, Proteomic and lipidomic signatures of lipid metabolism in NASH-associated hepatocellular carcinoma, Cancer research, 73 (2013) 4722-4731.
[154] J. Amezaga, G. Ugartemendia, A. Larraioz, N. Bretana, A. Iruretagoyena, J. Camba, A. Urruticoechea, C. Ferreri, I. Tueros, Altered Levels of Desaturation and omega-6 Fatty Acids in Breast Cancer Patients' Red Blood Cell Membranes, Metabolites, 10 (2020).
[155] T. Vargas, J. Moreno-Rubio, J. Herranz, P. Cejas, S. Molina, M. Mendiola, E. Burgos, A.B. Custodio, M. De Miguel, R. Martin-Hernandez, G. Reglero, J. Feliu, A. Ramirez de Molina, 3'UTR Polymorphism in ACSL1 Gene Correlates with Expression Levels and Poor Clinical Outcome in Colon Cancer Patients, PloS one, 11 (2016) e0168423.
[156] R. Sanchez-Martinez, S. Cruz-Gil, M.S. Garcia-Alvarez, G. Reglero, A. Ramirez de Molina, Complementary ACSL isoforms contribute to a non-Warburg advantageous energetic status characterizing invasive colon cancer cells, Scientific reports, 7 (2017) 11143.
[157] S. Cruz-Gil, R. Sanchez-Martinez, M. Gomez de Cedron, R. Martin-Hernandez, T. Vargas, S. Molina, J. Herranz, A. Davalos, G. Reglero, A. Ramirez de Molina, Targeting the lipid metabolic axis ACSL/SCD in colorectal cancer progression by therapeutic miRNAs: miR-19b-1 role, Journal of lipid research, 59 (2018) 14-24.
[158] D. Zhang, P. Wang, M.N. Slipchenko, J.X. Cheng, Fast vibrational imaging of single cells and tissues by stimulated Raman scattering microscopy, Accounts of chemical research, 47 (2014) 2282-2290.

[159] J.X. Cheng, X.S. Xie, Vibrational spectroscopic imaging of living systems: An emerging platform for biology and medicine, Science, 350 (2015) aaa8870.
[160] Y. Luo, S. Huang, J. Wei, H. Zhou, W. Wang, J. Yang, Q. Deng, H. Wang, Z. Fu, Long noncoding RNA LINC01606 protects colon cancer cells from ferroptotic cell death and promotes stemness by SCD1-Wnt/beta-catenin-TFE3 feedback loop signalling, Clinical and translational medicine, 12 (2022) e752.
[161] A. Koeberle, K. Loser, M. Thurmer, Stearoyl-CoA desaturase-1 and adaptive stress signaling, Biochimica et biophysica acta, 1861 (2016) 1719-1726.
[162] R. Sanchez-Martinez, S. Cruz-Gil, M. Gomez de Cedron, M. Alvarez-Fernandez, T. Vargas, S. Molina, B. Garcia, J. Herranz, J. Moreno-Rubio, G. Reglero, M. Perez-Moreno, J. Feliu, M. Malumbres, A. Ramirez de Molina, A link between lipid metabolism and epithelial-mesenchymal transition provides a target for colon cancer therapy, Oncotarget, 6 (2015) 38719-38736.
[163] J. Zhang, F. Song, X. Zhao, H. Jiang, X. Wu, B. Wang, M. Zhou, M. Tian, B. Shi, H. Wang, Y. Jia, H. Wang, X. Pan, Z. Li, EGFR modulates monounsaturated fatty acid synthesis through phosphorylation of SCD1 in lung cancer, Molecular cancer, 16 (2017) 127.
[164] S.J. Kim, H. Choi, S.S. Park, C. Chang, E. Kim, Stearoyl CoA desaturase (SCD) facilitates proliferation of prostate cancer cells through enhancement of androgen receptor transactivation, Molecules and cells, 31 (2011) 371-377.
[165] M.L. Doria, A.S. Ribeiro, J. Wang, C.Z. Cotrim, P. Domingues, C. Williams, M.R. Domingues, L.A. Helguero, Fatty acid and phospholipid biosynthetic pathways are regulated throughout mammary epithelial cell differentiation and correlate to breast cancer survival, FASEB journal : official publication of the Federation of American Societies for Experimental Biology, 28 (2014) 4247-4264.
[166] E.F. Contreras-Lopez, C.D. Cruz-Hernandez, S.A. Cortes-Ramirez, A. Ramirez-Higuera, C. Pena-Montes, M. Rodriguez-Dorantes, R.M. Oliart-Ros, Inhibition of Stearoyl-CoA Desaturase by Sterculic Oil Reduces Proliferation and Induces Apoptosis in Prostate Cancer Cell Lines, Nutrition and cancer, (2021) 1-14.
[167] V. Fritz, Z. Benfodda, G. Rodier, C. Henriquet, F. Iborra, C. Avances, Y. Allory, A. de la Taille, S. Culine, H. Blancou, J.P. Cristol, F. Michel, C. Sardet, L. Fajas, Abrogation of de novo lipogenesis by stearoyl-CoA desaturase 1 inhibition interferes with oncogenic signaling and blocks prostate cancer progression in mice, Molecular cancer therapeutics, 9 (2010) 1740-1754.
[168] D. Hess, J.W. Chisholm, R.A. Igal, Inhibition of stearoylCoA desaturase activity blocks cell cycle progression and induces programmed cell death in lung cancer cells, PloS one, 5 (2010) e11394.
[169] N. Scaglia, R.A. Igal, Inhibition of Stearoyl-CoA Desaturase 1 expression in human lung adenocarcinoma cells impairs tumorigenesis, International journal of oncology, 33 (2008) 839-850.
[170] M. Nashed, J.W. Chisholm, R.A. Igal, Stearoyl-CoA desaturase activity modulates the activation of epidermal growth factor receptor in human lung cancer cells, Experimental biology and medicine, 237 (2012) 1007-1017.
[171] H. Wang, Y. Zhang, Y. Lu, J. Song, M. Huang, J. Zhang, Y. Huang, The role of stearoyl-coenzyme A desaturase 1 in clear cell renal cell carcinoma, Tumour biology : the journal of the International Society for Oncodevelopmental Biology and Medicine, 37 (2016) 479-489.
[172] A.D. Southam, F.L. Khanim, R.E. Hayden, J.K. Constantinou, K.M. Koczula, R.H. Michell, M.R. Viant, M.T. Drayson, C.M. Bunce, Drug Redeployment to Kill Leukemia and Lymphoma Cells by Disrupting SCD1-Mediated Synthesis of Monounsaturated Fatty Acids, Cancer research, 75 (2015) 2530-2540.
[173] K. Vriens, S. Christen, S. Parik, D. Broekaert, K. Yoshinaga, A. Talebi, J. Dehairs, C. Escalona-Noguero, R. Schmieder, T. Cornfield, C. Charlton, L. Romero-Perez, M. Rossi, G. Rinaldi, M.F. Orth, R. Boon, A. Kerstens, S.Y. Kwan, B. Faubert, A. Mendez-Lucas, C.C. Kopitz, T. Chen, J. Fernandez-Garcia, J.A.G. Duarte, A.A. Schmitz, P. Steigemann, M. Najimi, A. Hagebarth, J.A. Van Ginderachter, E. Sokal, N.

Gotoh, K.K. Wong, C. Verfaillie, R. Derua, S. Munck, M. Yuneva, L. Beretta, R.J. DeBerardinis, J.V. Swinnen, L. Hodson, D. Cassiman, C. Verslype, S. Christian, S. Grunewald, T.G.P. Grunewald, S.M. Fendt, Evidence for an alternative fatty acid desaturation pathway increasing cancer plasticity, Nature, 566 (2019) 403-406.
[174] H.G. Park, K.S.D. Kothapalli, W.J. Park, C. DeAllie, L. Liu, A. Liang, P. Lawrence, J.T. Brenna, Palmitic acid (16:0) competes with omega-6 linoleic and omega-3 a-linolenic acids for FADS2 mediated Delta6-desaturation, Biochimica et biophysica acta, 1861 (2016) 91-97.
[175] M. Triki, G. Rinaldi, M. Planque, D. Broekaert, A.M. Winkelkotte, C.R. Maier, S. Janaki Raman, A. Vandekeere, J. Van Elsen, M.F. Orth, T.G.P. Grunewald, A. Schulze, S.M. Fendt, mTOR Signaling and SREBP Activity Increase FADS2 Expression and Can Activate Sapienate Biosynthesis, Cell reports, 31 (2020) 107806.
[176] L.S. Pike, A.L. Smift, N.J. Croteau, D.A. Ferrick, M. Wu, Inhibition of fatty acid oxidation by etomoxir impairs NADPH production and increases reactive oxygen species resulting in ATP depletion and cell death in human glioblastoma cells, Biochimica et biophysica acta, 1807 (2011) 726-734.
[177] E.A. Lee, L. Angka, S.G. Rota, T. Hanlon, A. Mitchell, R. Hurren, X.M. Wang, M. Gronda, E. Boyaci, B. Bojko, M. Minden, S. Sriskanthadevan, A. Datti, J.L. Wrana, A. Edginton, J. Pawliszyn, J.W. Joseph, J. Quadrilatero, A.D. Schimmer, P.A. Spagnuolo, Targeting Mitochondria with Avocatin B Induces Selective Leukemia Cell Death, Cancer research, 75 (2015) 2478-2488.
[178] Y. Ma, S.M. Temkin, A.M. Hawkridge, C. Guo, W. Wang, X.Y. Wang, X. Fang, Fatty acid oxidation: An emerging facet of metabolic transformation in cancer, Cancer letters, 435 (2018) 92-100.
[179] J. Shi, H. Fu, Z. Jia, K. He, L. Fu, W. Wang, High Expression of CPT1A Predicts Adverse Outcomes: A Potential Therapeutic Target for Acute Myeloid Leukemia, EBioMedicine, 14 (2016) 55-64.
[180] P.P. Liu, J. Liu, W.Q. Jiang, J.S. Carew, M.A. Ogasawara, H. Pelicano, C.M. Croce, Z. Estrov, R.H. Xu, M.J. Keating, P. Huang, Elimination of chronic lymphocytic leukemia cells in stromal microenvironment by targeting CPT with an antiangina drug perhexiline, Oncogene, 35 (2016) 5663-5673.
[181] T. Wang, J.F. Fahrmann, H. Lee, Y.J. Li, S.C. Tripathi, C. Yue, C. Zhang, V. Lifshitz, J. Song, Y. Yuan, G. Somlo, R. Jandial, D. Ann, S. Hanash, R. Jove, H. Yu, JAK/STAT3-Regulated Fatty Acid beta-Oxidation Is Critical for Breast Cancer Stem Cell Self-Renewal and Chemoresistance, Cell metabolism, 27 (2018) 136-150 e135.
[182] K. Zaugg, Y. Yao, P.T. Reilly, K. Kannan, R. Kiarash, J. Mason, P. Huang, S.K. Sawyer, B. Fuerth, B. Faubert, T. Kalliomaki, A. Elia, X. Luo, V. Nadeem, D. Bungard, S. Yalavarthi, J.D. Growney, A. Wakeham, Y. Moolani, J. Silvester, A.Y. Ten, W. Bakker, K. Tsuchihara, S.L. Berger, R.P. Hill, R.G. Jones, M. Tsao, M.O. Robinson, C.B. Thompson, G. Pan, T.W. Mak, Carnitine palmitoyltransferase 1C promotes cell survival and tumor growth under conditions of metabolic stress, Genes & development, 25 (2011) 1041-1051.
[183] Y. Wu, R. Hurren, N. MacLean, M. Gronda, Y. Jitkova, M.A. Sukhai, M.D. Minden, A.D. Schimmer, Carnitine transporter CT2 (SLC22A16) is over-expressed in acute myeloid leukemia (AML) and target knockdown reduces growth and viability of AML cells, Apoptosis : an international journal on programmed cell death, 20 (2015) 1099-1108.
[184] M.S. Padanad, G. Konstantinidou, N. Venkateswaran, M. Melegari, S. Rindhe, M. Mitsche, C. Yang, K. Batten, K.E. Huffman, J. Liu, X. Tang, J. Rodriguez-Canales, N. Kalhor, J.W. Shay, J.D. Minna, J. McDonald, Wistuba, II, R.J. DeBerardinis, P.P. Scaglioni, Fatty Acid Oxidation Mediated by Acyl-CoA Synthetase Long Chain 3 Is Required for Mutant KRAS Lung Tumorigenesis, Cell reports, 16 (2016) 1614-1628.
[185] K.L. Cook, D.R. Soto-Pantoja, P.A. Clarke, M.I. Cruz, A. Zwart, A. Warri, L. Hilakivi-Clarke, D.D. Roberts, R. Clarke, Endoplasmic Reticulum Stress Protein GRP78 Modulates Lipid Metabolism to Control Drug Sensitivity and Antitumor Immunity in Breast Cancer, Cancer research, 76 (2016) 5657-5670.

[186] K. Linher-Melville, S. Zantinge, T. Sanli, H. Gerstein, T. Tsakiridis, G. Singh, Establishing a relationship between prolactin and altered fatty acid beta-oxidation via carnitine palmitoyl transferase 1 in breast cancer cells, BMC cancer, 11 (2011) 56.
[187] M.D. Wang, H. Wu, S. Huang, H.L. Zhang, C.J. Qin, L.H. Zhao, G.B. Fu, X. Zhou, X.M. Wang, L. Tang, W. Wen, W. Yang, S.H. Tang, D. Cao, L.N. Guo, M. Zeng, M.C. Wu, H.X. Yan, H.Y. Wang, HBx regulates fatty acid oxidation to promote hepatocellular carcinoma survival during metabolic stress, Oncotarget, 7 (2016) 6711-6726.
[188] H. Lin, S. Patel, V.S. Affleck, I. Wilson, D.M. Turnbull, A.R. Joshi, R. Maxwell, E.A. Stoll, Fatty acid oxidation is required for the respiration and proliferation of malignant glioma cells, Neuro-oncology, 19 (2017) 43-54.
[189] R. Camarda, A.Y. Zhou, R.A. Kohnz, S. Balakrishnan, C. Mahieu, B. Anderton, H. Eyob, S. Kajimura, A. Tward, G. Krings, D.K. Nomura, A. Goga, Inhibition of fatty acid oxidation as a therapy for MYC-overexpressing triple-negative breast cancer, Nature medicine, 22 (2016) 427-432.
[190] J.H. Park, S. Vithayathil, S. Kumar, P.L. Sung, L.E. Dobrolecki, V. Putluri, V.B. Bhat, S.K. Bhowmik, V. Gupta, K. Arora, D. Wu, E. Tsouko, Y. Zhang, S. Maity, T.R. Donti, B.H. Graham, D.E. Frigo, C. Coarfa, P. Yotnda, N. Putluri, A. Sreekumar, M.T. Lewis, C.J. Creighton, L.C. Wong, B.A. Kaipparettu, Fatty Acid Oxidation-Driven Src Links Mitochondrial Energy Reprogramming and Oncogenic Properties in Triple-Negative Breast Cancer, Cell reports, 14 (2016) 2154-2165.
[191] I. Samudio, R. Harmancey, M. Fiegl, H. Kantarjian, M. Konopleva, B. Korchin, K. Kaluarachchi, W. Bornmann, S. Duvvuri, H. Taegtmeyer, M. Andreeff, Pharmacologic inhibition of fatty acid oxidation sensitizes human leukemia cells to apoptosis induction, The Journal of clinical investigation, 120 (2010) 142-156.
[192] H. Shao, E.M. Mohamed, G.G. Xu, M. Waters, K. Jing, Y. Ma, Y. Zhang, S. Spiegel, M.O. Idowu, X. Fang, Carnitine palmitoyltransferase 1A functions to repress FoxO transcription factors to allow cell cycle progression in ovarian cancer, Oncotarget, 7 (2016) 3832-3846.
[193] C.L. Merrill, H. Ni, L.W. Yoon, M.A. Tirmenstein, P. Narayanan, G.R. Benavides, M.J. Easton, D.R. Creech, C.X. Hu, D.C. McFarland, L.M. Hahn, H.C. Thomas, K.T. Morgan, Etomoxir-induced oxidative stress in HepG2 cells detected by differential gene expression is confirmed biochemically, Toxicol Sci, 68 (2002) 93-101.
[194] I.R. Schlaepfer, L. Rider, L.U. Rodrigues, M.A. Gijon, C.T. Pac, L. Romero, A. Cimic, S.J. Sirintrapun, L.M. Glode, R.H. Eckel, S.D. Cramer, Lipid catabolism via CPT1 as a therapeutic target for prostate cancer, Molecular cancer therapeutics, 13 (2014) 2361-2371.
[195] I.R. Schlaepfer, L.M. Glode, C.A. Hitz, C.T. Pac, K.E. Boyle, P. Maroni, G. Deep, R. Agarwal, S.M. Lucia, S.D. Cramer, N.J. Serkova, R.H. Eckel, Inhibition of Lipid Oxidation Increases Glucose Metabolism and Enhances 2-Deoxy-2-[(18)F]Fluoro-D-Glucose Uptake in Prostate Cancer Mouse Xenografts, Mol Imaging Biol, 17 (2015) 529-538.
[196] J.M. Tirado-Velez, I. Joumady, A. Saez-Benito, I. Cozar-Castellano, G. Perdomo, Inhibition of fatty acid metabolism reduces human myeloma cells proliferation, PloS one, 7 (2012) e46484.
[197] M.L. Gatza, G.O. Silva, J.S. Parker, C. Fan, C.M. Perou, An integrated genomics approach identifies drivers of proliferation in luminal-subtype human breast cancer, Nature genetics, 46 (2014) 1051-1059.
[198] Y.A. Wen, X. Xing, J.W. Harris, Y.Y. Zaytseva, M.I. Mitov, D.L. Napier, H.L. Weiss, B. Mark Evers, T. Gao, Adipocytes activate mitochondrial fatty acid oxidation and autophagy to promote tumor growth in colon cancer, Cell death & disease, 8 (2017) e2593.
[199] Y.Y. Wang, C. Attane, D. Milhas, B. Dirat, S. Dauvillier, A. Guerard, J. Gilhodes, I. Lazar, N. Alet, V. Laurent, S. Le Gonidec, D. Biard, C. Herve, F. Bost, G.S. Ren, F. Bono, G. Escourrou, M. Prentki, L. Nieto, P.

Valet, C. Muller, Mammary adipocytes stimulate breast cancer invasion through metabolic remodeling of tumor cells, JCI Insight, 2 (2017) e87489.
[200] I. Lazar, E. Clement, S. Dauvillier, D. Milhas, M. Ducoux-Petit, S. LeGonidec, C. Moro, V. Soldan, S. Dalle, S. Balor, M. Golzio, O. Burlet-Schiltz, P. Valet, C. Muller, L. Nieto, Adipocyte Exosomes Promote Melanoma Aggressiveness through Fatty Acid Oxidation: A Novel Mechanism Linking Obesity and Cancer, Cancer research, 76 (2016) 4051-4057.
[201] Y. Liu, L.S. Zuckier, N.V. Ghesani, Dominant uptake of fatty acid over glucose by prostate cells: a potential new diagnostic and therapeutic approach, Anticancer Res, 30 (2010) 369-374.
[202] Y. Liu, Fatty acid oxidation is a dominant bioenergetic pathway in prostate cancer, Prostate cancer and prostatic diseases, 9 (2006) 230-234.
[203] E.A. Maher, I. Marin-Valencia, R.M. Bachoo, T. Mashimo, J. Raisanen, K.J. Hatanpaa, A. Jindal, F.M. Jeffrey, C. Choi, C. Madden, D. Mathews, J.M. Pascual, B.E. Mickey, C.R. Malloy, R.J. DeBerardinis, Metabolism of [U-13C]glucose in human brain tumorsin vivo, NMR in Biomedicine, 25 (2012) 1234-1244.
[204] M.B. Paumen, Y. Ishida, M. Muramatsu, M. Yamamoto, T. Honjo, Inhibition of carnitine palmitoyltransferase I augments sphingolipid synthesis and palmitate-induced apoptosis, The Journal of biological chemistry, 272 (1997) 3324-3329.
[205] A. Giordano, M. Calvani, O. Petillo, P. Grippo, F. Tuccillo, M.A. Melone, P. Bonelli, A. Calarco, G. Peluso, tBid induces alterations of mitochondrial fatty acid oxidation flux by malonyl-CoA-independent inhibition of carnitine palmitoyltransferase-1, Cell Death Differ, 12 (2005) 603-613.
[206] A.K. Leamy, R.A. Egnatchik, J.D. Young, Molecular mechanisms and the role of saturated fatty acids in the progression of non-alcoholic fatty liver disease, Progress in lipid research, 52 (2013) 165-174.
[207] Z.T. Schafer, A.R. Grassian, L. Song, Z. Jiang, Z. Gerhart-Hines, H.Y. Irie, S. Gao, P. Puigserver, J.S. Brugge, Antioxidant and oncogene rescue of metabolic defects caused by loss of matrix attachment, Nature, 461 (2009) 109-113.
[208] M. Buzzai, D.E. Bauer, R.G. Jones, R.J. Deberardinis, G. Hatzivassiliou, R.L. Elstrom, C.B. Thompson, The glucose dependence of Akt-transformed cells can be reversed by pharmacologic activation of fatty acid beta-oxidation, Oncogene, 24 (2005) 4165-4173.
[209] S. Halldorsson, N. Rohatgi, M. Magnusdottir, K.S. Choudhary, T. Gudjonsson, E. Knutsen, A. Barkovskaya, B. Hilmarsdottir, M. Perander, G.M. Maelandsmo, S. Gudmundsson, O. Rolfsson, Metabolic re-wiring of isogenic breast epithelial cell lines following epithelial to mesenchymal transition, Cancer letters, 396 (2017) 117-129.
[210] A. Carracedo, D. Weiss, A.K. Leliaert, M. Bhasin, V.C. de Boer, G. Laurent, A.C. Adams, M. Sundvall, S.J. Song, K. Ito, L.S. Finley, A. Egia, T. Libermann, Z. Gerhart-Hines, P. Puigserver, M.C. Haigis, E. Maratos-Flier, A.L. Richardson, Z.T. Schafer, P.P. Pandolfi, A metabolic prosurvival role for PML in breast cancer, The Journal of clinical investigation, 122 (2012) 3088-3100.
[211] Y.N. Wang, Z.L. Zeng, J. Lu, Y. Wang, Z.X. Liu, M.M. He, Q. Zhao, Z.X. Wang, T. Li, Y.X. Lu, Q.N. Wu, K. Yu, F. Wang, H.Y. Pu, B. Li, W.H. Jia, M. Shi, D. Xie, T.B. Kang, P. Huang, H.Q. Ju, R.H. Xu, CPT1A-mediated fatty acid oxidation promotes colorectal cancer cell metastasis by inhibiting anoikis, Oncogene, 37 (2018) 6025-6040.
[212] H. Ye, B. Adane, N. Khan, T. Sullivan, M. Minhajuddin, M. Gasparetto, B. Stevens, S. Pei, M. Balys, J.M. Ashton, D.J. Klemm, C.M. Woolthuis, A.W. Stranahan, C.Y. Park, C.T. Jordan, Leukemic Stem Cells Evade Chemotherapy by Metabolic Adaptation to an Adipose Tissue Niche, Cell Stem Cell, 19 (2016) 23-37.
[213] I. Hermanova, A. Arruabarrena-Aristorena, K. Valis, H. Nuskova, M. Alberich-Jorda, K. Fiser, S. Fernandez-Ruiz, D. Kavan, A. Pecinova, M. Niso-Santano, M. Zaliova, P. Novak, J. Houstek, T. Mracek, G.

Kroemer, A. Carracedo, J. Trka, J. Starkova, Pharmacological inhibition of fatty-acid oxidation synergistically enhances the effect of l-asparaginase in childhood ALL cells, Leukemia, 30 (2016) 209-218.
[214] T. Farge, E. Saland, F. de Toni, N. Aroua, M. Hosseini, R. Perry, C. Bosc, M. Sugita, L. Stuani, M. Fraisse, S. Scotland, C. Larrue, H. Boutzen, V. Feliu, M.L. Nicolau-Travers, S. Cassant-Sourdy, N. Broin, M. David, N. Serhan, A. Sarry, S. Tavitian, T. Kaoma, L. Vallar, J. Iacovoni, L.K. Linares, C. Montersino, R. Castellano, E. Griessinger, Y. Collette, O. Duchamp, Y. Barreira, P. Hirsch, T. Palama, L. Gales, F. Delhommeau, B.H. Garmy-Susini, J.C. Portais, F. Vergez, M. Selak, G. Danet-Desnoyers, M. Carroll, C. Recher, J.E. Sarry, Chemotherapy-Resistant Human Acute Myeloid Leukemia Cells Are Not Enriched for Leukemic Stem Cells but Require Oxidative Metabolism, Cancer Discov, 7 (2017) 716-735.
[215] S. Tung, Y. Shi, K. Wong, F. Zhu, R. Gorczynski, R.C. Laister, M. Minden, A.K. Blechert, Y. Genzel, U. Reichl, D.E. Spaner, PPARalpha and fatty acid oxidation mediate glucocorticoid resistance in chronic lymphocytic leukemia, Blood, 122 (2013) 969-980.
[216] N. Casals, V. Zammit, L. Herrero, R. Fado, R. Rodriguez-Rodriguez, D. Serra, Carnitine palmitoyltransferase 1C: From cognition to cancer, Progress in lipid research, 61 (2016) 134-148.
[217] J.F. Barger, C.A. Gallo, P. Tandon, H. Liu, A. Sullivan, H.L. Grimes, D.R. Plas, S6K1 determines the metabolic requirements for BCR-ABL survival, Oncogene, 32 (2013) 453-461.
[218] H. Shinohara, M. Kumazaki, Y. Minami, Y. Ito, N. Sugito, Y. Kuranaga, K. Taniguchi, N. Yamada, Y. Otsuki, T. Naoe, Y. Akao, Perturbation of energy metabolism by fatty-acid derivative AIC-47 and imatinib in BCR-ABL-harboring leukemic cells, Cancer letters, 371 (2016) 1-11.
[219] S. Kitajima, A. Yoshida, S. Kohno, F. Li, S. Suzuki, N. Nagatani, Y. Nishimoto, N. Sasaki, H. Muranaka, Y. Wan, T.C. Thai, N. Okahashi, F. Matsuda, H. Shimizu, T. Nishiuchi, Y. Suzuki, K. Tominaga, N. Gotoh, M. Suzuki, M.E. Ewen, D.A. Barbie, O. Hirose, T. Tanaka, C. Takahashi, The RB-IL-6 axis controls self-renewal and endocrine therapy resistance by fine-tuning mitochondrial activity, Oncogene, 36 (2017) 5145-5157.
[220] J. Li, S. Zhao, X. Zhou, T. Zhang, L. Zhao, P. Miao, S. Song, X. Sun, J. Liu, X. Zhao, G. Huang, Inhibition of lipolysis by mercaptoacetate and etomoxir specifically sensitize drug-resistant lung adenocarcinoma cell to paclitaxel, PloS one, 8 (2013) e74623.
[221] C.L. Chen, D.B. Uthaya Kumar, V. Punj, J. Xu, L. Sher, S.M. Tahara, S. Hess, K. Machida, NANOG Metabolically Reprograms Tumor-Initiating Stem-like Cells through Tumorigenic Changes in Oxidative Phosphorylation and Fatty Acid Metabolism, Cell metabolism, 23 (2016) 206-219.
[222] C.K. Lee, S.H. Jeong, C. Jang, H. Bae, Y.H. Kim, I. Park, S.K. Kim, G.Y. Koh, Tumor metastasis to lymph nodes requires YAP-dependent metabolic adaptation, Science, 363 (2019) 644-649.
[223] A.M. Savino, S.I. Fernandes, O. Olivares, A. Zemlyansky, A. Cousins, E.K. Markert, S. Barel, I. Geron, L. Frishman, Y. Birger, C. Eckert, S. Tumanov, G. MacKay, J.J. Kamphorst, P. Herzyk, J. Fernandez-Garcia, I. Abramovich, I. Mor, M. Bardini, E. Barin, S. Janaki-Raman, J.R. Cross, M.G. Kharas, E. Gottlieb, S. Izraeli, C. Halsey, Metabolic adaptation of acute lymphoblastic leukemia to the central nervous system microenvironment is dependent on Stearoyl CoA desaturase, Nature cancer, 1 (2020) 998-1009.
[224] Y.P. Kang, J.H. Yoon, N.P. Long, G.B. Koo, H.J. Noh, S.J. Oh, S.B. Lee, H.M. Kim, J.Y. Hong, W.J. Lee, S.J. Lee, S.S. Hong, S.W. Kwon, Y.S. Kim, Spheroid-Induced Epithelial-Mesenchymal Transition Provokes Global Alterations of Breast Cancer Lipidome: A Multi-Layered Omics Analysis, Frontiers in oncology, 9 (2019) 145.
[225] C. Angelucci, A. D'Alessio, F. Iacopino, G. Proietti, A. Di Leone, R. Masetti, G. Sica, Pivotal role of human stearoyl-CoA desaturases (SCD1 and 5) in breast cancer progression: oleic acid-based effect of SCD1 on cell migration and a novel pro-cell survival role for SCD5, Oncotarget, 9 (2018) 24364-24380.
[226] M. Bellenghi, G. Talarico, L. Botti, R. Puglisi, C. Tabolacci, P. Portararo, A. Piva, G. Pontecorvi, A. Care, M.P. Colombo, G. Mattia, S. Sangaletti, SCD5-dependent inhibition of SPARC secretion hampers metastatic spreading and favors host immunity in a TNBC murine model, Oncogene, (2022).

[227] E. Gazi, P. Gardner, N.P. Lockyer, C.A. Hart, M.D. Brown, N.W. Clarke, Direct evidence of lipid translocation between adipocytes and prostate cancer cells with imaging FTIR microspectroscopy, Journal of lipid research, 48 (2007) 1846-1856.
[228] G. Pascual, D. Dominguez, M. Elosua-Bayes, F. Beckedorff, C. Laudanna, C. Bigas, D. Douillet, C. Greco, A. Symeonidi, I. Hernandez, S.R. Gil, N. Prats, C. Bescos, R. Shiekhattar, M. Amit, H. Heyn, A. Shilatifard, S.A. Benitah, Dietary palmitic acid promotes a prometastatic memory via Schwann cells, Nature, 599 (2021) 485-490.
[229] Y. Vivas-Garcia, P. Falletta, J. Liebing, P. Louphrasitthiphol, Y. Feng, J. Chauhan, D.A. Scott, N. Glodde, A. Chocarro-Calvo, S. Bonham, A.L. Osterman, R. Fischer, Z. Ronai, C. Garcia-Jimenez, M. Holzel, C.R. Goding, Lineage-Restricted Regulation of SCD and Fatty Acid Saturation by MITF Controls Melanoma Phenotypic Plasticity, Molecular cell, 77 (2020) 120-137 e129.
[230] C. Mounier, L. Bouraoui, E. Rassart, Lipogenesis in cancer progression (review), International journal of oncology, 45 (2014) 485-492.
[231] M. Lingrand, S. Lalonde, A. Jutras-Carignan, K.F. Bergeron, E. Rassart, C. Mounier, SCD1 activity promotes cell migration via a PLD-mTOR pathway in the MDA-MB-231 triple-negative breast cancer cell line, Breast cancer, 27 (2020) 594-606.
[232] C. Angelucci, G. Maulucci, A. Colabianchi, F. Iacopino, A. D'Alessio, A. Maiorana, V. Palmieri, M. Papi, M. De Spirito, A. Di Leone, R. Masetti, G. Sica, Stearoyl-CoA desaturase 1 and paracrine diffusible signals have a major role in the promotion of breast cancer cell migration induced by cancer-associated fibroblasts, British journal of cancer, 112 (2015) 1675-1686.
[233] D. Mauvoisin, C. Charfi, A.M. Lounis, E. Rassart, C. Mounier, Decreasing stearoyl-CoA desaturase-1 expression inhibits beta-catenin signaling in breast cancer cells, Cancer science, 104 (2013) 36-42.
[234] C. Liao, M. Li, X. Li, N. Li, X. Zhao, X. Wang, Y. Song, J. Quan, C. Cheng, J. Liu, A.M. Bode, Y. Cao, X. Luo, Trichothecin inhibits invasion and metastasis of colon carcinoma associating with SCD-1-mediated metabolite alteration, Biochimica et biophysica acta. Molecular and cell biology of lipids, 1865 (2020) 158540.
[235] H. Ran, Y. Zhu, R. Deng, Q. Zhang, X. Liu, M. Feng, J. Zhong, S. Lin, X. Tong, Q. Su, Stearoyl-CoA desaturase-1 promotes colorectal cancer metastasis in response to glucose by suppressing PTEN, Journal of experimental & clinical cancer research : CR, 37 (2018) 54.
[236] K. She, S. Fang, W. Du, X. Fan, J. He, H. Pan, L. Huang, P. He, J. Huang, SCD1 is required for EGFR-targeting cancer therapy of lung cancer via re-activation of EGFR/PI3K/AKT signals, Cancer cell international, 19 (2019) 103.
[237] G. Liu, S. Feng, L. Jia, C. Wang, Y. Fu, Y. Luo, Lung fibroblasts promote metastatic colonization through upregulation of stearoyl-CoA desaturase 1 in tumor cells, Oncogene, 37 (2018) 1519-1533.
[238] R. Pelaez, R. Ochoa, A. Pariente, A. Villanueva-Martinez, A. Perez-Sala, I.M. Larrayoz, Sterculic Acid Alters Adhesion Molecules Expression and Extracellular Matrix Compounds to Regulate Migration of Lung Cancer Cells, Cancers, 13 (2021).
[239] M. Lochner, L. Berod, T. Sparwasser, Fatty acid metabolism in the regulation of T cell function, Trends in immunology, 36 (2015) 81-91.
[240] H.H. Liu, Y. Xu, C.J. Li, S.J. Hsu, X.H. Lin, R. Zhang, J. Chen, J. Chen, D.M. Gao, J.F. Cui, X.R. Yang, Z.G. Ren, R.X. Chen, An SCD1-dependent mechanoresponsive pathway promotes HCC invasion and metastasis through lipid metabolic reprogramming, Mol Ther, 30 (2022) 2554-2567.
[241] H. Li, Z. Chen, Y. Zhang, P. Yuan, J. Liu, L. Ding, Q. Ye, MiR-4310 regulates hepatocellular carcinoma growth and metastasis through lipid synthesis, Cancer letters, 519 (2021) 161-171.

[242] S. Zhang, C. Balch, M.W. Chan, H.C. Lai, D. Matei, J.M. Schilder, P.S. Yan, T.H. Huang, K.P. Nephew, Identification and characterization of ovarian cancer-initiating cells from primary human tumors, Cancer research, 68 (2008) 4311-4320.
[243] I. Kryczek, S. Liu, M. Roh, L. Vatan, W. Szeliga, S. Wei, M. Banerjee, Y. Mao, J. Kotarski, M.S. Wicha, R. Liu, W. Zou, Expression of aldehyde dehydrogenase and CD133 defines ovarian cancer stem cells, International journal of cancer, 130 (2012) 29-39.
[244] J. Deng, L. Wang, H. Chen, J. Hao, J. Ni, L. Chang, W. Duan, P. Graham, Y. Li, Targeting epithelial-mesenchymal transition and cancer stem cells for chemoresistant ovarian cancer, Oncotarget, 7 (2016) 55771-55788.
[245] R.R. Somasagara, S.M. Spencer, K. Tripathi, D.W. Clark, C. Mani, L. Madeira da Silva, J. Scalici, H. Kothayer, A.D. Westwell, R.P. Rocconi, K. Palle, RAD6 promotes DNA repair and stem cell signaling in ovarian cancer and is a promising therapeutic target to prevent and treat acquired chemoresistance, Oncogene, 36 (2017) 6680-6690.
[246] S.K.Y. To, A.S.C. Mak, Y.M. Eva Fung, C.M. Che, S.S. Li, W. Deng, B. Ru, J. Zhang, A.S.T. Wong, beta-catenin downregulates Dicer to promote ovarian cancer metastasis, Oncogene, 36 (2017) 5927-5938.
[247] B. Beck, C. Blanpain, Unravelling cancer stem cell potential, Nature reviews. Cancer, 13 (2013) 727-738.
[248] C. Gonzalez-Torres, J. Gaytan-Cervantes, K. Vazquez-Santillan, E.A. Mandujano-Tinoco, G. Ceballos-Cancino, A. Garcia-Venzor, C. Zampedri, P. Sanchez-Maldonado, R. Mojica-Espinosa, L.E. Jimenez-Hernandez, V. Maldonado, NF-kappaB Participates in the Stem Cell Phenotype of Ovarian Cancer Cells, Archives of medical research, 48 (2017) 343-351.
[249] E.J. Seo, D.K. Kim, I.H. Jang, E.J. Choi, S.H. Shin, S.I. Lee, S.M. Kwon, K.H. Kim, D.S. Suh, J.H. Kim, Hypoxia-NOTCH1-SOX2 signaling is important for maintaining cancer stem cells in ovarian cancer, Oncotarget, 7 (2016) 55624-55638.
[250] L. Wang, R. Mezencev, N.J. Bowen, L.V. Matyunina, J.F. McDonald, Isolation and characterization of stem-like cells from a human ovarian cancer cell line, Molecular and cellular biochemistry, 363 (2012) 257-268.
[251] T. Ishiguro, A. Sato, H. Ohata, Y. Ikarashi, R.U. Takahashi, T. Ochiya, M. Yoshida, H. Tsuda, T. Onda, T. Kato, T. Kasamatsu, T. Enomoto, K. Tanaka, H. Nakagama, K. Okamoto, Establishment and Characterization of an In Vitro Model of Ovarian Cancer Stem-like Cells with an Enhanced Proliferative Capacity, Cancer research, 76 (2016) 150-160.
[252] A. Ghoneum, D. Gonzalez, A.Y. Abdulfattah, N. Said, Metabolic Plasticity in Ovarian Cancer Stem Cells, Cancers, 12 (2020).
[253] R. Mancini, A. Noto, M.E. Pisanu, C. De Vitis, M. Maugeri-Sacca, G. Ciliberto, Metabolic features of cancer stem cells: the emerging role of lipid metabolism, Oncogene, 37 (2018) 2367-2378.
[254] L. Potze, S. di Franco, J.H. Kessler, G. Stassi, J.P. Medema, Betulinic Acid Kills Colon Cancer Stem Cells, Current stem cell research & therapy, 11 (2016) 427-433.
[255] S. Choi, Y.J. Yoo, H. Kim, H. Lee, H. Chung, M.H. Nam, J.Y. Moon, H.S. Lee, S. Yoon, W.Y. Kim, Clinical and biochemical relevance of monounsaturated fatty acid metabolism targeting strategy for cancer stem cell elimination in colon cancer, Biochemical and biophysical research communications, 519 (2019) 100-105.
[256] Y. Yu, H. Kim, S. Choi, J. Yu, J.Y. Lee, H. Lee, S. Yoon, W.Y. Kim, Targeting a Lipid Desaturation Enzyme, SCD1, Selectively Eliminates Colon Cancer Stem Cells through the Suppression of Wnt and NOTCH Signaling, Cells, 10 (2021).
[257] M. Sun, Z. Yang, Metabolomic Studies of Live Single Cancer Stem Cells Using Mass Spectrometry, Analytical chemistry, 91 (2019) 2384-2391.

[258] H. Luo, C.Y. Chen, X. Li, X. Zhang, C.W. Su, Y. Liu, T. Cao, L. Hao, M. Wang, J.X. Kang, Increased lipogenesis is critical for self-renewal and growth of breast cancer stem cells: Impact of omega-3 fatty acids, Stem cells, 39 (2021) 1660-1670.
[259] S. Yu, Y. Lu, A. Su, J. Chen, J. Li, B. Zhou, X. Liu, Q. Xia, Y. Li, J. Li, M. Huang, Y. Ye, Q. Zhao, S. Jiang, X. Yan, X. Wang, C. Di, J. Pan, S. Su, A CD10-OGP Membrane Peptolytic Signaling Axis in Fibroblasts Regulates Lipid Metabolism of Cancer Stem Cells via SCD1, Advanced science, 8 (2021) e2101848.
[260] J.A. Colacino, S.P. McDermott, M.A. Sartor, M.S. Wicha, L.S. Rozek, Transcriptomic profiling of curcumin-treated human breast stem cells identifies a role for stearoyl-coa desaturase in breast cancer prevention, Breast cancer research and treatment, 158 (2016) 29-41.
[261] K. Kikuchi, H. Tsukamoto, Stearoyl-CoA desaturase and tumorigenesis, Chemico-biological interactions, 316 (2020) 108917.
[262] X.L. Ma, Y.F. Sun, B.L. Wang, M.N. Shen, Y. Zhou, J.W. Chen, B. Hu, Z.J. Gong, X. Zhang, Y. Cao, B.S. Pan, J. Zhou, J. Fan, W. Guo, X.R. Yang, Sphere-forming culture enriches liver cancer stem cells and reveals Stearoyl-CoA desaturase 1 as a potential therapeutic target, BMC cancer, 19 (2019) 760.
[263] C. Piao, X. Cui, B. Zhan, J. Li, Z. Li, Z. Li, X. Liu, J. Bi, Z. Zhang, C. Kong, Inhibition of stearoyl CoA desaturase-1 activity suppresses tumour progression and improves prognosis in human bladder cancer, Journal of cellular and molecular medicine, 23 (2019) 2064-2076.
[264] H. Wang, F. Dong, Y. Wang, X. Wang, D. Hong, Y. Liu, J. Zhou, Betulinic acid induces apoptosis of gallbladder cancer cells via repressing SCD1, Acta biochimica et biophysica Sinica, 52 (2020) 200-206.
[265] R. Kinstrie, M. Copland, Targeting chronic myeloid leukemia stem cells, Current hematologic malignancy reports, 8 (2013) 14-21.
[266] M. Song, H. Lee, M.H. Nam, E. Jeong, S. Kim, Y. Hong, N. Kim, H.Y. Yim, Y.J. Yoo, J.S. Kim, J.S. Kim, Y.Y. Cho, G.B. Mills, W.Y. Kim, S. Yoon, Loss-of-function screens of druggable targetome against cancer stem-like cells, FASEB journal : official publication of the Federation of American Societies for Experimental Biology, 31 (2017) 625-635.
[267] K. Pinkham, D.J. Park, A. Hashemiaghdam, A.B. Kirov, I. Adam, K. Rosiak, C.C. da Hora, J. Teng, P.S. Cheah, L. Carvalho, G. Ganguli-Indra, A. Kelly, A.K. Indra, C.E. Badr, Stearoyl CoA Desaturase Is Essential for Regulation of Endoplasmic Reticulum Homeostasis and Tumor Growth in Glioblastoma Cancer Stem Cells, Stem cell reports, 12 (2019) 712-727.
[268] Y. Gao, J. Li, H. Xi, J. Cui, K. Zhang, J. Zhang, Y. Zhang, W. Xu, W. Liang, Z. Zhuang, P. Wang, Z. Qiao, B. Wei, L. Chen, Stearoyl-CoA-desaturase-1 regulates gastric cancer stem-like properties and promotes tumour metastasis via Hippo/YAP pathway, British journal of cancer, 122 (2020) 1837-1847.
[269] A. Noto, S. Raffa, C. De Vitis, G. Roscilli, D. Malpicci, P. Coluccia, A. Di Napoli, A. Ricci, M.R. Giovagnoli, L. Aurisicchio, M.R. Torrisi, G. Ciliberto, R. Mancini, Stearoyl-CoA desaturase-1 is a key factor for lung cancer-initiating cells, Cell death & disease, 4 (2013) e947.
[270] A. Noto, C. De Vitis, M.E. Pisanu, G. Roscilli, G. Ricci, A. Catizone, G. Sorrentino, G. Chianese, O. Taglialatela-Scafati, D. Trisciuoglio, D. Del Bufalo, M. Di Martile, A. Di Napoli, L. Ruco, S. Costantini, Z. Jakopin, A. Budillon, G. Melino, G. Del Sal, G. Ciliberto, R. Mancini, Stearoyl-CoA-desaturase 1 regulates lung cancer stemness via stabilization and nuclear localization of YAP/TAZ, Oncogene, 36 (2017) 4573-4584.
[271] M.E. Pisanu, M. Maugeri-Sacca, L. Fattore, S. Bruschini, C. De Vitis, E. Tabbi, B. Bellei, E. Migliano, D. Kovacs, E. Camera, M. Picardo, Z. Jakopin, C. Cippitelli, A. Bartolazzi, S. Raffa, M.R. Torrisi, F. Fulciniti, P.A. Ascierto, G. Ciliberto, R. Mancini, Inhibition of Stearoyl-CoA desaturase 1 reverts BRAF and MEK inhibition-induced selection of cancer stem cells in BRAF-mutated melanoma, Journal of experimental & clinical cancer research : CR, 37 (2018) 318.

[272] B. Corominas-Faja, E. Cuyas, J. Gumuzio, J. Bosch-Barrera, O. Leis, A.G. Martin, J.A. Menendez, Chemical inhibition of acetyl-CoA carboxylase suppresses self-renewal growth of cancer stem cells, Oncotarget, 5 (2014) 8306-8316.
[273] R.C. Gimple, R.L. Kidwell, L.J.Y. Kim, T. Sun, A.D. Gromovsky, Q. Wu, M. Wolf, D. Lv, S. Bhargava, L. Jiang, B.C. Prager, X. Wang, Q. Ye, Z. Zhu, G. Zhang, Z. Dong, L. Zhao, D. Lee, J. Bi, A.E. Sloan, P.S. Mischel, J.M. Brown, H. Cang, T. Huan, S.C. Mack, Q. Xie, J.N. Rich, Glioma Stem Cell-Specific Superenhancer Promotes Polyunsaturated Fatty-Acid Synthesis to Support EGFR Signaling, Cancer Discov, 9 (2019) 1248-1267.
[274] R. El Helou, G. Pinna, O. Cabaud, J. Wicinski, R. Bhajun, L. Guyon, C. Rioualen, P. Finetti, A. Gros, B. Mari, P. Barbry, F. Bertucci, G. Bidaut, A. Harel-Bellan, D. Birnbaum, E. Charafe-Jauffret, C. Ginestier, miR-600 Acts as a Bimodal Switch that Regulates Breast Cancer Stem Cell Fate through WNT Signaling, Cell reports, 18 (2017) 2256-2268.
[275] K.K.Y. Lai, S.M. Kweon, F. Chi, E. Hwang, Y. Kabe, R. Higashiyama, L. Qin, R. Yan, R.P. Wu, K. Lai, N. Fujii, S. French, J. Xu, J.Y. Wang, R. Murali, L. Mishra, J.S. Lee, J.M. Ntambi, H. Tsukamoto, Stearoyl-CoA Desaturase Promotes Liver Fibrosis and Tumor Development in Mice via a Wnt Positive-Signaling Loop by Stabilization of Low-Density Lipoprotein-Receptor-Related Proteins 5 and 6, Gastroenterology, 152 (2017) 1477-1491.
[276] M. Knobloch, S.M. Braun, L. Zurkirchen, C. von Schoultz, N. Zamboni, M.J. Arauzo-Bravo, W.J. Kovacs, O. Karalay, U. Suter, R.A. Machado, M. Roccio, M.P. Lutolf, C.F. Semenkovich, S. Jessberger, Metabolic control of adult neural stem cell activity by Fasn-dependent lipogenesis, Nature, 493 (2013) 226-230.
[277] D.I. Sinner, G.J. Kim, G.C. Henderson, R.A. Igal, StearoylCoA desaturase-5: a novel regulator of neuronal cell proliferation and differentiation, PloS one, 7 (2012) e39787.
[278] O. Yanes, J. Clark, D.M. Wong, G.J. Patti, A. Sanchez-Ruiz, H.P. Benton, S.A. Trauger, C. Desponts, S. Ding, G. Siuzdak, Metabolic oxidation regulates embryonic stem cell differentiation, Nature chemical biology, 6 (2010) 411-417.
[279] J. Bradley, I. Pope, F. Masia, R. Sanusi, W. Langbein, K. Swann, P. Borri, Quantitative imaging of lipids in live mouse oocytes and early embryos using CARS microscopy, Development, 143 (2016) 2238-2247.
[280] D.O. Bauerschlag, N. Maass, P. Leonhardt, F.A. Verburg, U. Pecks, F. Zeppernick, A. Morgenroth, F.M. Mottaghy, R. Tolba, I. Meinhold-Heerlein, K. Brautigam, Fatty acid synthase overexpression: target for therapy and reversal of chemoresistance in ovarian cancer, Journal of translational medicine, 13 (2015) 146.
[281] E. Papaevangelou, G.S. Almeida, C. Box, N.M. deSouza, Y.L. Chung, The effect of FASN inhibition on the growth and metabolism of a cisplatin-resistant ovarian carcinoma model, International journal of cancer, 143 (2018) 992-1002.
[282] W. Peng, S. Tan, Y. Xu, L. Wang, D. Qiu, C. Cheng, Y. Lin, C. Liu, Z. Li, Y. Li, Y. Zhao, Q. Li, LCMS/MS metabolome analysis detects the changes in the lipid metabolic profiles of dMMR and pMMR cells, Oncology reports, 40 (2018) 1026-1034.
[283] I.R. Schlaepfer, C.A. Hitz, M.A. Gijon, B.C. Bergman, R.H. Eckel, B.M. Jacobsen, Progestin modulates the lipid profile and sensitivity of breast cancer cells to docetaxel, Molecular and cellular endocrinology, 363 (2012) 111-121.
[284] M. Hilvo, S. Gade, T. Hyotylainen, V. Nekljudova, T. Seppanen-Laakso, M. Sysi-Aho, M. Untch, J. Huober, G. von Minckwitz, C. Denkert, M. Oresic, S. Loibl, Monounsaturated fatty acids in serum triacylglycerols are associated with response to neoadjuvant chemotherapy in breast cancer patients, International journal of cancer, 134 (2014) 1725-1733.

[285] S. Bansal, M. Berk, N. Alkhouri, D.A. Partrick, J.J. Fung, A. Feldstein, Stearoyl-CoA desaturase plays an important role in proliferation and chemoresistance in human hepatocellular carcinoma, The Journal of surgical research, 186 (2014) 29-38.
[286] J. Tucci, T. Chen, K. Margulis, E. Orgel, R.L. Paszkiewicz, M.D. Cohen, M.J. Oberley, R. Wahhab, A.E. Jones, A.S. Divakaruni, C.C. Hsu, S.E. Noll, X. Sheng, R.N. Zare, S.D. Mittelman, Adipocytes Provide Fatty Acids to Acute Lymphoblastic Leukemia Cells, Frontiers in oncology, 11 (2021) 665763.
[287] G. Liu, S. Kuang, R. Cao, J. Wang, Q. Peng, C. Sun, Sorafenib kills liver cancer cells by disrupting SCD1-mediated synthesis of monounsaturated fatty acids via the ATP-AMPK-mTOR-SREBP1 signaling pathway, FASEB journal : official publication of the Federation of American Societies for Experimental Biology, 33 (2019) 10089-10103.
[288] P.W. Shueng, H.W. Chan, W.C. Lin, D.Y. Kuo, H.Y. Chuang, Orlistat Resensitizes Sorafenib-Resistance in Hepatocellular Carcinoma Cells through Modulating Metabolism, International journal of molecular sciences, 23 (2022).
[289] M.K.F. Ma, E.Y.T. Lau, D.H.W. Leung, J. Lo, N.P.Y. Ho, L.K.W. Cheng, S. Ma, C.H. Lin, J.A. Copland, J. Ding, R.C.L. Lo, I.O.L. Ng, T.K.W. Lee, Stearoyl-CoA desaturase regulates sorafenib resistance via modulation of ER stress-induced differentiation, Journal of hepatology, 67 (2017) 979-990.
[290] M.A. Lounis, B. Peant, K. Leclerc-Desaulniers, D. Ganguli, C. Daneault, M. Ruiz, A. Zoubeidi, A.M. Mes-Masson, F. Saad, Modulation of de Novo Lipogenesis Improves Response to Enzalutamide Treatment in Prostate Cancer, Cancers, 12 (2020).
[291] T. Zhang, Z. Guo, X. Huo, Y. Gong, C. Li, J. Huang, Y. Wang, H. Feng, X. Ma, C. Jiang, Q. Yin, L. Xue, Dysregulated lipid metabolism blunts the sensitivity of cancer cells to EZH2 inhibitor, EBioMedicine, 77 (2022) 103872.
[292] X. Hu, J. Xiang, Y. Li, Y. Xia, S. Xu, X. Gao, S. Qiao, Inhibition of Stearoyl-CoA Desaturase 1 Potentiates Anti-tumor Activity of Amodiaquine in Non-small Cell Lung Cancer, Biological & pharmaceutical bulletin, 45 (2022) 438-445.
[293] Q. Huang, Q. Wang, D. Li, X. Wei, Y. Jia, Z. Zhang, B. Ai, X. Cao, T. Guo, Y. Liao, Co-administration of 20(S)-protopanaxatriol (g-PPT) and EGFR-TKI overcomes EGFR-TKI resistance by decreasing SCD1 induced lipid accumulation in non-small cell lung cancer, Journal of experimental & clinical cancer research : CR, 38 (2019) 129.
[294] S. Dai, Y. Yan, Z. Xu, S. Zeng, L. Qian, L. Huo, X. Li, L. Sun, Z. Gong, SCD1 Confers Temozolomide Resistance to Human Glioma Cells via the Akt/GSK3beta/beta-Catenin Signaling Axis, Frontiers in pharmacology, 8 (2017) 960.
[295] S. Parik, J. Fernandez-Garcia, F. Lodi, K. De Vlaminck, M. Derweduwe, S. De Vleeschouwer, R. Sciot, W. Geens, L. Weng, F.M. Bosisio, G. Bergers, J. Duerinck, F. De Smet, D. Lambrechts, J.A. Van Ginderachter, S.M. Fendt, GBM tumors are heterogeneous in their fatty acid metabolism and modulating fatty acid metabolism sensitizes cancer cells derived from recurring GBM tumors to temozolomide, Frontiers in oncology, 12 (2022) 988872.
[296] M. Sun, X. Chen, Z. Yang, Single cell mass spectrometry studies reveal metabolomic features and potential mechanisms of drug-resistant cancer cell lines, Analytica chimica acta, 1206 (2022) 339761.
[297] M.J. Hangauer, V.S. Viswanathan, M.J. Ryan, D. Bole, J.K. Eaton, A. Matov, J. Galeas, H.D. Dhruv, M.E. Berens, S.L. Schreiber, F. McCormick, M.T. McManus, Drug-tolerant persister cancer cells are vulnerable to GPX4 inhibition, Nature, 551 (2017) 247-250.
[298] L. Tesfay, B.T. Paul, A. Konstorum, Z. Deng, A.O. Cox, J. Lee, C.M. Furdui, P. Hegde, F.M. Torti, S.V. Torti, Stearoyl-CoA Desaturase 1 Protects Ovarian Cancer Cells from Ferroptotic Cell Death, Cancer research, 79 (2019) 5355-5366.

[299] M. Carbone, G. Melino, Stearoyl CoA Desaturase Regulates Ferroptosis in Ovarian Cancer Offering New Therapeutic Perspectives, Cancer research, 79 (2019) 5149-5150.
[300] A. Konstorum, L. Tesfay, B.T. Paul, F.M. Torti, R.C. Laubenbacher, S.V. Torti, Systems biology of ferroptosis: A modeling approach, Journal of theoretical biology, 493 (2020) 110222.
[301] C.A. Wohlhieter, A.L. Richards, F. Uddin, C.H. Hulton, A. Quintanal-Villalonga, A. Martin, E. de Stanchina, U. Bhanot, M. Asher, N.S. Shah, O. Hayatt, D.J. Buonocore, N. Rekhtman, R. Shen, K.C. Arbour, M. Donoghue, J.T. Poirier, T. Sen, C.M. Rudin, Concurrent Mutations in STK11 and KEAP1 Promote Ferroptosis Protection and SCD1 Dependence in Lung Cancer, Cell reports, 33 (2020) 108444.
[302] G. Luis, A. Godfroid, S. Nishiumi, J. Cimino, S. Blacher, E. Maquoi, C. Wery, A. Collignon, R. Longuespee, L. Montero-Ruiz, I. Dassoul, N. Maloujahmoum, C. Pottier, G. Mazzucchelli, E. Depauw, A. Bellahcene, M. Yoshida, A. Noel, N.E. Sounni, Tumor resistance to ferroptosis driven by Stearoyl-CoA Desaturase-1 (SCD1) in cancer cells and Fatty Acid Biding Protein-4 (FABP4) in tumor microenvironment promote tumor recurrence, Redox biology, 43 (2021) 102006.
[303] B. Lettiero, M. Inasu, S. Kimbung, S. Borgquist, Insensitivity to atorvastatin is associated with increased accumulation of intracellular lipid droplets and fatty acid metabolism in breast cancer cells, Scientific reports, 8 (2018) 5462.
[304] H.E. Rasmussen, K.R. Blobaum, Y.K. Park, S.J. Ehlers, F. Lu, J.Y. Lee, Lipid extract of Nostoc commune var. sphaeroides Kutzing, a blue-green alga, inhibits the activation of sterol regulatory element binding proteins in HepG2 cells, The Journal of nutrition, 138 (2008) 476-481.
[305] J.S.V. Lally, S. Ghoshal, D.K. DePeralta, O. Moaven, L. Wei, R. Masia, D.J. Erstad, N. Fujiwara, V. Leong, V.P. Houde, A.E. Anagnostopoulos, A. Wang, L.A. Broadfield, R.J. Ford, R.A. Foster, J. Bates, H. Sun, T. Wang, H. Liu, A.S. Ray, A.K. Saha, J. Greenwood, S. Bhat, G. Harriman, W. Miao, J.L. Rocnik, W.F. Westlin, P. Muti, T. Tsakiridis, H.J. Harwood, Jr., R. Kapeller, Y. Hoshida, K.K. Tanabe, G.R. Steinberg, B.C. Fuchs, Inhibition of Acetyl-CoA Carboxylase by Phosphorylation or the Inhibitor ND-654 Suppresses Lipogenesis and Hepatocellular Carcinoma, Cell metabolism, 29 (2019) 174-182 e175.
[306] G. Falchook, M. Patel, J. Infante, H.-T. Arkenau, E. Dean, A. Brenner, E. Borazanci, J. Lopez, K. Moore, P. Schmid, A. Frankel, S. Jones, W. McCulloch, G. Kemble, H. Burris, Abstract CT153: First in human study of the first-in-class fatty acid synthase (FASN) inhibitor TVB-2640, (2017) CT153-CT153.
[307] Y. Choi, Y. Park, J.M. Storkson, M.W. Pariza, J.M. Ntambi, Inhibition of stearoyl-CoA desaturase activity by the cis-9,trans-11 isomer and the trans-10,cis-12 isomer of conjugated linoleic acid in MDA-MB-231 and MCF-7 human breast cancer cells, Biochemical and biophysical research communications, 294 (2002) 785-790.
[308] L.M.D. Reis, D. Adamoski, R. Ornitz Oliveira Souza, C.F. Rodrigues Ascencao, K.R. Sousa de Oliveira, F. Correa-da-Silva, F. Malta de Sa Patroni, M. Meira Dias, S.R. Consonni, P.M. Mendes de Moraes-Vieira, A.M. Silber, S.M.G. Dias, Dual inhibition of glutaminase and carnitine palmitoyltransferase decreases growth and migration of glutaminase inhibition-resistant triple-negative breast cancer cells, The Journal of biological chemistry, 294 (2019) 9342-9357.
[309] G. Galicia-Vazquez, R. Aloyz, Ibrutinib Resistance Is Reduced by an Inhibitor of Fatty Acid Oxidation in Primary CLL Lymphocytes, Frontiers in oncology, 8 (2018) 411.
[310] F. Veglia, V.A. Tyurin, M. Blasi, A. De Leo, A.V. Kossenkov, L. Donthireddy, T.K.J. To, Z. Schug, S. Basu, F. Wang, E. Ricciotti, C. DiRusso, M.E. Murphy, R.H. Vonderheide, P.M. Lieberman, C. Mulligan, B. Nam, N. Hockstein, G. Masters, M. Guarino, C. Lin, Y. Nefedova, P. Black, V.E. Kagan, D.I. Gabrilovich, Fatty acid transport protein 2 reprograms neutrophils in cancer, Nature, 569 (2019) 73-78.
[311] B. Raud, D.G. Roy, A.S. Divakaruni, T.N. Tarasenko, R. Franke, E.H. Ma, B. Samborska, W.Y. Hsieh, A.H. Wong, P. Stuve, C. Arnold-Schrauf, M. Guderian, M. Lochner, S. Rampertaap, K. Romito, J. Monsale, M. Bronstrup, S.J. Bensinger, A.N. Murphy, P.J. McGuire, R.G. Jones, T. Sparwasser, L. Berod, Etomoxir

Actions on Regulatory and Memory T Cells Are Independent of Cpt1a-Mediated Fatty Acid Oxidation, Cell metabolism, 28 (2018) 504-515 e507.
[312] A.S. Divakaruni, W.Y. Hsieh, L. Minarrieta, T.N. Duong, K.K.O. Kim, B.R. Desousa, A.Y. Andreyev, C.E. Bowman, K. Caradonna, B.P. Dranka, D.A. Ferrick, M. Liesa, L. Stiles, G.W. Rogers, D. Braas, T.P. Ciaraldi, M.J. Wolfgang, T. Sparwasser, L. Berod, S.J. Bensinger, A.N. Murphy, Etomoxir Inhibits Macrophage Polarization by Disrupting CoA Homeostasis, Cell metabolism, 28 (2018) 490-503 e497.
[313] S. Kamisuki, Q. Mao, L. Abu-Elheiga, Z. Gu, A. Kugimiya, Y. Kwon, T. Shinohara, Y. Kawazoe, S. Sato, K. Asakura, H.Y. Choo, J. Sakai, S.J. Wakil, M. Uesugi, A small molecule that blocks fat synthesis by inhibiting the activation of SREBP, Chemistry & biology, 16 (2009) 882-892.
[314] X. Li, Y.T. Chen, P. Hu, W.C. Huang, Fatostatin displays high antitumor activity in prostate cancer by blocking SREBP-regulated metabolic pathways and androgen receptor signaling, Molecular cancer therapeutics, 13 (2014) 855-866.
[315] X. Li, J.B. Wu, L.W. Chung, W.C. Huang, Anti-cancer efficacy of SREBP inhibitor, alone or in combination with docetaxel, in prostate cancer harboring p53 mutations, Oncotarget, 6 (2015) 41018-41032.
[316] S.K. Krol, M. Kielbus, A. Rivero-Muller, A. Stepulak, Comprehensive review on betulin as a potent anticancer agent, BioMed research international, 2015 (2015) 584189.
[317] Siqingaowa, S. Sekar, V. Gopalakrishnan, C. Taghibiglou, Sterol regulatory element-binding protein 1 inhibitors decrease pancreatic cancer cell viability and proliferation, Biochemical and biophysical research communications, 488 (2017) 136-140.
[318] Y. Gao, M.S. Islam, J. Tian, V.W. Lui, D. Xiao, Inactivation of ATP citrate lyase by Cucurbitacin B: A bioactive compound from cucumber, inhibits prostate cancer growth, Cancer letters, 349 (2014) 15-25.
[319] S.K. Koerner, J.I. Hanai, S. Bai, F.E. Jernigan, M. Oki, C. Komaba, E. Shuto, V.P. Sukhatme, L. Sun, Design and synthesis of emodin derivatives as novel inhibitors of ATP-citrate lyase, European journal of medicinal chemistry, 126 (2017) 920-928.
[320] C.T. Cramer, B. Goetz, K.L. Hopson, G.J. Fici, R.M. Ackermann, S.C. Brown, C.L. Bisgaier, W.G. Rajeswaran, D.C. Oniciu, M.E. Pape, Effects of a novel dual lipid synthesis inhibitor and its potential utility in treating dyslipidemia and metabolic syndrome, Journal of lipid research, 45 (2004) 1289-1301.
[321] S.L. Pinkosky, S. Filippov, R.A. Srivastava, J.C. Hanselman, C.D. Bradshaw, T.R. Hurley, C.T. Cramer, M.A. Spahr, A.F. Brant, J.L. Houghton, C. Baker, M. Naples, K. Adeli, R.S. Newton, AMP-activated protein kinase and ATP-citrate lyase are two distinct molecular targets for ETC-1002, a novel small molecule regulator of lipid and carbohydrate metabolism, Journal of lipid research, 54 (2013) 134-151.
[322] C.M. Ballantyne, M.H. Davidson, D.E. Macdougall, H.E. Bays, L.A. Dicarlo, N.L. Rosenberg, J. Margulies, R.S. Newton, Efficacy and safety of a novel dual modulator of adenosine triphosphate-citrate lyase and adenosine monophosphate-activated protein kinase in patients with hypercholesterolemia: results of a multicenter, randomized, double-blind, placebo-controlled, parallel-group trial, Journal of the American College of Cardiology, 62 (2013) 1154-1162.
[323] M.J. Gutierrez, N.L. Rosenberg, D.E. Macdougall, J.C. Hanselman, J.R. Margulies, P. Strange, M.A. Milad, S.J. McBride, R.S. Newton, Efficacy and safety of ETC-1002, a novel investigational low-density lipoprotein-cholesterol-lowering therapy for the treatment of patients with hypercholesterolemia and type 2 diabetes mellitus, Arteriosclerosis, thrombosis, and vascular biology, 34 (2014) 676-683.
[324] K.K. Ray, H.E. Bays, A.L. Catapano, N.D. Lalwani, L.T. Bloedon, L.R. Sterling, P.L. Robinson, C.M. Ballantyne, C.H. Trial, Safety and Efficacy of Bempedoic Acid to Reduce LDL Cholesterol, The New England journal of medicine, 380 (2019) 1022-1032.

[325] F.E. Jernigan, J.I. Hanai, V.P. Sukhatme, L. Sun, Discovery of furan carboxylate derivatives as novel inhibitors of ATP-citrate lyase via virtual high-throughput screening, Bioorganic & medicinal chemistry letters, 27 (2017) 929-935.
[326] T.A. Berkhout, L.M. Havekes, N.J. Pearce, P.H. Groot, The effect of (-)-hydroxycitrate on the activity of the low-density-lipoprotein receptor and 3-hydroxy-3-methylglutaryl-CoA reductase levels in the human hepatoma cell line Hep G2, The Biochemical journal, 272 (1990) 181-186.
[327] L. Schwartz, M. Abolhassani, A. Guais, E. Sanders, J.M. Steyaert, F. Campion, M. Israel, A combination of alpha lipoic acid and calcium hydroxycitrate is efficient against mouse cancer models: preliminary results, Oncology reports, 23 (2010) 1407-1416.
[328] A. Guais, G. Baronzio, E. Sanders, F. Campion, C. Mainini, G. Fiorentini, F. Montagnani, M. Behzadi, L. Schwartz, M. Abolhassani, Adding a combination of hydroxycitrate and lipoic acid (METABLOC) to chemotherapy improves effectiveness against tumor development: experimental results and case report, Investigational new drugs, 30 (2012) 200-211.
[329] G. Rose-Kahn, J. Bar-Tana, Inhibition of rat liver acetyl-CoA carboxylase by beta, beta'-tetramethyl-substituted hexadecanedioic acid (MEDICA 16), Biochimica et biophysica acta, 1042 (1990) 259-264.
[330] J.J. Li, H. Wang, J.A. Tino, J.A. Robl, T.F. Herpin, R.M. Lawrence, S. Biller, H. Jamil, R. Ponticiello, L. Chen, C.H. Chu, N. Flynn, D. Cheng, R. Zhao, B. Chen, D. Schnur, M.T. Obermeier, V. Sasseville, R. Padmanabha, K. Pike, T. Harrity, 2-hydroxy-N-arylbenzenesulfonamides as ATP-citrate lyase inhibitors, Bioorganic & medicinal chemistry letters, 17 (2007) 3208-3211.
[331] J. Wei, S. Leit, J. Kuai, E. Therrien, S. Rafi, H.J. Harwood, Jr., B. DeLaBarre, L. Tong, An allosteric mechanism for potent inhibition of human ATP-citrate lyase, Nature, 568 (2019) 566-570.
[332] G. Hatzivassiliou, F. Zhao, D.E. Bauer, C. Andreadis, A.N. Shaw, D. Dhanak, S.R. Hingorani, D.A. Tuveson, C.B. Thompson, ATP citrate lyase inhibition can suppress tumor cell growth, Cancer cell, 8 (2005) 311-321.
[333] Y. Sugimoto, Y. Naniwa, T. Nakamura, H. Kato, M. Yamamoto, H. Tanabe, K. Inoue, A. Imaizumi, A novel acetyl-CoA carboxylase inhibitor reduces de novo fatty acid synthesis in HepG2 cells and rat primary hepatocytes, Archives of biochemistry and biophysics, 468 (2007) 44-48.
[334] U.N.L.o. Medicine, Phase IB Metformin, Digoxin, Simvastatin in Solid Tumors, in, ClinicalTrials.gov, 2019.
[335] U.N.L.o. Medicine, Bicalutamide With or Without Metformin for Biochemical Recurrence in Overweight or Obese Prostate Cancer Patients (BIMET-1), in, ClinicalTrials.gov, 2019.
[336] U.N.L.o. Medicine, Nivolumab and Metformin Hydrochloride in Treating Patients With Stage III-IV Non-small Cell Lung Cancer That Cannot Be Removed by Surgery, in, ClinicalTrials.gov, 2018.
[337] U.N.L.o. Medicine, Vandetanib in Combination With Metformin in People With HLRCC or SDH-Associated Kidney Cancer or Sporadic Papillary Renal Cell Carcinoma, in, ClinicalTrials.gov, 2019.
[338] U.N.L.o. Medicine, Nivolumab and Metformin in Patients With Treatment Refractory MSS Colorectal Cancer, in, ClinicalTrials.gov, 2019.
[339] U.N.L.o. Medicine, A Trial of Pembrolizumab and Metformin Versus Pembrolizumab Alone in Advanced Melanoma, in, ClinicalTrials.gov, 2019.
[340] U.N.L.o. Medicine, Phase I/II Study OF Metformin in Combination With Cisplatin and Radiation in Head and Neck Squamous Cell Carcinoma, in, 2019.
[341] U.N.L.o. Medicine, Study of Paclitaxel, Carboplatin and Oral Metformin in the Treatment of Advanced Stage Ovarian Carcinoma, in, ClinicalTrials.gov, 2017.
[342] R.U. Svensson, S.J. Parker, L.J. Eichner, M.J. Kolar, M. Wallace, S.N. Brun, P.S. Lombardo, J.L. Van Nostrand, A. Hutchins, L. Vera, L. Gerken, J. Greenwood, S. Bhat, G. Harriman, W.F. Westlin, H.J. Harwood, Jr., A. Saghatelian, R. Kapeller, C.M. Metallo, R.J. Shaw, Inhibition of acetyl-CoA carboxylase

suppresses fatty acid synthesis and tumor growth of non-small-cell lung cancer in preclinical models, Nature medicine, 22 (2016) 1108-1119.
[343] G. Rose-Kahn, J. Bar-Tana, Inhibition of lipid synthesis by beta beta'-tetramethyl-substituted, C14-C22, alpha, omega-dicarboxylic acids in cultured rat hepatocytes, The Journal of biological chemistry, 260 (1985) 8411-8415.
[344] Q. Wei, L. Mei, Y. Yang, H. Ma, H. Chen, H. Zhang, J. Zhou, Design, synthesis and biological evaluation of novel spiro-pentacylamides as acetyl-CoA carboxylase inhibitors, Bioorganic & medicinal chemistry, 26 (2018) 3866-3874.
[345] K.D. Freeman-Cook, P. Amor, S. Bader, L.M. Buzon, S.B. Coffey, J.W. Corbett, K.J. Dirico, S.D. Doran, R.L. Elliott, W. Esler, A. Guzman-Perez, K.E. Henegar, J.A. Houser, C.S. Jones, C. Limberakis, K. Loomis, K. McPherson, S. Murdande, K.L. Nelson, D. Phillion, B.S. Pierce, W. Song, E. Sugarman, S. Tapley, M. Tu, Z. Zhao, Maximizing lipophilic efficiency: the use of Free-Wilson analysis in the design of inhibitors of acetyl-CoA carboxylase, Journal of medicinal chemistry, 55 (2012) 935-942.
[346] J.E. Jones, W.P. Esler, R. Patel, A. Lanba, N.B. Vera, J.A. Pfefferkorn, C. Vernochet, Inhibition of Acetyl-CoA Carboxylase 1 (ACC1) and 2 (ACC2) Reduces Proliferation and De Novo Lipogenesis of EGFRvIII Human Glioblastoma Cells, PloS one, 12 (2017) e0169566.
[347] D.F. Calvisi, C. Wang, C. Ho, S. Ladu, S.A. Lee, S. Mattu, G. Destefanis, S. Delogu, A. Zimmermann, J. Ericsson, S. Brozzetti, T. Staniscia, X. Chen, F. Dombrowski, M. Evert, Increased lipogenesis, induced by AKT-mTORC1-RPS6 signaling, promotes development of human hepatocellular carcinoma, Gastroenterology, 140 (2011) 1071-1083.
[348] M. Rios Garcia, B. Steinbauer, K. Srivastava, M. Singhal, F. Mattijssen, A. Maida, S. Christian, H. Hess-Stumpp, H.G. Augustin, K. Muller-Decker, P.P. Nawroth, S. Herzig, M. Berriel Diaz, Acetyl-CoA Carboxylase 1-Dependent Protein Acetylation Controls Breast Cancer Metastasis and Recurrence, Cell metabolism, 26 (2017) 842-855 e845.
[349] D. Buckley, G. Duke, T.S. Heuer, M. O'Farrell, A.S. Wagman, W. McCulloch, G. Kemble, Fatty acid synthase - Modern tumor cell biology insights into a classical oncology target, Pharmacology & therapeutics, 177 (2017) 23-31.
[350] R. Flavin, S. Peluso, P.L. Nguyen, M. Loda, Fatty acid synthase as a potential therapeutic target in cancer, Future oncology, 6 (2010) 551-562.
[351] A. Rivkin, Y.R. Kim, M.T. Goulet, N. Bays, A.D. Hill, I. Kariv, S. Krauss, N. Ginanni, P.R. Strack, N.E. Kohl, C.C. Chung, J.P. Varnerin, P.N. Goudreau, A. Chang, M.R. Tota, B. Munoz, 3-Aryl-4-hydroxyquinolin-2(1H)-one derivatives as type I fatty acid synthase inhibitors, Bioorganic & medicinal chemistry letters, 16 (2006) 4620-4623.
[352] E.S. Pizer, F.D. Wood, H.S. Heine, F.E. Romantsev, G.R. Pasternack, F.P. Kuhajda, Inhibition of fatty acid synthesis delays disease progression in a xenograft model of ovarian cancer, Cancer research, 56 (1996) 1189-1193.
[353] E.S. Pizer, C. Jackisch, F.D. Wood, G.R. Pasternack, N.E. Davidson, F.P. Kuhajda, Inhibition of fatty acid synthesis induces programmed cell death in human breast cancer cells, Cancer research, 56 (1996) 2745-2747.
[354] F.P. Kuhajda, E.S. Pizer, J.N. Li, N.S. Mani, G.L. Frehywot, C.A. Townsend, Synthesis and antitumor activity of an inhibitor of fatty acid synthase, Proceedings of the National Academy of Sciences of the United States of America, 97 (2000) 3450-3454.
[355] W. Zhou, P.J. Simpson, J.M. McFadden, C.A. Townsend, S.M. Medghalchi, A. Vadlamudi, M.L. Pinn, G.V. Ronnett, F.P. Kuhajda, Fatty acid synthase inhibition triggers apoptosis during S phase in human cancer cells, Cancer research, 63 (2003) 7330-7337.

[356] P.M. Alli, M.L. Pinn, E.M. Jaffee, J.M. McFadden, F.P. Kuhajda, Fatty acid synthase inhibitors are chemopreventive for mammary cancer in neu-N transgenic mice, Oncogene, 24 (2005) 39-46.
[357] H. Orita, J. Coulter, C. Lemmon, E. Tully, A. Vadlamudi, S.M. Medghalchi, F.P. Kuhajda, E. Gabrielson, Selective inhibition of fatty acid synthase for lung cancer treatment, Clinical cancer research : an official journal of the American Association for Cancer Research, 13 (2007) 7139-7145.
[358] H. Orita, J. Coulter, E. Tully, F.P. Kuhajda, E. Gabrielson, Inhibiting fatty acid synthase for chemoprevention of chemically induced lung tumors, Clinical cancer research : an official journal of the American Association for Cancer Research, 14 (2008) 2458-2464.
[359] W. Zhou, W.F. Han, L.E. Landree, J.N. Thupari, M.L. Pinn, T. Bililign, E.K. Kim, A. Vadlamudi, S.M. Medghalchi, R. El Meskini, G.V. Ronnett, C.A. Townsend, F.P. Kuhajda, Fatty acid synthase inhibition activates AMP-activated protein kinase in SKOV3 human ovarian cancer cells, Cancer research, 67 (2007) 2964-2971.
[360] D. Vance, I. Goldberg, O. Mitsuhashi, K. Bloch, Inhibition of fatty acid synthetases by the antibiotic cerulenin, Biochemical and biophysical research communications, 48 (1972) 649-656.
[361] H. Funabashi, A. Kawaguchi, H. Tomoda, S. Omura, S. Okuda, S. Iwasaki, Binding site of cerulenin in fatty acid synthetase, Journal of biochemistry, 105 (1989) 751-755.
[362] J.N. Thupari, M.L. Pinn, F.P. Kuhajda, Fatty acid synthase inhibition in human breast cancer cells leads to malonyl-CoA-induced inhibition of fatty acid oxidation and cytotoxicity, Biochemical and biophysical research communications, 285 (2001) 217-223.
[363] E.S. Pizer, J. Thupari, W.F. Han, M.L. Pinn, F.J. Chrest, G.L. Frehywot, C.A. Townsend, F.P. Kuhajda, Malonyl-coenzyme-A is a potential mediator of cytotoxicity induced by fatty-acid synthase inhibition in human breast cancer cells and xenografts, Cancer research, 60 (2000) 213-218.
[364] K. Brusselmans, E. De Schrijver, W. Heyns, G. Verhoeven, J.V. Swinnen, Epigallocatechin-3-gallate is a potent natural inhibitor of fatty acid synthase in intact cells and selectively induces apoptosis in prostate cancer cells, International journal of cancer, 106 (2003) 856-862.
[365] B.H. Li, W.X. Tian, Inhibitory effects of flavonoids on animal fatty acid synthase, Journal of biochemistry, 135 (2004) 85-91.
[366] K. Brusselmans, R. Vrolix, G. Verhoeven, J.V. Swinnen, Induction of cancer cell apoptosis by flavonoids is associated with their ability to inhibit fatty acid synthase activity, The Journal of biological chemistry, 280 (2005) 5636-5645.
[367] W.X. Tian, Inhibition of fatty acid synthase by polyphenols, Current medicinal chemistry, 13 (2006) 967-977.
[368] T. Puig, C. Turrado, B. Benhamu, H. Aguilar, J. Relat, S. Ortega-Gutierrez, G. Casals, P.F. Marrero, A. Urruticoechea, D. Haro, M.L. Lopez-Rodriguez, R. Colomer, Novel Inhibitors of Fatty Acid Synthase with Anticancer Activity, Clinical cancer research : an official journal of the American Association for Cancer Research, 15 (2009) 7608-7615.
[369] Y. Alwarawrah, P. Hughes, D. Loiselle, D.A. Carlson, D.B. Darr, J.L. Jordan, J. Xiong, L.M. Hunter, L.G. Dubois, J.W. Thompson, M.M. Kulkarni, A.N. Ratcliff, J.J. Kwiek, T.A. Haystead, Fasnall, a Selective FASN Inhibitor, Shows Potent Anti-tumor Activity in the MMTV-Neu Model of HER2(+) Breast Cancer, Cell chemical biology, 23 (2016) 678-688.
[370] T. Puig, H. Aguilar, S. Cufi, G. Oliveras, C. Turrado, S. Ortega-Gutierrez, B. Benhamu, M.L. Lopez-Rodriguez, A. Urruticoechea, R. Colomer, A novel inhibitor of fatty acid synthase shows activity against HER2+ breast cancer xenografts and is active in anti-HER2 drug-resistant cell lines, Breast cancer research : BCR, 13 (2011) R131.
[371] M.A. Hardwicke, A.R. Rendina, S.P. Williams, M.L. Moore, L. Wang, J.A. Krueger, R.N. Plant, R.D. Totoritis, G. Zhang, J. Briand, W.A. Burkhart, K.K. Brown, C.A. Parrish, A human fatty acid synthase

inhibitor binds beta-ketoacyl reductase in the keto-substrate site, Nature chemical biology, 10 (2014) 774-779.
[372] M.J. Vazquez, W. Leavens, R. Liu, B. Rodriguez, M. Read, S. Richards, D. Winegar, J.M. Dominguez, Discovery of GSK837149A, an inhibitor of human fatty acid synthase targeting the beta-ketoacyl reductase reaction, The FEBS journal, 275 (2008) 1556-1567.
[373] J.D. Oslob, R.J. Johnson, H. Cai, S.Q. Feng, L. Hu, Y. Kosaka, J. Lai, M. Sivaraja, S. Tep, H. Yang, C.A. Zaharia, M.J. Evanchik, R.S. McDowell, Imidazopyridine-Based Fatty Acid Synthase Inhibitors That Show Anti-HCV Activity and in Vivo Target Modulation, ACS medicinal chemistry letters, 4 (2013) 113-117.
[374] G. Zadra, C.F. Ribeiro, P. Chetta, Y. Ho, S. Cacciatore, X. Gao, S. Syamala, C. Bango, C. Photopoulos, Y. Huang, S. Tyekucheva, D.C. Bastos, J. Tchaicha, B. Lawney, T. Uo, L. D'Anello, A. Csibi, R. Kalekar, B. Larimer, L. Ellis, L.M. Butler, C. Morrissey, K. McGovern, V.J. Palombella, J.L. Kutok, U. Mahmood, S. Bosari, J. Adams, S. Peluso, S.M. Dehm, S.R. Plymate, M. Loda, Inhibition of de novo lipogenesis targets androgen receptor signaling in castration-resistant prostate cancer, Proceedings of the National Academy of Sciences of the United States of America, 116 (2019) 631-640.
[375] T. Lu, R. Alexander, G. Bignan, J. Bischoff, P. Connolly, M. Cummings, S. De Breucker, N. Esser, E. Fraiponts, R. Gilissen, Design and synthesis of a series highly potent and bioavailable FASN KR domain inhibitors for cancer, in, AACR, 2014.
[376] S.J. Kridel, F. Axelrod, N. Rozenkrantz, J.W. Smith, Orlistat is a novel inhibitor of fatty acid synthase with antitumor activity, Cancer research, 64 (2004) 2070-2075.
[377] J.A. Menendez, L. Vellon, R. Lupu, Antitumoral actions of the anti-obesity drug orlistat (XenicalTM) in breast cancer cells: blockade of cell cycle progression, promotion of apoptotic cell death and PEA3-mediated transcriptional repression of Her2/neu (erbB-2) oncogene, Annals of oncology : official journal of the European Society for Medical Oncology, 16 (2005) 1253-1267.
[378] M.A. Carvalho, K.G. Zecchin, F. Seguin, D.C. Bastos, M. Agostini, A.L. Rangel, S.S. Veiga, H.F. Raposo, H.C. Oliveira, M. Loda, R.D. Coletta, E. Graner, Fatty acid synthase inhibition with Orlistat promotes apoptosis and reduces cell growth and lymph node metastasis in a mouse melanoma model, International journal of cancer, 123 (2008) 2557-2565.
[379] S. Dowling, J. Cox, R.J. Cenedella, Inhibition of fatty acid synthase by Orlistat accelerates gastric tumor cell apoptosis in culture and increases survival rates in gastric tumor bearing mice in vivo, Lipids, 44 (2009) 489-498.
[380] M. Wu, S.B. Singh, J. Wang, C.C. Chung, G. Salituro, B.V. Karanam, S.H. Lee, M. Powles, K.P. Ellsworth, M.E. Lassman, C. Miller, R.W. Myers, M.R. Tota, B.B. Zhang, C. Li, Antidiabetic and antisteatotic effects of the selective fatty acid synthase (FAS) inhibitor platensimycin in mouse models of diabetes, Proceedings of the National Academy of Sciences of the United States of America, 108 (2011) 5378-5383.
[381] J.M. McFadden, G.L. Frehywot, C.A. Townsend, A flexible route to (5R)-thiolactomycin, a naturally occurring inhibitor of fatty acid synthesis, Organic letters, 4 (2002) 3859-3862.
[382] J.M. McFadden, S.M. Medghalchi, J.N. Thupari, M.L. Pinn, A. Vadlamudi, K.I. Miller, F.P. Kuhajda, C.A. Townsend, Application of a flexible synthesis of (5R)-thiolactomycin to develop new inhibitors of type I fatty acid synthase, Journal of medicinal chemistry, 48 (2005) 946-961.
[383] U.N.L.o. Medicine, TVB 2640 for Resectable Colon Cancer Other Resectable Cancers; a Window Trial., in, ClinicalTrials.gov, 2018.
[384] U.N.L.o. Medicine, FASN Inhibitor TVB-2640, Paclitaxel, and Trastuzumab in Treating Patients With HER2 Positive Advanced Breast Cancer, in, ClinicalTrials.gov, 2019.
[385] U.N.L.o. Medicine, TVB- 2640 in Combination With Bevacizumab in Patients With First Relapse of High Grade Astrocytoma, in, ClinicalTrials.gov, 2018.

[386] G. Falchook, J. Infante, H.T. Arkenau, M.R. Patel, E. Dean, E. Borazanci, A. Brenner, N. Cook, J. Lopez, S. Pant, A. Frankel, P. Schmid, K. Moore, W. McCulloch, K. Grimmer, M. O'Farrell, G. Kemble, H. Burris, First-in-human study of the safety, pharmacokinetics, and pharmacodynamics of first-in-class fatty acid synthase inhibitor TVB-2640 alone and with a taxane in advanced tumors, EClinicalMedicine, 34 (2021) 100797.
[387] R. Ventura, K. Mordec, J. Waszczuk, Z. Wang, J. Lai, M. Fridlib, D. Buckley, G. Kemble, T.S. Heuer, Inhibition of de novo Palmitate Synthesis by Fatty Acid Synthase Induces Apoptosis in Tumor Cells by Remodeling Cell Membranes, Inhibiting Signaling Pathways, and Reprogramming Gene Expression, EBioMedicine, 2 (2015) 808-824.
[388] G. Liu, Stearoyl-CoA desaturase inhibitors: update on patented compounds, Expert opinion on therapeutic patents, 19 (2009) 1169-1191.
[389] Z. Zhang, N.A. Dales, M.D. Winther, Opportunities and challenges in developing stearoyl-coenzyme A desaturase-1 inhibitors as novel therapeutics for human disease, Journal of medicinal chemistry, 57 (2014) 5039-5056.
[390] Y. Uto, Recent progress in the discovery and development of stearoyl CoA desaturase inhibitors, Chem Phys Lipids, 197 (2016) 3-12.
[391] C.A. von Roemeling, L.A. Marlow, J.J. Wei, S.J. Cooper, T.R. Caulfield, K. Wu, W.W. Tan, H.W. Tun, J.A. Copland, Stearoyl-CoA desaturase 1 is a novel molecular therapeutic target for clear cell renal cell carcinoma, Clinical cancer research : an official journal of the American Association for Cancer Research, 19 (2013) 2368-2380.
[392] J.Y. Leung, W.Y. Kim, Stearoyl co-A desaturase 1 as a ccRCC therapeutic target: death by stress, Clinical cancer research : an official journal of the American Association for Cancer Research, 19 (2013) 3111-3113.
[393] Y. Liu, X. Liu, H. Wang, P. Ding, C. Wang, Agrimonolide inhibits cancer progression and induces ferroptosis and apoptosis by targeting SCD1 in ovarian cancer cells, Phytomedicine, 101 (2022) 154102.
[394] Y. Uto, T. Ogata, J. Harada, Y. Kiyotsuka, Y. Ueno, Y. Miyazawa, H. Kurata, T. Deguchi, N. Watanabe, T. Takagi, S. Wakimoto, R. Okuyama, M. Abe, N. Kurikawa, S. Kawamura, M. Yamato, J. Osumi, Novel and potent inhibitors of stearoyl-CoA desaturase-1. Part I: Discovery of 3-(2-hydroxyethoxy)-4-methoxy-N-[5-(3-trifluoromethylbenzyl)thiazol-2-yl]benzamid e, Bioorganic & medicinal chemistry letters, 19 (2009) 4151-4158.
[395] Y. Uto, T. Ogata, Y. Kiyotsuka, Y. Miyazawa, Y. Ueno, H. Kurata, T. Deguchi, M. Yamada, N. Watanabe, T. Takagi, S. Wakimoto, R. Okuyama, M. Konishi, N. Kurikawa, K. Kono, J. Osumi, Novel and potent inhibitors of stearoyl-CoA desaturase-1. Part II: Identification of 4-ethylamino-3-(2-hydroxyethoxy)-N-[5-(3-trifluoromethylbenzyl)thiazol-2-yl]benzamide and its biological evaluation, Bioorganic & medicinal chemistry letters, 19 (2009) 4159-4166.
[396] D.O. Koltun, N.I. Vasilevich, E.Q. Parkhill, A.I. Glushkov, T.M. Zilbershtein, E.I. Mayboroda, M.A. Boze, A.G. Cole, I. Henderson, N.A. Zautke, S.A. Brunn, N. Chu, J. Hao, N. Mollova, K. Leung, J.W. Chisholm, J. Zablocki, Orally bioavailable, liver-selective stearoyl-CoA desaturase (SCD) inhibitors, Bioorganic & medicinal chemistry letters, 19 (2009) 3050-3053.
[397] D.O. Koltun, T.M. Zilbershtein, V.A. Migulin, N.I. Vasilevich, E.Q. Parkhill, A.I. Glushkov, M.J. McGregor, S.A. Brunn, N. Chu, J. Hao, N. Mollova, K. Leung, J.W. Chisholm, J. Zablocki, Potent, orally bioavailable, liver-selective stearoyl-CoA desaturase (SCD) inhibitors, Bioorganic & medicinal chemistry letters, 19 (2009) 4070-4074.
[398] D.A. Powell, Y. Ramtohul, M.E. Lebrun, R. Oballa, S. Bhat, J.P. Falgueyret, S. Guiral, Z. Huang, K. Skorey, P. Tawa, L. Zhang, 2-Aryl benzimidazoles: human SCD1-specific stearoyl coenzyme-A desaturase inhibitors, Bioorganic & medicinal chemistry letters, 20 (2010) 6366-6369.

[399] E. Isabel, D.A. Powell, W.C. Black, C.C. Chan, S. Crane, R. Gordon, J. Guay, S. Guiral, Z. Huang, J. Robichaud, K. Skorey, P. Tawa, L. Xu, L. Zhang, R. Oballa, Biological activity and preclinical efficacy of azetidinyl pyridazines as potent systemically-distributed stearoyl-CoA desaturase inhibitors, Bioorganic & medicinal chemistry letters, 21 (2011) 479-483.
[400] H. Matter, G. Zoller, A.W. Herling, J.A. Sanchez-Arias, C. Philippo, C. Namane, M. Kohlmann, A. Pfenninger, M.D. Voss, Benzimidazole-carboxamides as potent and bioavailable stearoyl-CoA desaturase (SCD1) inhibitors from ligand-based virtual screening and chemical optimization, Bioorganic & medicinal chemistry letters, 23 (2013) 1817-1822.
[401] P.C. Theodoropoulos, S.S. Gonzales, S.E. Winterton, C. Rodriguez-Navas, J.S. McKnight, L.K. Morlock, J.M. Hanson, B. Cross, A.E. Owen, Y. Duan, J.R. Moreno, A. Lemoff, H. Mirzaei, B.A. Posner, N.S. Williams, J.M. Ready, D. Nijhawan, Discovery of tumor-specific irreversible inhibitors of stearoyl CoA desaturase, Nature chemical biology, 12 (2016) 218-225.
[402] Y. Uto, T. Ogata, Y. Kiyotsuka, Y. Ueno, Y. Miyazawa, H. Kurata, T. Deguchi, N. Watanabe, M. Konishi, R. Okuyama, N. Kurikawa, T. Takagi, S. Wakimoto, J. Ohsumi, Novel benzoylpiperidine-based stearoyl-CoA desaturase-1 inhibitors: Identification of 6-[4-(2-methylbenzoyl)piperidin-1-yl]pyridazine-3-carboxylic acid (2-hydroxy-2-pyridin-3-ylethyl)amide and its plasma triglyceride-lowering effects in Zucker fatty rats, Bioorganic & medicinal chemistry letters, 20 (2010) 341-345.
[403] Y. Deng, Z. Yang, G.W. Shipps, Jr., S.M. Lo, R. West, J. Hwa, S. Zheng, C. Farley, J. Lachowicz, M. van Heek, A.S. Bass, D.P. Sinha, C.R. Mahon, M.E. Cartwright, Discovery of liver-targeted inhibitors of stearoyl-CoA desaturase (SCD1), Bioorganic & medicinal chemistry letters, 23 (2013) 791-796.
[404] Y.K. Ramtohul, D. Powell, J.P. Leclerc, S. Leger, R. Oballa, C. Black, E. Isabel, C.S. Li, S. Crane, J. Robichaud, J. Guay, S. Guiral, L. Zhang, Z. Huang, Bicyclic heteroaryl inhibitors of stearoyl-CoA desaturase: from systemic to liver-targeting inhibitors, Bioorganic & medicinal chemistry letters, 21 (2011) 5692-5696.
[405] N. Scaglia, J.W. Chisholm, R.A. Igal, Inhibition of stearoylCoA desaturase-1 inactivates acetyl-CoA carboxylase and impairs proliferation in cancer cells: role of AMPK, PloS one, 4 (2009) e6812.
[406] K. Imamura, N. Tomita, Y. Kawakita, Y. Ito, K. Ono, N. Nii, T. Miyazaki, K. Yonemori, M. Tawada, H. Sumi, Y. Satoh, Y. Yamamoto, I. Miyahisa, M. Sasaki, Y. Satomi, M. Hirayama, R. Nishigaki, H. Maezaki, Discovery of Novel and Potent Stearoyl Coenzyme A Desaturase 1 (SCD1) Inhibitors as Anticancer Agents, Bioorganic & medicinal chemistry, 25 (2017) 3768-3779.
[407] S. Nishizawa, H. Sumi, Y. Satoh, Y. Yamamoto, S. Kitazawa, K. Honda, H. Araki, K. Kakoi, K. Imamura, M. Sasaki, I. Miyahisa, Y. Satomi, R. Nishigaki, M. Hirayama, K. Aoyama, H. Maezaki, T. Hara, In vitro and in vivo antitumor activities of T-3764518, a novel and orally available small molecule stearoyl-CoA desaturase 1 inhibitor, European journal of pharmacology, 807 (2017) 21-31.
[408] M. Issandou, A. Bouillot, J.M. Brusq, M.C. Forest, D. Grillot, R. Guillard, S. Martin, C. Michiels, T. Sulpice, A. Daugan, Pharmacological inhibition of stearoyl-CoA desaturase 1 improves insulin sensitivity in insulin-resistant rat models, European journal of pharmacology, 618 (2009) 28-36.
[409] C. Yang, Y.Y. Jin, J. Mei, D. Hu, X. Jiao, H.L. Che, C.L. Tang, Y. Zhang, G.S. Wu, Identification of icaritin derivative IC2 as an SCD-1 inhibitor with anti-breast cancer properties through induction of cell apoptosis, Cancer cell international, 22 (2022) 202.
[410] S. Leger, W.C. Black, D. Deschenes, S. Dolman, J.P. Falgueyret, M. Gagnon, S. Guiral, Z. Huang, J. Guay, Y. Leblanc, C.S. Li, F. Masse, R. Oballa, L. Zhang, Synthesis and biological activity of a potent and orally bioavailable SCD inhibitor (MF-438), Bioorganic & medicinal chemistry letters, 20 (2010) 499-502.
[411] M.E. Pisanu, A. Noto, C. De Vitis, S. Morrone, G. Scognamiglio, G. Botti, F. Venuta, D. Diso, Z. Jakopin, F. Padula, A. Ricci, S. Mariotta, M.R. Giovagnoli, E. Giarnieri, I. Amelio, M. Agostini, G. Melino, G.

Ciliberto, R. Mancini, Blockade of Stearoyl-CoA-desaturase 1 activity reverts resistance to cisplatin in lung cancer stem cells, Cancer letters, 406 (2017) 93-104.
[412] R.M. Oballa, L. Belair, W.C. Black, K. Bleasby, C.C. Chan, C. Desroches, X. Du, R. Gordon, J. Guay, S. Guiral, M.J. Hafey, E. Hamelin, Z. Huang, B. Kennedy, N. Lachance, F. Landry, C.S. Li, J. Mancini, D. Normandin, A. Pocai, D.A. Powell, Y.K. Ramtohul, K. Skorey, D. Sorensen, W. Sturkenboom, A. Styhler, D.M. Waddleton, H. Wang, S. Wong, L. Xu, L. Zhang, Development of a liver-targeted stearoyl-CoA desaturase (SCD) inhibitor (MK-8245) to establish a therapeutic window for the treatment of diabetes and dyslipidemia, Journal of medicinal chemistry, 54 (2011) 5082-5096.
[413] U.N.L.o. Medicine, Pharmacokinetics and Pharmacodynamics of MK-8245 in Participants With Type 2 Diabetes (MK-8245-012), in, ClinicalTrials.gov, 2010.
[414] K.A. Atkinson, E.E. Beretta, J.A. Brown, M. Castrodad, Y. Chen, J.M. Cosgrove, P. Du, J. Litchfield, M. Makowski, K. Martin, T.J. McLellan, C. Neagu, D.A. Perry, D.W. Piotrowski, C.M. Steppan, R. Trilles, N-benzylimidazole carboxamides as potent, orally active stearoylCoA desaturase-1 inhibitors, Bioorganic & medicinal chemistry letters, 21 (2011) 1621-1625.
[415] D.A. Powell, W.C. Black, K. Bleasby, C.C. Chan, D. Deschenes, M. Gagnon, R. Gordon, J. Guay, S. Guiral, M.J. Hafey, Z. Huang, E. Isabel, Y. Leblanc, A. Styhler, L.J. Xu, L. Zhang, R.M. Oballa, Nicotinic acids: liver-targeted SCD inhibitors with preclinical anti-diabetic efficacy, Bioorganic & medicinal chemistry letters, 21 (2011) 7281-7286.
[416] H. Zhao, M.D. Serby, H.T. Smith, N. Cao, T.S. Suhar, T.K. Surowy, H.S. Camp, C.A. Collins, H.L. Sham, G. Liu, Discovery of 1-(4-phenoxypiperidin-1-yl)-2-arylaminoethanone stearoyl-CoA desaturase 1 inhibitors, Bioorganic & medicinal chemistry letters, 17 (2007) 3388-3391.
[417] N. Lachance, S. Guiral, Z. Huang, J.P. Leclerc, C.S. Li, R.M. Oballa, Y.K. Ramtohul, H. Wang, J. Wu, L. Zhang, Discovery of potent and liver-selective stearoyl-CoA desaturase (SCD) inhibitors in an acyclic linker series, Bioorganic & medicinal chemistry letters, 22 (2012) 623-627.
[418] N. Lachance, Y. Gareau, S. Guiral, Z. Huang, E. Isabel, J.P. Leclerc, S. Leger, E. Martins, C. Nadeau, R.M. Oballa, S.G. Ouellet, D.A. Powell, Y.K. Ramtohul, G.K. Tranmer, T. Trinh, H. Wang, L. Zhang, Discovery of potent and liver-targeted stearoyl-CoA desaturase (SCD) inhibitors in a bispyrrolidine series, Bioorganic & medicinal chemistry letters, 22 (2012) 980-984.
[419] Z. Xin, H. Zhao, M.D. Serby, B. Liu, M. Liu, B.G. Szczepankiewicz, L.T. Nelson, H.T. Smith, T.S. Suhar, R.S. Janis, N. Cao, H.S. Camp, C.A. Collins, H.L. Sham, T.K. Surowy, G. Liu, Discovery of piperidine-aryl urea-based stearoyl-CoA desaturase 1 inhibitors, Bioorganic & medicinal chemistry letters, 18 (2008) 4298-4302.
[420] D.O. Koltun, E.Q. Parkhill, N.I. Vasilevich, A.I. Glushkov, T.M. Zilbershtein, A.V. Ivanov, A.G. Cole, I. Henderson, N.A. Zautke, S.A. Brunn, N. Mollova, K. Leung, J.W. Chisholm, J. Zablocki, Novel, potent, selective, and metabolically stable stearoyl-CoA desaturase (SCD) inhibitors, Bioorganic & medicinal chemistry letters, 19 (2009) 2048-2052.
[421] Z. Zhang, S. Sun, V. Kodumuru, D. Hou, S. Liu, N. Chakka, S. Sviridov, S. Chowdhury, D.G. McLaren, L.G. Ratkay, K. Khakh, X. Cheng, H.W. Gschwend, R. Kamboj, J. Fu, M.D. Winther, Discovery of piperazin-1-ylpyridazine-based potent and selective stearoyl-CoA desaturase-1 inhibitors for the treatment of obesity and metabolic syndrome, Journal of medicinal chemistry, 56 (2013) 568-583.
[422] J.G. Meingassner, H. Aschauer, A.P. Winiski, N. Dales, D. Yowe, M.D. Winther, Z. Zhang, A. Stutz, A. Billich, Pharmacological inhibition of stearoyl CoA desaturase in the skin induces atrophy of the sebaceous glands, The Journal of investigative dermatology, 133 (2013) 2091-2094.
[423] M.D. Voss, G. Zoller, H. Matter, A.W. Herling, G. Biemer-Daub, A. Pfenninger, S. Haag-Diergarten, S. Keil, M. Kohlmann, H.L. Schmidts, Discovery and pharmacological characterization of SAR707 as novel

and selective small molecule inhibitor of stearoyl-CoA desaturase (SCD1), European journal of pharmacology, 707 (2013) 140-146.
[424] Y. Uto, Y. Kiyotsuka, Y. Ueno, Y. Miyazawa, H. Kurata, T. Ogata, T. Deguchi, M. Yamada, N. Watanabe, M. Konishi, N. Kurikawa, T. Takagi, S. Wakimoto, K. Kono, J. Ohsumi, Novel spiropiperidine-based stearoyl-CoA desaturase-1 inhibitors: Identification of 1'-{6-[5-(pyridin-3-ylmethyl)-1,3,4-oxadiazol-2-yl]pyridazin-3-yl}-5-(trifluorome thyl)-3,4-dihydrospiro[chromene-2,4'-piperidine], Bioorganic & medicinal chemistry letters, 20 (2010) 746-754.
[425] Y. Uto, Y. Ueno, Y. Kiyotsuka, Y. Miyazawa, H. Kurata, T. Ogata, M. Yamada, T. Deguchi, M. Konishi, T. Takagi, S. Wakimoto, J. Ohsumi, Synthesis and evaluation of novel stearoyl-CoA desaturase 1 inhibitors: 1'-{6-[5-(pyridin-3-ylmethyl)-1,3,4-oxadiazol-2-yl]pyridazin-3-yl}-3,4-dihydrospi ro[chromene-2,4'-piperidine] analogs, European journal of medicinal chemistry, 45 (2010) 4788-4796.
[426] Y. Uto, Y. Ueno, Y. Kiyotsuka, Y. Miyazawa, H. Kurata, T. Ogata, T. Takagi, S. Wakimoto, J. Ohsumi, Discovery of novel SCD1 inhibitors: 5-alkyl-4,5-dihydro-3H-spiro[1,5-benzoxazepine-2,4'-piperidine] analogs, European journal of medicinal chemistry, 46 (2011) 1892-1896.
[427] Y.K. Ramtohul, C. Black, C.C. Chan, S. Crane, J. Guay, S. Guiral, Z. Huang, R. Oballa, L.J. Xu, L. Zhang, C.S. Li, SAR and optimization of thiazole analogs as potent stearoyl-CoA desaturase inhibitors, Bioorganic & medicinal chemistry letters, 20 (2010) 1593-1597.
[428] C.S. Li, L. Belair, J. Guay, R. Murgasva, W. Sturkenboom, Y.K. Ramtohul, L. Zhang, Z. Huang, Thiazole analog as stearoyl-CoA desaturase 1 inhibitor, Bioorganic & medicinal chemistry letters, 19 (2009) 5214-5217.
[429] T. Iida, M. Ubukata, I. Mitani, Y. Nakagawa, K. Maeda, H. Imai, Y. Ogoshi, T. Hotta, S. Sakata, R. Sano, H. Morinaga, T. Negoro, S. Oshida, M. Tanaka, T. Inaba, Discovery of potent liver-selective stearoyl-CoA desaturase-1 (SCD1) inhibitors, thiazole-4-acetic acid derivatives, for the treatment of diabetes, hepatic steatosis, and obesity, European journal of medicinal chemistry, 158 (2018) 832-852.
[430] S. Sun, Z. Zhang, V. Raina, N. Pokrovskaia, D. Hou, R. Namdari, K. Khakh, L.G. Ratkay, D.G. McLaren, M. Mork, J. Fu, S. Ferreira, B. Hubbard, M.D. Winther, N. Dales, Discovery of thiazolylpyridinone SCD1 inhibitors with preferential liver distribution and reduced mechanism-based adverse effects, Bioorganic & medicinal chemistry letters, 24 (2014) 526-531.
[431] S. Sun, Z. Zhang, N. Pokrovskaia, S. Chowdhury, Q. Jia, E. Chang, K. Khakh, R. Kwan, D.G. McLaren, C.C. Radomski, L.G. Ratkay, J. Fu, N.A. Dales, M.D. Winther, Discovery of triazolone derivatives as novel, potent stearoyl-CoA desaturase-1 (SCD1) inhibitors, Bioorganic & medicinal chemistry, 23 (2015) 455-465.
[432] U.N.L.o. Medicine, TPST-1120 as Monotherapy and in Combination With (Nivolumab, Docetaxel or Cetuximab) in Subjects With Advanced Cancers, in, ClinicalTrials.gov, 2019.
[433] R. Perets, G.A. Wyant, K.W. Muto, J.G. Bijron, B.B. Poole, K.T. Chin, J.Y. Chen, A.W. Ohman, C.D. Stepule, S. Kwak, A.M. Karst, M.S. Hirsch, S.R. Setlur, C.P. Crum, D.M. Dinulescu, R. Drapkin, Transformation of the fallopian tube secretory epithelium leads to high-grade serous ovarian cancer in Brca;Tp53;Pten models, Cancer cell, 24 (2013) 751-765.
[434] K. Vriens, S. Christen, S. Parik, D. Broekaert, K. Yoshinaga, A. Talebi, J. Dehairs, C. Escalona-Noguero, R. Schmieder, T. Cornfield, C. Charlton, L. Romero-Pérez, M. Rossi, G. Rinaldi, M.F. Orth, R. Boon, A. Kerstens, S.Y. Kwan, B. Faubert, A. Méndez-Lucas, C.C. Kopitz, T. Chen, J. Fernandez-Garcia, J.A.G. Duarte, A.A. Schmitz, P. Steigemann, M. Najimi, A. Hägebarth, J.A. Van Ginderachter, E. Sokal, N. Gotoh, K.-K. Wong, C. Verfaillie, R. Derua, S. Munck, M. Yuneva, L. Beretta, R.J. DeBerardinis, J.V. Swinnen, L. Hodson, D. Cassiman, C. Verslype, S. Christian, S. Grünewald, T.G.P. Grünewald, S.-M. Fendt, Evidence for an alternative fatty acid desaturation pathway increasing cancer plasticity, Nature, 566 (2019) 403-406.

[435] K.J. Livak, T.D. Schmittgen, Analysis of Relative Gene Expression Data Using Real-Time Quantitative PCR and the 2−ΔΔCT Method, Methods, 25 (2001) 402-408.
[436] H. Huang, Y. Wang, M. Kandpal, G. Zhao, H. Cardenas, Y. Ji, A. Chaparala, E.J. Tanner, J. Chen, R.V. Davuluri, D. Matei, FTO-Dependent N6-Methyladenosine Modifications Inhibit Ovarian Cancer Stem Cell Self-Renewal by Blocking cAMP Signaling, Cancer research, 80 (2020) 3200-3214.
[437] Y. Wang, G. Zhao, S. Condello, H. Huang, H. Cardenas, E.J. Tanner, J. Wei, Y. Ji, J. Li, Y. Tan, R.V. Davuluri, M.E. Peter, J.X. Cheng, D. Matei, Frizzled-7 Identifies Platinum-Tolerant Ovarian Cancer Cells Susceptible to Ferroptosis, Cancer Res, 81 (2021) 384-399.
[438] S. Condello, L. Sima, C. Ivan, H. Cardenas, G. Schiltz, R.K. Mishra, D. Matei, Tissue Tranglutaminase Regulates Interactions between Ovarian Cancer Stem Cells and the Tumor Niche, Cancer Research, 78 (2018) 2990-3001.
[439] G.J. Horacio Cardenas, Jessica Thomes Pepin, J. Brandon Parker, Salvatore Condello, Kenneth P. Nephew, Harikrishna Nakshatri, Debabrata Chakravarti, Yunlong Liu, and Daniela Matei, Interferon-γ Signaling is Associated with BRCA1 Loss-of-Function Mutations in High Grade Serous Ovarian Cancer, Npj Precision Oncology, in press (2019).
[440] M. Song, T.A. Sandoval, C.-S. Chae, S. Chopra, C. Tan, M.R. Rutkowski, M. Raundhal, R.A. Chaurio, K.K. Payne, C. Konrad, S.E. Bettigole, H.R. Shin, M.J.P. Crowley, J.P. Cerliani, A.V. Kossenkov, I. Motorykin, S. Zhang, G. Manfredi, D. Zamarin, K. Holcomb, P.C. Rodriguez, G.A. Rabinovich, J.R. Conejo-Garcia, L.H. Glimcher, J.R. Cubillos-Ruiz, IRE1α–XBP1 controls T cell function in ovarian cancer by regulating mitochondrial activity, Nature, 562 (2018) 423-428.
[441] C.A. Schneider, W.S. Rasband, K.W. Eliceiri, NIH Image to ImageJ: 25 years of image analysis, Nature methods, 9 (2012) 671-675.
[442] Z. Xie, C.R. Ferreira, A.A. Virequ, R.G. Cooks, Multiple reaction monitoring profiling (MRM profiling): Small molecule exploratory analysis guided by chemical functionality, Chemistry and Physics of Lipids, 235 (2021) 105048.
[443] E.G. Bligh, W.J. Dyer, A Rapid Method of Total Lipid Extraction and Purification, Canadian Journal of Biochemistry and Physiology, 37 (1959) 911-917.
[444] J.A. Vogt, U. Wachter, M. Georgieff, Non-linearity in the quadrupole detector system: implications for the determination of the13C mass distribution of an ion fragment, Journal of Mass Spectrometry, 38 (2003) 222-230.
[445] S.S. Dipali, C.R. Ferreira, L.T. Zhou, M.T. Pritchard, F.E. Duncan, Histologic analysis and lipid profiling reveal reproductive age-associated changes in peri-ovarian adipose tissue, Reproductive Biology and Endocrinology, 17 (2019).
[446] A. Suarez-Trujillo, S.M. Luecke, L. Logan, C. Bradshaw, K.R. Stewart, R.C. Minor, C. Ramires Ferreira, T.M. Casey, Changes in sow milk lipidome across lactation occur in fatty acyl residues of triacylglycerol and phosphatidylglycerol lipids, but not in plasma membrane phospholipids, Animal, 15 (2021) 100280.
[447] A. Suarez-Trujillo, K. Huff, C. Ramires Ferreira, T.J. Paschoal Sobreira, K.K. Buhman, T. Casey, High-fat-diet induced obesity increases the proportion of linoleic acyl residues in dam serum and milk and in suckling neonate circulation, Biology of Reproduction, 103 (2020) 736-749.
[448] J.A.B. Claydon, C.E. Clyde-Brockway, C.R. Ferreira, E.A. Flaherty, F.V. Paladino, Lipid profiling suggests species specificity and minimal seasonal variation in Pacific Green and Hawksbill Turtle plasma, PloS one, 16 (2021) e0253916.
[449] M.E. Edwards, T. De Luca, C.R. Ferreira, K.S. Collins, M.T. Eadon, E.A. Benson, T.J.P. Sobreira, R.G. Cooks, Multiple reaction monitoring profiling as an analytical strategy to investigate lipids in extracellular vesicles, Journal of Mass Spectrometry, 56 (2020).

[450] Z. Pang, J. Chong, S. Li, J. Xia, MetaboAnalystR 3.0: Toward an Optimized Workflow for Global Metabolomics, Metabolites, 10 (2020).
[451] E. Fahy, S. Subramaniam, R.C. Murphy, M. Nishijima, C.R. Raetz, T. Shimizu, F. Spener, G. van Meer, M.J. Wakelam, E.A. Dennis, Update of the LIPID MAPS comprehensive classification system for lipids, Journal of lipid research, 50 Suppl (2009) S9-14.
[452] J. Li, Y. Tan, G. Zhao, K.-C. Huang, H. Cardenas, D. Matei, J.-X. Cheng, Metabolic Reprogramming from Glycolysis to Fatty Acid Uptake and beta-Oxidation in Platinum-Resistant Cancer Cells, bioRxiv, (2021) 2021.2005.2017.444564.
[453] H. Lin, H.J. Lee, N. Tague, J.B. Lugagne, C. Zong, F. Deng, J. Shin, L. Tian, W. Wong, M.J. Dunlop, J.X. Cheng, Microsecond fingerprint stimulated Raman spectroscopic imaging by ultrafast tuning and spatial-spectral learning, Nature communications, 12 (2021) 3052.
[454] B.L. Aken, P. Achuthan, W. Akanni, M.R. Amode, F. Bernsdorff, J. Bhai, K. Billis, D. Carvalho-Silva, C. Cummins, P. Clapham, L. Gil, C.G. Giron, L. Gordon, T. Hourlier, S.E. Hunt, S.H. Janacek, T. Juettemann, S. Keenan, M.R. Laird, I. Lavidas, T. Maurel, W. McLaren, B. Moore, D.N. Murphy, R. Nag, V. Newman, M. Nuhn, C.K. Ong, A. Parker, M. Patricio, H.S. Riat, D. Sheppard, H. Sparrow, K. Taylor, A. Thormann, A. Vullo, B. Walts, S.P. Wilder, A. Zadissa, M. Kostadima, F.J. Martin, M. Muffato, E. Perry, M. Ruffier, D.M. Staines, S.J. Trevanion, F. Cunningham, A. Yates, D.R. Zerbino, P. Flicek, Ensembl 2017, Nucleic acids research, 45 (2017) D635-D642.
[455] A. Dobin, C.A. Davis, F. Schlesinger, J. Drenkow, C. Zaleski, S. Jha, P. Batut, M. Chaisson, T.R. Gingeras, STAR: ultrafast universal RNA-seq aligner, Bioinformatics, 29 (2013) 15-21.
[456] H. Li, B. Handsaker, A. Wysoker, T. Fennell, J. Ruan, N. Homer, G. Marth, G. Abecasis, R. Durbin, S. Genome Project Data Processing, The Sequence Alignment/Map format and SAMtools, Bioinformatics, 25 (2009) 2078-2079.
[457] S. Anders, P.T. Pyl, W. Huber, HTSeq--a Python framework to work with high-throughput sequencing data, Bioinformatics, 31 (2015) 166-169.
[458] M.D. Robinson, D.J. McCarthy, G.K. Smyth, edgeR: a Bioconductor package for differential expression analysis of digital gene expression data, Bioinformatics, 26 (2010) 139-140.
[459] A. Subramanian, P. Tamayo, V.K. Mootha, S. Mukherjee, B.L. Ebert, M.A. Gillette, A. Paulovich, S.L. Pomeroy, T.R. Golub, E.S. Lander, J.P. Mesirov, Gene set enrichment analysis: a knowledge-based approach for interpreting genome-wide expression profiles, Proceedings of the National Academy of Sciences of the United States of America, 102 (2005) 15545-15550.
[460] G. Yu, L.-G. Wang, Y. Han, Q.-Y. He, clusterProfiler: an R Package for Comparing Biological Themes Among Gene Clusters, OMICS: A Journal of Integrative Biology, 16 (2012) 284-287.
[461] A. Tsherniak, F. Vazquez, P.G. Montgomery, B.A. Weir, G. Kryukov, G.S. Cowley, S. Gill, W.F. Harrington, S. Pantel, J.M. Krill-Burger, R.M. Meyers, L. Ali, A. Goodale, Y. Lee, G. Jiang, J. Hsiao, W.F.J. Gerath, S. Howell, E. Merkel, M. Ghandi, L.A. Garraway, D.E. Root, T.R. Golub, J.S. Boehm, W.C. Hahn, Defining a Cancer Dependency Map, Cell, 170 (2017) 564-576.e516.
[462] T.Z. Tan, H. Yang, J. Ye, J. Low, M. Choolani, D.S. Tan, J.P. Thiery, R.Y. Huang, CSIOVDB: a microarray gene expression database of epithelial ovarian cancer subtype, Oncotarget, 6 (2015) 43843-43852.
[463] N. Cancer Genome Atlas Research, Integrated genomic analyses of ovarian carcinoma, Nature, 474 (2011) 609-615.
[464] M.A. Surma, M.J. Gerl, R. Herzog, J. Helppi, K. Simons, C. Klose, Mouse lipidomics reveals inherent flexibility of a mammalian lipidome, Scientific reports, 11 (2021) 19364.
[465] M. Ghandi, F.W. Huang, J. Jane-Valbuena, G.V. Kryukov, C.C. Lo, E.R. McDonald, 3rd, J. Barretina, E.T. Gelfand, C.M. Bielski, H. Li, K. Hu, A.Y. Andreev-Drakhlin, J. Kim, J.M. Hess, B.J. Haas, F. Aguet, B.A.

Weir, M.V. Rothberg, B.R. Paolella, M.S. Lawrence, R. Akbani, Y. Lu, H.L. Tiv, P.C. Gokhale, A. de Weck, A.A. Mansour, C. Oh, J. Shih, K. Hadi, Y. Rosen, J. Bistline, K. Venkatesan, A. Reddy, D. Sonkin, M. Liu, J. Lehar, J.M. Korn, D.A. Porter, M.D. Jones, J. Golji, G. Caponigro, J.E. Taylor, C.M. Dunning, A.L. Creech, A.C. Warren, J.M. McFarland, M. Zamanighomi, A. Kauffmann, N. Stransky, M. Imielinski, Y.E. Maruvka, A.D. Cherniack, A. Tsherniak, F. Vazquez, J.D. Jaffe, A.A. Lane, D.M. Weinstock, C.M. Johannessen, M.P. Morrissey, F. Stegmeier, R. Schlegel, W.C. Hahn, G. Getz, G.B. Mills, J.S. Boehm, T.R. Golub, L.A. Garraway, W.R. Sellers, Next-generation characterization of the Cancer Cell Line Encyclopedia, Nature, 569 (2019) 503-508.
[466] R. Volmer, K. van der Ploeg, D. Ron, Membrane lipid saturation activates endoplasmic reticulum unfolded protein response transducers through their transmembrane domains, Proceedings of the National Academy of Sciences of the United States of America, 110 (2013) 4628-4633.
[467] M. Calfon, H. Zeng, F. Urano, J.H. Till, S.R. Hubbard, H.P. Harding, S.G. Clark, D. Ron, IRE1 couples endoplasmic reticulum load to secretory capacity by processing the XBP-1 mRNA, Nature, 415 (2002) 92-96.
[468] H.P. Harding, Y. Zhang, D. Ron, Protein translation and folding are coupled by an endoplasmic-reticulum-resident kinase, Nature, 397 (1999) 271-274.
[469] H.P. Harding, I. Novoa, Y. Zhang, H. Zeng, R. Wek, M. Schapira, D. Ron, Regulated translation initiation controls stress-induced gene expression in mammalian cells, Molecular cell, 6 (2000) 1099-1108.
[470] C. Hetz, The unfolded protein response: controlling cell fate decisions under ER stress and beyond, Nature Reviews Molecular Cell Biology, 13 (2012) 89-102.
[471] J.D. Wikstrom, T. Israeli, E. Bachar-Wikstrom, A. Swisa, Y. Ariav, M. Waiss, D. Kaganovich, Y. Dor, E. Cerasi, G. Leibowitz, AMPK regulates ER morphology and function in stressed pancreatic beta-cells via phosphorylation of DRP1, Molecular endocrinology, 27 (2013) 1706-1723.
[472] B. Gyorffy, A. Lanczky, Z. Szallasi, Implementing an online tool for genome-wide validation of survival-associated biomarkers in ovarian-cancer using microarray data from 1287 patients, Endocrine-related cancer, 19 (2012) 197-208.
[473] S. Schoors, U. Bruning, R. Missiaen, K.C. Queiroz, G. Borgers, I. Elia, A. Zecchin, A.R. Cantelmo, S. Christen, J. Goveia, W. Heggermont, L. Godde, S. Vinckier, P.P. Van Veldhoven, G. Eelen, L. Schoonjans, H. Gerhardt, M. Dewerchin, M. Baes, K. De Bock, B. Ghesquiere, S.Y. Lunt, S.M. Fendt, P. Carmeliet, Fatty acid carbon is essential for dNTP synthesis in endothelial cells, Nature, 520 (2015) 192-197.
[474] D. Wang, S.J. Lippard, Cellular processing of platinum anticancer drugs, Nature reviews. Drug discovery, 4 (2005) 307-320.
[475] L. Galluzzi, L. Senovilla, I. Vitale, J. Michels, I. Martins, O. Kepp, M. Castedo, G. Kroemer, Molecular mechanisms of cisplatin resistance, Oncogene, 31 (2012) 1869-1883.
[476] K. Apostolov, W. Barker, D. Catovsky, J. Goldman, E. Matutes, Reduction in the stearic to oleic acid ratio in leukaemic cells--a possible chemical marker of malignancy, Blut, 50 (1985) 349-354.
[477] J.A. Petrek, L.C. Hudgins, M. Ho, D.R. Bajorunas, J. Hirsch, Fatty acid composition of adipose tissue, an indication of dietary fatty acids, and breast cancer prognosis, Journal of clinical oncology : official journal of the American Society of Clinical Oncology, 15 (1997) 1377-1384.
[478] V. Chajes, K. Hulten, A.L. Van Kappel, A. Winkvist, R. Kaaks, G. Hallmans, P. Lenner, E. Riboli, Fatty-acid composition in serum phospholipids and risk of breast cancer: an incident case-control study in Sweden, International journal of cancer, 83 (1999) 585-590.
[479] S. Sharad, A. Srivastava, S. Ravulapalli, P. Parker, Y. Chen, H. Li, G. Petrovics, A. Dobi, Prostate cancer gene expression signature of patients with high body mass index, Prostate cancer and prostatic diseases, 14 (2011) 22-29.

[480] J. Macasek, M. Vecka, A. Zak, M. Urbanek, T. Krechler, L. Petruzelka, B. Stankova, M. Zeman, Plasma fatty acid composition in patients with pancreatic cancer: correlations to clinical parameters, Nutrition and cancer, 64 (2012) 946-955.
[481] J.E. Chavarro, S.A. Kenfield, M.J. Stampfer, M. Loda, H. Campos, H.D. Sesso, J. Ma, Blood levels of saturated and monounsaturated fatty acids as markers of de novo lipogenesis and risk of prostate cancer, American journal of epidemiology, 178 (2013) 1246-1255.
[482] A.M. Holder, A.M. Gonzalez-Angulo, H. Chen, A. Akcakanat, K.A. Do, W. Fraser Symmans, L. Pusztai, G.N. Hortobagyi, G.B. Mills, F. Meric-Bernstam, High stearoyl-CoA desaturase 1 expression is associated with shorter survival in breast cancer patients, Breast cancer research and treatment, 137 (2013) 319-327.
[483] A. Budhu, S. Roessler, X. Zhao, Z. Yu, M. Forgues, J. Ji, E. Karoly, L.X. Qin, Q.H. Ye, H.L. Jia, J. Fan, H.C. Sun, Z.Y. Tang, X.W. Wang, Integrated metabolite and gene expression profiles identify lipid biomarkers associated with progression of hepatocellular carcinoma and patient outcomes, Gastroenterology, 144 (2013) 1066-1075 e1061.
[484] L. Byberg, L. Kilander, E. Warensjo Lemming, K. Michaelsson, B. Vessby, Cancer death is related to high palmitoleic acid in serum and to polymorphisms in the SCD-1 gene in healthy Swedish men, The American journal of clinical nutrition, 99 (2014) 551-558.
[485] C.A. Pickens, A. Lane-Elliot, S.S. Comstock, J.I. Fenton, Altered Saturated and Monounsaturated Plasma Phospholipid Fatty Acid Profiles in Adult Males with Colon Adenomas, Cancer epidemiology, biomarkers & prevention : a publication of the American Association for Cancer Research, cosponsored by the American Society of Preventive Oncology, 25 (2016) 498-506.
[486] M. Zemanova, M. Vecka, L. Petruzelka, B. Stankova, A. Zak, M. Zeman, Plasma Phosphatidylcholines Fatty Acids in Men with Squamous Cell Esophageal Cancer: Chemoradiotherapy Improves Abnormal Profile, Medical science monitor : international medical journal of experimental and clinical research, 22 (2016) 4092-4099.
[487] J. Wang, Y. Xu, L. Zhu, Y. Zou, W. Kong, B. Dong, J. Huang, Y. Chen, W. Xue, Y. Huang, J. Zhang, High Expression of Stearoyl-CoA Desaturase 1 Predicts Poor Prognosis in Patients with Clear-Cell Renal Cell Carcinoma, PloS one, 11 (2016) e0166231.
[488] A. Manni, J.P. Richie, S.E. Schetter, A. Calcagnotto, N. Trushin, C. Aliaga, K. El-Bayoumy, Stearoyl-CoA desaturase-1, a novel target of omega-3 fatty acids for reducing breast cancer risk in obese postmenopausal women, European journal of clinical nutrition, 71 (2017) 762-765.
[489] L.P. Fernandez, R. Ramos-Ruiz, J. Herranz, R. Martin-Hernandez, T. Vargas, M. Mendiola, L. Guerra, G. Reglero, J. Feliu, A. Ramirez de Molina, The transcriptional and mutational landscapes of lipid metabolism-related genes in colon cancer, Oncotarget, 9 (2018) 5919-5930.
[490] B. Scazzocchio, R. Vari, A. Silenzi, S. Giammarioli, A. Masotti, A. Baldassarre, C. Santangelo, M. D'Archivio, C. Giovannini, M. Del Corno, L. Conti, S. Gessani, R. Masella, Dietary habits affect fatty acid composition of visceral adipose tissue in subjects with colorectal cancer or obesity, European journal of nutrition, 59 (2020) 1463-1472.
[491] M.T. Nakamura, T.Y. Nara, Structure, function, and dietary regulation of delta6, delta5, and delta9 desaturases, Annu Rev Nutr, 24 (2004) 345-376.
[492] M.C. Beauchamp, A. Yasmeen, A. Knafo, W.H. Gotlieb, Targeting insulin and insulin-like growth factor pathways in epithelial ovarian cancer, Journal of oncology, 2010 (2010) 257058.
[493] K.J. Williams, J.P. Argus, Y. Zhu, M.Q. Wilks, B.N. Marbois, A.G. York, Y. Kidani, A.L. Pourzia, D. Akhavan, D.N. Lisiero, E. Komisopoulou, A.H. Henkin, H. Soto, B.T. Chamberlain, L. Vergnes, M.E. Jung, J.Z. Torres, L.M. Liau, H.R. Christofk, R.M. Prins, P.S. Mischel, K. Reue, T.G. Graeber, S.J. Bensinger, An

essential requirement for the SCAP/SREBP signaling axis to protect cancer cells from lipotoxicity, Cancer research, 73 (2013) 2850-2862.
[494] B.G. Ward, K. Wallace, J.H. Shepherd, F.R. Balkwill, Intraperitoneal xenografts of human epithelial ovarian cancer in nude mice, Cancer research, 47 (1987) 2662-2667.
[495] Y. Zou, W.S. Henry, E.L. Ricq, E.T. Graham, V.V. Phadnis, P. Maretich, S. Paradkar, N. Boehnke, A.A. Deik, F. Reinhardt, J.K. Eaton, B. Ferguson, W. Wang, J. Fairman, H.R. Keys, V. Dancik, C.B. Clish, P.A. Clemons, P.T. Hammond, L.A. Boyer, R.A. Weinberg, S.L. Schreiber, Plasticity of ether lipids promotes ferroptosis susceptibility and evasion, Nature, 585 (2020) 603-608.
[496] M. Minville-Walz, A.S. Pierre, L. Pichon, S. Bellenger, C. Fevre, J. Bellenger, C. Tessier, M. Narce, M. Rialland, Inhibition of stearoyl-CoA desaturase 1 expression induces CHOP-dependent cell death in human cancer cells, PloS one, 5 (2010) e14363.
[497] Q. Zhang, S. Yu, M.M.T. Lam, T.C.W. Poon, L. Sun, Y. Jiao, A.S.T. Wong, L.T.O. Lee, Angiotensin II promotes ovarian cancer spheroid formation and metastasis by upregulation of lipid desaturation and suppression of endoplasmic reticulum stress, Journal of experimental & clinical cancer research : CR, 38 (2019) 116.
[498] K. Skrypek, S. Balog, Y. Eriguchi, K. Asahina, Inhibition of Stearoyl-CoA Desaturase Induces the Unfolded Protein Response in Pancreatic Tumors and Suppresses Their Growth, Pancreas, 50 (2021) 219-226.
[499] X.Y. Qin, T. Su, W. Yu, S. Kojima, Lipid desaturation-associated endoplasmic reticulum stress regulates MYCN gene expression in hepatocellular carcinoma cells, Cell death & disease, 11 (2020) 66.
[500] H. Xie, C.H. Tang, J.H. Song, A. Mancuso, J.R. Del Valle, J. Cao, Y. Xiang, C.V. Dang, R. Lan, D.J. Sanchez, B. Keith, C.C. Hu, M.C. Simon, IRE1alpha RNase-dependent lipid homeostasis promotes survival in Myc-transformed cancers, The Journal of clinical investigation, 128 (2018) 1300-1316.
[501] L. Potze, S. Di Franco, C. Grandela, M.L. Pras-Raves, D.I. Picavet, H.A. van Veen, H. van Lenthe, F.B. Mullauer, N.N. van der Wel, A. Luyf, A.H. van Kampen, S. Kemp, V. Everts, J.H. Kessler, F.M. Vaz, J.P. Medema, Betulinic acid induces a novel cell death pathway that depends on cardiolipin modification, Oncogene, 35 (2016) 427-437.
[502] L. Chen, J. Ren, L. Yang, Y. Li, J. Fu, Y. Li, Y. Tian, F. Qiu, Z. Liu, Y. Qiu, Stearoyl-CoA desaturase-1 mediated cell apoptosis in colorectal cancer by promoting ceramide synthesis, Scientific reports, 6 (2016) 19665.
[503] R.H. Zheng, Y.B. Zhang, F.N. Qiu, Z.H. Liu, Y. Han, R. Huang, Y. Zhao, P. Yao, Y. Qiu, J. Ren, NF-kappaB pathway play a role in SCD1 deficiency-induced ceramide de novo synthesis, Cancer biology & therapy, 22 (2021) 164-174.
[504] D. Hanahan, R.A. Weinberg, Hallmarks of cancer: the next generation, Cell, 144 (2011) 646-674.
[505] M. Bowers, T. Liang, D. Gonzalez-Bohorquez, S. Zocher, B.N. Jaeger, W.J. Kovacs, C. Rohrl, K.M.L. Cramb, J. Winterer, M. Kruse, S. Dimitrieva, R.W. Overall, T. Wegleiter, H. Najmabadi, C.F. Semenkovich, G. Kempermann, C. Foldy, S. Jessberger, FASN-Dependent Lipid Metabolism Links Neurogenic Stem/Progenitor Cell Activity to Learning and Memory Deficits, Cell Stem Cell, 27 (2020) 98-109 e111.
[506] J. Lu, Q. Wang, L. Huang, H. Dong, L. Lin, N. Lin, F. Zheng, J. Tan, Palmitate causes endoplasmic reticulum stress and apoptosis in human mesenchymal stem cells: prevention by AMPK activator, Endocrinology, 153 (2012) 5275-5284.
[507] J.M. van Rijn, M. van Hoesel, C. de Heus, A.H.M. van Vugt, J. Klumperman, E.E.S. Nieuwenhuis, R.H.J. Houwen, S. Middendorp, DGAT2 partially compensates for lipid-induced ER stress in human DGAT1-deficient intestinal stem cells, Journal of lipid research, 60 (2019) 1787-1800.
[508] H. Mujcic, A. Nagelkerke, K.M. Rouschop, S. Chung, N. Chaudary, P.N. Span, B. Clarke, M. Milosevic, J. Sykes, R.P. Hill, M. Koritzinsky, B.G. Wouters, Hypoxic activation of the PERK/eIF2alpha arm of the

unfolded protein response promotes metastasis through induction of LAMP3, Clinical cancer research : an official journal of the American Association for Cancer Research, 19 (2013) 6126-6137.
[509] Y.X. Feng, E.S. Sokol, C.A. Del Vecchio, S. Sanduja, J.H. Claessen, T.A. Proia, D.X. Jin, F. Reinhardt, H.L. Ploegh, Q. Wang, P.B. Gupta, Epithelial-to-mesenchymal transition activates PERK-eIF2alpha and sensitizes cells to endoplasmic reticulum stress, Cancer Discov, 4 (2014) 702-715.
[510] S. Yue, J. Li, S.Y. Lee, H.J. Lee, T. Shao, B. Song, L. Cheng, T.A. Masterson, X. Liu, T.L. Ratliff, J.X. Cheng, Cholesteryl ester accumulation induced by PTEN loss and PI3K/AKT activation underlies human prostate cancer aggressiveness, Cell metabolism, 19 (2014) 393-406.
[511] J. Li, D. Gu, S.S. Lee, B. Song, S. Bandyopadhyay, S. Chen, S.F. Konieczny, T.L. Ratliff, X. Liu, J. Xie, J.X. Cheng, Abrogating cholesterol esterification suppresses growth and metastasis of pancreatic cancer, Oncogene, 35 (2016) 6378-6388.
[512] K.C. Huang, J. Li, C. Zhang, Y. Tan, J.X. Cheng, Multiplex Stimulated Raman Scattering Imaging Cytometry Reveals Lipid-Rich Protrusions in Cancer Cells under Stress Condition, iScience, 23 (2020) 100953.
[513] S.K. Clinton, E.L. Giovannucci, S.D. Hursting, The World Cancer Research Fund/American Institute for Cancer Research Third Expert Report on Diet, Nutrition, Physical Activity, and Cancer: Impact and Future Directions, The Journal of nutrition, 150 (2020) 663-671.
[514] M.C. Mentella, F. Scaldaferri, C. Ricci, A. Gasbarrini, G.A.D. Miggiano, Cancer and Mediterranean Diet: A Review, Nutrients, 11 (2019).
[515] D.D. Weber, S. Aminzadeh-Gohari, J. Tulipan, L. Catalano, R.G. Feichtinger, B. Kofler, Ketogenic diet in the treatment of cancer - Where do we stand?, Molecular metabolism, 33 (2020) 102-121.
[516] E.C. Lien, A.M. Westermark, Y. Zhang, C. Yuan, Z. Li, A.N. Lau, K.M. Sapp, B.M. Wolpin, M.G. Vander Heiden, Low glycaemic diets alter lipid metabolism to influence tumour growth, Nature, 599 (2021) 302-307.
[517] D. Mauvoisin, C. Mounier, Hormonal and nutritional regulation of SCD1 gene expression, Biochimie, 93 (2011) 78-86.
[518] J.M. Ntambi, Regulation of stearoyl-CoA desaturase by polyunsaturated fatty acids and cholesterol, Journal of lipid research, 40 (1999) 1549-1558.
[519] M.Y. Park, H.H. Jang, J.B. Kim, H.N. Yoon, J.Y. Lee, Y.M. Lee, J.H. Kim, D.S. Park, Hog millet (Panicum miliaceum L.)-supplemented diet ameliorates hyperlipidemia and hepatic lipid accumulation in C57BL/6J-ob/ob mice, Nutrition research and practice, 5 (2011) 511-519.
[520] S. Ducheix, E. Piccinin, C. Peres, O. Garcia-Irigoyen, J. Bertrand-Michel, A. Fouache, M. Cariello, J.M. Lobaccaro, H. Guillou, C. Sabba, J.M. Ntambi, A. Moschetta, Reduction in gut-derived MUFAs via intestinal stearoyl-CoA desaturase 1 deletion drives susceptibility to NAFLD and hepatocarcinoma, Hepatology communications, (2022).
[521] S. Ducheix, C. Peres, J. Hardfeldt, C. Frau, G. Mocciaro, E. Piccinin, J.M. Lobaccaro, S. De Santis, M. Chieppa, J. Bertrand-Michel, M. Plateroti, J.L. Griffin, C. Sabba, J.M. Ntambi, A. Moschetta, Deletion of Stearoyl-CoA Desaturase-1 From the Intestinal Epithelium Promotes Inflammation and Tumorigenesis, Reversed by Dietary Oleate, Gastroenterology, 155 (2018) 1524-1538 e1529.
[522] E. Magnotti, W.A. Marasco, The latest animal models of ovarian cancer for novel drug discovery, Expert opinion on drug discovery, 13 (2018) 249-257.
[523] A.B. Cordero, Y. Kwon, X. Hua, A.K. Godwin, In vivo imaging and therapeutic treatments in an orthotopic mouse model of ovarian cancer, Journal of visualized experiments : JoVE, (2010).
[524] R. Rudalska, J. Harbig, M.T. Snaebjornsson, S. Klotz, S. Zwirner, L. Taranets, F. Heinzmann, T. Kronenberger, M. Forster, W. Cui, L. D'Artista, E. Einig, M. Hinterleitner, W. Schmitz, A. Dylawerska, T.W. Kang, A. Poso, M.T. Rosenfeldt, N.P. Malek, M. Bitzer, S. Laufer, B.J. Pichler, N. Popov, A. Schulze, L.

Zender, D. Dauch, LXRalpha activation and Raf inhibition trigger lethal lipotoxicity in liver cancer, Nature cancer, 2 (2021) 201-217.

Guangyuan Zhao

guangyuanzhao2022@u.northwestern.edu

EDUCATION

Feinberg School of Medicine, Northwestern University – Chicago, IL *Aug 2016 – Oct 2022*

PhD Candidate in Biomedical Sciences Cumulative GPA: 3.84/4.00
MS in Clinical Investigation

Imperial College of Science, Technology and Medicine – London, UK *Sept 2012 – Nov 2013*

MRes in Chemical Biology of Crop Sustainability and Protection

College of Chemistry and Molecular Sciences, Wuhan University – Hubei, China *Sept 2008 – Jun 2012*

BS in Chemistry

RESEARCH EXPERIENCE

Fatty Acid Metabolism in Ovarian Cancer
Department of Ob/Gyn, Feinberg School of Medicine, Northwestern University
PI: Daniela Matei, MD *Aug 2017 – Oct 2022*

- Generated stearoyl CoA desaturase (SCD) knockdown (KD) via shRNA and overexpression via lentiviral transfection stable ovarian cancer cell lines
- Assessed gene expression at mRNA and protein level using RT-qPCR and Western blotting
- Examined cellular apoptosis/ferroptosis of ovarian cancer cells upon SCD inhibition via flow cytometry
- Performed RNA-seq and lipidomics library preparation and analyses to examine global effect of SCD KD on fatty acid metabolism in ovarian cancer cells
- Directed research intern to examine XBP1 splicing in ovarian cancer cells depleted of SCD
- Utilized athymic nude mice to study impact of SCD KD on tumorigenesis and tumor growth *in vivo*

Platinum Resistance in Ovarian Cancer
Department of Ob/Gyn, Feinberg School of Medicine, Northwestern University
PI: Daniela Matei, MD *Aug 2017 – Jul 2022*

- Developed platinum-resistant ovarian cancer cell lines *in vitro*
- Conducted RNA-seq and metabolomics library preparation and analyses to investigate the alternation in cellular metabolism in acquiring platinum resistance
- Established 2D and 3D cell models from primary solid tumor and ascites from ovarian cancer patients
- Customized in-house pipeline for analyzing metabolomics data
- Enabled cross-functional collaboration on mechanistic studies of platinum-sensitive and

resistant ovarian cancer via high-resolution imaging

Bioinformatics skills

Linux OS, R (RNA-seq, metabolomics and lipidomics analyses), GraphPad, SPSS, SnapGene, BLAST

PUBLICATIONS

1. **Zhao, G.**, Tan, Y., Cardenas, H., Vayngart, D., Wang, Y., Huang, H., Keathley, R., Wei, J.J., Ferreira, C.R., Orsulic, S. and Cheng, J.X., 2022. Ovarian cancer cell fate regulation by the dynamics between saturated and unsaturated fatty acids. *Proceedings of the National Academy of Sciences*, 119(41), p.e2203480119.
2. Tan, Y.[#], Li, J.[#], **Zhao, G.[#]**, Huang, K.C., Cardenas, H., Wang, Y., Matei, D. and Cheng, J.X., 2022. Metabolic reprogramming from glycolysis to fatty acid uptake and beta-oxidation in platinum-resistant cancer cells. *Nature communications*, 13(1), pp.1-16. (# equal contribution, accepted).
3. Zhang, Y., Wang, Y., **Zhao, G.**, Tanner, E.J., Adli, M. and Matei, D., 2022. FOXK2 promotes ovarian cancer stemness by regulating the unfolded protein response pathway. *The Journal of Clinical Investigation*, 132(10).
4. Sima, L.E., Chen, S., Cardenas, H., **Zhao, G.**, Wang, Y., Ivan, C., Huang, H., Zhang, B. and Matei, D., 2021. Loss of host tissue transglutaminase boosts antitumor T cell immunity by altering STAT1/STAT3 phosphorylation in ovarian cancer. *Journal for immunotherapy of cancer*, 9(9).
5. Zhuge, M., Huang, K.C., Lee, H.J., Jiang, Y., Tan, Y., Lin, H., Dong, P.T., **Zhao, G.**, Matei, D., Yang, Q. and Cheng, J.X., 2021. Ultrasensitive Vibrational Imaging of Retinoids by Visible Preresonance Stimulated Raman Scattering Microscopy. *Advanced Science*, p.2003136.
6. Wang, Y., **Zhao, G.**, Condello, S., Huang, H., Cardenas, H., Tanner, E.J., Wei, J., Ji, Y., Li, J., Tan, Y. and Davuluri, R.V., 2020. Frizzled-7 Identifies Platinum-Tolerant Ovarian Cancer Cells Susceptible to Ferroptosis. *Cancer Research*, 81(2), pp.384-399.
7. Huang, H., Wang, Y., Kandpal, M., **Zhao, G.**, Cardenas, H., Ji, Y., Chaparala, A., Tanner, E.J., Chen, J., Davuluri, R.V. and Matei, D., 2020. FTO-Dependent N6-Methyladenosine Modifications Inhibit Ovarian Cancer Stem Cell Self-Renewal by Blocking cAMP Signaling. *Cancer Research*, 80(16), pp.3200-3214.
8. **Zhao, G.**, Cardenas, H. and Matei, D., 2019. Ovarian Cancer—Why Lipids Matter. *Cancers*, 11(12), p.1870.
9. Delaney, M. K., Malikov, V., Chai, Q., **Zhao, G.**, & Naghavi, M. H. (2017). Distinct functions of diaphanous-related formins regulate HIV-1 uncoating and transport. *Proceedings of the National Academy of Sciences*, 114(33), E6932-E6941.
10. O'Donnelly, K., **Zhao, G.**, Patel, P., Butt, M., Mak, L., Kretschmer, S., Woscholski, R., and Barter, L. (2014). Isolation and kinetic characterisation of hydrophobically distinct populations of form I Rubisco. *Plant Methods*, *10*, 17-27.
11. Dong, J.X., **Zhao, G.Y.**, Yu, Q.L., Li, R., Yuan, L., Chen, J., and Liu, Y. (2013). Mitochondrial Dysfunction Induced by Honokiol. *The Journal of membrane biology*, *246*, 375-381.
12. Li, J.H., Liu, X.R., Zhang, Y., Tian, F.F., **Zhao, G.Y.**, Yu, Q.L.Y., Jiang, F.L., and Liu, Y. (2012). Toxicity of nano zinc oxide to mitochondria. *Toxicol Res-Uk*, *1*, 137-144.
13. Li, J., Zhang, Y., Xiao, Q., Tian, F., Liu, X., Li, R., **Zhao, G.**, Jiang, F., and Liu, Y. (2011). Mitochondria as target of quantum dots toxicity. *J Hazard Mater*, 194, 440-444.

HONORS AND AWARDS

Constance Campbell Trainee Travel Award, Northwestern University *2020*

Scholarship for Outstanding Performance throughout an academic year, Wuhan University *2009 – 2011*

Class-A Scholarship for Excellent Performance in National University Entrance Examination, Wuhan University *2008*

OTHER ACTIVITIES

Teaching Assistant – Investigative Lab, Northwestern University *Apr 2019 – Jun 2019*

- Presented core theoretical knowledge and lab skills to students before weekly lab session
- Supervised students to complete their weekly experiments and lab reports
- Guided students in their scientific writing and scientific presentation